The Pathophysiological Role and Therapeutic Potential of C-Type Natriuretic Peptide in Pulmonary Hypertension

A thesis submitted in partial fulfilment of the requirements of the Degree of Doctor of Philosophy

Joshua Patrick Dignam

Centre for Translational Medicine & Therapeutics

William Harvey Research Institute

Barts & The London School of Medicine & Dentistry

Queen Mary University of London

Charterhouse Square

London EC1M 6BQ

United Kingdom

Statement of originality

I, Joshua Patrick Dignam, confirm that the research included within this thesis is my own work or that where it has been carried out in collaboration with, or supported by others, that this is duly acknowledged below, and my contribution indicated. Previously published material is also acknowledged below.

I attest that I have exercised reasonable care to ensure that the work is original and does not to the best of my knowledge break any UK law, infringe any third party's copyright or other Intellectual Property Right, or contain any confidential material.

I accept that the College has the right to use plagiarism detection software to check the electronic version of the thesis.

I confirm that this thesis has not been previously submitted for the award of a degree by this or any other university.

Date: 21/10/2022

List of publications

Dignam, J. P., Scott, T. E., Kemp-Harper, B. K., & Hobbs, A. J. (2022). Animal models of pulmonary hypertension: Getting to the heart of the problem. British Journal of Pharmacology, 179(5), 811– 837.

Grange, R. M. H., Preedy, M. E. J., Renukanthan, A., **Dignam, J. P.**, Lowe, V. J., Moyes, A. J., Pérez-Ternero, C., Aubdool, A. A., Baliga, R. S., & Hobbs, A. J. (2022). Multidrug resistance proteins preferentially regulate natriuretic peptide-driven cGMP signalling in the heart and vasculature. British Journal of Pharmacology, 179(11), 2443– 2459.

Presentations

Dignam, J. P., Perez-Ternero, C., Aubdool, A., & Hobbs, A. J. C-type natriuretic peptide offsets the development of pulmonary hypertension. 10th International Conference on cGMP: Generators, Effectors and Therapeutic Implications; Augsburg, Germany, June 2022. Poster and flash talk (Young Investigator Prize).

Dignam, J. P., Perez-Ternero, C., Aubdool, A., & Hobbs, A. J. The pathophysiological role and therapeutic potential of C-type natriuretic peptide in pulmonary hypertension. BHF 4-year PhD student conference; virtual meeting, April 2021. Oral presentation.

Abstract

Background

Pulmonary hypertension (PH) is a multi-faceted disease characterised by vascular remodelling and elevated pressure in the pulmonary arteries. Whilst targeted pharmacological and surgical treatments significantly improve outcomes in some PH subgroups, many patients still develop fatal right heart failure, even with optimal therapy. In the systemic circulation, C-type natriuretic peptide (CNP) acts on two biological receptors, natriuretic peptide receptor (NPR)-B, and NPR-C, to modulate vascular tone, angiogenesis, inflammation, smooth muscle and endothelial cell proliferation, cardiomyocyte hypertrophy and fibrosis. In addition, NPR-C also functions as a clearance receptor. A (patho)physiological function for this signalling pathway in the cardiopulmonary circulation has not been established. Exploiting cell-specific transgenic mouse strains, the role of CNP in the development of experimental PH and right ventricular hypertrophy (RVH) was explored.

Methods

Wildtype (WT), global CNP knockout (gbCNP$^{-/-}$), endothelial CNP knockout (ecCNP$^{-/-}$), cardiomyocyte CNP knockout (cmCNP$^{-/-}$) and global natriuretic peptide receptor (NPR)-C null animals (NPR-C$^{-/-}$) were exposed to normoxia (21% O_2; 5 weeks; 'controls') or hypoxia (10% O_2; 5 weeks) plus the vascular endothelial growth factor (VEGF) receptor antagonist Sugen (3x20mg/kg; subcutaneous; days 0, 7 & 14). PH was quantified by determination of right ventricular systolic pressure (RVSP) and heart chamber weights were measured to evaluate RVH (right ventricle to left ventricle plus septum ratio; RV/[LV+S]). Pulmonary vascular remodelling and RV fibrosis were assessed by α-smooth muscle actin staining and picrosirius red staining, respectively. To investigate the therapeutic potential of CNP, and to examine the effects of receptor specific CNP signalling, the peptide was administered to WT and NPR-C$^{-/-}$ mice with established PH via subcutaneous minipump.

Results

Male gbCNP$^{-/-}$ mice exposed to exposed to Sugen plus hypoxia (SuHx) exhibited increased RVSP versus WT SuHx animals. This phenotype was recapitulated in male ecCNP$^{-/-}$ mice, with the addition of accentuated pulmonary vascular remodelling and elevated RVH. Cardiopulmonary pressure and pulmonary vascular remodelling were unaltered in male NPR-C$^{-/-}$ animals, suggesting the protective effects of endogenous CNP are primarily mediated by NPR-B in the pulmonary vasculature. Whilst loss of cardiomyocyte derived CNP was compensated by other cell types in the heart, global NPR-C deficiency exacerbated the development of RVH and fibrosis in male mice, highlighting a key cardioprotective role for NPR-C in the right heart. These effects were highly sex-dependent; deletion of CNP or NPR-C from female SuHx mice did not exacerbate the development of PH or RV remodelling. CNP infusion reduced RVSP in male WT SuHx mice by promoting anti-proliferative, anti-remodelling bone morphogenetic protein (BMP) signalling in the lungs. Reversal of PH was also achieved in NPR-C$^{-/-}$ animals, further highlighting the critical vasoprotective action of NPR-B in the pulmonary circulation.

Conclusions

In sum, these data elucidate the protective role of endogenous CNP signalling against the development of PH and suggest that targeting NPR-B and NPR-C, respectively, may be of therapeutic benefit in the context of pulmonary vascular disease and right heart remodelling.

COVID-19 Impact Statement

The COVID-19 pandemic and subsequent restrictions had a significant effect on this body of work. The major impact was on the *in vivo* component of the project, as the closure of the lab resulted in the discontinuation and non-commencement of numerous cohorts of animals. Furthermore, colonies were reduced to a maintenance level during the closure period, limiting the availability of transgenic animals when the lab reopened. As a result, the final *in vivo* experiments were completed much later than anticipated, and a planned CNP infusion study to 'rescue' the detrimental phenotype in male endothelial C-type natriuretic peptide knockout (ecCNP$^{-/-}$) mice could not be undertaken.

As social distancing and room occupancy restrictions severely limited access to the animal facility during the initial reopening period, processing of previously generated tissue samples was prioritised during this time. Still, due to the aforementioned disruption to the *in vivo* component of the project, the majority of the frozen and fixed lung and right ventricle (RV) samples only became available very late in the course of the project. As such, it was not possible to complete all planned gene expression studies (the greatest impact being on the ecCNP$^{-/-}$ cohorts), and for those datasets in which changes in gene expression were identified, there was insufficient time to confirm these changes at the protein level with immunoblotting. Likewise, α-smooth muscle actin immunohistochemistry was not completed for male cardiomyocyte C-type natriuretic peptide knockout (cmCNP$^{-/-}$) lungs, and picrosirius red staining (for collagen content) was not completed for RVs from ecCNP$^{-/-}$ and cmCNP$^{-/-}$ mice.

The final component of this project impacted by the pandemic was a planned gene expression study using human pulmonary arterial smooth muscle cells (HPASMCs) isolated from pulmonary arterial hypertension (PAH) patients. Whilst RNA was isolated from PAH (n=3) and non-PAH controls (n=3), these samples were collected in my final few days in the lab, and so further analysis could not be completed.

On a final note, I would like to sincerely thank the BHF for granting me a 5-month extension to the project, which significantly mitigated the disruption caused to my studies.

Acknowledgments

First and foremost, I would like to thank my supervisor Prof. Adrian Hobbs for the opportunity to undertake this project, and for the constant guidance and support that saw it come to fruition. Whenever I felt disheartened, you had an uncanny ability to reinvigorate my drive and passion for science. I will miss our chats, and (maybe) your jokes, but the thing I will miss most is your pragmatic and realistic approach to research.

Secondly, I must acknowledge Dr. Aisah Aubdool, my 'Yoda,' with her great wisdom in all things science, who taught me everything I know about molecular biology. Your firm hand steered (and sometimes dragged) me through the lowest points of my PhD and pushed me up the hill to reach the peaks. You are a great mentor and a fantastic friend Aisah; I hope we can work together again someday in the future.

Dr. Vanessa Lowe, where do I begin? Your echo tips and cowboy tricks made me a much more efficient PhD student. You never failed to lift my spirits with your stories and antics, or to tell me when to shut up when I was moaning too much. Not many people could make a whole day of echo fun, but you somehow managed it. Most of all, you kept me sane, by always reminding me there is a life outside the lab (filled with bikes and cats, apparently).

I must also thank Dr. Cristina Perez Ternero, who always offered help, advice, encouragement, and cake in times of need. The week we spent together doing organ bath experiments was one of the most enjoyable of my PhD (despite all the maths). I would also like to acknowledge Dr. Reshma Baliga and Dr. Tara Scott, who looked after me during my MRes and taught me many of the techniques and skills that are detailed in this thesis, and the remaining members of the Hobbs Lab, Dr. Amie Moyes, Dr. Aemun Salam, and Dr. Michael Preedy, who made my time in the lab so much more enjoyable.

I would also like to acknowledge the staff of the Charterhouse Square BSU, for supporting my research and being a genuine joy to work (and socialise!) with.

Stefan, Shireen, Monja, Kaya, Yaseen, James, and Mason; my friends, and my support group. You were always there when I needed you.

To Mum, Dad, Nan, Kanah, Sam, Natasha, Marcus, and Max. You'll probably never understand how much you each contributed, but I hope you all feel proud.

Finally, I extend by thanks to the British Heart Foundation for making this project possible.

"We got there."

Abbreviations

$[Ca^{2+}]cyt$	cytosolic Ca^{2+} concentration
16OHE1	16α-hydroxyestrone
16OHE2	16α-hydroxyestradiol
2ME2	2-methoxyestradiol
5-HT	5-hydroxytryptamine
6MWD	six-minute walk distance
AA	arachidonic acid
aa	amino acid
ACE	angiotensin converting enzyme
ACh	acetylcholine
ActRIIA/B	activin receptor type IIA/B
ADAM	a disintegrin and metalloprotease
ADMA	asymmetric dimethylarginine
ALK	anaplastic lymphoma kinase
AMPK	adenosine monophosphate-activated protein kinase
Ang II	angiotensin II
ANOVA	analysis of variance
ANP	atrial natriuretic peptide
ARB	angiotensin II receptor blocker
ARRIVE	animal research: reporting of *in vivo* experiments
ASK1	apoptosis signal-regulating kinase 1
BCI	Barts Cancer Institute
Bcl	B-cell lymphoma
BET	bromodomain and extraterminal protein
BMP	bone morphogenetic protein
BNP	brain natriuretic peptide
BMPR2	bone morphogenetic protein receptor 2
bp	base pair
BRD4	bromodomain-containing protein 4
CaMK	calmodulin-dependent protein kinase
cAMP	cyclic adenosine -3',5'-monophosphate
CCB	calcium channel blocker
CCL	chemokine (C-C motif) ligand
cDNA	complementary DNA
cGMP	cyclic guanosine-3',5'-monophosphate
CH	chronic hypoxia
CHD	congenital heart disease
CLD	chronic lung disease
$cmCNP^{-/-}$	cardiomyocyte C-type natriuretic peptide knockout
CNP	C-type natriuretic peptide

CNS	central nervous system
CO	cardiac output
COPD	chronic obstructive pulmonary disease
COX	cyclo-oxygenase
CpcPH	combined pre- and post-capillary pulmonary hypertension
Ct	cycle threshold
CTD	connective tissue disease
CTEPH	chronic thromboembolic pulmonary hypertension
DCA	dichloroacetate
DHEA	dehydroepiandrosterone
DNP	*Dendroaspis* natriuretic peptide
E2	17β-oestradiol
EC_{50}	half maximal effective concentration
$ecCNP^{-/-}$	endothelial C-type natriuretic peptide knockout
ECG	electrocardiogram
ECM	extracellular matrix
EC	endothelial cell
ELISA	enzyme-linked immunosorbent assay
E_{max}	maximum effect
EMT	endothelial-to-mesenchymal transition
ENG	endoglin
eNOS	endothelial nitric oxide synthase
ERA	endothelin receptor antagonist
ECM	extracellular matrix
ERK	extracellular signal-regulated kinase
ET	endothelin
ET_A	endothelin receptor A
ET_B	endothelin receptor B
EtOH	ethanol
FAK	focal adhesion kinase
FAO	fatty acid oxidation
FGF-2	fibroblast growth factor
FKBP12	FK-binding protein-12
GATA4	GATA binding protein 4
$gbCNP^{-/-}$	global CNP knockout
GC	guanylyl cyclase
GIRK	G-protein-gated inwardly rectifying potassium channel
GERD	gastroesophageal reflux disease
GPCR	G-protein coupled receptor
GTP	guanosine-5'-triphosphate
GWAS	genome-wide association study
H2R	H2 receptor

H2RA	H2R antagonist
HF	heart failure
HFpEF	heart failure with preserved ejection fraction
HIF	hypoxia-inducible factor
HPASMC	human pulmonary artery/arterial smooth muscle cell
HPV	hypoxic pulmonary vasoconstriction
HPAEC	human pulmonary artery endothelial cell
HR	heart rate
ICAM-1	intercellular adhesion molecule 1
IL	interleukin
IP	prostacyclin receptor
IPAH	idiopathic pulmonary arterial hypertension
IpcPH	isolated post-capillary pulmonary hypertension
KO	knockout
LHD	left heart disease
LOX	lysyl oxidase
LV	left ventricle, left ventricular
LVEF	left ventricular ejection fraction
MABP	mean arterial blood pressure
MAPK	mitogen-activated protein kinase
MCT	monocrotaline
MEF	myocyte enhancer factor
MEK	mitogen-activated protein kinase kinase
MHC	myosin heavy chain
MMP	matrix metalloproteinase
mPAP	mean pulmonary artery pressure
mRNA	messenger RNA
mTOR	mechanistic target of rapamycin
MI	myocardial infarction
n	number of samples
NEP	neutral endopeptidase, neprilysin
NFAT	nuclear factor of activated T-cells
NF-κB	nuclear factor kappa-light-chain-enhancer of activated B cells
NmOx	normoxic
NO	nitric oxide
NPR	natriuretic peptide receptor
NPR-C$^{-/-}$	global NPR-C knockout
Nrf2	nuclear factor erythroid 2-related factor 2
NSAID	non-steroidal anti-inflammatory drug
NT	N-terminal
P	probability value
p21	cyclin-dependent kinase inhibitor 1

p-Smad2/3	phosphorylated Smad2/3
PAB	pulmonary artery banding
PAC	pulmonary artery compliance
PAEC	pulmonary artery endothelial cell
PAH	pulmonary arterial hypertension
PAP	pulmonary artery pressure
PARP	poly [adenosine diphosphate-ribose] polymerase
PASMC	pulmonary artery/arterial smooth muscle cell
PAT	pulmonary acceleration time
PAWP	pulmonary artery wedge pressure
PBS	phosphate-buffered saline
PCNA	proliferating cell nuclear antigen
PCR	polymerase chain reaction
PDE	phosphodiesterase
PDGF	platelet-derived growth factor
PDGFR	platelet-derived growth factor receptor
PDH	pyruvate dehydrogenase
PDK	pyruvate dehydrogenase kinase
PEA	pulmonary endarterectomy
PGI_2	prostacyclin
PH	pulmonary hypertension
Phe	phenylephrine
PLB	phospholamban
PKA	protein kinase A
PKC	protein kinase C
PKG	protein kinase G
PLC	phospholipase C
PPARγ	peroxisome proliferator-activated receptor-γ
PPHN	persistent PH of the new-born
PVD	pulmonary vascular disease
PVR	pulmonary vascular resistance
PVT	pulmonary vascular tone
PW	pulsed wave
RAP	right atrial pressure
RAAS	renin-angiotensin-aldosterone system
RHRR	right heart reverse remodelling
RPL-19	ribosomal protein L19
ROCK	rho-associated protein kinase
ROS	reactive oxygen species
RTK	receptor tyrosine kinase
RT-qPCR	reverse transcription quantitative polymerase chain reaction
RV	right ventricle, right ventricular

RV/(LV+S)	right ventricle to left ventricle plus septum ratio
RVEF	right ventricular ejection fraction
RVFWd	end-diastolic right ventricular free wall thickness
RVH	right ventricular hypertrophy
RVP	right ventricular pressure
RVSP	right ventricular systolic pressure
SA-HRP	Streptavidin-horseradish peroxidase
SEM	standard error of the mean
SERCA2a	sarco/endoplasmic reticulum Ca^{2+}-ATPase 2a
sGC	soluble guanylyl cyclase
SiMFi	singular millimetric fibrovascular lesion
SIRT3	sirtuin 3
Smad	suppressor of mothers against decapentaplegic
SNP	single nucleotide polymorphism
SNS	sympathetic nervous system
SR	sarcoplasmic reticulum
SSc	systemic sclerosis
SSRI	serotonin reuptake inhibitor
SV	stroke volume
t-Smad2/3	total Smad2/3
TAE	tris-acetate-ethylenediaminetetraacetic acid
TAPSE	tricuspid annular plane systolic excursion
TGF	transforming growth factor
TGF-βR2	transforming growth factor-β receptor 2
TIMP	tissue inhibitor of metalloproteinase
TnI	troponin I
TPH1	tryptophan hydroxylase 1
TV	tricuspid valve
UBC	ubiquitin C
UCP2	uncoupling protein 2
V/Q	ventilation/perfusion
VCAM-1	vascular cell adhesion molecule 1
VEGF	endothelial cell
VEGFR-2	vascular endothelial growth factor receptor 2
VIP	vasoactive intestinal peptide
VSMC	vascular smooth muscle cell
vWF	von Willebrand factor
WT	wildtype
WU	Wood units
α-SMA	α-smooth muscle actin
β-ME	β-mercaptoethanol

Table of Contents

CHAPTER I: INTRODUCTION 21

1.1 Overview 22
1.2 Classification of pulmonary hypertension 23
1.3 Pathophysiology of pulmonary hypertension 26
1.3.1 Overview 26
1.3.2 Endothelial dysfunction 26
1.3.3 Vascular remodelling 30
1.3.4 Right ventricular pressure overload 40
1.4 Pharmacological treatment of pulmonary hypertension 44
1.4.1 Pulmonary arterial hypertension 44
1.4.2 Groups 2, 3 and 5 44
1.4.3 Chronic thromboembolic pulmonary hypertension 45
1.4.4 Challenges 48
1.5 Novel pharmacological targets in pulmonary hypertension 49
1.5.1 Bone morphogenetic protein receptor 2 50
1.5.2 Serotonin 51
1.5.3 Apelin 52
1.5.4 Vasoactive intestinal peptide 52
1.5.5 Oestrogens 53
1.5.6 Dehydroepiandrosterone 54
1.5.7 Receptor tyrosine kinases 55
1.5.8 Mechanistic target of rapamycin 56
1.5.9 Rho-kinase family 56
1.5.10 Immunomodulation 57
1.5.11 Elafin 57
1.5.12 Oxidative stress 58
1.5.13 Altered metabolism 59
1.5.14 Systemic metabolism 60
1.5.15 Epigenetics 61
1.5.16 Neurohormones 62
1.5.17 Histamine 63
1.6 Natriuretic peptides 64
1.6.1 C-type natriuretic peptide 64
1.7 Natriuretic peptide receptor signalling 67
1.7.1 Natriuretic peptide receptor B 67
1.7.2 Natriuretic peptide receptor C 68
1.7.3 Natriuretic peptide inactivation 69

1.8 Prospective role for CNP in pulmonary hypertension 71
1.9 Working hypothesis and specific aims 73

CHAPTER II: METHODS 74

2.1 Genetically modified animals 75
2.1.1 Generation 75
2.1.2 Genotyping 75
2.1.3 Tamoxifen administration 76
2.2 Sugen + hypoxia model 81
2.2.1 Overview 81
2.2.2 Sugen preparation 81
2.3 Administration of CNP 83
2.3.1 Minipump preparation 83
2.3.2 Implantation 83
2.4 Echocardiography 84
2.5 Invasive pressure measurements 90
2.5.1 Right ventricular pressure 90
2.5.2 Systemic blood pressure 90
2.5.3 Analysis 91
2.6 Plasma and tissue collection 93
2.6.1 Plasma collection 93
2.6.2 Tissue weights and processing 93
2.6.3 Tissue fixation 93
2.7 Pulmonary artery organ bath pharmacology 94
2.8 Molecular biology 97
2.8.1 Natriuretic peptide and disease-related gene expression 97
2.8.2 Natriuretic peptide bioassays 107
2.9 Immunohistochemistry 108
2.9.1 Assessment of small artery muscularisation 108
2.9.2 Assessment of RV fibrosis 108
2.10 Statistical analysis 109

CHAPTER III: RESULTS I 110

3.1 Overview 111
3.2 Pulmonary vascular reactivity to CNP and cANF$^{4-23}$ is blunted in SuHx mice 112
3.3 Cardiopulmonary expression of CNP and NPRs is altered in SuHx mice 119
3.4 Global CNP deletion has sex-specific effects on experimental PH 122

CHAPTER IV: RESULTS II 125

4.1 Overview 126

4.2 Ablation of endothelial CNP accentuates experimental PH in male mice 127
4.3 Loss of cardiomyocyte CNP does not alter experimental RVH 131
4.4 Global deletion of NPR-C exacerbates RVH and fibrosis in male SuHx mice 136

CHAPTER V: RESULTS III 141

5.1 Overview 142
5.2 Exogenous CNP reverses established experimental PH via NPR-B-signalling 143
5.3 Pulmonary haemodynamics in CNP-treated WT and NPR-C$^{-/-}$ SuHx mice 146
5.4 Cardiac function in CNP-treated WT and NPR-C$^{-/-}$ SuHx mice 148
5.5 CNP infusion tempers the expression of remodelling-associated genes 153
5.6 Principal findings 156

CHAPTER VI: DISCUSSION 158

6.1 Overview and key findings 159
6.2 Cardiopulmonary CNP/NPR expression is altered in PH 160
6.3 CNP regulates pulmonary vascular tone 162
6.4 Endogenous CNP protects against PH 165
6.5 CNP protects against remodelling in the RV 167
6.6 CNP/NPR-C modulate cardiac function in PH 171
6.7 Cardiopulmonary sex differences in CNP signalling 173
6.8 The therapeutic potential of CNP in PH 175
6.9 CNP therapeutic agents 178
6.10 Limitations of the present study, and future work 181
6.11 Limitations of the SuHx mouse model 182
6.12 Limitations of echocardiography 184
6.13 Conclusions 186

BIBLIOGRAPHY 188

APPENDIX 277

List of Figures

Figure 1: Endothelial regulation of vascular tone 27

Figure 2: Overview of the molecular mechanisms involved in vascular remodelling 32

Figure 3: Summary of pulmonary arterial remodelling 33

Figure 4: The response of the right ventricle to chronic pressure overload 43

Figure 5: Current therapeutic targets in pulmonary arterial hypertension 47

Figure 6: Amino acid structures of the natriuretic peptides 66

Figure 7: Schematic representation of CNP-receptor signalling 70

Figure 8: Experimental time-course for the SU5416/hypoxia model of PH 82

Figure 9: Assessment of pulmonary artery function using echocardiography 85

Figure 10: Assessment of left ventricular function using echocardiography 86

Figure 11: Assessment of right ventricular structure using echocardiography 87

Figure 12: Assessment of right ventricular function using echocardiography 88

Figure 13: Haemodynamic measurements 92

Figure 14: Concentration-response curves to CNP in pulmonary arteries from male and female NmOx and SuHx mice 113

Figure 15: Concentration-response curves to $cANF^{4-23}$ in pulmonary arteries from male and female NmOx and SuHx mice 114

Figure 16: Concentration-response curves to ACh in pulmonary arteries from male and female NmOx and SuHx mice 116

Figure 17: Concentration-response curves to Phe in pulmonary arteries from male and female NmOx and SuHx mice 117

Figure 18: Expression of CNP, NPR-B and NPR-C in the lungs of animals with experimental PH 120

Figure 19: Expression of CNP, NPR-B and NPR-C in the RV of animals with experimental PH 121

Figure 20: The effect of global CNP deletion on cardiopulmonary and systemic arterial pressure in experimental PH..... 123

Figure 21: The effect of global CNP deletion on RV hypertrophy following pressure overload... 124

Figure 22: The effect of endothelial CNP deletion on cardiopulmonary and systemic arterial pressure in experimental PH..... 128

Figure 23: The effect of endothelial CNP deletion on pulmonary vascular remodelling in experimental PH..... 129

Figure 24: The effect of endothelial CNP deletion on RV hypertrophy following pressure overload 130

Figure 25: The effect of cardiomyocyte CNP deletion on cardiopulmonary and systemic arterial pressure in experimental PH..... 132

Figure 26: The effect of cardiomyocyte CNP deletion on RV hypertrophy following pressure overload 133

Figure 27: The effect of cardiomyocyte CNP depletion on remodelling-associated gene expression in the right heart of male mice following pressure overload..... 134

Figure 28: The effect of cardiomyocyte CNP depletion on pulmonary vascular remodelling in female mice with experimental PH 135

Figure 29: The effect of global NPR-C deletion on cardiopulmonary and systemic arterial pressure in experimental PH..... 137

Figure 30: The effect of global NPR-C deletion on pulmonary vascular remodelling in experimental PH 138

Figure 31: The effect of global NPR-C deletion on RV hypertrophy in experimental PH 139

Figure 32: The effect of global NPR-C depletion on the development of RV fibrosis following pressure overload 140

Figure 33: The effect of CNP infusion on cardiopulmonary pressure, systemic arterial pressure, RV hypertrophy, and RV fibrosis in male WT and NPR-C$^{-/-}$ mice with experimental PH..... 144

Figure 34: Plasma natriuretic peptide levels in male WT and NPR-C$^{-/-}$ mice with experimental PH 145

Figure 35: The effect of CNP infusion on pulmonary artery function in male WT and NPR-C$^{-/-}$ mice with experimental PH 147

Figure 36: The effect of CNP infusion on cardiopulmonary structure and function in male WT and NPR-C$^{-/-}$ mice with experimental PH 149

Figure 37: The effect of CNP infusion on global heart function in male WT and NPR-C$^{-/-}$ mice with experimental PH 150

Figure 38: The effect of CNP infusion on remodelling-associated gene expression in the lungs of male WT mice with experimental PH 154

Figure 39: The effect of CNP infusion on remodelling-associated gene expression in the right heart of male WT mice with experimental PH 155

Figure 40: Summary of key findings 187

Supplementary Figures

Supplementary Figure 1: Comparison of housekeeping gene mRNA expression in NmOx and SuHx mice 278

Supplementary Figure 2: Expression of CNP, NPR-B and NPR-C in the lungs of animals with experimental PH 279

Supplementary Figure 3: Expression of CNP, NPR-B and NPR-C in the RV of animals with experimental PH 280

Supplementary Figure 4: The effect of global CNP deletion on the development of experimental PH 281

Supplementary Figure 5: The effect of endothelial CNP deletion on the development of experimental PH 282

Supplementary Figure 6: The effect of cardiomyocyte CNP depletion on the development of experimental PH 283

Supplementary Figure 7: The effect of global NPR-C deletion on the development of experimental PH 284

List of Tables

Table 1: Clinical classification of pulmonary hypertension 24

Table 2: Haemodynamic classification of pulmonary hypertension 25

Table 3: Drugs approved for the treatment of pulmonary arterial hypertension 46

Table 4: Nucleic acid sequences of primers used in genotyping 77

Table 5: Polymerase chain reaction components 78

Table 6: Polymerase chain reaction protocols 79

Table 7: Summary of parameters assessed using echocardiography 89

Table 8: Krebs Ringer 1X working solution 96

Table 9: Reverse transcription reaction components 100

Table 10: Thermal cycler conditions for reverse transcription 101

Table 11: qPCR reaction components 102

Table 12: Thermal cycler conditions for qPCR reactions 103

Table 13: Primers used for qPCR – natriuretic peptide signalling 104

Table 14: Primers used for qPCR – vascular disease markers 105

Table 15: Primers used for qPCR – cardiac disease markers 106

Table 16: CNP-induced relaxation of mouse isolated pulmonary arteries 115

Table 17: $cANF^{4-23}$-induced relaxation of mouse isolated pulmonary arteries 115

Table 18: ACh-induced relaxation of mouse isolated pulmonary arteries 118

Table 19: Phe-induced contraction of mouse isolated pulmonary arteries 118

Table 20: Cardiopulmonary function in NPR-$C^{-/-}$ mice 151

Table 21: Global heart function in NPR-$C^{-/-}$ mice 152

Table 22: Summary of CNP/NPR expression data 157

Table 23: Summary of CNP/NPR-C knockout data 157

Table 24: Summary of CNP infusion data 157

Chapter I: Introduction

1.1 Overview

Pulmonary hypertension (PH) is a multi-factorial condition driven by rising blood pressure within the pulmonary circulation (McLaughlin et al., 2009; Hoeper et al., 2013b). The overarching paradigm is that endothelial dysfunction and obstructive remodelling of the pulmonary vascular tree produces a gradual rise in pulmonary vascular resistance (PVR) and pulmonary artery pressure (PAP). The progressive increase in afterload (the pressure the heart must overcome to propel blood into the circulation with each ventricular contraction) forces the right ventricle (RV) into a state hypertrophic remodelling, culminating in functional decline, heart failure, and death (Humbert et al., 2019).

PH is uncommon, with a global prevalence of ~1% (rising to 10% in individuals aged more than 65 years), but accompanied by significant morbidity (Hoeper et al., 2016a). Initially, patients are debilitated on exertion by dyspnoea, fatigue, angina, and syncope, however in advanced disease these symptoms are also present at rest (Galiè et al., 2016). Currently, PH management is limited to optimisation of symptoms with vasodilators. Critically, for pulmonary arterial hypertension (PAH), five-year survival is approximately 60% (Badesch et al., 2010; Gall et al., 2017). Consequently, there is a desperate need for new therapies that address pulmonary vascular remodelling and cardiac dysfunction.

C-type natriuretic peptide (CNP) is an endogenous signalling molecule that plays an important role in systemic cardiovascular homeostasis, including regulation of vascular tone, smooth muscle and endothelial cell proliferation, and cardiac hypertrophy and fibrosis (Moyes and Hobbs, 2019). Plasma CNP levels correlate with PAP (Palmer et al., 2009) and the receptors for this peptide are highly expressed in the RV (Kim et al., 1999), alluding to an important role for CNP in the regulation of cardiopulmonary haemodynamics and PH.

Akin to some of the approved therapeutics for PH, CNP increases intracellular cyclic guanosine-3',5'-monophosphate (cGMP) levels by acting on natriuretic peptide receptor (NPR)-B (Potter et al., 2006), but may have additional anti-remodelling and cardioprotective actions through the activation of a second cognate receptor, NPR-C (Moyes et al., 2014, 2020). However, the therapeutic potential of CNP in PH has yet to be fully explored.

1.2 Classification of pulmonary hypertension

PH is an umbrella term for a group of aetiologically unique clinical entities, each having a distinct pathophysiology (Galiè et al., 2016; Simonneau et al., 2019). On this basis, PH is classified into five clinically recognised groups, which are listed in ***Table 1***. Proper classification of PH is critical, as each presentation has a different management strategy which may be of harm to other clinical groups (Simonneau et al., 2019).

Haemodynamic characterisation is a defining factor for all PH clinical groups (***Table 2***). A mean pulmonary arterial pressure (mPAP) of ≥20 mmHg at rest, determined by right heart catheterisation, is essential for any PH diagnosis (Hatano and Strasser, 1975; Hoeper et al., 2013b). PAP elevation can result from structural changes in small pulmonary arteries (i.e. isolated pre-capillary disease), or may be due to backwards transmission of post-capillary pressure elevation, such is the case in left heart disease (LHD)-PH (Galiè et al., 2016). Post-capillary PH is delineated by a pulmonary artery wedge pressure (PAWP; an estimate of left atrial pressure) of >15 mmHg, measured by inflating a balloon-tipped, multi-lumen catheter to occlude a branch of the pulmonary artery (Viray et al., 2020). In the absence of elevated PAWP, PVR ([mPAP – PAWP]/CO) of ≥3 Wood units (WU) is used as a confirmatory measure of isolated pulmonary vascular disease. In rare cases, combined pre- and post-capillary PH (CpcPH) may be present (Simonneau et al., 2019).

Table 1: Clinical classification of pulmonary hypertension

1. **Pulmonary Arterial Hypertension (PAH)**
    - 1.1 Idiopathic PAH
    - 1.2 Heritable PAH
    - 1.3 Drug and toxin induced
    - 1.4 Associated with:
        - 1.4.1 Connective tissue disease
        - 1.4.2 HIV infection
        - 1.4.3 Portal hypertension
        - 1.4.4 Congenital heart diseases
        - 1.4.5 Schistosomiasis
    - 1.5 PAH long-term responders to calcium channel blockers
    - 1.6 PH with overt features of venous/capillaries (PVOD/PCH) involvement
    - 1.7 Persistent PH of the new-born (PPHN)
2. **Pulmonary hypertension due to left heart disease**
    - 2.1 PH due to heart failure with preserved LVEF
    - 2.2 PH due to heart failure with reduced LVEF
    - 2.3 Valvular disease
    - 2.4 Congenital/acquired cardiovascular conditions leading to post-capillary PH
3. **Pulmonary hypertension due to lung diseases and/or hypoxia**
    - 3.1 Obstructive pulmonary disease
    - 3.2 Restrictive lung disease
    - 3.3 Other lung disease with mixed restrictive/obstructive pattern
    - 3.4 Hypoxia without lung disease
    - 3.5 Developmental lung disorders
4. **PH due to pulmonary artery obstructions**
    - 4.1 Chronic thromboembolic PH
    - 4.2 Other pulmonary artery obstructions
5. **Pulmonary hypertension with unclear multifactorial mechanisms**
    - 5.1 Hematologic disorders
    - 5.2 Systemic and metabolic disorders
    - 5.3 Others
    - 5.4 Complex congenital heart disease

PVOD, pulmonary veno-occlusive disease; PCH, pulmonary capillary haemangiomatosis; LVEF, left ventricular ejection fraction.

Table 2: Haemodynamic classification of pulmonary hypertension

Definition	PH Group	mPAP (mmHg)	PAWP (mmHg)	PVR (WU)
Pre-capillary PH	1, 3, 4, 5	>20	≤15	≥3
Isolated post-capillary PH (IpcPH)	2 and 5	>20	>15	<3
Combined pre- and post-capillary PH (CpcPH)	2 and 5	>20	>15	≥3

mPAP, mean pulmonary arterial pressure; PAWP, pulmonary arterial wedge pressure; PVR, pulmonary vascular resistance; WU, Wood units.

1.3 Pathophysiology of pulmonary hypertension

1.3.1 Overview

The heterogeneous origins of PH produce a variable pathophysiology influenced by genetic predisposition and environmental factors, such as hypoxia. However, there are three pathophysiological hallmarks common to all clinical groups: persistent vasoconstriction, vascular remodelling, and RV dysfunction (Shimoda and Laurie, 2013). An amalgamation of cellular and molecular mechanisms contribute to this disease, including vasoconstriction, proliferation, inflammation, coagulation, apoptosis, autoimmunity, and cell-cell and cell-matrix interactions (Schermuly et al., 2011; Tuder et al., 2013).

1.3.2 Endothelial dysfunction

1.3.2.1 *Increased vascular tone*

Vascular tone, the contractile activity of vascular smooth muscle cells (VSMCs) in the walls of small arteries and arterioles, is the major determinant of the resistance to blood flow through the circulation (Barnes and Liu, 1995; Goldenberg and Kuebler, 2015). The pulmonary endothelium is highly metabolically active and liberates various vasoactive compounds such as nitric oxide (NO), prostacyclin (PGI_2), and endothelin (ET)-1, that influence PVR by altering pulmonary vascular tone (PVT; Celermajer et al., 1994; Liu and Barnes, 1994; ***Figure 1***). In comparison to the systemic circulation, pulmonary arterioles have such remarkably low basal tone (Goldenberg and Kuebler, 2015) that inhaled or intravenous vasodilators have little effect on PAP in healthy individuals (Fritts et al., 1958; Bueltmann et al., 2009; Yin et al., 2009).

Endothelial injury by genetic and/or environmental factors (e.g. hypoxia, shear stress, chronic low-grade inflammation) has long been recognised as a precipitating event in PH pathogenesis (Humbert et al., 2004, 2019). One hallmark of the subsequent dysfunction is excessive and persistent vasoconstriction, which may account for the initial rise in PVR (Budhiraja et al., 2004; Huertas et al., 2018).

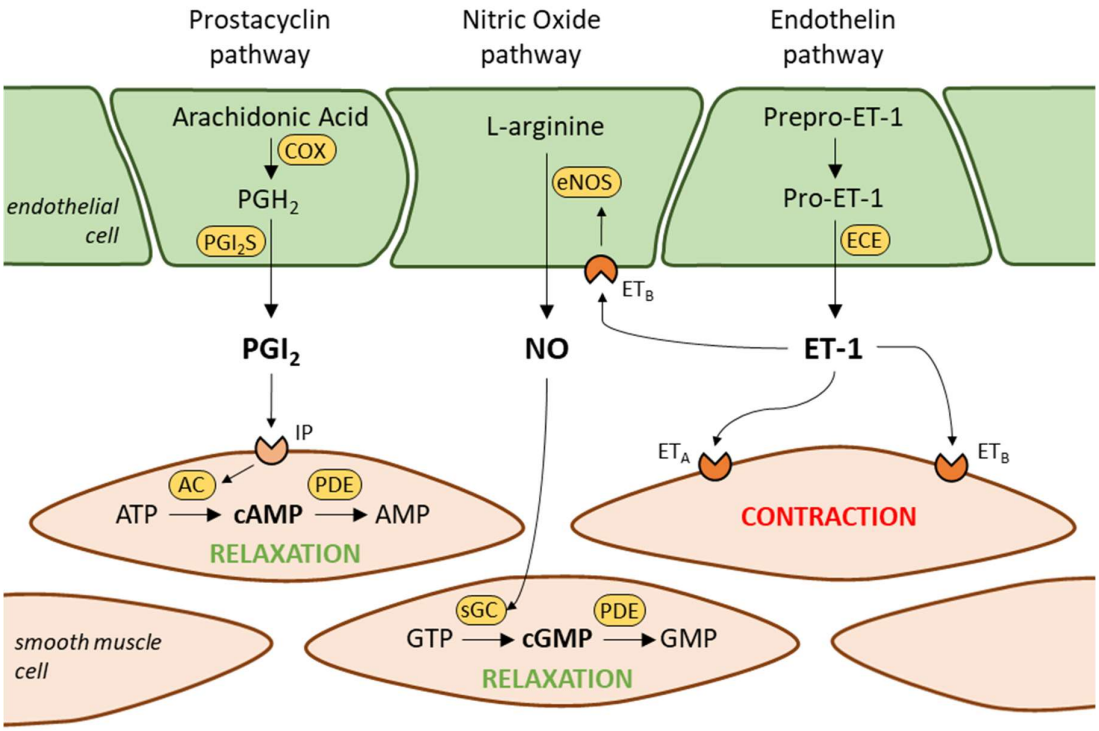

Figure 1: Endothelial regulation of vascular tone

The major pathways involved in the regulation of pulmonary vascular tone. eNOS, endothelial NO synthase; NO, nitric oxide, sGC, soluble guanylyl cyclase; GTP, guanosine triphosphate; cGMP, cyclic guanosine monophosphate; GMP, guanosine monophosphate; PDE, phosphodiesterase; COX, cyclooxygenase; PGH_2, prostaglandin H2; PGI_2S, prostacyclin synthase; PGI_2, prostacyclin; IP, PGI_2 receptor; AC, adenylyl cyclase; ATP, adenosine triphosphate; cAMP, cyclic adenosine monophosphate; AMP, adenosine monophosphate; ECE, endothelin-converting enzyme, ET-1, endothelin-1; ET_A, endothelin receptor A; ET_B, endothelin receptor B.

1.3.2.2 *Nitric oxide pathway*

NO, a diatomic free radical released constitutively from the endothelium in response to pulsatile flow and shear stress (Goldenberg and Kuebler, 2015), is essential for upholding basal vessel tone. This molecule freely diffuses into the underlying VSMCs to activate soluble guanylyl cyclase (sGC), increasing levels of the second messenger cGMP. The subsequent activation of protein kinase G (PKG) initiates several downstream cascades culminating in decreased cytosolic Ca^{2+} ($[Ca^{2+}]_{cyt}$) and vasodilatation (Goldenberg and Kuebler, 2015; Lo et al., 2018). NO also inhibits VSMC proliferation through both cGMP-dependant (Lehners et al., 2018) and cGMP-independent mechanisms (Kibbe et al., 2000; Bauer et al., 2001; Zuckerbraun et al., 2007). Critically, targeted disruption of the murine endothelial nitric oxide synthase (eNOS) gene increases PVR (Steudel et al., 1997), an effect which can be replicated in healthy humans with pharmacological eNOS inhibition (Stamler et al., 1994).

Despite a compensatory upregulation of sGC in the pulmonary arteries of subjects with PH (Schermuly et al., 2008), the overall function of the enzyme is limited by decreased NO bioavailability. Indeed, eNOS expression is dampened in the lungs of PAH patients (Giaid and Saleh, 1995). Also, smoking, an important risk factor for both LHD and chronic lung disease (CLD), has a similar effect on pulmonary arterial eNOS expression (Barberà et al., 2001). Levels of asymmetric dimethylarginine (ADMA), an endogenous competitive inhibitor of NOS, are elevated in individuals with chronic thromboembolic PH (CTEPH), idiopathic PAH (IPAH), congenital heart disease (CHD)-PAH, systemic sclerosis (SSc)-PAH, and PAH related to sickle cell disease (Gorenflo et al., 2001; Kielstein et al., 2005; Pullamsetti et al., 2005; Skoro-Sajer et al., 2007; Dimitroulas et al., 2008; Landburg et al., 2008). Of note, ADMA levels predict survival in CTEPH patients (Skoro-Sajer et al., 2007).

NO bioavailability may be further reduced by the increased production of reactive oxygen species (ROS), another hallmark of endothelial dysfunction. Oxidation converts NO to the less acutely active nitrite and nitrate (Crosswhite and Sun, 2010). In addition, superoxide, a major player in oxidative stress, reacts with NO, forming peroxynitrite, which in turn oxidises and uncouples eNOS (Laursen et

al., 2001). Another consequence of oxidative stress is oxidation of the sGC heme-moiety, rendering the enzyme less responsive to NO (Dasgupta et al., 2015). Finally, increased expression of phosphodiesterase (PDE)-5 in the pulmonary arteries (Murray et al., 2002) may accelerate cGMP breakdown, further limiting NO-evoked vasodilatation.

1.3.2.3 *Prostacyclin pathway*

Eicosanoids are fatty acid derivatives formed when arachidonic acid (AA) is metabolised by cyclo-oxygenase (COX) enzymes (Goldenberg and Kuebler, 2015). PGI_2 is the primary eicosanoid produced by endothelial cells (ECs), and like NO, is a well-defined potent endothelium-dependent vasodilator (Lo et al., 2018). PGI_2 selectively binds and activates a G-protein coupled receptor (GPCR), known as the prostacyclin or IP receptor. Upon activation of this receptor, adenylyl cyclase is stimulated to produce cyclic adenosine -3',5'-monophosphate (cAMP), with downstream effects mediated by protein kinase A (PKA; Mitchell et al., 2008). Like PKG, PKA mediates vasodilatation by lowering $[Ca^{2+}]_{cyt}$ (Morgado et al., 2012). PGI_2 also has anti-proliferative effects on human pulmonary artery smooth muscle cells (HPASMCs), ascribed to elevation of cAMP and activation of peroxisome proliferator-activated receptor-γ (PPARγ; Wharton et al., 2000; Clapp et al., 2002; Falcetti et al., 2010). In PAH patients, pulmonary expression of prostacyclin synthase is decreased and urinary markers of PGI_2 are diminished (Christman et al., 1992; Tuder et al., 1999).

1.3.2.4 *Endothelin pathway*

Endothelin is a vasoconstrictive peptide that exerts its activity via two GPCRs expressed on VSMCs, endothelin receptor A (ET_A) and endothelin receptor B (ET_B; Seo et al., 1994). When activated, these receptors increase $[Ca^{2+}]_{cyt}$ by stimulating phospholipase C (PLC), resulting in vasoconstriction (Pollock et al., 1995). Concurrent $ET_{A/B}$ blockade is necessary to completely abolish ET-1-mediated vasoconstriction, suggesting crosstalk occurs between the two (Sauvageau et al., 2007). Additionally, activation of these receptors has also been shown to induce HPASMC proliferation *in vitro* and arterial hyperplasia *in vivo* (Davie et al., 2002; Dao et al., 2006). In human pulmonary arteries, ET_A is more highly expressed in

larger vessels, though the abundance of ET_B increases in arterioles (Davie et al., 2002). Notably, ET_B is also expressed on ECs (Migneault et al., 2005) where, in a role unique to the lungs, it functions as a clearance receptor (Fukuroda et al., 1994; Kelland et al., 2010). Activation of endothelial ET_B also facilitates cross-talk with other vasomotor signalling pathways, by enhancing NO and PGI_2 release (Hirata et al., 1993; Lal et al., 1996).

Since ET-1 expression is downregulated by NO (Boulanger and Luscher, 1990), this peptide may be particularly potent in dysfunctional blood vessels with blunted NO production. Indeed, heightened ET-1 levels are reported in the lungs and circulation of subjects with PAH, CTEPH, and CLD-PAH (Giaid et al., 1993; Yamakami et al., 1997; Rubens et al., 2001; Bauer et al., 2002). ET-1 may further suppress NO production, as dual $ET_{A/B}$ blockade boosts exhaled and urinary NO metabolites to control levels in PAH patients (Girgis et al., 2005).

1.3.2.5 *Enhanced platelet aggregation and inflammation*

Hypercoagulability, another consequence of endothelial dysfunction, is also noted in some IPAH patients (Tournier et al., 2010). Furthermore, levels of von Willebrand factor (vWF), an endothelium-derived glycoprotein essential for platelet adhesion to subendothelial collagen, are increased in IPAH and correlate negatively with survival (Pfeffer et al., 2000). Crucially, dysfunctional ECs adopt a pro-inflammatory phenotype, characterised by increased surface expression of adhesion molecules (E-selectin, intercellular adhesion molecule 1, ICAM-1 and vascular cell adhesion molecule 1, VCAM-1; Le Hiress et al., 2015), and excessive release of cytokines, including interleukin (IL)-6 and IL-1β; Humbert et al., 2019), chemokines (Le Hiress et al., 2015) and growth factors (e.g. fibroblast growth factor, (FGF)-2; Izikki et al., 2009). Altered expression of vasoactive mediators may also contribute to these processes; ET-1 is pro-aggregatory and pro-inflammatory (Galié et al., 2004), whilst NO and PGI_2 have anti-thrombotic and anti-inflammatory properties (Vane, 1971; Moncada et al., 1977; Gkaliagkousi and Ferro, 2011).

1.3.3 Vascular remodelling

Though much remains to be understood, it is increasing recognised that the genetic and environmental factors driving PH pathogenesis induce or accelerate

irreversible remodelling of the pulmonary vascular bed by dysregulating growth factors, ion channels, hormones, and cytokines. Complex signalling cascades culminate in altered transcription factor activity and gene expression, inducing and sustaining a pro-inflammatory, pro-proliferative, anti-apoptotic, and de-differentiated phenotype (Humbert et al., 2019). These pathways are briefly summarised in ***Figure 2***.

1.3.3.1 *Vessel involvement*

PH is primarily attributed to proliferative lesions occurring in small muscular-type arteries, affecting all vessel layers (medial hypertrophy/hyperplasia, intimal and adventitial fibrosis) and resulting in a loss of cross-sectional area (Tuder, 2009; ***Figure 3***). There is also involvement of the pre-capillary arterioles, through abnormal muscularisation, perivascular inflammation, and obliteration (Rabinovitch, 2012). Whilst these changes account for the primary influence on PVR, fibrosis of the large proximal pulmonary arteries and the ensuing reduction in compliance (i.e. inability to deform under loading; Ghio et al., 2015), also contribute to RV pressure overload (Lammers et al., 2012).

A growing body of evidence suggests that pulmonary venous remodelling is present in all forms of PH (Dorfmüller et al., 2007, 2014; Overbeek et al., 2008b; Humbert et al., 2019). In some cases the trigger is obvious, e.g. the chronically elevated post-capillary pressure in LHD-PH (Fayyaz et al., 2018) or parenchymal inflammation and destruction in CLD-PH (Barberà, 2013; Agrawal et al., 2016). In PAH and CTEPH, the mechanisms of post-capillary involvement are less clear, as the venous compartment should be protected from increased arteriolar pressure by the capillaries (Dorfmüller et al., 2014). Recent findings suggest the high pressure in the pulmonary arteries may facilitate shunting to bronchial arteries and pulmonary veins through anastomotic connections, leading to shear stress and remodelling in these vessels (Tio et al., 2013; Dorfmüller et al., 2014; Galambos et al., 2016; Ghigna et al., 2016).

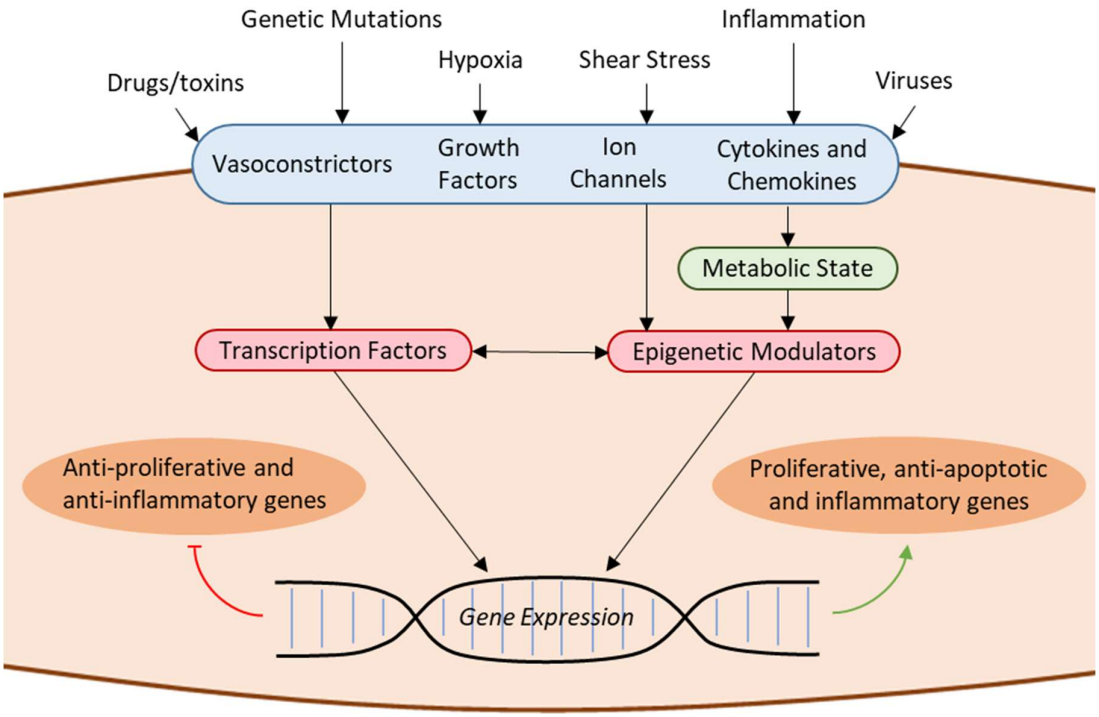

Figure 2: Overview of the molecular mechanisms involved in vascular remodelling

Growth factors, ion channels, hormones and cytokines activate classical signalling pathways and downstream transcriptional factors, leading to altered gene expression and vascular remodelling. Metabolic dysregulation will affect levels of the metabolites required by chromatin-modifying enzymes to modify both histones and DNA. Epigenetic dysregulation may lead to crosstalk with transcription factors.

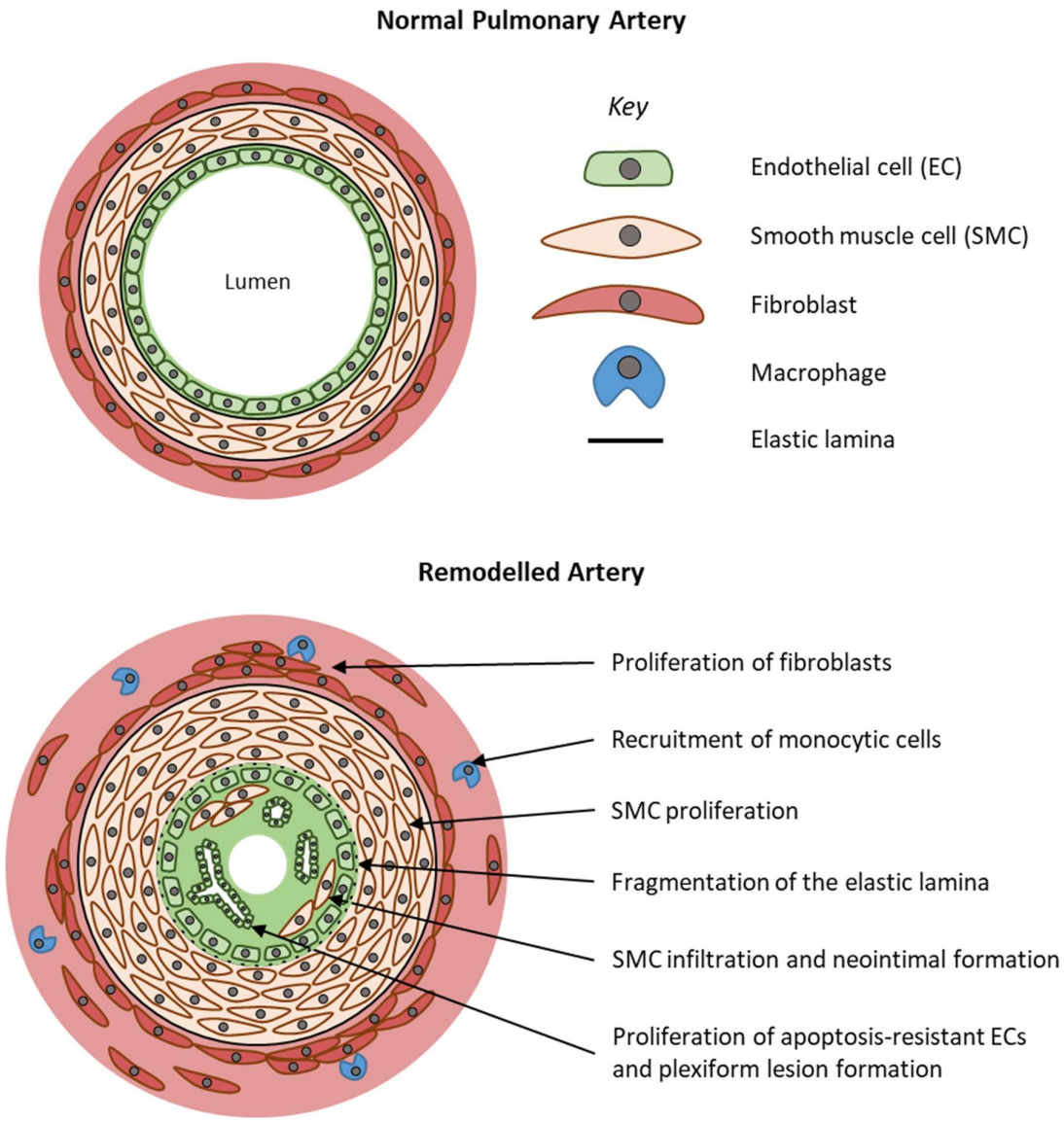

Figure 3: Summary of pulmonary arterial remodelling

The vessel lumen is occluded due to thickening of the pulmonary arteriolar wall. Medial smooth muscle cells begin to proliferate and invade the endothelial cell layer, forming a neointima. Immune cells migrate into the adventitia and resident fibroblasts begin to proliferate. Plexiform lesions, capillary-like channels of proliferating endothelial cells, are mainly associated with PAH but also present in other severe cases of PH.

1.3.3.2 *Intimal remodelling and vessel loss*

In healthy individuals, the intima exists as an endothelial monolayer. In PAH patients, the fractional thickness of this layer may increase as much as threefold, equating to a 40-fold increase in PVR (Stacher et al., 2012; Tuder, 2017). Intimal thickening is both cellular and fibrous, characterised by hyper-proliferative ECs, invading VSMCs and (myo)fibroblasts, with extensive deposition of a collagen-rich extracellular matrix (ECM; Tuder et al., 2007). Overproduction of key remodelling mediators (cytokines and growth factors) by the endothelium fuels intimal thickening by sustaining EC dysfunction (in an autocrine manner) and stimulating the growth of other cells (namely VSMCs) in the vascular wall (Humbert et al., 2008).

Isolated human pulmonary artery ECs (HPAECs) from subjects with IPAH retain a hyper-proliferative phenotype *in vitro* and fail to form normal tubes (Masri et al., 2005), which may explain why occluded and obliterated precapillary vessels are not restored or replaced (Rabinovitch, 2012). Pericytes are vascular supporting cells that stabilise new vessels during sprouting (Yuan et al., 2021). Recent findings suggest that abnormal EC-pericyte interactions, particularly reduced pericyte recruitment, may contribute to vessel loss in PH (Yuan et al., 2016, 2019).

1.3.3.3 *Plexiform lesions*

Severe PH (particularly PAH) is also associated with the appearance of complex plexiform lesions (Croix and Steinhorn, 2016), disorganised networks of tortuous vascular channels that arise at arterial bifurcations and may completely obstruct the vessel lumen (Lee et al., 1998; Cool et al., 1999). These lesions are encircled by ECM, platelet aggregates, VSMCs, (myo)fibroblasts, and inflammatory cells, which may percolate the core of the lesion (Tuder et al., 2007; Lee et al., 2020). Plexiform lesions arise from disordered angiogenesis in a process which has been likened to malignancy. Endothelial injury is posited to result in substantial apoptosis, selecting for a dysfunctional, apoptosis-resistant, and hyper-proliferative EC population (Taraseviciene-Stewart et al., 2001; Sakao et al., 2005, 2009). Loss of contact inhibition drives the clonal expansion of these cells, giving rise to cellular masses which are further fuelled by over-expression of pro-angiogenic factors. including vascular endothelial growth factor (VEGF) and

hypoxia-inducible factor (HIF)-1α (Geiger et al., 2000; Tuder et al., 2001), and under-expression of pro-apoptotic factors, like transforming growth factor (TGF)-β receptor 2 (TGF-βR2) and B-cell lymphoma (Bcl)-2 (Yeager et al., 2001). These lesions demonstrate further neoplastic traits, such as metabolic alterations and increased expression of cell adhesion molecules, chemokines and anti-apoptotic markers (Xu et al., 2007; Rai et al., 2008; Jonigk et al., 2011; Cool et al., 2020; Lee et al., 2020).

It remains contentious whether plexiform lesions play an active role in disease progression or are simply a morphological indicator of irreversible, end-stage disease (Jonigk et al., 2011). Indeed, the occurrence and distribution of plexiform lesions appears not to correlate with haemodynamic parameters such as mPAP and PVR (Stacher et al., 2012). On the other hand, the close association of plexiform lesions and dilated bronchial micro-vessels has led to the suggestion that plexiform lesions function as anastomotic structures between the pulmonary and bronchial circulation (Galambos et al., 2016). SiMFis (singular millimetric fibrovascular lesions) another type of complex lesion recently identified in PAH lungs, may also connect the systemic vasculature to pulmonary arteries and veins (Ghigna et al., 2016).

1.3.3.4 *Smooth muscle proliferation*

Medial thickening of muscular arteries by VSMC hyperplasia and increased ECM (elastin and collagen) deposition is regarded as a signature process in PH (Tuder et al., 2007; Tuder, 2009). Partially- and non- muscular peripheral arteries may also become muscularised by migration and proliferation of pre-existing VSMCs (Sheikh et al., 2014, 2015). In explanted PAH lungs, medial thickness is increased by approximately 20% and correlates with pre-transplanted elevated PVR and mPAP (Stacher et al., 2012).

VSMC growth has been extensively investigated within the context of PH. In culture, PASMCs isolated from PAH patients exhibit increased levels of proliferative markers, like proliferating cell nuclear antigen (PCNA), and anti-apoptotic factors, such as Bcl-2 (Perros et al., 2019). Early in the disease process, disruption of the endothelium (by apoptosis) may expose the underlying smooth muscle to circulating growth factors and cytokines, evoking a phenotypic switch

from quiescence to a state of active proliferation (Budhiraja et al., 2004; Zhou et al., 2018). As PH develops, the hyper-proliferative phenotype of VSMCs is sustained by the excessive release of growth factors (e.g. FGF-2; Thompson and Rabinovitch, 1996) and reduced secretion of anti-mitogens (e.g. apelin; Alastalo et al., 2011) by dysfunctional ECs.

Lineage tracing suggest that ~95% of VSMCs in remodelled vessels derive from expansion of existing smooth muscle (Sheikh et al., 2014). The remaining 5% are likely derived from other cell types with multi-lineage differentiation potential. Endothelial-to-mesenchymal transition (EMT), resident/circulating vascular progenitor cells and multifunctional pro-fibrotic/inflammatory cells (fibrocytes) are all thought to contribute (Arciniegas et al., 2007; Yeager et al., 2011). Notably, the pericyte coverage of pulmonary arterioles is disproportionately increased (two - threefold) in experimental and human PAH (Ricard et al., 2014). These cells have been shown to differentiate into VSMCs in a TGF-β-dependant manner (Ricard et al., 2014; Bordenave et al., 2020).

Evidence from animal models of PH suggests that VSMC proliferation does not continue unabated, but wanes with time (Stenmark et al., 2018). In accordance, α-smooth muscle actin (α-SMA) positive VSMCs in the medial layer of remodelled pulmonary arteries from late stage IPAH and hereditary PAH (HPAH) patients do not demonstrate significant Ki-67 expression (Majka et al., 2008). If VSMC proliferation is limited to the early stages of disease, then it is possible that alternative smooth muscle phenotypes play a key role in established disease.

An emerging paradigm of VMSC involvement in PH is stress-induced cellular senescence. Senescent cells exist in a state of permanent, irreversible growth arrest characterised by apoptosis resistance and a pro-inflammatory, secretory phenotype (Van Der Feen et al., 2019a). In lung tissue sections from patients with chronic obstructive pulmonary disease (COPD)-PH, the expression of senescence markers in VSMCs correlates closely with the degree of vascular remodelling (Wang et al., 2021). In culture, senescent VSMCs stimulate the growth and migration of phenotypically ‘normal’ HPASMCs through the production and release of inflammatory mediators, including IL-6 and chemokine (C-C motif) ligand (CCL)-2. In early disease, senescence may act as a brake to disengage continuous smooth muscle proliferation. However, as senescent VSMCs accumulate, this

altered metabolic state may become pathological, by promoting persistent inflammation, proliferation of non-senescent cells, progenitor cell recruitment and ECM accumulation (Stenmark et al., 2018).

1.3.3.5 *Adventitial fibrosis*

Adventitial fibrosis is a common pathological finding in PH patients (Tuder et al., 2007). The principal cell population in the adventitia are fibroblasts, which are responsible for the production of ECM and matricellular proteins (Stenmark et al., 2011, 2013). In response to vessel injury, adventitial fibroblasts proliferate and differentiate into myofibroblasts, augmenting deposition of ECM components, including collagen, elastin and fibronectin (Nogueira-Ferreira et al., 2014), and secretion of mediators of tissue remodelling, such as matrix metalloproteinases (MMPs) and tissue inhibitors of metalloproteinases (TIMPs; Stenmark et al., 2013). Studies in animal models suggest that fibroblast proliferation precedes and exceeds that of ECs and VSMCs (Stenmark et al., 2006), implying that reduced vascular compliance is a precipitating factor for the initial rise in PVR (Thenappan et al., 2016).

Activated fibroblasts also adopt an inflammatory phenotype, characterised by increased expression of adhesion molecules (such as VCAM-1) and release of chemokines and cytokines, including CCL2, CCL23, IL-6 and IL1β. These molecules influence the activity of ECs and VSMCs, and signal circulating leukocytes (primarily macrophages) to infiltrate the adventitial compartment and adopt a pro-inflammatory/pro-fibrotic phenotype (Stenmark et al., 2012; El Kasmi et al., 2014). Adventitial fibrosis appears to be dependent on the recruitment of circulating monocytes, as depletion of these cells blocks adventitial remodelling (Frid et al., 2006).

Adventitial fibrosis causes the large proximal arteries to become stiff, limiting the compliance of the pulmonary arterial tree and exerting an additional pulsatile stress on the RV (Wang and Chesler, 2011; Thenappan et al., 2016). Clinically, decreased pulmonary artery compliance (PAC) is independently associated with RV dysfunction, dilatation, hypertrophy (Stevens et al., 2012; Prins et al., 2016) and poor patient outcome (Douwes et al., 2013). Some studies even suggest PAC

is of greater prognostic value than PVR (Mahapatra et al., 2006a, 2006b; Hunter et al., 2008).

1.3.3.6 *Extracellular matrix remodelling*

It is increasingly recognised that expansion of the ECM contributes to pulmonary vascular fibrosis and vessel stiffening (Thenappan et al., 2018a). Evidence from CHD-PAH patients and experimental models indicates that degradation and fragmentation of the internal elastic lamina are early events in remodelled pulmonary arteries, even preceding VSMC proliferation (Rabinovitch et al., 1986; Rosenberg et al., 1987; Todorovich-Hunter et al., 1988, 1992). Furthermore, there is evidence of increased collagen deposition in proximal and distal pulmonary arteries; particularly in the intima, but also in the medial, adventitial, and perivascular compartments (Poiani et al., 1990; Botney et al., 1993; Estrada and Chesler, 2009; Hoffmann et al., 2015b; Wang et al., 2017b). Collagen cross-linking is also enhanced, increasing the ratio of insoluble to soluble fibres (Wang and Chesler, 2012; Wang et al., 2013; Bertero et al., 2016). The expression of other ECM components, including tenascin (Jones and Rabinovitch, 1996; Jones et al., 1997), fibronectin (Jones et al., 1997), and osteopontin (Anwar et al., 2012; Saker et al., 2016), is also increased. Accordingly, the lungs of subjects with IPAH show signs of calcification (Ruffenach et al., 2016).

ECM remodelling is driven by altered expression and activity of proteolytic enzymes, including MMPs, proteins with a disintegrin and metalloprotease domain (ADAMs), serine elastases, lysyl oxidases (LOXs), and TIMPs (Lepetit et al., 2005; Chelladurai et al., 2012; Hoffmann et al., 2015; Bertero et al., 2016; Thenappan et al., 2018a). Crucially, degradation of the ECM releases elastin peptides and growth factors such as TGF-β and FGF-2 (which normally are stored in an inactive form in the ECM), promoting VSMC cell proliferation, survival, and motility and also acting as chemoattractant molecules for inflammatory cells (Thompson and Rabinovitch, 1996). Increased ECM stiffness may also enhance mechano-activation of growth pathways in pulmonary artery ECs (PAECs) and PASMCs, leading to proliferation (Thenappan et al., 2018a).

1.3.3.7 *Inflammation*

Infiltrates of T- and B- lymphocytes, macrophages, dendritic cells and mast cells are present within vascular lesions of PAH patients and animal models (Rabinovitch et al., 2014), accompanied by organised perivascular lymphoid aggregates of T- and B- cells (Perros et al., 2012). Infiltrating inflammatory cells play a direct role in vascular remodelling, by inducing an inflammatory and proliferative phenotype in ECs, VSMCs, and (myo)fibroblasts (Humbert et al., 2019). Indeed, the expression of several chemokines, including CCL2, CCL5 and fractalkine, is increased within the lungs and remodelled pulmonary arteries of individuals with PAH (Dorfmüller et al., 2002; Sanchez et al., 2007; Perros et al., 2008). Moreover, circulating concentrations of inflammatory cytokines (notably IL-1β and IL-6) correlate strongly with disease severity in IPAH (Humbert et al., 1995; Soon et al., 2010). Inflammasomes, multiprotein complexes of the innate immune system, are also gaining interest in the context of PH (Scott et al., 2019) and RV failure (Al-Qazazi et al., 2022).

1.3.3.8 *Thrombosis and embolism*

In PAH, the release of pro-inflammatory and pro-thrombotic mediators from the endothelium predisposes to *in-situ* thrombosis (Lannan et al., 2014). In small occluded vessels, micro-thrombi may undergo an organising process orchestrated by fibroblasts, in which the thrombus is percolated with several recanalized vessels (Tuder et al., 2007; Humbert et al., 2019).

Abnormal blood clotting is a core component of CTEPH pathobiology. Following unresolved pulmonary embolism, material left adhering to the wall of large and/or middle-sized pulmonary arteries (Bernard and Yi, 2007) may become organised, forming fibrous obstructions that redirect blood flow to non-occluded vessels (Bernard and Yi, 2007; Banks et al., 2014). The increased passage of blood through small downstream arteries results in shear stress, endothelial dysfunction and a pattern of vascular remodelling reminiscent of PAH (Moser and Bloor, 1993; Pietra et al., 2004; Lang et al., 2016; Simonneau et al., 2017). There may also be involvement of small vessels downstream of totally- and partially-obstructed arteries, due to distal thrombosis or propagation of the macrovasculopathy (Kim, 2016; Simonneau et al., 2017).

1.3.4 Right ventricular pressure overload

The ultimate consequence of pulmonary vascular remodelling is increased RV afterload (Lammers et al., 2012; Chemla et al., 2015). As vascular remodelling progresses, the steady rise in afterload forces the right heart into a state of chronic pressure overload (Borgdorff et al., 2015). To curtail wall stress and maintain cardiac output (CO), the RV progressively hypertrophies (Ryan and Archer, 2014). This ability of the right heart to remodel and maintain a functional status is the ultimate decider of outcome in PH; RV mass, size, and ejection fraction (RVEF) are independent predictors of survival (Humbert et al., 2010; Howard, 2011). Impaired RVEF predicts clinical worsening more accurately than elevated PVR (Van De Veerdonk et al., 2011).

1.3.4.1 *Adaptive hypertrophy*

Pressure overload is detected in cardiomyocytes by integrins and stretch-sensitive ion channels ('mechanoreceptors') which respond to wall stretch by activating intracellular messengers such as focal adhesion kinase (FAK), mitogen-activated protein kinase kinase (MEK) and calmodulin-dependent protein kinase (CaMK) II; (Ruwhof and Van Der Laarse, 2000; Ren et al., 2019). These signalling pathways lead to augmented synthesis of contractile proteins, assembly of new sarcomeres (the basic contractile unit of a muscle fibre), cytoskeletal reorganisation and increased cell size (Hynes, 1992; Shyy and Chien, 1997; Ross et al., 1998; Mann, 2004; Bogaard et al., 2009a). The resulting increase in RV mass-to-volume ratio normalises wall tension and increases contractility such that right heart function is compensated (Van de Veerdonk et al., 2016).

Akin to LV hypertrophy, RV hypertrophy (RVH) is accompanied by the re-appearance of a foetal gene expression pattern (Friedberg and Redington, 2014). A hallmark of this process is a transition from the expression of α-myosin heavy chain (MHC) to β-MHC (Lowes et al., 1997), which requires less energy but may also have lower force-generating ability (Gupta, 2007). Other changes include elevated levels of the cardiac hormones atrial and brain natriuretic peptide (ANP and BNP; Ikeda et al., 2014), and decreased expression of the sarco/endoplasmic reticulum Ca^{2+}-ATPase (SERCA2a; Wu et al., 2012).

1.3.4.2 *RV failure*

RVEF, CO and exercise capacity are initially maintained at the expense of right heart remodelling (Ryan and Archer, 2015). Yet, without intervention the continuous rise in mPAP will inevitably exceed the adaptive countermeasures, at which point RVH becomes maladaptive. Maladaptation is characterised by progressive dilatation of the ventricle, which may be acutely beneficial as stroke volume (SV) is increased by the Frank–Starling mechanism (van de Veerdonk et al., 2016). However, this occurs at the expense of escalating filling pressures, wall stress and energy exhaustion, ultimately culminating in dramatic functional decline (decompensation; Bogaard et al., 2009a; Vonk Noordegraaf and Galiè, 2011; Vonk-Noordegraaf et al., 2013; 2017; Thenappan et al., 2018).

In comparison to the muscular LV, the thin, compliant RV is much less adept at generating high pressures (Ventetuolo and Klinger, 2014). Furthermore, the RV of a PH patient may face a fivefold elevation in afterload, dwarfing the 50% uptick of LV afterload associated with systemic hypertension and resulting in a far greater level of functional decline (Friedberg and Redington, 2014; Sanz et al., 2019). Consequently, the acute morality rate of RV failure requiring inotropic support is ≥40% (Sztrymf et al., 2010; Campo et al., 2011), far exceeding that of LV failure requiring inotropes (13-14%; Abraham et al., 2005).

1.3.4.3 *Ventricular interdependence*

In the absence of LHD, PH is defined by normal LV filling pressures. However, as the maladapted RV begins to dilate, the septum bows outwards, compressing the left heart and impairing LV filling (Gan et al., 2006). Furthermore, reduced RV CO diminishes venous return to the left heart, resulting in decreased workload and oxygen demand (LV unloading). The subsequent atrophy of the free wall ultimately decreases the force-generating capacity of the LV (Manders et al., 2014). Due to mutually encircling epicardial muscle fibres approximately one-third of right ventricular systolic pressure (RVSP) and CO is generated by contraction of the LV (Santamore et al., 1976). In consequence, a cycle of dysfunction may exist between the two ventricles; RV pressure overload impairs LV function, which in turn diminishes the contribution of the left heart to RV output, aggravating RV dysfunction.

1.3.4.4 *Mechanisms of maladaptation*

In PH, the primary cause of right heart remodelling is irrefutably pulmonary vascular disease (PVD), exemplified by the near total recuperation of RV homeostasis just weeks after lung transplantation (Kasimir et al., 2004) or pulmonary endarterectomy (PEA; Iino et al., 2008). Still, the capacity of the right heart to adapt to adverse loading is heterogeneous between PH groups. Despite comparable mPAP, patients with Eisenmenger's syndrome exhibit RVH from birth, yet remain free from RV failure for decades (Hopkins et al., 1996), whilst SSc-PAH is associated with rapid and severe RV failure (Overbeek et al., 2008a). Likewise, disparities in the degree of RVH and the occurrence of RV failure between different animal models of RV pressure overload cannot be explained by differences in afterload alone (Bogaard et al., 2009b).

The cellular and molecular events dictating the transition from adaptive remodelling into a state of maladaptation are largely unknown. Emerging evidence suggests the severity of RV dysfunction may be altered by abnormal neurohormonal signalling, disturbed angiogenesis, metabolic changes, oxidative stress, ischaemia, inflammation, apoptosis and fibrosis (Maron and Leopold, 2015; Thenappan et al., 2018; ***Figure 4***). Although RV remodelling is phenotypically classified as adaptive or maladaptive, the remodelling process is best considered a progressive continuum (Vonk Noordegraaf et al., 2019). Indeed, some pathological changes may begin in the adaptive state, and others may be simple by-products of maladaptation, with no influence on outcome (Ren et al., 2019).

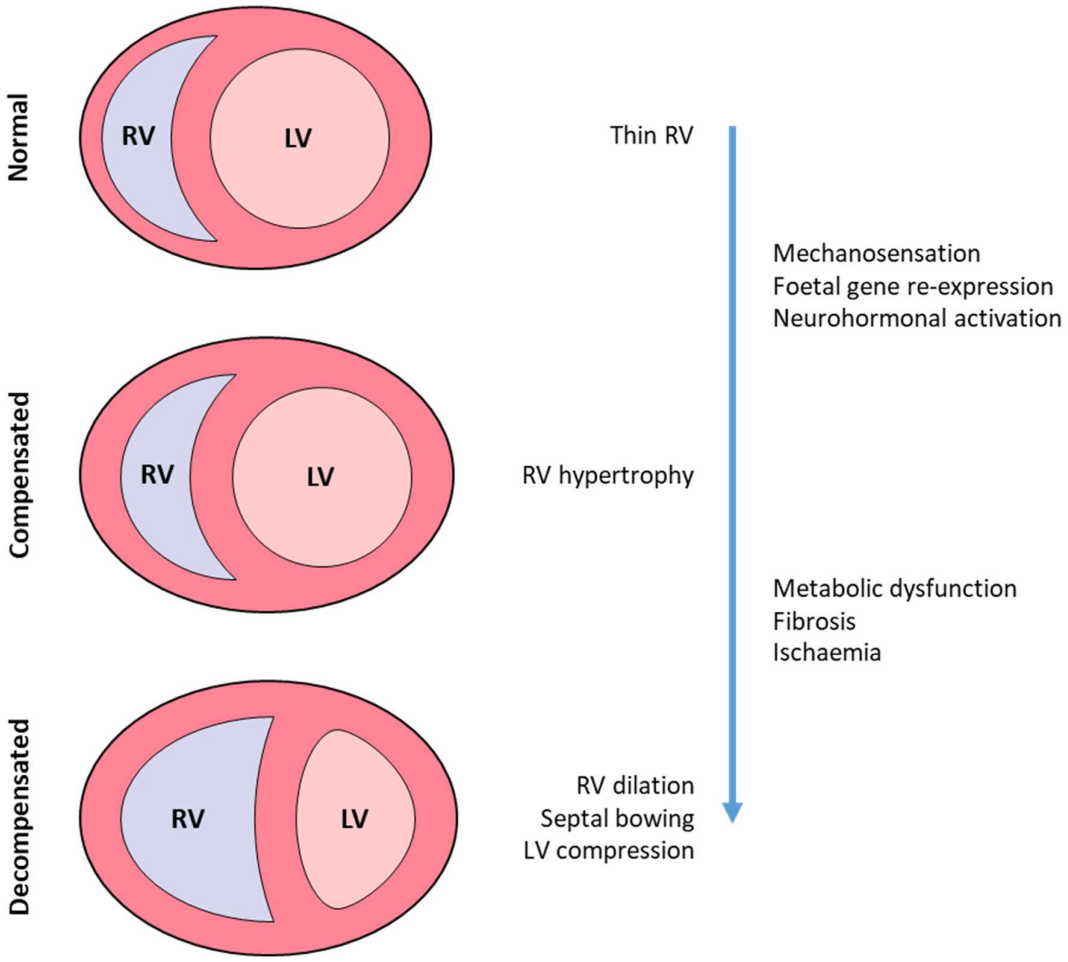

Figure 4: The response of the right ventricle to chronic pressure overload

Coupling of the ventricle to the RV to high arterial load is initially maintained by increasing muscle mass. Chronic afterload elevation may give rise to metabolic dysfunction, fibrosis, and ischaemia, marking the onset of RV failure. Dilation of the RV shifts the interventricular septum leftward, impacting LV geometry and impeding filling. RV, right ventricle; LV, left ventricle.

1.4 Pharmacological treatment of pulmonary hypertension

1.4.1 Pulmonary arterial hypertension

For many years, endothelial dysfunction has been recognised as an important factor in the initiation and progression of PAH. Consequently, all approved therapies have been developed to correct excessive pulmonary vasoconstriction; either by bolstering the effects of endogenous vasodilators, or dampening the effects of endogenous vasoconstrictors (Montani et al., 2014; Yaoita et al., 2016).

A small subset of IPAH patients (5-10%) demonstrate a favourable response to acute vasodilator challenge and show significant long-term haemodynamic improvement and prognosis with calcium channel blockers (CCBs; Rich et al., 1992; Sitbon et al., 2005). Outside of this small minority, subjects with PAH rarely experience long-term benefit with CCBs, even if they respond favourably during acute vasoreactivity testing (Montani et al., 2010).

Most PAH patients will receive one or more PAH-specific therapies. These drugs target the NO, PGI_2, and ET-1 pathways and fall into one of five pharmacological classes: an sGC stimulator, PDE5 inhibitors, PGI_2 analogues, an IP receptor agonist, and ET-1 receptor antagonists (ERAs; ***Table 3***; Humbert et al., 2014). The mechanism of action for each of these drug classes is summarised in ***Figure 5***. For the management of patients with PAH, early combination therapy according to risk profile is recommended; upfront triple combination therapy (including a parenteral PGI_2) for high-risk patients, and upfront dual oral combination therapy for the majority of low- and intermediate-risk subjects (Galiè et al., 2016, 2019; Hoeper et al., 2018).

1.4.2 Groups 2, 3 and 5

As there are no specific therapies for group 2 or 3 PH, management is limited to optimisation of the primary disease (Rose-Jones et al., 2015). Randomised controlled trials failed to demonstrate an improvement in symptoms or prognosis with PAH drugs in CLD-PH (Stolz et al., 2008; Zisman et al., 2010; Goudie et al., 2014; Nathan et al., 2019) or LHD (Hoeper et al., 2016b; Vachiéry et al., 2019). The use of vasodilators may be contraindicated in CLD-PH due to the risk of ventilation/perfusion (V/Q) mismatch secondary to dilatation of vessels perfusing

poorly ventilated regions of lung (i.e. impairment of hypoxic pulmonary vasoconstriction, HPV; Stolz et al., 2008; Blanco et al., 2010). Due to the heterogeneous nature of Group 5 PH, little data from randomised controlled trials exists and therapy is usually decided on a case-by-case basis (Galiè et al., 2016).

1.4.3 Chronic thromboembolic pulmonary hypertension

CTEPH is the only form of PH which has a curative treatment. PEA, a surgical procedure involving removal of the obstructive thrombi from the pulmonary arteries (Kim et al., 2013; Jenkins, 2015), results in rapid and near normalisation of mPAP and PVR (Mayer et al., 2011; Berman et al., 2012; Madani et al., 2012), with subsequent improvements in biventricular cardiac structure and function (Reesink et al., 2007; Iino et al., 2008; Surie et al., 2011; Mauritz et al., 2012).

Although long-term survival post-PEA is excellent (Delcroix et al., 2016), ~40% of CTEPH patients are inoperable due to inaccessible vascular obstruction, PAP out of proportion to morphological lesions, or prohibitive comorbidities (Pepke-Zaba et al., 2011). Furthermore, persistent/residual PH (usually caused by distal small vessel vasculopathy) may be present in up to 35% of patients post-PEA (Cannon et al., 2016). Riociguat, is approved for the treatment of inoperable and persistent/recurrent CTEPH on the basis of improvements in six-minute walk distance (6MWD) and pulmonary haemodynamics (Ghofrani et al., 2013; Simonneau et al., 2016).

Table 3: Drugs approved for the treatment of pulmonary arterial hypertension

Drug Class	Pathway	Examples
Soluble guanylyl cyclase stimulators	NO	Riociguat
Phosphodiesterase type 5 inhibitors	NO	Sildenafil, tadalafil
Endothelin receptor antagonists	ET-1	Bosentan, macitentan, ambrisentan
Prostacyclin analogues	PGI_2	Epoprostenol, iloprost, treprostinil
Prostacyclin receptor agonists	PGI_2	Selexipag

NO, nitric oxide; ET-1, endothelin; PGI_2, prostacyclin.

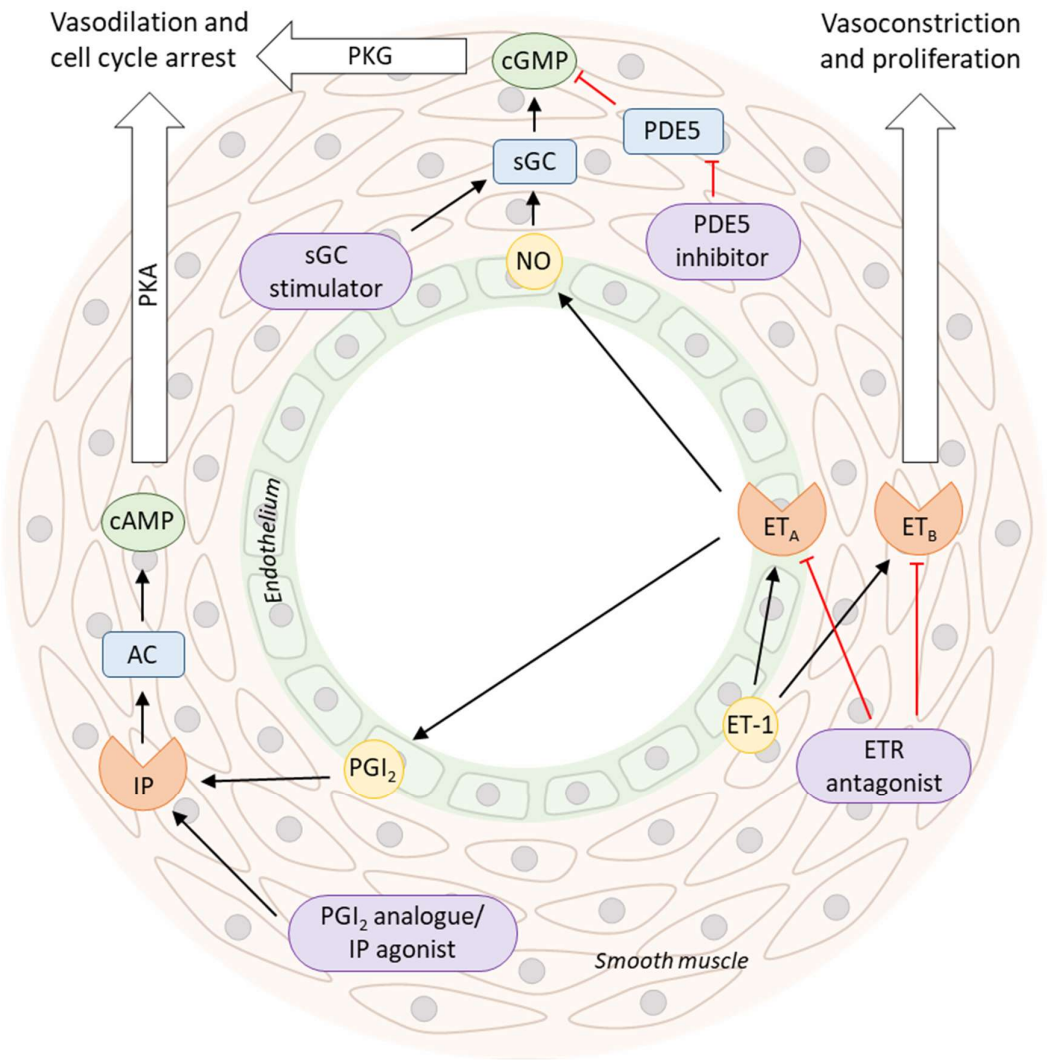

Figure 5: Current therapeutic targets in pulmonary arterial hypertension

PGI_2 analogues and IP receptor agonists induce vasodilatation by activating G_s-coupled IP receptors and elevating intracellular cAMP. Exogenous NO activates sGC, increasing cGMP to induce vasodilatation. PDE5 inhibitors prevent the metabolism of the cGMP pool, thus maintaining vessel dilation. As such, PDE5 inhibitors rely predominantly on endogenous NO to exert their effects. On the other hand, direct sGC stimulators increase cGMP production independent of endogenous NO bioavailability. ET receptor antagonists block the actions of ET-1 at its two cognate G_q-coupled receptors, ETR_A and ETR_B, preventing initiation of a contractile response. PGI_2, prostacyclin; IP, PGI_2 receptor; cAMP, cyclic adenosine monophosphate; PKA, protein kinase A; NO, nitric oxide; sGC, soluble guanylyl cyclase; cGMP, cyclic guanosine monophosphate; PDE5, phosphodiesterase type 5; PKG, protein kinase G; ET-1, endothelin; ETR_A, endothelin receptor A; ETR_B, endothelin receptor B.

1.4.4 Challenges

Current PAH therapies mitigate symptomatic burden, enhance exercise capacity and slow the rate of clinical deterioration (Pulido et al., 2013; McLaughlin et al., 2015; Sitbon et al., 2015). However, even with optimised therapy, the average fall in mPAP is just 10% (i.e. ≤6 mmHg; Dasgupta et al., 2015) and most patients continue to have significant or deteriorating PH (Pullamsetti et al., 2014). Furthermore, the only therapy demonstrated to reduce mortality alone (i.e. not a composite end point) in a randomised study is epoprostenol (Barst et al., 1996; Sitbon and Vonk Noordegraaf, 2017), which requires continuous intravenous infusion and carries risks of infection and thrombosis (Toshner et al., 2020). In addition, whilst the introduction of these drugs led to improvements in long-term survival versus historical figures (Benza et al., 2012), 5-year survival for patients with PAH remains at only 60% (Badesch et al., 2010; Gall et al., 2017). In end-stage disease, the only treatment option is organ replacement. Double-lung or heart-lung transplantation is associated with excellent long-term survival, but the shortage of donor organs and need for chronic immunosuppression render this approach far from ideal (Fadel et al., 2010; Lordan and Corris, 2011).

1.4.4.1 *Pulmonary vascular remodelling*

Owing to the distensibility and large recruitment capacity of the pulmonary vasculature, 70% of the vascular bed may be obstructed before an increase in resting PAP is evident (Magliano et al., 2002; Vonk-Noordegraaf et al., 2005). Consequently, excessive vasoconstriction may be a relatively minor pathophysiological feature of PH at diagnosis, and the limited efficacy of current PAH therapies might be related to an inability to reverse vascular remodelling. Indeed, although these drugs inhibit VSMC proliferation *in vivo* (Tilton et al., 2000; Schermuly et al., 2004; Liu et al., 2007), complex pulmonary vascular lesions persist in long-term drug-treated PAH patients (Achcar et al., 2006; Pogoriler et al., 2012; Stacher et al., 2012). This discrepancy might be related to the relatively moderate degree of pulmonary vascular remodelling in the classical animal models of PH, which may be particularly amenable to treatment (Maarman et al., 2013). As such, it is now evident that a curative therapy must address extensive multi-

cellular vascular lesions (Sommer et al., 2021), shifting the focus to novel experimental models that feature extensive EC-driven, proliferative remodelling.

1.4.4.2 *Cardiac dysfunction*

At present, afterload optimisation is the sole strategy for managing RV dysfunction and preventing RV failure (Cassady and Ramani, 2020). Notably, a small clinical study of patients with PAH found that sildenafil reduced RV mass, precipitating greater improvement in cardiac function and exercise capacity than the dual ET receptor antagonist bosentan, which did not alter RVH (Wilkins et al., 2005). As PDE5 is expressed in the hypertrophied human RV, but not in healthy hearts (Nagendran et al., 2007), a direct anti-hypertrophic action of sildenafil on cardiac muscle cannot be ruled out. Still, studies of sildenafil in animal models of isolated RV dysfunction have yielded mixed results in terms of both remodelling and function (Borgdorff et al., 2015).

A growing body of evidence suggests that the clinical benefit of PAH therapies is determined by their effect on RV function, rather than pulmonary haemodynamics. In accordance, subjects with the greatest reductions in PVR after the initiation of pharmacotherapy exhibit right heart reverse remodelling (RHRR), increased RVEF and an excellent 5-year survival of >90% (Van De Veerdonk et al., 2011; Badagliacca et al., 2018a). With monotherapy, <20% of patients demonstrate RHRR, though recent findings suggest a greater number of subjects may experience this benefit with upfront combination therapy (Van de Veerdonk et al., 2017; Badagliacca et al., 2018b; D'Alto et al., 2020). Unfortunately, despite a therapeutic decrease in PVR, some 25% patients exhibit deteriorating RV function, in which case the prognosis is poor (Van De Veerdonk et al., 2011). Consequently, cardioprotection is an attractive therapeutic avenue, particularly in the absence of therapies able to reverse vascular remodelling (Dignam et al., 2022).

1.5 Novel pharmacological targets in pulmonary hypertension

New therapies are desperately needed to increase the quality of life and survival of PH patients (Grinnan et al., 2019). Current research is focused on targeting the proliferation, migration, and apoptosis pathways driving pulmonary vascular remodelling (Sommer et al., 2021). A growing number of clinical trials have not met

their primary endpoint or have reported major safety concerns (Sitbon et al., 2019). Still, a plethora of diverse novel targets remain under investigation in the clinic, including bone morphogenetic protein (BMP) signalling, metabolism, sex hormones, neurohormones, the ECM and epigenetic factors (Groeneveldt et al., 2019; Sommer et al., 2021; Zolty, 2021; Condon et al., 2022), offering hope for a curative therapy that will revolutionise patient outcomes.

1.5.1 Bone morphogenetic protein receptor 2

The TGF-β/BMP signalling pathway is critical to cell growth and adult tissue homeostasis (Hogan, 1996). TGFβ/BMP signalling is transduced by heteromeric transmembrane receptor complexes consisting of two type 1 receptors (anaplastic lymphoma kinases, ALKs 1-7), two type 2 receptors (e.g. TGFβR2; bone morphogenetic protein receptor 2, BMPR2; activin receptor type IIA/B, ActRIIA/B) and co-receptors (e.g. endoglin; Gomez-Puerto et al., 2019; Agnew et al., 2021). These multicomponent receptors activate downstream signalling via suppressor of mothers against decapentaplegic (Smad)-2/3 (TGFβR2, ActRIIA/B) or Smad1/5/8 (BMPR2). Activation of Smad2/3 signalling by TGF-β or activins promotes proliferation and survival of PAECs and PASMCs, whereas activation of Smad1/5/8 signalling by BMPs favours quiescence (Yang et al., 2005; Upton et al., 2009; Rol et al., 2018).

PAH is associated with dysregulation of the BMPR2-Smad1/5/8 pathway, curtailing anti-proliferative signalling and shifting the balance toward pro-proliferative TGF-β/activin-Smad2/3 signalling, ultimately leading to pulmonary vascular remodelling (Morrell, 2006). The pivotal role of this pathway was highlighted following the discovery of mutations that cause heritable PAH in several of its members, including *BMPR2*, *ALK-1*, endoglin (*ENG*) and *SMAD9* (Austin and Loyd, 2014). Critically, heterozygous mutations in *BMPR2* are present in ~75% of heritable PAH cases, 12% of sporadic cases and 8% of anorexigen-exposed cases (Gräf et al., 2018). Furthermore, *BMPR2* expression is dampened even in patients without mutations (Atkinson et al., 2002; Lavoie et al., 2014), and in several non-genetic experimental models (Takahashi et al., 2006; Morty et al., 2007; Long et al., 2009).

Naturally, attempts have been made to rebalance growth-promoting and growth-inhibiting signalling for therapeutic benefit in PH. Tacrolimus (FK506) is a potent, indirect BMPR2 activator that binds FK-binding protein-12 (FKBP12), a repressor of BMP signalling. Tacrolimus reverses endothelial dysfunction in HPAECs isolated from subjects with PAH and offsets neointima formation and distal artery muscularisation in experimental models (Spiekerkoetter et al., 2013). Compassionate use yielded promising results in three end-stage IPAH patients (Spiekerkoetter et al., 2015), yet a Phase 2a trial found no effect on exercise capacity (6MWD), N-terminal (NT)-proBNP (a serological marker of cardiac dysfunction; Lewis et al., 2020), or echocardiographic parameters of RV function. The negative result of this trial may be attributed to the small sample size, as patients that demonstrated increased BMPR2 expression tended to show improvement (Spiekerkoetter et al., 2017).

An alternative to increasing BMP signalling is to inhibit Smad2/3 signalling. Sotatercept is an ActRIIA fusion protein that acts as a ligand trap, competitively binding and neutralising TGF-β superfamily ligands (Humbert et al., 2021). In pre-clinical studies, sotatercept attenuated the proliferation of PASMCs and pulmonary microvascular ECs from PAH patients, and had favourable effects on pulmonary vascular remodelling and RV function in animal models (Joshi et al., 2019; Yung et al., 2020). In Phase 2 clinical trials, sotatercept-treated patients demonstrated significant improvements in PVR, 6MWD and NT-proBNP (Humbert et al., 2021). Following these promising results, sotatercept is progressing to a Phase 3 clinical trial (NCT04576988) with the primary end point of 6MWD distance at 24 weeks.

1.5.2 Serotonin

The link between serotonin (5-hydroxytryptamine; 5-HT) and PH was identified following a surge in cases associated with the use of anorexigens (MacLean, 2018), which increase 5-HT availability by enhancing release and suppressing reuptake and degradation (Eddahibi and Adnot, 2001). Further investigation revealed that 5-HT is a potent pulmonary vasoconstrictor and a mitogenic agent for VSMC and fibroblasts (MacLean et al., 2000). As such, serotonergic signalling is under exploration as a therapeutic target in PH.

Initial results were disappointing; terguride, a dual 5-HT_{2A} and 5-HT_{2B} receptor inhibitor, failed to show efficacy in a Phase 2 trial of PAH patients outside of a subgroup on background therapy with ERAs (Ghofrani et al., 2012). Still, 5-HT_{1B} is the most highly expressed 5-HT receptor in the pulmonary arteries of experimental models and humans with PAH (Keegan et al., 2001; Wang et al., 2001; Launay et al., 2002; Morecroft et al., 2005), and thus may be a more rewarding target. Recently, an open-label pilot study of a selective serotonin reuptake inhibitor (SSRI) in PAH patients found no effect on the primary endpoint of PVR (Sodimu et al., 2020). On the other hand, early clinical experience with an inhibitor (rodatristat ethyl) of tryptophan hydroxylase 1 (TPH1), the rate-limiting enzyme in 5-HT biosynthesis, was promising (Paralkar et al., 2017; Carpenter et al., 2019). A Phase 2 study evaluating rodatristat ethyl in PAH patients is underway (Lazarus et al., 2021; NCT04712669).

1.5.3 Apelin

Apelin is an endogenous peptide that has both vasodilatory and positive inotropic effects (Folino et al., 2015). PAH is associated with reduced apelin expression in HPAECs (Alastalo et al., 2011), which may account for lower circulating levels of the peptide (Chandra et al., 2011). The G protein-coupled apelin receptor is also downregulated in PAH lungs (Yang et al., 2017) and agonism of this receptor has salutary effects in animal models (Falcão-Pires et al., 2009; Yang et al., 2017). A crossover study of 19 patients with PAH reported that short-term administration of the peptide reduced PVR and increased CO (Brash et al., 2018). The results of a Phase 1 trial in PAH patients are pending (NCT01590108).

1.5.4 Vasoactive intestinal peptide

Vasoactive intestinal peptide (VIP) is a hormone with important biological actions in the nervous, digestive, and cardiovascular systems. Owing to its vasodilatory and positive inotropic effects (Henning and Sawmiller, 2001), VIP has been extensively investigated in the context of PH. In IPAH patients, levels of the hormone are depressed in the circulation and lungs whilst VIP receptor expression is elevated in the pulmonary arteries. Deficiency of the hormone produces spontaneous PH in mice (Said et al., 2007) and exogenous VIP inhibits the

proliferation of HPASMCs from subjects with PAH *in vitro* (Petkov et al., 2003). In a preliminary study of eight PAH patients, inhaled VIP decreased mPAP and boosted CO and exercise capacity (Petkov et al., 2003). However, the results of a Phase 2 study with inhaled VIP were negative (Said, 2012). Due to concerns relating to the bioavailability of the inhaled formulation, a sustained-release analogue (PB1046) suitable for subcutaneous administration was developed and is currently under investigation in a Phase 2 trial (NCT03556020).

1.5.5 Oestrogens

The 'sex' or 'oestrogen' paradox of PAH is born from the seemingly contradictory association of female sex with greater incidence of PAH (McGoon and Miller, 2012; Ghofrani et al., 2013; Skride et al., 2018) but also superior outcome (Escribano-Subias et al., 2012; Shapiro et al., 2012; Kjellström et al., 2019). The role of oestrogens in PAH has yet to be fully elucidated, but evidence suggests the vascular effects of oestrogens are mediated by metabolites of 17β-oestradiol (E2), the major female sex hormone (Morris et al., 2021). Some of these metabolites have proliferative effects (e.g. 16α-hydroxyestrone, 16OHE1; 16α-hydroxyestradiol, 16OHE2; White et al., 2012; Hood et al., 2016; Denver et al., 2020), whilst others are anti-mitogenic (e.g. 2-Methoxyestradiol, 2ME2; Docherty et al., 2019). Consequently, it is postulated that dysfunctional oestrogen metabolism and a subsequent accumulation of mitogenic metabolites underlies the high female-male patient ratio of PAH (Morris et al., 2021). Interestingly, elevated plasma levels of E2 are associated with PAH severity, even in post-menopausal women and men (Ventetuolo et al., 2016; Baird et al., 2018). In these individuals, oestrogens are thought to be derived from extra-gonadal sites, including the lungs and adipose tissue (Mair et al., 2020; Morris et al., 2021).

On the other side of the paradox, the female survival advantage has been linked to superior RV compensation to pressure overload (Jacobs et al., 2014). Accordingly, protective effects of exogenous and ovarian-derived circulating oestrogens on RVH and RV function are reported in experimental animals (Lahm et al., 2012, 2016; Frump et al., 2021). One explanation for the seemingly polar actions of oestrogenic signalling in the lungs and heart is that local alterations in oestrogen metabolism have pathogenic consequences in the pulmonary

circulation. To test this hypothesis, anti-oestrogen drugs currently in use for the treatment of breast cancer are under for investigation for repurposing in PH (Morris et al., 2021).

One example are aromatase inhibitors like anastrozole, which is widely used in the treatment of oestrogen-sensitive breast cancer (Ratre et al., 2020). Aromatase converts androgens to E2 and is highly expressed in the pulmonary vasculature of individuals with PAH (Mair et al., 2014). In a small, placebo-controlled, randomised clinical trial of post-menopausal women and men with PAH, anastrozole was well tolerated and improved 6MWD over a 12-week period, having no detrimental effects on RV function (Kawut et al., 2017). A Phase 2 trial of anastrozole in PAH is ongoing (NCT03229499). The expression of oestrogen receptors is increased in PASMCs from PAH patients (Wright et al., 2015). Fulvestrant, an oestrogen receptor antagonist, was found to be well-tolerated in a small proof-of-concept study of five post-menopausal women with PAH, and showed trends towards higher 6MWD, increased SV and decreased 16OHE2 levels (Kawut et al., 2019). Fulvestrant and anastrozole are contraindicated in pre-menopausal women due to their strong anti-oestrogenic activity and induction of menopause. In contrast, the oestrogen receptor inhibitor tamoxifen is safely used in pre-menopausal women to treat oestrogen-sensitive breast cancer (Pistelli et al., 2018). A Phase 2 study to determine the safety of tamoxifen in males and pre- and post- menopausal females with PAH is currently in progress (NCT03528902).

1.5.6 Dehydroepiandrosterone

Dehydroepiandrosterone (DHEA), a precursor to oestrogens and androgens, is another steroid hormone under investigation in PH (Traish et al., 2011). Circulating DHEA is reduced in men and women with PAH and independently associates with poorer RV function, NT-proBNP, exercise capacity and survival (Ventetuolo et al., 2016; Rhodes et al., 2017; Baird et al., 2018, 2021). Exogenous DHEA normalises the proliferative/apoptotic mediator balance in PAH-PASMCs (Paulin et al., 2011) and moderately reverses PH in experimental models (Bonnet et al., 2003; Hampl et al., 2003; Paulin et al., 2011). The hormone has more pronounced effects in the heart, alleviating oxidative stress, capillary rarefaction, apoptosis and fibrosis, thereby normalising some indices of RV function (Alzoubi et al., 2013). In a small

trial of COPD-PH patients, DHEA significantly improved 6MWD, pulmonary haemodynamics, and diffusion capacity, without worsening gas exchange (Dumas de La Roque et al., 2012). The cardioprotective effects of DHEA in PAH are now being examined in a Phase 2 study (Walsh et al., 2021; NCT03648385).

1.5.7 Receptor tyrosine kinases

The expression and function of different growth factors and their respective receptor tyrosine kinases (RTKs) is altered in PH (Voelkel et al., 2012). Platelet-derived growth factor (PDGF), a potent mitogen and chemoattractant for VSMCs and fibroblasts (Yu et al., 2003; Malenfant et al., 2013; Zhao et al., 2014), is upregulated in PAH lungs (Humbert et al., 1998; Schermuly et al., 2005), particularly within the vasculature (Perros et al., 2008). In experimental models of PH, PDGF receptor antagonists were found to improve haemodynamics, reverse remodelling and boost survival (Schermuly et al., 2005; Klein et al., 2008; Medarametla et al., 2014).

Imatinib, a selective inhibitor of RTKs, including PDGF receptors (PDGFRs) α and β, was the first compound to directly target vascular remodelling used in a Phase 3 trial of subjects with PAH. This landmark trial reported improvements in 6MWD, reduced PVR and increased CO (Hoeper et al., 2013a). Despite being the first drug to demonstrate considerable benefit in patients since the advent of vasodilator therapy, imatinib was ultimately not approved due severe adverse effects (e.g. subdural haematoma) and a failure to delay clinical worsening. Regardless, imatinib may be of use in patients with optimal risk-benefit ratios (Sommer et al., 2021). A new dry powder inhaled imatinib formulation is currently under investigation in a Phase 2b/3 trial (NCT05036135).

The efficacy of imatinib paved the way for investigations of several other RTK inhibitors in PH. Unfortunately, efforts to date have been hampered by concerns regarding cardiotoxicity and unfavourable pulmonary haemodynamics (Minami et al., 2017; Weatherald et al., 2017). A Phase 2 study of seratunib (GB002) in PAH is underway (Frantz et al., 2021; NCT04456998).

1.5.8 Mechanistic target of rapamycin

Mechanistic target of rapamycin (mTOR) is a serine/threonine protein kinase that integrates signals from growth factors, insulin and nutrients (e.g. glucose) to promote cell growth, proliferation, and survival (Saxton and Sabatini, 2017). Expression of phosphorylated mTOR is elevated in the pulmonary arteries of IPAH and CHD-PAH patients (Huang et al., 2011; Goncharov et al., 2014). Furthermore, mTOR signalling is an essential driver of PASMC proliferation in IPAH (Wilson et al., 2015; Kudryashova et al., 2016; Liu et al., 2019) and CTEPH (Ogawa et al., 2009) and promotes vascular remodelling in numerous experimental models (Paddenberg et al., 2007; Krymskaya et al., 2011; Houssaini et al., 2013; Wang et al., 2015; Liu et al., 2019; Guo et al., 2020). A phase 1 trial of the mTOR inhibitor rapamycin in PAH patients is ongoing (NCT02587325); preliminary safety, functional and hemodynamic data are positive (Simon et al., 2019).

1.5.9 Rho-kinase family

The Rho-kinase family of small GTPases are key regulators of many actin-dependent processes intimately related to cardiovascular remodelling, such as adhesion, migration, cell cycle regulation and apoptosis (Nunes et al., 2010). RhoA and its downstream effector Rho-associated protein kinase (ROCK) mediate the vascular effects of numerous vasoactive substances pertinent to the pathophysiology of PH , including ET-1 (Liu et al., 2014), PDGF (Kamiyama et al., 2003) and 5-HT (Matsusaka and Wakabayashi, 2005; Mair et al., 2008). RhoA/ROCK signalling has also been implicated in crosstalk between 5-HT and BMPR2 signalling (Liu et al., 2009). However, despite trends towards improved pulmonary haemodynamics, the ROCK inhibitor fasudil did not improve 6MWD in a Phase 2 trial of PAH patients (Fukumoto et al., 2013). Other ROCK inhibitors have shown promise in animal studies and remain under investigation (Wu et al., 2017; Wang et al., 2019; Zhang et al., 2019).

Other Rho-kinase signalling pathways are also being examined. Deletion of RhoB (a homologous sibling of RhoA) attenuates pulmonary vascular remodelling in mice (Wojciak-Stothard et al., 2012), indicating a causative role in PH pathology. Indeed, the RhoB gene was recently identified as a vascular remodelling-associated gene in IPAH and CTEPH patients (Tan et al., 2022). From a

therapeutic standpoint, the farnesyltransferase inhibitor tipifarnib was found to prevent the development of hypoxia-induced PH in a manner attributed, at least in part, to RhoB inhibition (Duluc et al., 2017). Farnesyltransferase inhibitors have yet to be further explored for treatment of PH.

1.5.10 Immunomodulation

Inflammation appears to be a predisposing factor for the development of PH, as abnormal inflammatory cell number and function are features of several PAH-associated conditions, including systemic sclerosis, HIV infection and systemic lupus erythematosus (Speich et al., 1991; Bonelli et al., 2009; Radstake et al., 2009). However, the involvement of the immune system is not limited to these PH subgroups; inflammation is observed in almost all forms of human and experimental PH (Stenmark et al., 2009; Tuder et al., 2013).

Despite the clear rationale for immunomodulation, the non-steroidal anti-inflammatory drug (NSAID) aspirin was found to be of no benefit in PAH patients (Kawut et al., 2011), and the response to immunosuppression varies depending on the underlying inflammatory disease (Sanchez et al., 2006). Likewise, the results of a Phase 2 study of B cell depletion (with the anti CD20 antibody rituximab) in SSc-PAH were negative outside of a trend towards increased 6MWD (Zamanian et al., 2021). Furthermore, a Phase 2 trial of targeted anti-IL-6 therapy (tocilizumab) reported no overall efficacy outside of a small subgroup of patients with connective tissue disease (CTD)-associated PAH (Toshner et al., 2022), implying that immunomodulation may only be beneficial in subjects with strong inflammatory phenotypes, or at certain stages in the disease course (Scott et al., 2021). Anakinra, a recombinant IL-1 receptor antagonist, was found to be safe in a short open-label study of subjects with PAH (Trankle et al., 2019), setting the foundation for larger, randomised trials.

1.5.11 Elafin

Elafin is an inhibitor of serine proteases (including neutrophil elastase) that regulates vascular structure by preventing degradation of the ECM (chiefly elastin) and restraining the activity of MMPs (Chun and Yu, 2015). Elafin supplementation restores normal tube formation in HPAECs from subjects with PAH and regresses

occlusive pulmonary artery lesions in rats with severe angioproliferative PH (Nickel et al., 2015). Likewise, overexpression of this protein offsets the development of hypoxic PH (Zaidi et al., 2002). The mechanism of action involves amplification of BMPR2 signalling and heightened production of apelin (Nickel et al., 2015). Results are pending from a Phase 1 study of elafin in individuals with PAH (NCT03522935).

1.5.12 Oxidative stress

Markers of oxidative stress are evident in the plasma, urine and lungs of PAH patients (Irodova et al., 2002; Bowers et al., 2004; Reis et al., 2013) and are associated with unfavourable pulmonary haemodynamics (Cracowski et al., 2001; Zhang et al., 2015). Evidence from animal models suggests the RV is particularly vulnerable to ROS (Redout et al., 2007, 2010; Wang et al., 2017; Pak et al., 2018).

A small open-label trial of the antioxidant coenzyme Q10 in subjects with PAH reported slight improvements in RV haemodynamics, but no alterations in 6MWD (Sharp et al., 2014). At low concentrations, ROS are important regulators of various cellular functions (Di Meo et al., 2016), therefore consensus is building around the need to target specific ROS pathways to achieve a therapeutic effect. One such approach is inhibition of apoptosis signal-regulating kinase 1 (ASK1), a mitogen-activated protein kinase (MAPK) that promotes fibrosis and apoptosis under conditions of oxidative stress (Hayakawa et al., 2012). Whilst pharmacological inhibition of ASK1 demonstrated efficacy against vascular remodelling and right heart fibrosis in experimental models of PH and RVH (Boehm et al., 2015; Budas et al., 2018; Wilson et al., 2020), a phase 2 study of PAH patients failed to show clinical benefit (Rosenkranz et al., 2022).

Bardoxolone methyl is a promising potential therapy for PAH that activates nuclear factor erythroid 2-related factor 2 (Nrf2). Nrf2 reduces ROS by promoting antioxidant gene transcription, repleting ATP reserves, improving the efficiency of oxidative phosphorylation and suppressing activation of the pro-inflammatory factor nuclear factor kappa-light-chain-enhancer of activated B cells (NF-κB; Holmström et al., 2013; Ahmed et al., 2017). A Phase 2 trial of subjects with PAH reported significant improvement in the exercise capacity of the CTD subgroup (Oudiz et al., 2017). Unfortunately, a follow-up trial in patients with CTD-PAH (NCT02657356) and a Phase 3 study to assess long-term safety of bardoxolone

(NCT03068130) were cancelled due to safety concerns relating to clinical visits during the COVID-19 pandemic. A Phase 2 clinical trial of another Nrf2 activator and NF-κB suppressor (CXA-10) was terminated due to lack of efficacy (NCT03449524).

1.5.13 Altered metabolism

PAH is associated with a transition in the metabolism of PASMCs, PAECs and adventitial fibroblasts from oxidative phosphorylation to glycolysis (Bonnet et al., 2006; Xu et al., 2007; Marsboom et al., 2012; Paulin and Michelakis, 2014; Diebold et al., 2015; Li et al., 2016). This metabolic shift ('the Warburg Effect;' Warburg, 1956) was first described in cancer and supports rapid growth and apoptosis avoidance (Paulin and Michelakis, 2014). One hallmark of this process is an increase in the activity of pyruvate dehydrogenase kinase (PDK), an inhibitor of the mitochondrial gatekeeper between glycolysis and the Krebs cycle, pyruvate dehydrogenase (PDH; Piao et al., 2010; Sutendra et al., 2013). Metabolic dysfunction is also evident in the pressure-overloaded RV. Whereas the normal myocardium uses fatty acid oxidation (FAO) as an energy source, the maladapted myocardium reverts to a foetal-like dependence on glucose metabolism (Borgdorff et al., 2015). Furthermore, in parallel to the vasculature, complete oxidation of glucose in the mitochondria is suppressed by PDK upregulation (Piao et al., 2010), reducing O_2 demand at the expense of RV function (Piao et al., 2010; Sutendra et al., 2013).

In an animal model of isolated RV pressure overload, the PDK inhibitor dichloroacetate (DCA) partially restored CO, though even greater improvement in RV function was achieved in an experimental model of PH (Piao et al., 2010), presumably due to a synergistic effect on the pulmonary vasculature (McMurtry et al., 2004). A first-in-human trial of DCA in IPAH reported reductions in mPAP and PVR, and increased RVEF. However, the clinical response to DCA was limited by common single-nucleotide polymorphisms associated with deficiencies in sirtuin 3 (SIRT3) and uncoupling protein 2 (UCP2), which activate PDH in a PDK-independent manner (Michelakis et al., 2017).

Also under investigation are the piperazine derivatives trimetazidine and ranolazine, which promote glucose oxidation by inhibiting FAO, and are approved

for the treatment of chronic stable angina (Guarini et al., 2018). In addition, ranolazine is thought to reduce the inward late Na^+ current in cardiomyocytes and has been shown to alleviate Ca^{2+} overload in failing myocytes, improving RV performance (Hawwa and Menon, 2013). In a model of isolated RVH, ranolazine attenuated RVH, increasing CO and exercise capacity (Fang et al., 2012). In addition to reversing RVH, trimetazidine and ranolazine were unexpectedly found to reverse PVD in multiple experimental models (Sutendra et al., 2010; Rocchetti et al., 2014).

A Phase 1 study of ranolazine in PAH reported reduced RV size and improved RV function (Khan et al., 2015). A second study round no effects on haemodynamics, functional capacity, or RV function, though this may be due to underdosing as the plasma concentration of ranolazine did not consistently reach therapeutic levels (Gomberg-Maitland et al., 2015). Ranolazine has also shown promise in PH associated with heart failure with preserved ejection fraction (HFpEF; Finch et al., 2016). Results of a Phase 4 trial examining the effects of ranolazine on RV function in PAH patients are eagerly awaited (NCT02829034, NCT01839110; Han et al., 2018). Early results from a Phase 2 trial of Trimetazidine indicate significant improvements in RVEF and functional capacity (Sakti Muliawan et al., 2020); a further study is ongoing (NCT02102672).

1.5.14 Systemic metabolism

Insulin resistance is a common co-morbidity of PAH (Zamanian et al., 2009; Benson et al., 2014; Hemnes et al., 2019) and may contribute to the pathogenesis of both PVD and right heart dysfunction. Metformin, the first-line anti-diabetic drug, has beneficial effects in animal models of PAH (Agard et al., 2009; Hemnes et al., 2014; Dean et al., 2016) and PH-HFpEF (Goncharov et al., 2018), which are ascribed to activation of adenosine monophosphate-activated protein kinase (AMPK). The downstream mechanisms through which metformin may work are multiple, including increased eNOS activity, decreased ROCK activity, inhibition of MAPK (Agard et al., 2009) and enhanced RV FAO (Hemnes et al., 2014). A pilot study of CHD-PAH patients found that combination therapy with metformin and bosentan produced a superior reduction in PVR and a greater increase in exercise capacity than bosentan alone (Liao et al., 2018). A Phase 2 trial of metformin in

subjects with PAH reported a modest improvement in RV function (Brittain et al., 2020).

Another systemic metabolic alteration noted in PAH patients is iron deficiency (in the absence of anaemia), which is associated with reduced survival (Krasuski et al., 2011; Rhodes et al., 2011). In animal models, iron deficiency promotes proliferation and apoptosis resistance in PASMCs by enhancing mitochondrial dysfunction and disturbing glycolysis. Correspondingly, pulmonary vascular remodelling can be reversed with iron supplementation (Cotroneo et al., 2015; Lakhal-Littleton et al., 2019). There are reports of increased exercise capacity in open-label studies of iron supplementation in PAH patients (Viethen et al., 2014; Ruiter et al., 2015; Olsson et al., 2020; Ghio et al., 2021), however two recently completed randomised, double-blind, placebo-controlled crossover studies found no benefit (Howard et al., 2021).

1.5.15 Epigenetics

An emerging area of focus is the contribution of epigenetic changes and DNA damage to the pathobiology of PH. Bromodomain-containing protein 4 (BRD4), an epigenetic and transcriptional regulator implicated in cancer (Donati et al., 2018), is upregulated in the lungs, distal pulmonary arteries, and PASMCs of PAH patients. BRD4 upregulates oncogenic genes, including nuclear factor of activated T-cells (NFAT), Bcl-2, survivin, and cyclin-dependent kinase inhibitor 1 (p21), which promote proliferation and apoptosis resistance in PASMCs (Meloche et al., 2015). BRD4 also regulates several key processes related to PH pathophysiology, including inflammation, angiogenesis, oxidative stress, mitochondrial hyperpolarisation and DNA damage (Lin and Du, 2020). Apabetalone, a clinically available inhibitor of bromodomain and extraterminal (BET) proteins, including BRD4, improved pulmonary vascular remodelling, haemodynamics and RV function in experimental models (Van Der Feen et al., 2019b). In an open-label study of subjects with PAH, apabetalone demonstrated improvements in PVR, CO and SV (Provencher et al., 2022). A planned Phase 2 trial will further investigate this efficacy signal (NCT04915300).

The use of alkylating chemotherapeutic agents, which induce DNA damage, has been linked to development of PAH (Perros et al., 2015; Ranchoux et al.,

2015). Oxidative stress and inflammation are known to promote DNA damage, and as discussed previously, are key drivers of pulmonary vascular remodelling (Ranchoux et al., 2015). In the distal pulmonary arteries of PAH patients, DNA damage is accompanied by augmented activity of poly [adenosine diphosphate-ribose] polymerase (PARP)-1, a DNA repair protein that promotes cell survival and proliferation (Krietsch et al., 2012; Meloche et al., 2014). Accordingly, a PARP inhibitor (veliparib) was found to reverse PH in experimental rat models (Meloche et al., 2014). The PARP1 inhibitor olaparib, which is used in the treatment of ovarian cancer (Lorusso et al., 2018), is under investigation in a Phase 1 trial of PAH patients (NCT03782818).

1.5.16 Neurohormones

Various pre-clinical studies have demonstrated that hyperactivity of the sympathetic nervous system and renin-angiotensin-aldosterone system (SNS and RAAS, respectively) contribute to the pathophysiology of PAH and RV failure. Akin to LV failure, stimulation of the pressure-overloaded RV by the SNS and RAAS is initially compensatory, but becomes maladaptive over time (Kimura et al., 2007). In experimental models of PH, β-blockers and RAAS antagonists (mainstay therapies for the management of LV failure) reverse vascular remodelling (Tual et al., 2006; Bogaard et al., 2010; Maron et al., 2012; Preston et al., 2013), facilitate RHRR, and improve RV function (Tual et al., 2006; Okada et al., 2009; Bogaard et al., 2010; De Man et al., 2012; Preston et al., 2013). However, results have not been uniformly positive; the combination of an angiotensin II receptor blocker (ARB) and an aldosterone antagonist or β-blocker proved ineffective in models of both PH and isolated RV pressure overload (Borgdorff et al., 2013; Andersen et al., 2014).

Evidence from small clinical studies suggests that carefully titrated use of β-blockers is safe in stable PAH (i.e. in the absence of decompensated heart failure), but the impact on cardiac function is variable, and there is little improvement in exercise capacity or mortality (Thenappan et al., 2014; Bandyopadhyay et al., 2015; Van Campen et al., 2016; Farha et al., 2017). A post-hoc analysis of the ARIES trials found that PAH patients administered the ET_A inhibitor ambrisentan, and in whom spironolactone use (an aldosterone antagonist) was reported,

demonstrated additional improvement in 6MWD and a greater reduction in plasma BNP concentration (Maron et al., 2013). A further retrospective analysis identified an association between background spironolactone therapy and an increased rate of all-cause hospitalisations, albeit with no difference in hospitalisations for heart failure or PAH (Corkish et al., 2019). One explanation for this finding is that spironolactone use is indicative of baseline disease burden, a possibility also raised by Maron et al. Two large scale trials are in progress to assess spironolactone in PAH and right heart failure (NCT01712620, NCT03344159).

A new avenue of pursuit is recombinant angiotensin converting enzyme (ACE) 2, which functions as a negative regulator of the angiotensin system by metabolising angiotensin II (Ang II) to a putative protective peptide, angiotensin-(1-7; Shenoy et al., 2011). An open-label pilot study of 5 subjects found a single infusion of recombinant human ACE2 was well-tolerated by patients with PAH, and improved CO and plasma markers of oxidative stress and inflammation without altering mPAP or systemic blood pressures (Hemnes et al., 2018). However, a later dose escalation study reported no effect on acute cardiopulmonary haemodynamics (Simon et al., 2022). Larger and longer duration trials are needed to assess effects on vascular remodelling.

1.5.17 Histamine

The number of circulating mast cell progenitors is elevated in PAH patients (Montani et al., 2011; Farha et al., 2012). In accordance, mature mast cells (and progenitors) are found surrounding remodelled arteries (Hamada et al., 1999; Mitani et al., 1999; Farha et al., 2012) and within vascular lesions (Heath and Yacoub, 1991; Mitani et al., 1999; Montani et al., 2011). In animal models, mast cell targeted therapy attenuates pulmonary vascular remodelling when administered early in the disease course, but does not reverse established PH (Baňasová et al., 2008; Dahal et al., 2011; Gambaryan et al., 2011; Bartelds et al., 2012). These findings are supported by a small clinical study (Farha et al., 2012).

Recent focus has shifted to the therapeutic potential of H2R antagonists (H2RAs) in the right heart, due to the positive inotropic and chronotropic effects of H2 receptor (H2R) activation in the myocardium (Bristow et al., 1982). In a large cohort of individuals using H2RAs for gastroesophageal reflux disease (GERD),

lower RV mass and end diastolic volume were reported (Leary et al., 2014). It was subsequently shown that H2RA use for GERD reduces mortality risk by 10% in individuals with PH (Leary et al., 2018). A H2RA (famotidine) is now under investigation in a Phase 2 study of PAH patients (NCT03554291).

1.6 Natriuretic peptides

ANP, BNP and CNP are a family of polypeptide hormones involved in cardiovascular homeostasis. ANP and BNP are primarily expressed in the heart where they are released in response to volume-induced stretch of the atria and ventricles, respectively (Edwards et al., 1988; McGrath et al., 2005; Potter et al., 2006). These peptides function as endocrine hormones, governing blood volume and pressure, and cardiac structure (Fu et al., 2018). CNP, which has a different tissue distribution and mode of action to its siblings, regulates vascular tone and integrity, leukocyte activation, smooth muscle and endothelial cell proliferation, angiogenesis, cardiac hypertrophy and fibrosis, coronary blood flow and heart rate (HR; Moyes and Hobbs, 2019).

Of the natriuretic peptides, CNP is the most structurally conserved across species, including fish, amphibians, birds and mammals (Takei, 2001). In fact, it has been suggested that tandem duplication of an ancestral CNP gene in early evolution gave rise to ANP and BNP (Inoue et al., 2005). As such, all three peptides are encoded by distinct genes, but share a 17 amino acid (aa) disulphide ring with 11 conserved residues that are critical to their biological activity and receptor selectivity (D'Souza et al., 2004; Del Ry et al., 2013). On the other hand, ANP and BNP possess variable length C- and N-terminal tails whilst CNP lacks a C-terminal tail altogether (***Figure 6***).

1.6.1 C-type natriuretic peptide

In 1990, Sudoh et. al isolated a novel natriuretic peptide from porcine brain, which was termed CNP (Sudoh et al., 1990). This peptide is highly expressed in the central nervous system (CNS), by chondrocytes (Chusho et al., 2001), and is constitutively released by ECs (Stingo et al., 1992; Suga et al., 1992b). Other cellular sources include cardiomyocytes (Del Ry et al., 2011), fibroblasts (Horio et al., 2003) and VSMCs (Kelsall et al., 2006). The plasma half-life of CNP is 2-3

minutes (Hunt et al., 1994) and thus the plasma concentration is normally very low (fmol–pmol range; Wei et al., 1993; Sangaralingham et al., 2015), suggesting it functions predominantly as a local paracrine/autocrine regulator (Kuhn, 2004; Volpe et al., 2016). Secretion is stimulated by numerous factors, including shear stress (Chun et al., 1997), inflammatory cytokines (TGF-β, TNF-α and IL-1β; Suga et al., 1993; Mendonça et al., 2010), and bacterial lipopolysaccharide (Suga et al., 1993). ANP and BNP can also stimulate CNP production (Nazario et al., 1995), and this may account for some of their biological activity. In contrast, CNP release is attenuated by oxidised low-density lipoprotein (Sugiyama et al., 1995) and VEGF (Doi et al., 1996).

The human gene encoding CNP (*NPPC*) is located on chromosome 2 and consists of only two exons and one intron (Ogawa et al., 1994). The peptide is secreted as preproCNP (126 aa; Tawaragi et al., 1991), which is processed by a signal peptidase to form proCNP (103 aa) and then cleaved by the endoprotease furin, forming mature CNP-53 (53 aa; Wu et al., 2003). CNP-53 is further processed by an unknown protease to the shorter, more abundant CNP-22 (22 aa; Moyes and Hobbs, 2019). Though the two forms have comparable activity and function, CNP-53 is largely found in the brain (Brown et al., 1997), endothelium (Stingo et al., 1992) and heart (Minamino et al., 1991), whereas CNP-22 predominates in cerebral spinal fluid and plasma (Togashi et al., 1992). Notably, there is considerable interspecies homology in CNP; the mouse, rat, dog and chimp genes share 91-99% homology with *NPPC*, and the mature circulating (22 aa) peptide is completely identical in these species (Potter et al., 2009).

Endothelial-specific deletion of murine CNP leads to a significantly elevated mean arterial blood pressure (MABP) and impaired responses to endothelium-dependent vasodilators (Moyes et al., 2014; Nakao et al., 2017), suggesting the local action of CNP on vascular tone makes an important contribution to the regulation of blood pressure. Indeed, single nucleotide polymorphisms (SNPs) in the CNP and furin genes are associated with hypertension (Ono et al., 2002; Li et al., 2010). Outside the cardiovascular system, CNP plays an essential role in bone growth and thus transgenic mice with a global deficiency of the peptide exhibit dwarfism (Chusho et al., 2001; Komatsu et al., 2002).

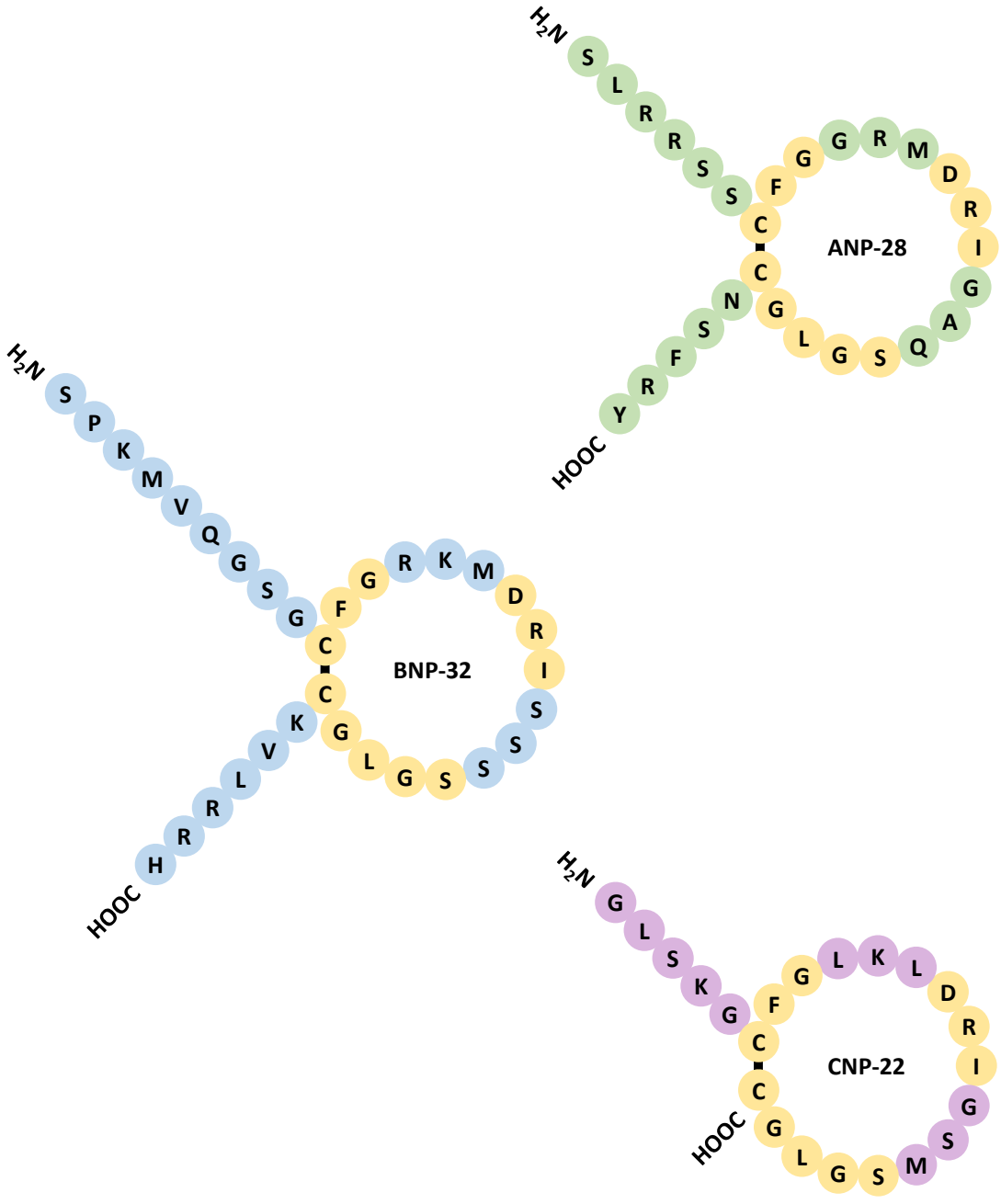

Figure 6: Amino acid structures of the natriuretic peptides

Atrial natriuretic peptide (ANP), Brain natriuretic peptide (BNP), and C-type natriuretic peptide (CNP). Residues shown in yellow are conserved across all three peptides. Disulphide bonds are indicated by black lines.

1.7 Natriuretic peptide receptor signalling

The biological effects of natriuretic peptides are mediated by binding to a family of three transmembrane natriuretic peptide receptors (NPRs): NPR-A, NPR-B, and NPR-C. NPRs are homodimeric and exhibit high homology in their relatively large (~450 aa) extracellular ligand binding domain and single membrane-spanning region of about 20 residues (Potter et al., 2009). CNP exerts its biological effects via NPR-B and NPR-C, which activate distinct signalling pathways (Potter et al., 2006; ***Figure 7***). The peptide has the highest binding affinity for NPR-C, closely followed by NPR-B, and very low affinity for NPR-A, the endogenous receptor for ANP and BNP (He et al., 2006).

1.7.1 Natriuretic peptide receptor B

The human NPR-B gene (*NPR2*) is located on chromosome 9 (Lowe et al., 1990) and consists of 22 exons and 21 introns (Tamura and Garbers, 2003), producing a 1,047 aa protein (Kone, 2001). NPR-B is localised to the brain, vasculature, kidney, adrenal glands, and cartilage (Llis et al., 1998; Kone, 2001; Schulz, 2005). Akin to NPR-A, this receptor possesses a large intracellular domain comprising of a kinase homology domain, a dimerisation domain and a C-terminus guanylyl cyclase (GC) domain (Misono, 2002; Misono et al., 2011).

CNP selectively binds NPR-B with fifty or five hundred-fold greater affinity than ANP or BNP, respectively (Koller et al., 1991). Receptor activation involves a conformational change that disinhibits GC functionality by the kinase homology domain (Ogawa et al., 2004). Subsequent conversion of guanosine-5'-triphosphate (GTP) to the second messenger cGMP leads to altered cellular function via phosphorylation of specific target proteins by PKG I and II (Koller et al., 1991; Miyazawa et al., 2002; Schlossmann et al., 2005). Downstream regulatory proteins underpinning the biology activity of natriuretic peptides include cGMP-regulated PDEs, cGMP-gated ion channels and cGMP-dependent protein kinases (Garbers et al., 1994; Misono et al., 2011).

NPR-B is highly phosphorylated (Potter and Hunter, 1998) and dephosphorylation by prolonged CNP exposure, elevated $[Ca^{2+}]_{cyt}$, or activation of protein kinase C (PKC) results in reduced receptor activity (Potter, 1998; Potter and Hunter, 2000; Potthast et al., 2004). In mice, targeted disruption of the NPR-B

gene results in dwarfism and female sterility, with preserved vascular function and blood pressure. As extensive cardiovascular phenotyping of these mice is precluded by severe skeletal malformation and premature death (Tamura et al., 2004), NPR-B dominant negative mutant transgenic rats were generated. These animals exhibit a mild growth retardation of the long bones, in addition to blood pressure-independent cardiac hypertrophy and elevated HR (Langenickel et al., 2006). More recently, cell-restricted NPR-B knockout (KO) mice have been described. Targeted disruption of NPR-B under the control of the PDGFRβ promotor results in a hypertensive phenotype, suggesting that CNP regulates peripheral vascular resistance by facilitating paracrine communications between ECs and pericytes (Špiranec et al., 2018). Basal cardiac morphology and function are preserved in cardiomyocyte-specific NPR-B KO mice, but pressure overload results in a mild diastolic dysfunction driven by increased cardiomyocyte stiffness (Michel et al., 2020).

1.7.2 Natriuretic peptide receptor C

The human NPR-C gene (*NPR3*), comprising 8 exons and 7 introns, is located on chromosome 5 and encodes a 540 aa acid protein (Lowe et al., 1990; Rahmutula et al., 2002). This receptor has a large extracellular ligand-binding domain that shares ~30% homology with NPR-A and NPR-B, and a small 37 aa intracellular region (Porter et al., 1990; Anand-Srivastava, 2005). Notably, NPR-C lacks GC activity and thus was historically considered a clearance receptor only (Maack et al., 1987; Matsukawa et al., 1999; Potter et al., 2009). However, this dogma was challenged by the discovery of overlapping *Pertussis* toxin sensitive $G_{i/0}$ binding sequences in the C-terminal tail (Pagano and Anand-Srivastava, 2001). These sequences couple to adenylyl cyclase inhibition (via the G_i α subunit) and PLC-β activation (via G_i βγ subunits; Hirata et al., 1989; Anand-Srivastava et al., 1996; Murthy and Makhlouf, 1999; Murthy et al., 2000; Pagano and Anand-Srivastava, 2001), indicating direct signalling activity.

NPR-C possesses high affinity for all three natriuretic peptides, with a selectivity profile of ANP > CNP > BNP (Suga et al., 1992a). The receptor is predominantly expressed in major endocrine glands, the lungs, the kidneys, and the vascular wall (Kone, 2001), constituting >90% of the total NPR population in

some tissues (Maack, 1992). On a cellular level, NPR-C is highly concentrated on ECs (Leitman et al., 1986). There is speculation that the seemingly divergent functions of this receptor (i.e. clearance versus signalling) emanate from multiple bindings sites, or different receptor subpopulations (Savoie et al., 1995). In support of this notion, a study in isolated rat glomerular membranes reported the existence of two NPR-C subtypes, a 67 kDa receptor that couples to G_i proteins, and a 77 kDa receptor involved in ligand internalisation, with lower affinity for CNP (Brown and Zuo, 1994).

Global deletion of NPR-C prolongs the plasma half-life of ANP without altering the plasma concentration of the peptide, resulting in mild diuresis, diluted urine, and blood volume depletion (Matsukawa et al., 1999). Furthermore, NPR-C KO mice demonstrate increased bone turnover and growth, producing striking skeletal abnormalities (Jaubert et al., 1999; Matsukawa et al., 1999). It is proposed that this is an indirect effect secondary to reduced CNP clearance and increased activation of NPR-B (Lumsden et al., 2011). Interestingly, male NPR-C KO mice are hypotensive (Matsukawa et al., 1999; Moyes et al., 2014), indicative of reduced natriuretic peptide clearance, yet female mice are hypertensive, suggestive of deficient CNP signalling (Moyes et al., 2014). Still, a genome-wide association study (GWAS) linking NPR-C variants with hypertension did not reveal a sex disparity (Ehret et al., 2011). On the other hand, an SNP in the NPR-C gene that results in diastolic dysfunction has been identified. Altered downstream signalling is proposed to drive excessive fibroblast proliferation, increasing myocardial stiffness (Pereira et al., 2014).

1.7.3 Natriuretic peptide inactivation

Natriuretic peptide inactivation is driven by two main pathways: NPR-C-mediated internalisation (Kenny et al., 1993; Watanabe et al., 1997) and cleavage by neutral endopeptidase (neprilysin, NEP; Cohen et al., 1996). Under normal conditions, each pathway appears to contribute equally to clearance (Charles et al., 1996). However, when NPR-C is saturated due to pathological (e.g. heart failure) or pharmacological elevations in circulating natriuretic peptides, NEP activity is enhanced (Hashimoto et al., 1994).

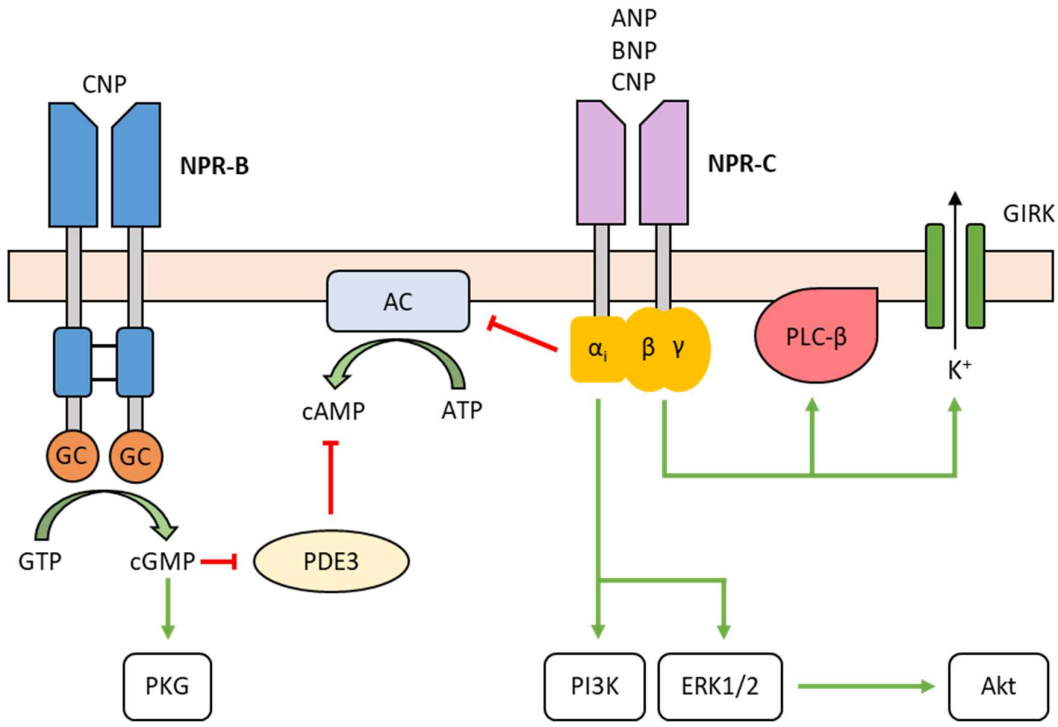

Figure 7: Schematic representation of CNP-receptor signalling

The cellular effects of CNP are mediated via two cognate receptors, NPR-B and NPR-C. NPR-B is a particulate guanylyl cyclase receptor and stimulation results in the production of cGMP and the activation of protein kinase G (PKG) I. NPR-C is a G_i protein-linked receptor that modulates various intracellular enzymes including adenylyl cyclase (AC), phospholipase (PLC)-β, extracellular signal-related kinase (ERK) 1/2, phosphoinositide-3-kinase (PI3K), and protein kinase B (Akt). NPR-C activation also triggers the opening of G-protein-gated inwardly rectifying potassium (GIRK) channels. Crosstalk occurs between the two receptor signalling pathways via cGMP-mediated inhibition of phosphodiesterase (PDE) 3, the enzyme responsible for the hydrolysis of cAMP.

1.7.3.1 *Receptor-mediated clearance*

Receptor-based clearance systems are relatively uncommon for cardiovascular signalling peptides (ET-1 being the other notable example), which tend to be preferentially degraded by extracellular proteases, like NEP (Potter, 2011). NPR-C mediated internalisation and degradation follows similar mechanics to those of other clearance receptors: peptide binding is proceeded by endocytosis, lysosomal ligand degradation, and shuttling of the free receptor back to the plasma membrane (Volpe et al., 2016). NPR-C internalisation is a constitutive process that occurs even in the absence of ligand, at a rate comparable to that of clearance and transport receptors endocytosed by clathrin-coated pits. However, NPR-C lacks cytoplasmic internalisation motifs common to other receptors internalised in this way (Nussenzveig et al., 1990; Cohen et al., 1996).

1.7.3.2 *Neutral endopeptidase*

NEP is an extracellular membrane-bound zinc-dependent metalloproteinase that cleaves peptides at the amino side of hydrophobic residues (Kerr and Kenny, 1974). Of the natriuretic peptides, CNP is particularly susceptible to degradation by NEP (Kenny et al., 1993; Gardner et al., 2007), which may underpin its short half-life (Hunt et al., 1994). Several other peptides are also inactivated by this enzyme, including Ang II, ET-1, substance P, neurotensin, oxytocin, and bradykinin (Whyteside and Turner, 2008). NEP is particularly abundant in the kidneys, lungs, and heart, and is widely expressed on the surface of ECs, VSMCs, cardiomyocytes, fibroblasts, and neutrophils (Mangiafico et al., 2013).

1.8 Prospective role for CNP in pulmonary hypertension

A significant body of evidence suggests that endogenous natriuretic peptides have protective effects in the context of PH. Firstly, the development of PH is exacerbated in NPR-A KO mice (Zhao et al., 1999, 2003; Klinger et al., 2002), and the beneficial effects of PDE5 inhibition on pulmonary vascular remodelling and RVH are blunted in these animals, indicating that the favourable actions of cGMP are predominantly mediated by natriuretic peptides (Zhao et al., 2003). In further support of this notion, NEP inhibition boosts the efficaciousness of PDE5 inhibitors in models of hypoxic and pulmonary fibrosis-associated PH (Baliga et al., 2008,

2014); this positive pharmacodynamic effect is also diminished in NPR-A KO mice (Baliga et al., 2014). By virtue of these findings, the NEP inhibitor racecadotril was recently examined in a randomised, double-blind, placebo-controlled Phase 2a trial of PAH patients on stable PDE5 inhibitor therapy. Racecadotril augmented plasma ANP levels to synergise with PDE5 inhibition, evoking a greater increase in plasma cGMP, and a greater reduction in PVR, than PDE5 inhibition alone (Hobbs et al., 2019).

Akin to ANP, evidence points to a protective role for CNP in the cardiopulmonary circuit, particularly in the context of PH. In patients requiring cardiac catheterisation for cardiovascular morbidities, circulating CNP strongly correlates with PAP (Palmer et al., 2009). In addition, experimental PH models exhibit elevated plasma CNP, decreased levels of the peptide in the lung (Klinger et al., 1998a), and NPR downregulation in the RV (Kim et al., 1999), indicating that PH is associated with deficient CNP signalling. Compared to ANP, CNP more potently inhibits VSMC proliferation by eliciting greater cGMP production in these cells (Hutchinson et al., 1997). CNP also has superior cGMP synthesising capability in the RV endocardium, where NPR-B is the major GC-coupled NPR (Kim et al., 1999). These observations suggest that CNP has greater potential to harness the disease-modifying actions of cGMP-dependent signalling.

Beyond the CNP/NPR-B axis, novel homeostatic roles for NPR-C signalling were recently identified in the systemic circulation, including modulation of vascular and cardiac remodelling (Moyes et al., 2014, 2020). In the vasculature, the biological activity of the CNP/NPR-C axis is increased when the NO signalling pathway is inhibited or lost (Wright et al., 1996; Hobbs et al., 2004), such that the effects of CNP may be amplified in the hypertensive pulmonary vasculature. Furthermore, NPR-C is even more highly expressed than NPR-B in the RV (Kim et al., 1999). Though these findings suggest CNP may regulate pulmonary arterial pressure and RV function through cGMP-dependant and cGMP-independent effects, a direct role in the pathophysiology of PH has yet to be identified.

1.9 Working hypothesis and specific aims

This thesis describes studies aimed at elucidating the role(s) of CNP in regulating cardiopulmonary pressure, structure, and function, in health, and in the context of PH. Specifically, I tested the following principal hypotheses:

1. Genetic deletion of CNP worsens disease severity in experimental PH
2. Administration of exogenous CNP alleviates experimental PH

To investigate these hypotheses, the following aims were addressed:

Chapter III:

- To establish how the expression of CNP/NPRs is altered in experimental PH
- To assess pulmonary vascular reactivity to CNP and cANF$^{4-23}$ in vessels isolated from healthy mice and animals with PH
- To assess cardiopulmonary pressure and RV structure in mice with a global CNP deficiency, in health, and following the induction of PH

Chapter IV:

- To define the contribution of different cellular sources of CNP (endothelial, cardiomyocyte) to the actions of the peptide in the pulmonary circulation and RV using cell-restricted CNP KO mouse strains
- To identify the NPR subtype(s) that underpins the bioactivity of CNP (identified in the previous aim) using a global NPR-C KO mouse strain

Chapter V:

- To evaluate the propensity of exogenous CNP to reverse experimental PH
- To provide further evidence of the cognate receptor(s) responsible for the actions of CNP in the cardiopulmonary circulation by administering the peptide to global NPR-C KO mice
- To assess the impact of CNP treatment on pulmonary haemodynamics and RV structure/function in mice with experimental PH

Chapter II: Methods

2.1 Genetically modified animals

All animal procedures were conducted in accordance with the UK Home Office Animals (Scientific Procedures) Act of 1986, adhered to ARRIVE (Animal Research: Reporting of *In Vivo* Experiments) guidelines, and were approved by a local animal welfare and ethical review board. Power calculations were undertaken prospectively based on the principal endpoint of RVSP. In the SuHx mouse model, the average standard deviation (SD) for RVSP is 5%. As such, 8 animals per group are required to detect a 5 mmHg change in RVSP with a power of 80%. The sample size for biochemical and histological analyses was influenced by the need to divide tissue samples for either freezing or fixation.

2.1.1 Generation

Nppc LoxP-flanked mice (*Nppc*$^{fl/fl}$) mice were generated in-house using a targeting vector constructed with 2 LoxP sites flanking the entire peptide coding region for CNP in exons 1 and 2 (Moyes et al., 2014). These mice were subsequently crossed with animals expressing either a tamoxifen-inducible ubiquitin C (UBC)-driven Cre-ERT2 fusion gene (UBC-Cre/ERT2; Perez-Ternero et al., 2022), an angiopoietin Tie^2 receptor-driven Cre recombinase (Moyes et al., 2014), or an α-MHC-driven Cre recombinase (a kind gift of Prof. M. Schneider, Imperial College London; Moyes et al., 2020), to produce *Nppc*$^{fl/fl}$ UBC-Cre/ERT2$^+$ (global CNP KO), *Nppc*$^{fl/fl}$ Tie^2-Cre$^+$ (endothelial-specific CNP KO), and Nppc$^{fl/fl}$ αMHC-Cre$^+$ (cardiomyocyte-specific CNP KO) mice, respectively. Global NPR-C KO mice were a kind gift of Prof. Oliver Smithies (University of North Carolina, USA; Matsukawa et al., 1999). Wildtype (WT) littermates (Nppc$^{+/+}$ Cre$^-$ or Nppc$^{+/+}$ Cre$^+$) were used as controls. All animals were based on a C57BL/6 genetic background.

2.1.2 Genotyping

Genomic DNA was prepared from ear biopsies for analysis by polymerase chain reaction (PCR). Ear clips were digested in 25 mM NaOH (75 µl) for 30 min at 85°C before neutralisation with 40 mM Tris-HCl (75 µl). For each PCR reaction, a master mix was created, composed of MyTaq^{TM} Red Mix (Bioline 25044, London, UK) biomix, primers (see ***Table 4***), genomic DNA and nuclease-free H_2O, in a total volume of 25 µl (for further details, see ***Table 5***). PCRs were conducted using a

thermal cycler (Bio-Rad S1000, UK); conditions for each reaction are listed in ***Table 6***.

PCR products were loaded into wells on a 2% agarose gel made with tris-acetate-EDTA (TAE) buffer (2M tris acetate and 100 mM EDTA; Fisher Scientific, Loughborough, UK) and containing Midori Green nucleic acid stain (5 µl/100 ml gel; Nippon Genetics, Europe). The gel was run for 1 h at 100 mV and the bands were visualised under UV light using the G:BOX Chemi XRQ gel documentation system (Syngene, Cambridge UK). KO animals were identified by the presence of a 956 base pair (bp) floxed CNP band (as opposed to an 842 bp WT band), plus either a 700 bp UBC-Cre/ERT2 band, a 512 bp Tie^2-Cre band, or a 990 bp αMHC-Cre band.

2.1.3 Tamoxifen administration

In tamoxifen-inducible gbCNP$^{-/-}$ animals, gene deletion was achieved by injecting tamoxifen (Sigma, Poole, UK) at 6-8 weeks of age for five consecutive days (40 mg/kg/day, i.p.). Tamoxifen was prepared in a mixture of 90% sunflower oil and 10% absolute ethanol, wrapped in foil to avoid light, and heated on a heating block at 50-55°C for 5 min, or until the crystals were completely dissolved. To control for any adverse effects associated with tamoxifen administration, WT controls were also injected, and a recovery period of 2 weeks was allowed prior to use in experiments.

Table 4: Nucleic acid sequences of primers used in genotyping

Target		Primer Sequence (5'-3')
Floxed CNP	Forward:	TGCAGAAGTGCAGTGCTCTGTGTACTTG
	Reverse:	GCAAACTGAAAATTCAAGTCCTCAGACTCC
UBC-Cre/ERT2	Forward:	ATCCGAAAAGAAAACGTTGA
	Reverse:	ATCCAGGTTACGGATATAGT
Tie^2-Cre	Forward:	CCCTGTGCTCAGACAGAAATGAG
	Reverse:	CGCATAACCAGTGAAACAGCATTGC
αMHC-Cre	Forward:	CCAATTTACTGACCGTACACC
	Reverse:	GTTTCACTATCCAGGTTACGG
NPR-C	Forward:	CTTGGATGTAGCGCACTATGTC
	Reverse:	CACAAGGACACGGAATACTC
	NEO:	ACGCGTCACCTTAATATGCG

A, adenine; C, cytosine; G, guanine; T, thymine; NEO, neomycin.

Table 5: Polymerase chain reaction components

Target	*Biomix (µl)*	*Forward Primer (µl)*	*Reverse Primer (µl)*	*NEO primer (µl)*	*Nuclease-free water (µl)*	*Sample DNA (µl)*
Floxed CNP	12.5	2	2	-	5.5	3
UBC-Cre/ERT2	12.5	2.5	2.5	-	4.5	3
Tie^2-Cre	12.5	2	2	-	5.5	3
αMHC-Cre	12.5	2.5	2.5	-	4.5	3
NPR-C	12.5	0.5	0.5	0.5	8	3

The total volume for each reaction was 25 µl. The working stock concentrations for each primer were as follows: floxed CNP, 100 µM; Tie^2, 10 µM; α-MHC Cre, 10 µM; NPR-C, 2.5 µM.

Table 6: Polymerase chain reaction protocols

	Step	Temp	Time	Number of cycles
Floxed CNP	Initial denaturation	94°C	10 min	Hold
	Denaturation	94°C	30 s	35
	Annealing	60°C	30 s	
	Polymerisation	68°C	1 min	
	Extension	68°C	10 min	Hold
UBC-Cre/ERT2	Initial denaturation	93°C	1 min	Hold
	Denaturation	93°C	20 s	35
	Annealing	68°C	3 min	
	Polymerisation	72°C	1 min	
	Extension	72°C	10 min	Hold
Tie^2-Cre	Initial denaturation	95°C	10 min	Hold
	Denaturation	95°C	30 s	40
	Annealing	58°C	1 min	
	Polymerisation	72°C	1 min	
	Extension	72°C	10 min	Hold
αMHC-Cre	Initial denaturation	94°C	2 min	Hold
	Denaturation	94°C	1 min	35
	Annealing	60°C	1 min	
	Polymerisation	72°C	1 min	
	Extension	72°C	5 min	Hold

Table 6: continued

	Step	Temp	Time	Number of cycles
NPR-C	Initial denaturation	95°C	5 min	Hold
	Denaturation	93°C	1 min	35
	Annealing	60°C	1 min	
	Polymerisation	72°C	1 min	
	Extension	72°C	10 min	Hold

2.2 Sugen + hypoxia model

2.2.1 Overview

Male and female global (gbCNP$^{-/-}$), endothelial-specific (ecCNP$^{-/-}$), and cardiomyocyte-specific (cmCNP$^{-/-}$) CNP KO mice, and global NPR-C KO (NPR-C$^{-/-}$) animals, were used to investigate the role of CNP signalling in experimental PH. WT controls were colony-mates and littermates where possible. Mice aged 7-11 weeks were injected with the VEGF receptor-2 (VEGFR-2) antagonist, Sugen 5416 (SU5416, Sugen; 20 mg/kg, s.c.; synthesised in-house), and exposed to chronic normobaric hypoxia (collectively referred to as SuHx) for five weeks in a ventilated plexiglass chamber. The O_2 level was maintained at 10% by a controlled purge system (Plas Labs MI, USA). Mice received additional injections of SU5416 (20 mg/kg, s.c.) one- and two-weeks post hypoxia induction. Age-matched normoxic (NmOx) control mice were housed in room air (21% O_2) and administered vehicle (see below for details). The experimental time course is summarised in ***Figure 8***.

2.2.2 Sugen preparation

SU5416 was suspended in a mixture of carboxymethylcellulose (CMC; 0.5% w/v; Sigma Aldrich, UK), sodium chloride (NaCL; 0.9% w/v; Sigma Aldrich, UK), polysorbate 80 (Tween 80; 0.4% v/v; Sigma Aldrich, UK), and benzyl alcohol (0.9% v/v; Sigma Aldrich, UK) in double distilled water (ddH_2O). To produce a uniform suspension, the mixture was vigorously vortexed and sonicated for 6 min.

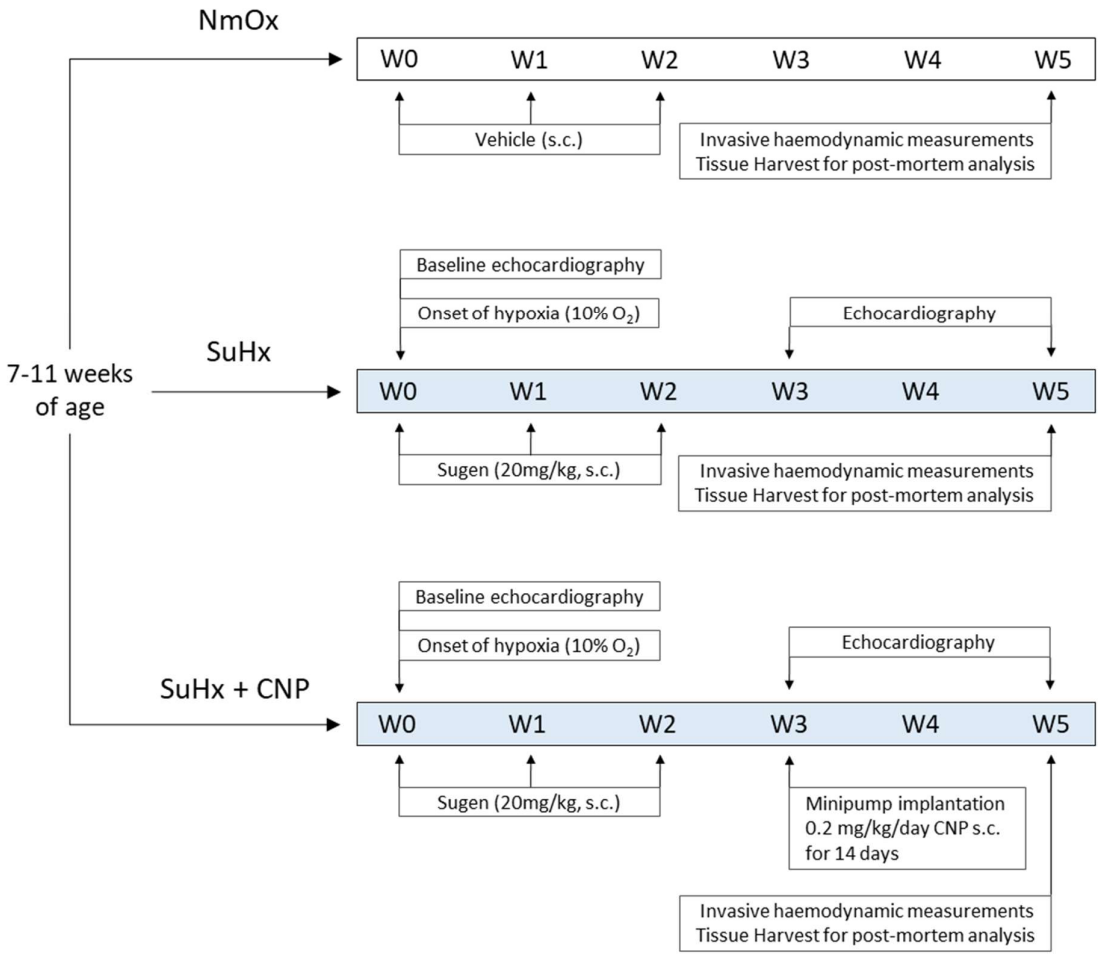

Figure 8: Experimental time-course for the SU5416/hypoxia model of PH

Normoxic (NmOx) control mice were housed in standard laboratory conditions (21% O_2) and administered vehicle (10 ml/kg, s.c.) on weeks 0, 1 and 2. SU5416/hypoxia (SuHx) animals were dosed with SU5416 (20 mg/kg; 10 ml/kg; s.c.) on week 0 and were subsequently placed inside a normobaric hypoxia chamber (10% O_2) for five weeks. Additional doses of SU5416 (20 mg/kg; 10 ml/kg; s.c.) were administered on weeks 1 and 2. Some mice underwent baseline echocardiography prior to SuHx exposure, and on weeks 3 and 5, to map disease progression. SuHx + CNP mice were implanted with an osmotic minipump containing CNP (0.2 mg/kg/day, s.c., for 14 days, following echocardiography on week 3. All animals (regardless of treatment group) underwent invasive haemodynamic measurements on week 5 to determine right ventricular systolic pressure and mean arterial blood pressure and were subsequently culled humanely for tissue collection.

2.3 Administration of CNP

In some experiments, male WT and NPRC$^{-/-}$ mice were delivered a continuous infusion of CNP by osmotic minipump (s.c.) for 14 days (0.2 mg/kg/day), initiated after three weeks of hypoxic exposure. This dose was previously shown to have sub-pressor efficacy against vascular and cardiac remodelling (Bubb et al., 2019; Moyes et al., 2020). The aim of these experiments was to explore the therapeutic potential of CNP in PH and examine the effects of receptor specific CNP signalling.

2.3.1 Minipump preparation

CNP (Genescript, New Jersey, US) was reconstituted at the desired concentration (based on the bodyweight of the animals) in 5% dextrose (Sigma Aldrich, UK). Osmotic minipumps (Azlet, model 1002; California, USA) were filled with CNP solution (100 µl) in an aseptic laminar flow hood. A flow moderator was inserted into the pump which was then submerged in saline and placed in an incubator overnight at 37°C to equilibrate.

2.3.2 Implantation

Mice were anesthetised with isoflurane (4%, 0.8 ml/min O_2; Abbott Laboratories Ltd, Queenborough, UK) and placed supine on a thermostatically regulated heating mat (TCAT-2LV Controller; Physitemp, Norfolk, UK) maintained at 37°C. Isoflurane delivery was reduced to 2 ± 0.5% and the upper right flank of the mouse was prepared with depilatory cream (Veet; Hull, UK). The patch of skin was then disinfected with chlorhexidine (Vetasept®; Animalcare Ltd, York, UK), and 100 µl buprenorphine (vetergesic®, 0.03 mg/ml, s.c.; Centeur, Somerset, UK) was administered at the surgical site for post-operative pain relief.

A small skin incision was made under sterile conditions, and a pair of blunt tip scissors were introduced. The skin and muscle layers were separated down to the most caudal right ventral region of the mouse by blunt dissection, creating a subcutaneous pocket which was irrigated with sterile saline. Next, the minipump was inserted into the subcutaneous space with the flow moderator facing away from the incision site and carefully guided into a caudal position by gentle manipulation of the skin. Once the pump was in-situ, the incision was closed with 6.0 absorbable sutures (Vicryl, Ethicon, USA). A tissue adhesive (3M™ Vetbond™,

St. Paul, USA) was used to seal the wound and prevent reopening, and a local anaesthetic cream (EMLA™, 5% lidocaine/prilocaine, APP Pharmaceuticals, UK) was applied. Animals were recovered on a heat pad and monitored closely for three days.

2.4 Echocardiography

Pulmonary artery function and cardiac morphology/function were assessed by echocardiography using the Visualsonics Vevo 3100 ultrasound system, and a MX550D probe (32-55 MHz frequency). Baseline recordings were taken prior to hypoxic exposure. Further recordings were taken after 3 and 5 weeks of hypoxic exposure, to map disease progression.

Mice were anesthetised in an induction chamber with isoflurane (4%, 0.8 ml/min O_2; Abbott Laboratories Ltd, Queenborough, UK) before placement on a heated platform. Body temperature was maintained at 37°C and anaesthesia delivered by nose cone (1-2% isoflurane, 0.8 ml/min O_2). Conduction gel was applied to all four paws, which were then attached to electrocardiogram (ECG) pads. The chest was prepared for imaging using depilatory cream (Veet; Hull, UK), followed by a small amount of ultrasound gel (Aquasonic, Parker; the Netherland).

The pulmonary artery was visualised first, in B mode, using a modified left parasternal long-axis view. Colour Doppler was used to pinpoint the region with greatest flow, and pulsed wave (PW) Doppler was employed to assess pulmonary artery outflow (***Figure 9***). Then, the LV was imaged in B-Mode using a left parasternal short-axis view and M-mode imaging was employed to assess wall motion (***Figure 10***). Next, the RV was visualised in B mode using a right parasternal long-axis view and M-mode was used to assess motion of the RV free wall (***Figure 11***). Finally, the apical-4 chamber view was obtained in B-Mode. Colour Doppler and PW Doppler were used to assess flow across the tricuspid valve (TV), and TV motion was visualised by placing the M-Mode sample volume through the lateral annulus of the TV plane (***Figure 12***).

Analysis was carried out using the Vevo LAB 5.5.0 software. Each parameter was measured three times, and a mean value taken. Parameters assessed in the current study are detailed in ***Table 7***.

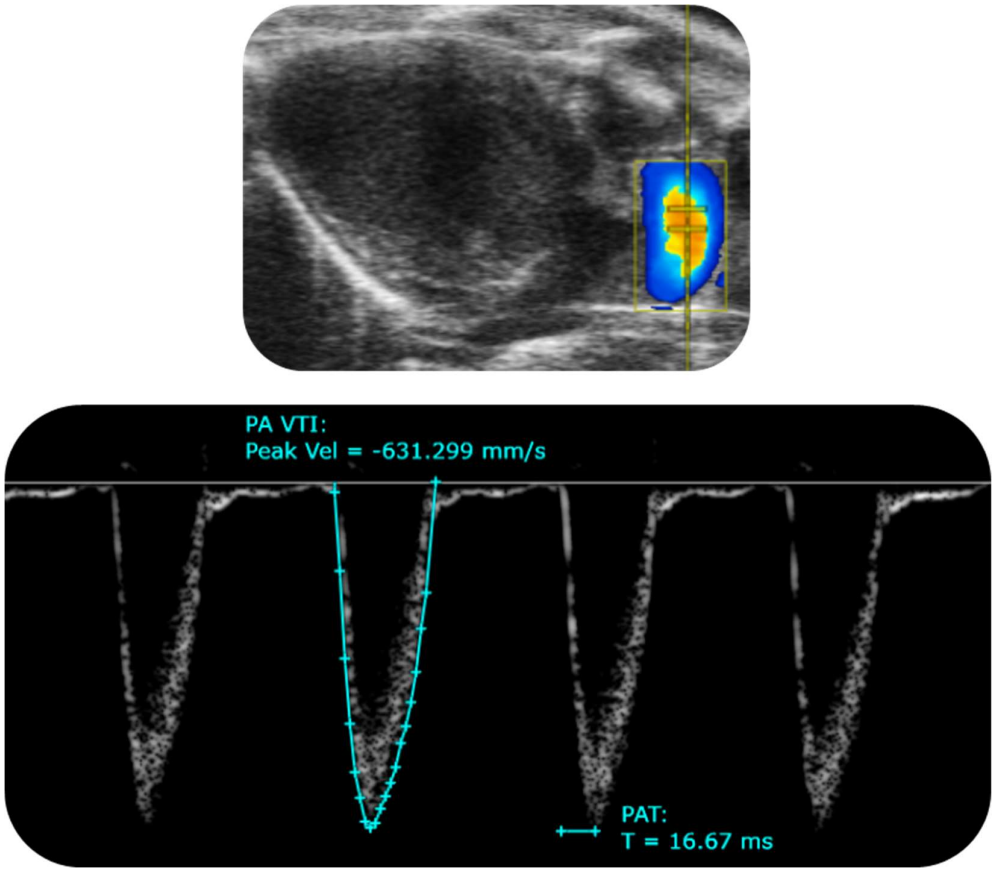

Figure 9: Assessment of pulmonary artery function using echocardiography

Top: colour Doppler of the pulmonary artery in a modified left parasternal long-axis view, with positioning of the pulsed wave Doppler sample volume indicated in yellow. Bottom: pulsed wave Doppler of pulmonary outflow, with measurement of pulmonary acceleration time (PAT) and pulmonary artery velocity time integral (PA VTI) peak velocity (Peak Vel) denoted.

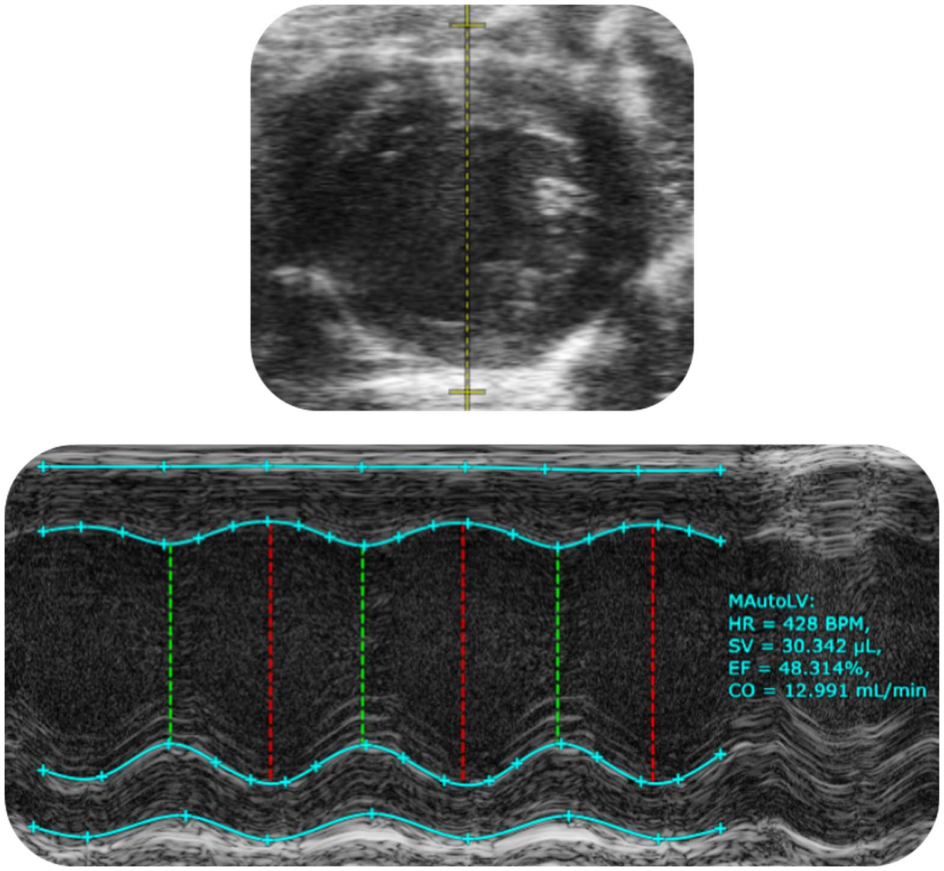

Figure 10: Assessment of left ventricular function using echocardiography

Top: left parasternal short axis view with M-mode sample volume placement indicated in yellow. Bottom: M-mode of the left ventricle, showing assessment of LV function using the 'autoLV' tool. HR, heart rate; SV, stroke volume; EF, ejection fraction; CO; cardiac output.

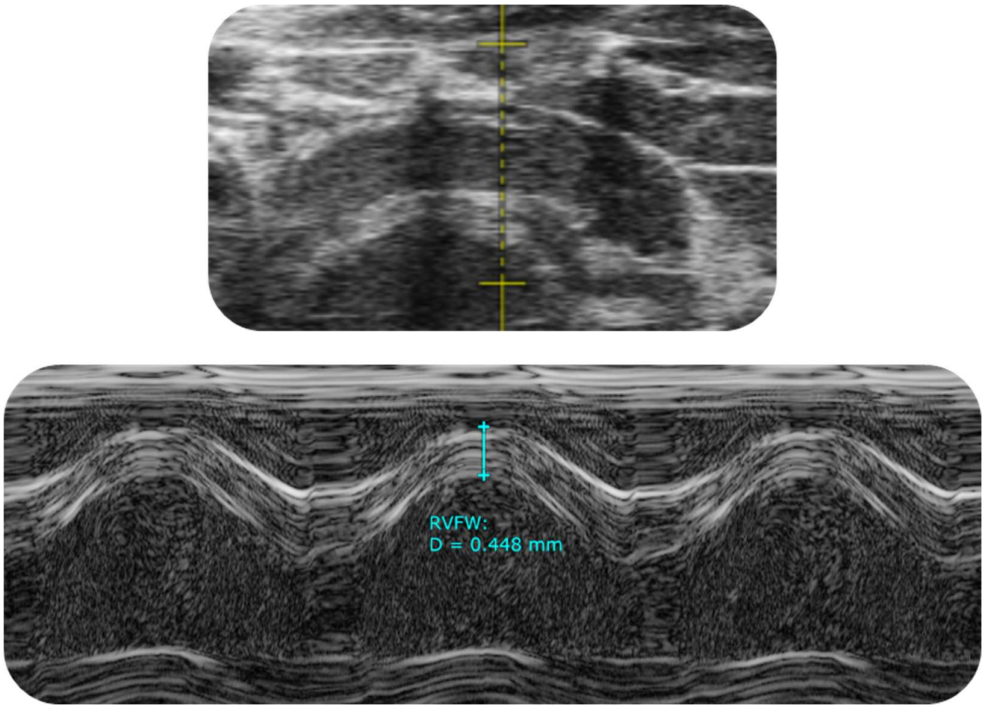

Figure 11: Assessment of right ventricular structure using echocardiography

Top: right parasternal long axis view of the heart with M-mode sample volume placement indicated in yellow. Bottom: M-mode of the right ventricular free wall (RVFW), showing measurement of wall thickness.

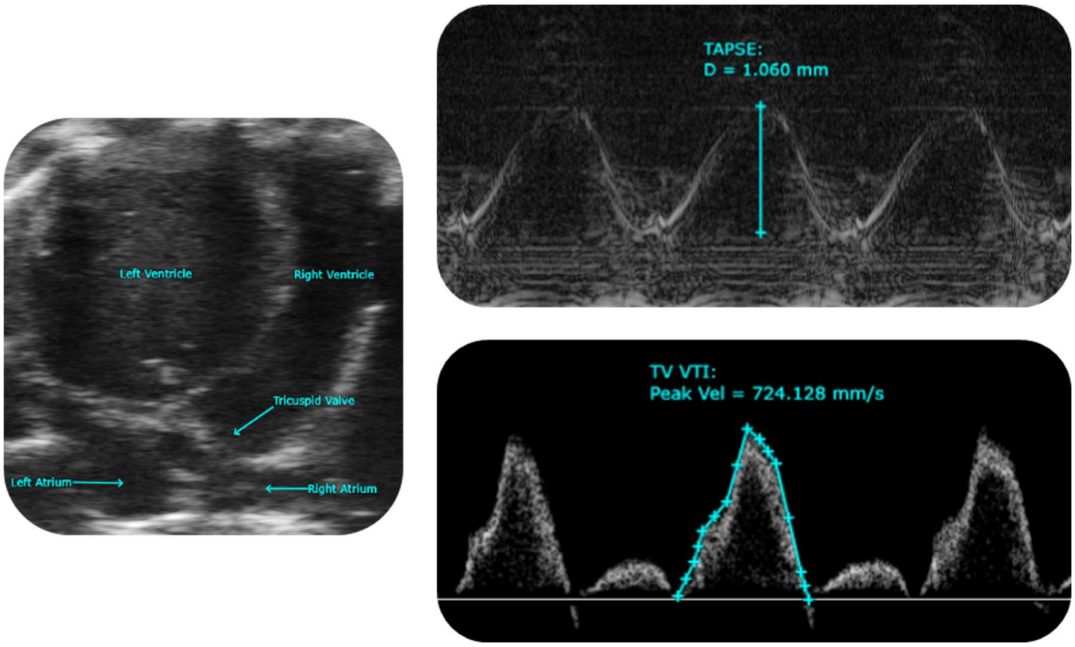

Figure 12: Assessment of right ventricular function using echocardiography

Left: apical four chamber view of the heart. Top right: M-mode of the tricuspid valve, showing measurement of tricuspid annular plan systolic excursion (TAPSE). Bottom right: pulsed wave Doppler of tricuspid outflow, showing measurement of tricuspid valve velocity time integral (TV VTI) peak velocity (Peak Vel).

Table 7: Summary of parameters assessed using echocardiography

Parameter	Units	Description
Pulmonary acceleration time (PAT)	ms	Interval between the onset of flow and peak flow through the pulmonary artery
Pulmonary artery peak velocity	mm/s	Peak velocity of flow through the pulmonary artery
Diastolic right ventricular free wall (RVFWd)	mm	End-diastolic right ventricular free wall thickness
Tricuspid annular plane systolic excursion (TAPSE)	mm	The displacement of the lateral tricuspid annulus toward the apex during systole
Tricuspid valve peak velocity	mm/s	Peak velocity of flow through the tricuspid valve
Cardiac output	ml/min	The volume of blood pumped by the heart per minute
Stroke volume	ml	The volume of blood ejected from the LV per beat
Heart rate	bpm	The number of times the heart beats per minute (bpm)
Left ventricular ejection fraction (LVEF)	%	The percentage of blood the LV expels with each contraction

2.5 Invasive pressure measurements

2.5.1 Right ventricular pressure

To quantify PH, right ventricular pressure (RVP) was determined by right heart catheterisation and used to calculate RVSP. Mice were anesthetised in an induction chamber with isoflurane (4%, 0.8 ml/min O_2; Abbott Laboratories Ltd, Queenborough, UK) then placed supine on a thermostatically regulated heating mat (TCAT-2LV Controller; Physitemp, Norfolk, UK) set to 37°C with anaesthesia maintained by nose cone (2 ± 0.5% isoflurane, 0.8 ml/min O_2).

Under the guidance of a light microscope, a small incision was made in the neck, exposing the salivary glands. The glands were then separated to visualise the right jugular vein, which was gently isolated from the surrounding tissue with fine forceps. Two sutures (silk, 4-0; Surgical Specialities, UK) were looped around the vein; the most cephalic suture was tied off, and the most caudal suture was pulled tight, temporarily interrupting blood flow to facilitate catheterisation. A Millar Mikro-Tip® pressure catheter (Millar; SPR-671, size 1.4F; Houston, USA) was introduced into a small incision made in the vein and secured in place by the caudal suture. The catheter was then advanced through the superior vena cava and into the RV.

For recording, anaesthesia was adjusted to achieve a stable respiration rate of approximately 100 breaths per minute. RVP was recorded over a stable continuous period of five minutes using an in-line P23 XL transducer (Viggo-Spectramed, Oxnard, USA) with a pre-calibrated PowerLab System (ADInstruments Ltd., Castle Hill, Australia) and LabChart 6.0 software. See ***Figure 13*** for representative trace. Following recording, the catheter was removed, and the caudal suture tied to prevent blood loss.

2.5.2 Systemic blood pressure

Immediately following RVP recording, the carotid artery was cannulated to determine systemic blood pressure. Briefly, the left common carotid artery was isolated and surrounded by three sutures (silk, 6-0; Surgical Specialities, UK). The most cephalic suture was tied to permanently cease blood flow, the most caudal was pulled tight to interrupt blood flow. A fluid-filled (heparin; 100 U/ml diluted in

0.9% saline) cannula (0.28 mm internal diameter; Critchley Electrical Products Pty Ltd, Castle Hill, Australia) was introduced into the artery through a small incision and secured using the third suture. The caudal suture was then released to restore blood flow, and systemic blood pressure was recorded as described above for RVP. See ***Figure 13*** for representative trace.

2.5.3 Analysis

Labchart Reader v8.1.21 was used to calculate right ventricular systolic pressure (RVSP) and mean arterial blood pressure (MABP) from 10 s snapshots of stable periods of recording.

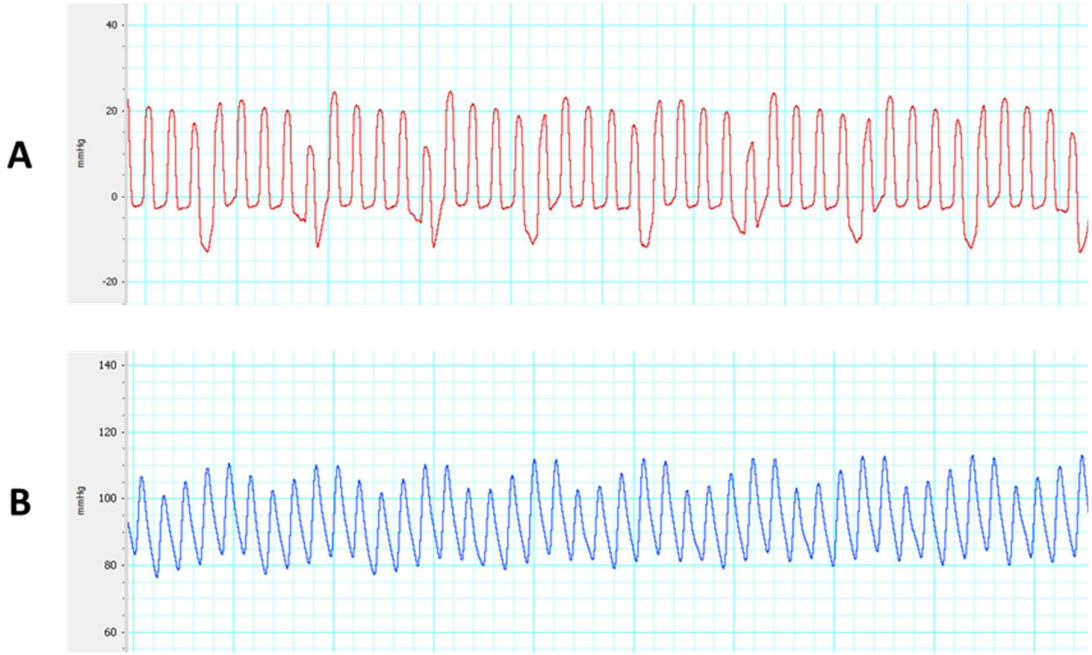

Figure 13: Haemodynamic measurements

Representative traces of right ventricular pressure (RVP) obtained by right heart catheterisation (*A*) and systemic arterial blood pressure obtained by cannulation of the carotid artery (*B*).

2.6 Plasma and tissue collection

2.6.1 Plasma collection

Following blood pressure recording, animals were humanely euthanised by a combination of isoflurane overdose (4%) and exsanguination. Whole blood samples were collected via the carotid catheter and centrifuged (14,000 RPM; 2 min; 4°C). Plasma was snap frozen in liquid nitrogen and stored at -80°C for further analyses.

2.6.2 Tissue weights and processing

The lungs and heart were excised together and then separated. The atria were trimmed from the rest of the heart and the right ventricle was cut away from the left ventricle and septum. Each ventricle was weighed separately to determine right ventricle to left ventricle plus septum ratio; RV/(LV+S), also known as Fulton's index. The lungs and RV were then snap frozen on liquid nitrogen in separate 2 ml cryogenic tubes and stored at -80°C for molecular biology.

2.6.3 Tissue fixation

In a subset of mice, the heart and lungs were formalin fixed for histological analysis. With the heart in-situ, the left atrium was removed, and a 22-gauge needle was inserted into the RV. Approximately 10 ml of phosphate-buffered saline (PBS) was injected to flush residual blood from the pulmonary vasculature. Then, a cannula coupled to a 22-gauge blunt needle was introduced to the trachea through a small incision and secured with a suture (silk, 4-0; Surgical Specialities, UK). The lungs were gradually inflated by gentle infusion of 10% neutral-buffered formalin (4% formaldehyde, Sigma Aldrich, UK) from a reservoir, at a constant fluid pressure of 20 cm H_2O. Once the lungs were fully inflated, the heart and lungs were removed from the chest together and immersed in 10% formalin overnight. After 24 h, the samples were removed from formalin and washed with PBS, before being transferred into 70% EtOH (Fisher Scientific Ltd, Leicestershire, UK) and stored at 4°C for paraffin wax embedding.

2.7 Pulmonary artery organ bath pharmacology

Pulmonary vascular reactivity to CNP and the NPR-C agonist cANF$^{4-23}$ was investigated in NmOx and SuHx mice using organ bath pharmacology. Male and female animals (C57BL/6, 13 weeks old; Envigo, UK) were anesthetised with 4% isoflurane and euthanised by exsanguination. Second order conduit pulmonary arteries were carefully dissected and cleaned of connective tissue, then cut into rings of approximately 4 mm in length. Vessels were mounted in a multi-wire myograph system (Danish Myo Technology, Hinnerup Denmark) containing Krebs Ringer solution (Sigma-Aldrich, Poole, UK; for composition see ***Table 8***) and gassed continuously with carbogen (5% CO_2, 95% O_2; British Oxygen Company, Guildford, UK). The tissues were allowed to equilibrate for ~45 min during which time tension was maintained at 0.3 g and Krebs buffer was refreshed every 15 min.

After equilibration, the contractile potential of each vessel was assessed by the addition of 80 mM KCl (Sigma Aldrich, Poole, UK). Once a stable maximal tension was achieved, tissues were thoroughly washed with fresh Krebs buffer to recover baseline levels of contraction. The vessels were then contracted again with the addition of U-46619 (1 μM; Santa Cruz Biotechnology, Dallas, Texas, USA) and washed after a stable maximum tension was observed. In preparation for the addition of test agents, tissues were pre-contracted to 80% of the maximal tension elicited by U-46619. Relaxation concentration-response curves to CNP (1 nM - 1 μM; Genescript, New Jersey, US) or cANF$^{4-23}$ (1 nM - 10 μM; Genescript, New Jersey, US) were then constructed. Subsequently, vessels were washed thoroughly, and a contraction concentration-response curve to phenylephrine (Phe; 1 nM - 100 μM; Sigma Aldrich, Poole, UK) was constructed. Alternatively, vessels were again pre-contracted with U-46619, and once a stable response was achieved, a relaxation concentration–response curve to acetylcholine (ACh; 1 nM - 10 μM; Sigma Aldrich, Poole, UK) was constructed.

Data was recorded using LabChart Pro v8.1.19 and analysed using Labchart Reader v8.1.21. Relaxation was calculated as percentage reversal of U46619-induced tone. Curves were fitted to the data using nonlinear regression (GraphPad Prism software, ver. 9.02, San Diego, CA) and the -log [M] of each drug. From these curves, EC_{50} and E_{max} were determined, which are the log

concentration necessary to achieve a half-maximal response (used to compare potency) and the maximum response (used to compare efficacy), respectively.

Table 8: Krebs Ringer 1X working solution

Component	Chemical Formula	Concentration	
Sodium Chloride	NaCl	6.9	g/l
Potassium Chloride	KCl	0.35	g/l
D-(+)-Glucose	$C_6H_{12}O_6$	2.0	g/l
Potassium Phosphate (monobasic, anhydrous)	KH_2PO_4	0.16	g/l
Magnesium Sulphate (anhydrous)	$MgSO_4$	0.14	g/l
Sodium Bicarbonate	$NaHCO_3$	2.1	g/l
Calcium Chloride	$CaCl_2$	2.5	mM

2.8 Molecular biology

2.8.1 Natriuretic peptide and disease-related gene expression

Quantitative reverse transcription polymerase chain reaction (RT-qPCR) was used to investigate changes in CNP signalling and remodelling gene expression in the pulmonary vasculature and RV.

2.8.1.1 *Tissue homogenisation*

Frozen tissue (10 - 20 mg) was added to a Precellys® lysing CKMix 2 ml tube (Bertin Technologies, France) and dissociated using a solution of 350 µl RLT buffer (Qiagen, UK) and 1% β-mercaptoethanol (β-ME; Sigma-Aldrich, Poole, UK). The dissociated tissue was homogenised at 0°C using a Precellys® Evolution tissue homogenizer (Bertin Technologies, France). Samples were agitated at 6000 RPM in six 13 s bursts, with a 30 s interval in between cycles. Finally, the homogenate was centrifuged (10,000 x g; min; 4°C) to remove any foam that may have formed during agitation.

2.8.1.2 *RNA isolation and purification*

Total RNA was extracted from the homogenate using a standard extraction kit (RNeasy Mini Kit, Qiagen, UK). Lysate supernatant was transferred to 1.5 ml Eppendorf tubes containing 590 µl of nuclease-free H_2O and 10 µl of proteinase K (Invitrogen, USA) and incubated at 55°C for 10 min. Following centrifugation (10,000 x g, 3 min, room temperature), 700-900 µl of each sample was transferred to a fresh Eppendorf. A 0.5x volume (350-450 µl) of 100% ethanol (EtOH; Fisher Scientific Ltd, Leicestershire, UK) was added to each tube, and the contents were mixed well by pipetting. Of each sample, 700 µl was transferred to RNeasy spin columns in collection tubes and centrifuged (8000 x g, 15 s; room temperature); inside each column, EtOH promotes selective binding of RNA to the RNeasy membrane. This was then repeated with the remainder of the sample.

Following the RNA binding step, each column was washed by centrifugation with a series of buffers to discard excess ethanol and unwanted molecules (e.g. DNA). The columns were transferred to new collection tubes and 700 µl of RW1 buffer was added before centrifugation (8000 x g, 15 s; room temperature). The columns were again transferred to fresh collection tubes and washed twice more

with 500 µl of RPE buffer (8000 x g, 15 s; room temperature). To eliminate any buffer carryover, the columns underwent a 'dry run' in new collection tubes (10000 x g, 1 min; room temperature).

For RNA elution, the columns were placed in 1.5 ml Eppendorf tubes and 30 µl of nuclease-free H_2O was added. The samples were then centrifuged (10000 x g, 1 min; room temperature). Finally, the eluents were re-applied onto the spin columns and centrifuged again, for maximal RNA yield.

2.8.1.3 *Measurement of RNA quantity and quality*

RNA yield and purity was quantified using a Nano-drop®ND-1000 spectrophotometer (Thermo Fisher Scientific, UK). RNA concentration was determined by measuring absorbance at 260 nm. RNA purity was determined by the ratio of absorbance at 260 nm and 280 nm (A260/A280), which indicates protein contamination, and the ratio of absorbance at 260 nm and 230 nm (A260/A230), which indicates contamination with ethanol and/or guanidine. Ratios in the range of 1.8 - 2.2 were considered indicative of sufficient purity. Purified RNA was stored at -80°C.

2.8.1.4 *Reverse transcription*

Of the RNA, 1 µg was transcribed into complementary DNA (cDNA) by reverse transcription (RT; High-Capacity cDNA Reverse Transcription Kit; Thermo Fisher Scientific, UK) according to the manufacturer's instructions. A RT master mix was added to the RNA (see ***Table 9*** for details). Reaction mixtures without RT enzyme were also aliquoted as a negative control for contamination of genomic DNA. Samples were reverse transcribed in a thermal cycler (Bio-Rad S1000, UK) under the conditions listed in ***Table 10***. The cDNA was then diluted 1:40 in nuclease-free H_2O and stored at -20°C.

2.8.1.5 *Real-time qPCR*

For real time qPCR, specific primers for each molecular target (10 µM) were added to cDNA template and PowerUp™ SYBR™ Green Master Mix (Thermo Fisher Scientific, UK). For reaction mixture details, see ***Table 11***. For each sample, cDNA was amplified using quantitative real-time PCR over 45 cycles (***Table 12***) on a Bio-Rad CFX96 Connect Real-Time PCR detection system (BioRad, California, USA).

To confirm amplification efficiency and specificity, samples were subjected to melting curve analysis using CFX Maestro™ Software 2.3 (Bio-Rad Laboratories Ltd., Hertfordshire, UK). Messenger RNA (mRNA) expression was determined by expressing the cycle threshold (Ct) value as 2-ΔΔCt relative to the levels of the housekeeping gene ribosomal protein L19 (RPL-19) and normalised as a fold change to NmOx WT samples. All primer sequences are listed in ***Table 13 - 15***.

Table 9: Reverse transcription reaction components

Component	Volume
10X RT Buffer	2.0 µl
25X dNTP Mix (100 mM)	0.8 µl
10X RT Random Primers	2.0 µl
MultiScribe™ Reverse Transcriptase	1.0 µl
Nuclease-free H_2O	4.2 µl
RNA Sample (1µg)	10 µl

The total volume for each reaction was 20 µl.

Table 10: Thermal cycler conditions for reverse transcription

Step	Temperature	Time
1	25°C	10 min
2	37°C	120 min
3	85°C	5 min
4	4°C	hold

Table 11: qPCR reaction components

Component	Volume
PowerUp™ SYBR™ Green Master Mix	10 µl
Forward Primer (10µM)	1 µl
Reverse Primer (10µM)	1 µl
Nuclease-free water (µl)	7 µl
Sample cDNA (diluted)	1 µl

The total volume for each reaction was 20µl.

Table 12: Thermal cycler conditions for qPCR reactions

Step	Stage	Temp	Time
1	Polymerase activation	95°C	3 min
2	Denaturation	95°C	10 s
3	Annealing	57.3°C	30 s
	Repeat steps 2 & 3 x 45 cycles		
4	Extension	95°C	10 s
5	Dissociation I	65°C	31 s
6	Dissociation II	65°C	5 s
	Repeat step 6 x 60 cycles, +0.5 C/cycle		

Table 13: Primers used for qPCR – natriuretic peptide signalling

Target		Primer Sequence (5'-3')
RPL-19	Forward:	GCTTGCCTCTAGTGTCCTCC
	Reverse:	TTGGCGATTTCATTGGTCTCA
CNP	Forward:	CCAACGCGCGCAAATACAAA
	Reverse:	GCACAGAGCAGTTCCCAATC
NPRB	Forward:	AACGGGCGCATTGTGTATATCT
	Reverse:	TCAGGATTTGGGGGTTCTCG
NPRC	Forward:	CTTGGATGTAGCGCACTATGTC
	Reverse:	CACAAGGACACGGAATACTC

A, adenine; C, cytosine; G, guanine; T, thymine.

Table 14: Primers used for qPCR – vascular disease markers

Target		Primer Sequence (5'-3')
RPL-19	Forward:	GCTTGCCTCTAGTGTCCTCC
	Reverse:	TTGGCGATTTCATTGGTCTCA
BMPR2	Forward:	TTGACAGGAGACCGGAAACAG
	Reverse:	CGTATCGACCCCGTCCAATC
Smad3	Forward:	CAGCATGGACGCAGGTTCT
	Reverse:	TGTGTCGCCTTGTAAGTTCC
Smad5	Forward:	CAGCATATCCAGCAGAGATGTTCA
	Reverse:	CCTCCCCACCAACCAACGTAGTAT
Smad7	Forward:	AGAGGCTGTGTTGCTGTGAA
	Reverse:	AAGAAGTTGGGAATCTGAAAGCC

A, adenine; C, cytosine; G, guanine; T, thymine.

Table 15: Primers used for qPCR – cardiac disease markers

Target		Primer Sequence (5'-3')
RPL-19	Forward:	GCTTGCCTCTAGTGTCCTCC
	Reverse:	TTGGCGATTTCATTGGTCTCA
β-MHC	Forward:	ACTGTCAACACTAAGAGGGTCA
	Reverse:	TTGGATGATTTGATCTTCCAGGG
BNP	Forward:	TGGGCTGTAACGCACTGAA
	Reverse:	TGTTGTGGCAAGTTTGTGCTT
CTGF	Forward:	GGGCCTCTTCTGCGATTC
	Reverse:	ATCCAGGCAAGTGCATTGGTA
Fibronectin	Forward:	CCGGTGGCTGTCAGTCAGA
	Reverse:	CCGTTCCCACTGCTGATTTATC
TGFβ1	Forward:	TCAGACATTCGGGAAGCAGT
	Reverse:	GCCCTGTATTCCGTCTCCTTG
SERCA2a	Forward:	TGGAACCTTTGCCGCTCATTT
	Reverse:	CAGAGGCTGGTAGATGTGTT

A, adenine; C, cytosine; G, guanine; T, thymine.

2.8.2 Natriuretic peptide bioassays

2.8.2.1 *Overview*

The plasma concentrations of ANP and CNP were quantified using commercial enzyme-linked immunosorbent assay (ELISA) kits (Phoenix Pharmaceuticals; Karlsruhe, Germany). These assays are 'competitive' enzyme immunoassays, whereby the target peptide (in either the sample or standard) competes with a biotinylated peptide to bind the primary antibody (which in turn binds the secondary antibody coating the immunoplate). The biotinylated peptide interacts with streptavidin-horseradish peroxidase (SA-HRP), which catalyses the substrate solution. The intensity of the resulting yellow colour is directly proportional to the amount of biotinylated peptide-SA-HRP complex, but inversely proportional to the amount of the targeted peptide. Based on this principle, a standard curve can be established by plotting the measured optical density versus the various standard peptide concentrations. The peptide concentration can then be determined by extrapolation of the standard curve. A positive control is included to confirm the accuracy of the ELISA.

2.8.2.2 *Peptide extraction*

Plasma samples from male WT and NPRC$^{-/-}$ mice were thawed on ice (4°C). The samples were acidified with an equal amount of Buffer A and centrifuged (14,000 RPM, 20 min, 4°C). The acidified samples were then extracted using pre-equilibrated C18 SEP-columns as per the manufacturer's instructions. The eluent was evaporated to dryness by a centrifugal concentrator and stored at -80°C overnight (Speedvac, Thermo Fisher Scientific, UK).

2.8.2.3 *ELISA assay*

The following day, samples were reconstituted in 250 µl 1x assay buffer. To a 96-well immunoplate, 50 µl/well of standard, sample, or positive control was added, along with 25 µl/well of primary antibody plus biotinylated peptide. The plate was then incubated at room temperature (~20°C) for 2 h. Next, the plate was washed 4 times with 350 µl/well 1x assay buffer and 100 µl/well of SA-HRP solution was added. After a 1 h incubation at room temperature, the plate was washed as previously described and 100µl/well of TMB substrate solution was added. After a

final 1 h room temperature incubation, the reaction was terminated with 100 µl/well of 2M HCl (stop solution) and the optical density of each well was read at an absorbance of 450 nm using a microtiter plate reader (VICTOR Multilabel Plate Reader, PerkinElmer Ltd., UK).

2.9 Immunohistochemistry

2.9.1 Assessment of small artery muscularisation

Whole lungs were separated into individual lobes, each of which was bisected along the transverse plane. The bottom half of each lobe was sent to Barts Cancer Institute (BCI) Pathology Services (London, UK) for embedding, sectioning, mounting, and staining. Paraffin-embedded sagittal lung sections (4 µm; 5 lobes per section) were stained with an anti-α-SMA antibody, which stains smooth muscle brown, and lightly counterstained with haematoxylin, which stains nucleic acids a purplish-blue colour. Slides were imaged using a NanoZoomer S210 slide scanner (Hamamatsu, Hertfordshire, UK) at 20x magnification. For each lobe, pulmonary arteries with an external diameter of ≤80 µm (Baliga et al., 2014; Bubb et al., 2014) were identified in a randomly selected field. Vessels were scored in a blinded manner as either non-muscularised (staining covers ≤50% of vessel circumference) or muscularised (staining covers ≥50% of vessel circumference). Percentage muscularisation was defined for each animal as the number of remodelled arteries divided by the total number of vessels counted (≥30 per section).

2.9.2 Assessment of RV fibrosis

RV fibrosis was assessed by quantifying collagen deposition using picrosirius red, which stains cytoplasm and muscle fibres yellow, and collagen red. Fixed hearts were sent to Barts Cancer Institute (BCI) Pathology Services (London, UK) for embedding, sectioning, and mounting. Paraffin-embedded transverse heart sections (5 µm) were deparaffinised by washing in xylene (Sigma Aldrich, UK) for 10 min and then rehydrated by washing in sequential EtOH solutions (100%, 10 min; 95%, 10 min; 80%, 10 min; 70%, 5 min; 50%, 5 min; Fisher Scientific Ltd, Leicestershire, UK), followed by ddH_2O for 5 min. For the staining, sections were submerged in phosphomolybdic acid (0.1%; Sigma Aldrich, UK) for 2 min, rinsed

with distilled water and then immersed in picrosirius red (0.1% w/v Direct Red 80 in picric acid; Sigma Aldrich, UK) for 2 h. The sections were then washed in acidified water (0.5% acetic acid; Sigma Aldrich, UK) and dehydrated by rapid washing in sequential EtOH solutions (25%, 50%, 75%, 100%, then placed in xylene. Slides were mounted with DPX mounting medium (Merck, UK) and glass coverslips, and left to dry overnight at room temperature. A NanoZoomer S210 slide scanner (Hamamatsu, Hertfordshire, UK) was used to capture images of the tissue slides (20x magnification). Images were analysed by threshold analysis using Image J (NIH, USA) with investigator blinded to treatment. Values of fibrosis were expressed as a percentage of the whole section area.

2.10 Statistical analysis

All values are expressed as mean ± standard error of the mean (*SEM*). The *n* (number of samples) value denotes the number of vessels studied in each group. Individual data points are show for *in vivo* experiments. For the comparison of two groups of data, a two-tailed, unpaired Student's *t*-test was used. When comparing three or more groups of data a one-way or two-way analysis of variance (ANOVA) was used, followed by a Šidák post hoc test with adjustment for multiplicity. A probability (*P)* value ≤ 0.05 was considered statistically significant.

Chapter III: Results I

3.1 Overview

The studies described within this chapter build on previous work characterising the multi-faceted regulatory roles of CNP and NPR-C in the systemic vasculature and LV (Moyes et al., 2014, 2020). The data presented herein provide preliminary evidence of a pivotal role for the peptide in governing pulmonary vascular and RV homeostasis under pathological conditions. A multi-disciplinary strategy was employed, including organ bath pharmacology and gene expression analysis, culminating with an *in vivo* investigation that utilised mice in which CNP is deleted globally to determine the impact of the peptide on cardiopulmonary haemodynamics and RV structure. Of note, a systemic hypertensive phenotype has been previously described in female ecCNP$^{-/-}$ mice only, implying that male sex is associated with a reduced reliance on CNP to regulate vascular homeostasis (Moyes et al., 2014). As such, both sexes were investigated independently in the present study; composite data can be found in the Appendix.

3.2 Pulmonary vascular reactivity to CNP and cANF$^{4-23}$ is blunted in SuHx mice

Pulmonary vascular reactivity to CNP and cANF$^{4-23}$ was investigated *ex vivo*, using second order conduit pulmonary arteries isolated from NmOx and SuHx WT mice. CNP elicited concentration-dependent relaxation in pre-contracted pulmonary arteries from male NmOx and SuHx animals (***Figure 14***). Whilst pulmonary arteries from female NmOx mice were also readily relaxed by CNP, this effect was significantly blunted in female SuHx mice (***Figure 14***), resulting in a significantly reduced E_{max} (***Table 16***). cANF$^{4-23}$ also had a vasorelaxant effect in pulmonary arteries isolated from NmOx animals, albeit with reduced efficacy (i.e. lower E_{max}) than CNP, which was particularly evident in female mice (***Table 16 & 17***). Notably, cANF$^{4-23}$-mediated relaxation was near-totally ablated in vessels from SuHx animals (***Figure 15***, ***Table 17***).

Pulmonary vascular reactivity to other vasoactive mediators was also assessed. The ability of ACh to relax vessels was moderately tempered in vessels from male SuHx mice (***Figure 16***), which trended towards a higher EC_{50} (***Table 18***) but was unaltered in female SuHx vessels (***Figure 16***). The response to Phe was highly concentration-dependant in vessels from male SuHx animals. At lower concentrations, the contractile response to Phe was impaired versus vessels from NmOx mice (***Figure 17***), with a trend towards higher EC_{50}. Paradoxically, the contractile activity of Phe was potentiated at higher concentrations, leading to a significantly higher E_{max} (***Table 19***).

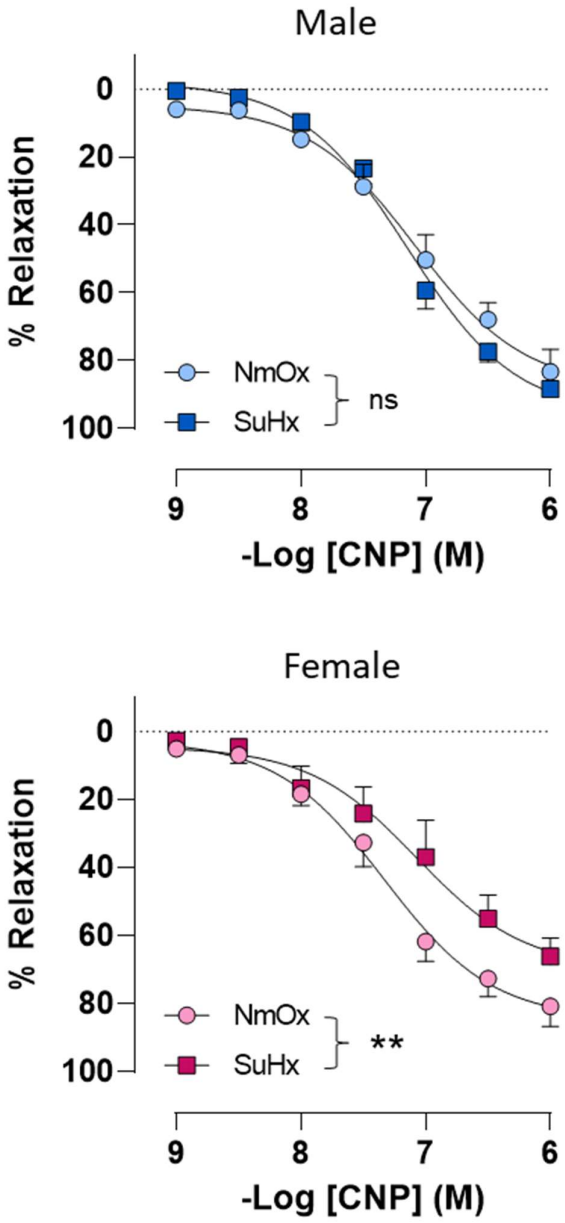

Figure 14: Concentration-response curves to CNP in pulmonary arteries from male and female NmOx and SuHx mice

Relaxation to CNP in isolated pulmonary arteries from normoxic (NmOx) and Sugen + hypoxia (SuHx) WT mice. Relaxation is expressed as percentage reversal of U-46619-induced tone. Data presented as mean ± *SEM*. *n*=5-6. Statistical analysis by two-way ANOVA across the entire concentration–response curve. $^{**}P \leq 0.01$; *ns*, not significant (adjusted for multiplicity).

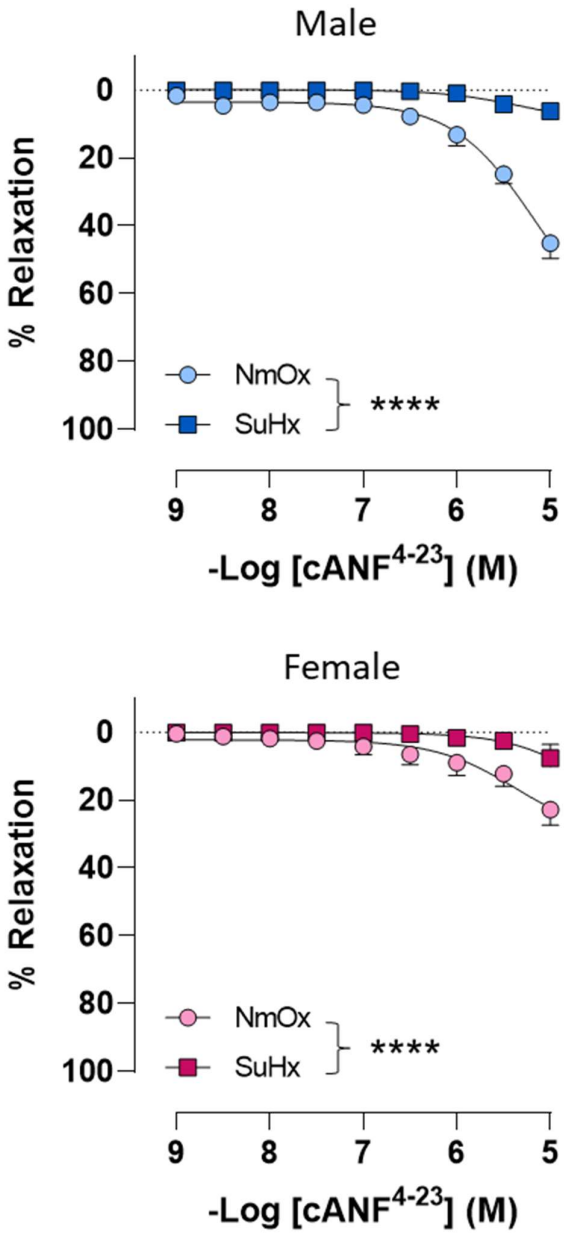

Figure 15: Concentration-response curves to cANF$^{4-23}$ in pulmonary arteries from male and female NmOx and SuHx mice

Relaxation to cANF$^{4-23}$ in isolated pulmonary arteries from normoxic (NmOx) and Sugen + hypoxia (SuHx) WT mice. Relaxation is expressed as percentage reversal of U-46619-induced tone. Data presented as mean ± *SEM*. *n*=5-6. Statistical analysis by two-way ANOVA across the entire concentration–response curve. ****$P \leq 0.0001$ (adjusted for multiplicity).

Table 16: CNP-induced relaxation of mouse isolated pulmonary arteries

	Log EC_{50} (M)			E_{max} (%)		
	NmOx	*SuHx*	*P* Value	*NmOx*	*SuHx*	*P* Value
Male	-7.08 ± 0.17	-7.14 ± 0.07	0.96	83.42 ± 6.31	80.84 ± 5.97	0.93
Female	-7.32 ± 0.08	-7.07 ± 0.28	0.53	88.31 ± 2.15	66.09 ± 5.22	0.02*

NmOx, normoxic; SuHx, Sugen + hypoxia. Data presented as mean ± *SEM*; *n*=5-6. Statistical analysis by two-way ANOVA with Šidák post hoc test (adjusted for multiplicity). *$P \leq 0.05$.

Table 17: $cANF^{4-23}$-induced relaxation of mouse isolated pulmonary arteries

	E_{max} (%)		
	NmOx	*SuHx*	*P* Value
Male	45.01 ± 4.58	6.71 ± 1.61	<0.0001****
Female	22.79 ± 4.61	9.31 ± 4.45	0.06

NmOx, normoxic; SuHx, Sugen + hypoxia. Data presented as mean ± *SEM*; *n*=5-6. Statistical analysis by two-way ANOVA with Šidák post hoc test (adjusted for multiplicity). ****$P \leq 0.0001$.

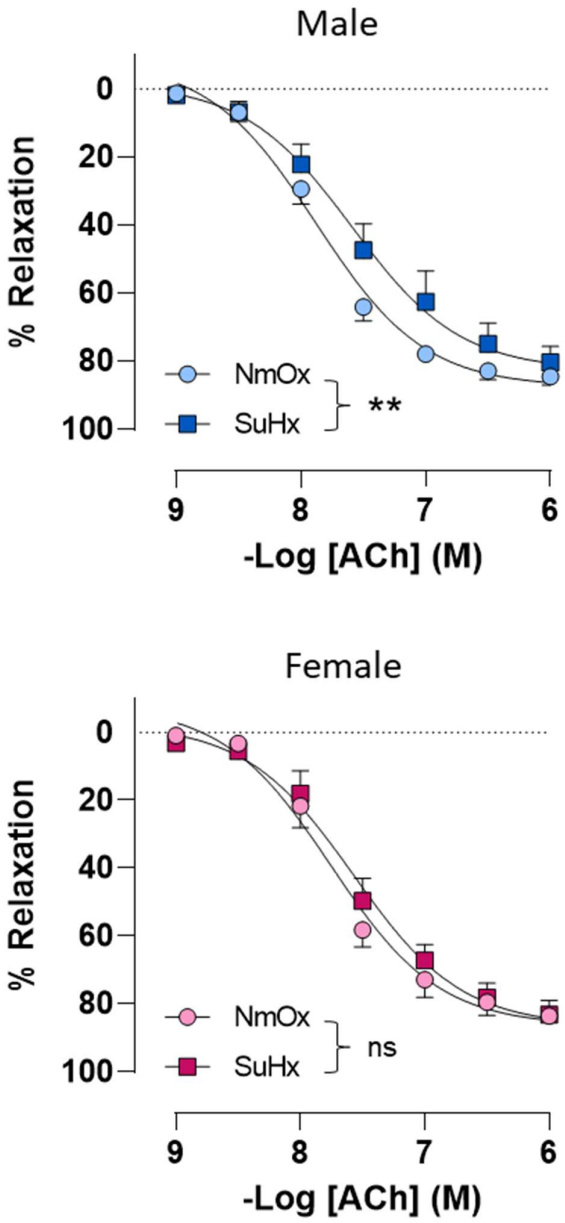

Figure 16: Concentration-response curves to ACh in pulmonary arteries from male and female NmOx and SuHx mice

Relaxation to acetylcholine in isolated pulmonary arteries from normoxic (NmOx) and Sugen + hypoxia (SuHx) WT mice. Relaxation is expressed as percentage reversal of U-46619-induced tone. Data presented as mean ± *SEM*. *n*=4-5. Statistical analysis by two-way ANOVA across the entire concentration–response curve. $^{**}P \leq 0.01$; *ns*, not significant (adjusted for multiplicity).

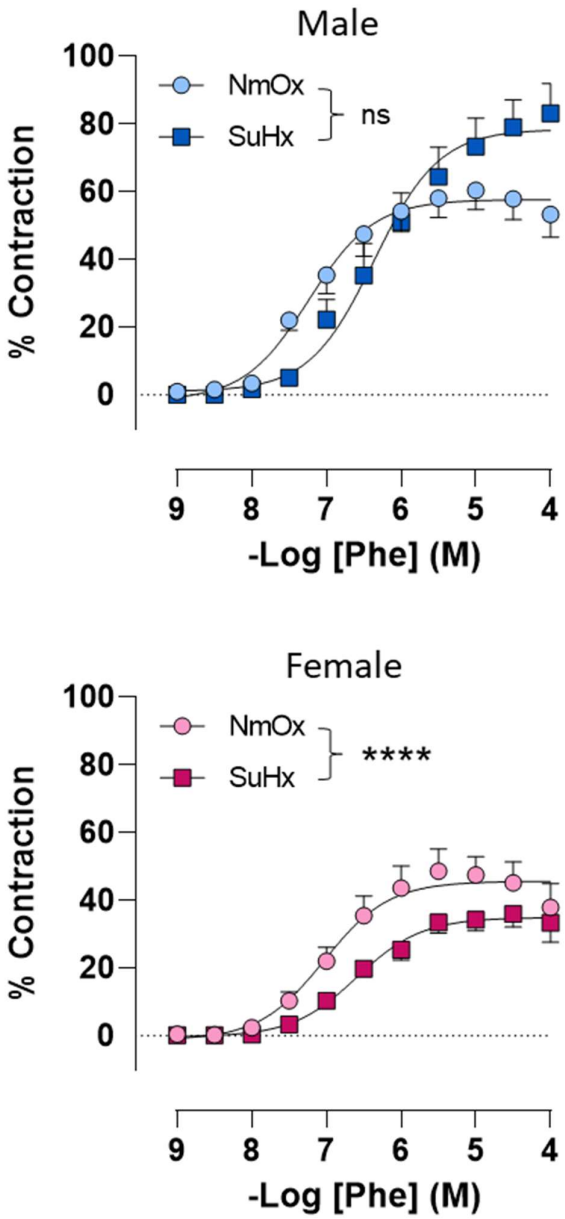

Figure 17: Concentration-response curves to Phe in pulmonary arteries from male and female NmOx and SuHx mice

Contraction to pheylephrine in isolated pulmonary arteries from normoxic (NmOx) and Sugen + hypoxia (SuHx) WT mice. Contraction is expressed as a percentage of KCl-induced tone Data presented as mean ± *SEM*. *n*=6. Statistical analysis by two-way ANOVA across the entire concentration–response curve. ****$P \leq 0.0001$; *ns*, not significant (adjusted for multiplicity).

Table 18: ACh-induced relaxation of mouse isolated pulmonary arteries

	Log EC_{50} (M)			E_{max} (%)		
	NmOx	*SuHx*	*P* Value	*NmOx*	*SuHx*	*P* Value
Male	-7.87 ± 0.04	-7.54 ± 0.15	0.08	88.34 ± 2.18	83.74 ± 4.16	0.55
Female	-7.75 ± 0.07	-7.58 ± 0.08	0.47	87.32 ± 2.41	87.49 ± 2.80	>0.99

NmOx, normoxic; SuHx, Sugen + hypoxia. Data presented as mean ± *SEM*; *n*=4-5. Statistical analysis by two-way ANOVA with Šidák post hoc test (adjusted for multiplicity).

Table 19: Phe-induced contraction of mouse isolated pulmonary arteries

	Log EC_{50} (M)			E_{max} (%)		
	NmOx	*SuHx*	*P* Value	*NmOx*	*SuHx*	*P* Value
Male	-7.21 ± 0.10	-6.38 ± 0.25	0.003**	62.52 ± 5.42	83.32 ± 8.74	0.06
Female	-6.96 ± 0.09	-6.58 ± 0.16	0.21	51.38 ± 6.08	37.82 ± 3.89	0.26

NmOx, normoxic; SuHx, Sugen + hypoxia. Data presented as mean ± *SEM*; *n*=6. Statistical analysis by two-way ANOVA with Šidák post hoc test (adjusted for multiplicity). ***P* ≤ 0.01.

3.3 Cardiopulmonary expression of CNP and NPRs is altered in SuHx mice

One mechanism by which vascular reactivity to CNP and cANF$^{4-23}$ may be impaired in SuHx mice is receptor downregulation. Accordingly, the cardiopulmonary mRNA expression of CNP, NPR-B and NPR-C was investigated in SuHx mice.

The expression of the housekeeping gene RPL-19 was not altered by SuHx exposure in either the lung (***Supplementary Figure 1A***) or RV (***Supplementary Figure 1B***). Pulmonary CNP expression was unchanged in WT SuHx animals versus NmOx controls (***Figure 18A & B; Supplementary Figure 2A***), though a marked downregulation of both NPR-B and NPR-C was noted in male and female mice (***Figure 18C - F; Supplementary Figure 2B & C***). In contrast to the lung, CNP mRNA levels were significantly reduced in the hypertrophic right heart of male animals only (***Figure 19A & B; Supplementary Figure 3A***). A sexual dimorphism was also noted in the expression of NPR-B, which was upregulated in male SuHx mice (***Figure 19C; Supplementary Figure 3B***) but unchanged in female animals (***Figure 19D; Supplementary Figure 3B***). Finally, there was no significant difference in NPR-C expression in the RV between NmOx and SuHx mice in either sex (***Figure 19E & F; Supplementary Figure 3C***).

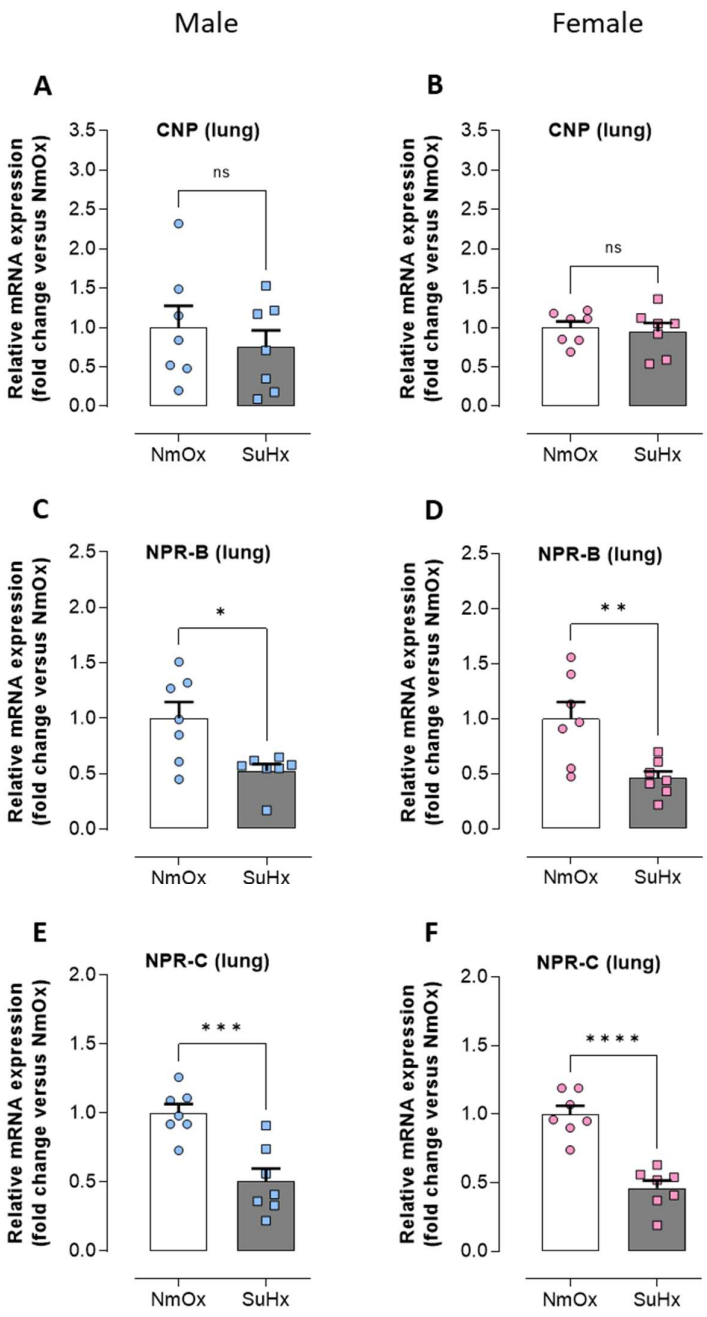

Figure 18: Expression of CNP, NPR-B and NPR-C in the lungs of animals with experimental PH

Pulmonary mRNA expression of (*A & B*) CNP, (*C & D*) NPR-B, and (*E & F*) NPR-C in normoxic (NmOx) and Sugen + hypoxia (SuHx) wildtype mice. Data presented as mean ± *SEM*; symbols represent individual data points. Statistical analysis by Student's *t*-test. **P* ≤ 0.05, ***P* ≤ 0.01, ****P* ≤ 0.001, *****P* ≤ 0.0001; *ns*, not significant.

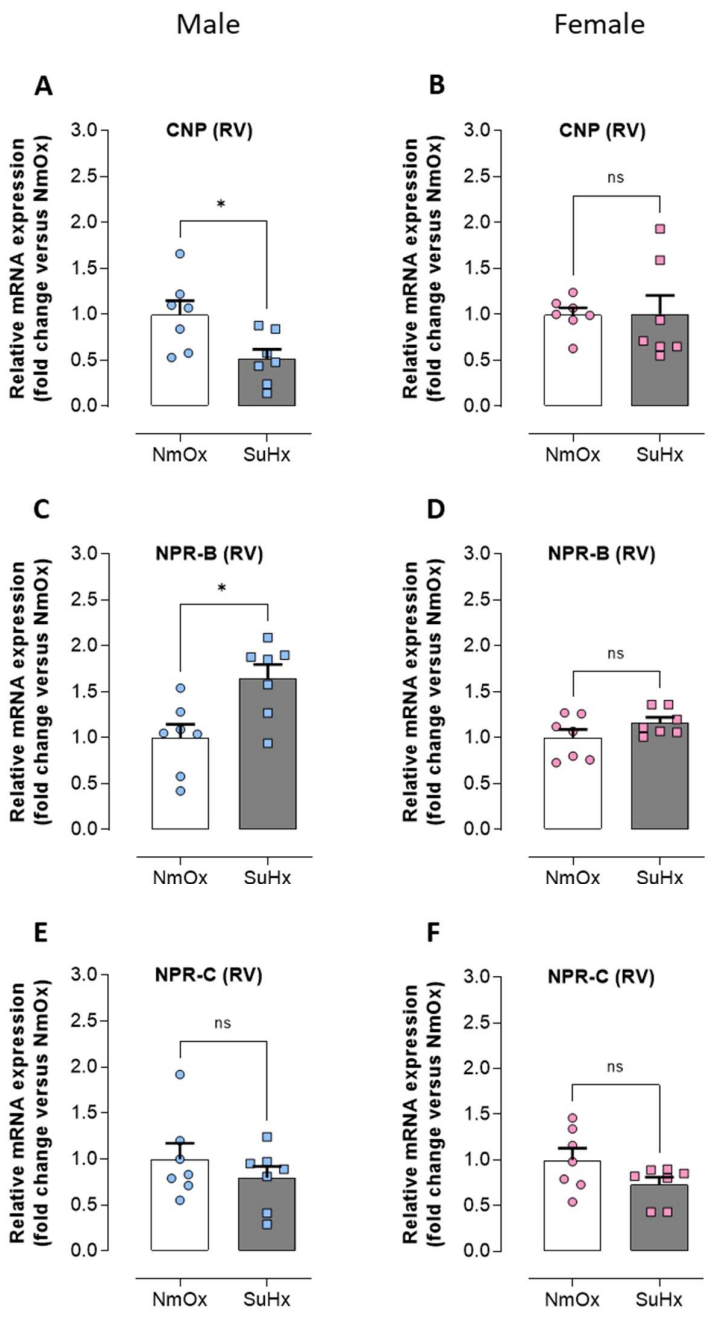

Figure 19: Expression of CNP, NPR-B and NPR-C in the RV of animals with experimental PH

Right ventricular (RV) mRNA expression of (*A & B*) CNP, (*C & D*) NPR-B, and (*E & F*) NPR-C in normoxic (NmOx) and Sugen + hypoxia (SuHx) wildtype mice. Data presented as mean ± *SEM*; symbols represent individual data points. Statistical analysis by Student's *t*-test. **P* ≤ 0.05; *ns*, not significant.

3.4 Global CNP deletion has sex-specific effects on experimental PH

Having established that experimental PH is associated with deficient CNP signalling in the lung and RV, the haemodynamic and structural impact of CNP loss on the cardiopulmonary circuit was delineated *in vivo*, using gbCNP$^{-/-}$ mice.

SuHx mice developed augmented RVSP (***Figure 20A & B***) and increased RV/(LV+S) ratio (***Figure 21A & B***) compared with NmOx animals, confirming the induction of a PH phenotype. Regardless of sex, loss of CNP did not significantly alter RVSP (***Figure 20A & B; Supplementary Figure 4A***) or right heart weight (***Figure 21A & B; Supplementary Figure 4C***) in NmOx mice. However, SuHx challenge unmasked a phenotype of increased cardiopulmonary pressure in male gbCNP$^{-/-}$ SuHx animals (***Figure 20A; Supplementary Figure 4A***) and decreased pressure in female gbCNP$^{-/-}$ mice (***Figure 20B; Supplementary Figure 4A***). In contrast, MABP was commensurate in WT and KO animals of either sex (***Figure 20C & D; Supplementary Figure 4B***). Whilst statistically significant, the deviations in RVSP observed in these mice did not alter the development of RVH, as in both sexes RV/(LV+S) was comparable between WT and gbCNP$^{-/-}$ animals (***Figure 21A & B; Supplementary Figure 4C***).

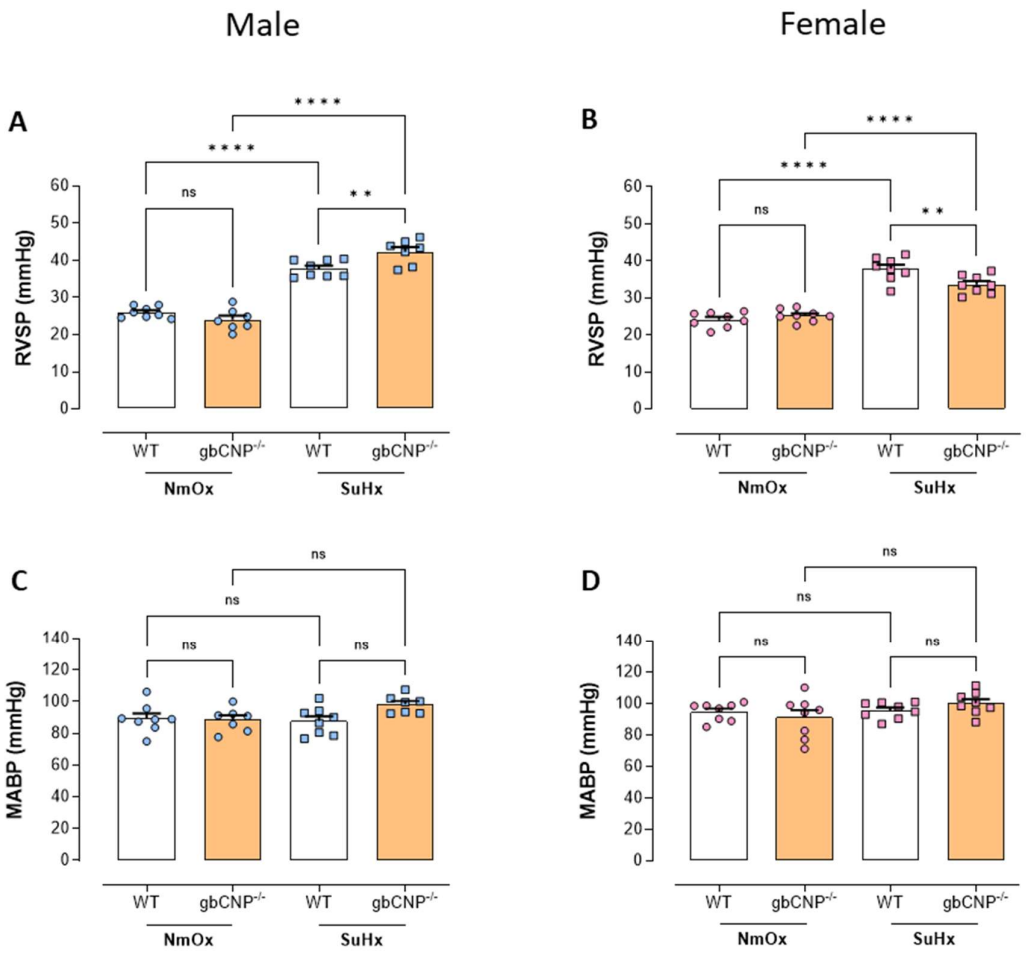

Figure 20: The effect of global CNP deletion on cardiopulmonary and systemic arterial pressure in experimental PH

(A & B) Right ventricular systolic pressure (RVSP) and (*C & D*) mean arterial blood pressure (MABP) in normoxic (NmOx) and Sugen + hypoxia (SuHx) wildtype (WT) and global CNP knockout (gbCNP$^{-/-}$) mice. Data presented as mean ± *SEM*; symbols represent individual data points. Statistical analysis by one-way ANOVA with Šidák post hoc test. ***P* ≤ 0.01, *****P* ≤ 0.0001; *ns*, not significant (adjusted for multiplicity).

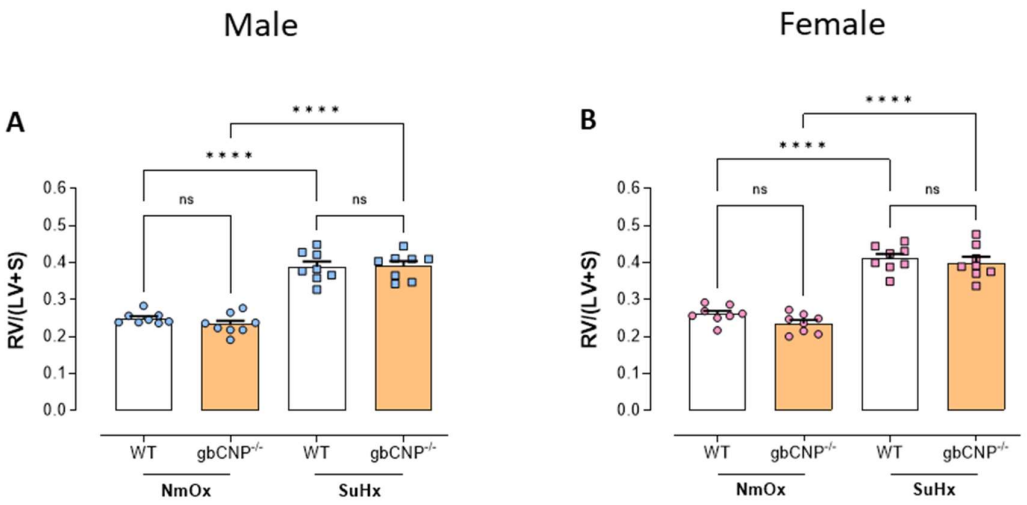

Figure 21: The effect of global CNP deletion on RV hypertrophy following pressure overload

Right ventricle to left ventricle plus septum ratio; RV/(LV+S), in normoxic (NmOx) and Sugen + hypoxia (SuHx) wildtype (WT) and global CNP knockout (gbCNP$^{-/-}$) mice. Data presented as mean ± *SEM*; symbols represent individual data points. Statistical analysis by one-way ANOVA with Šidák post hoc test. ****$P \leq 0.0001$; *ns*, not significant (adjusted for multiplicity).

Chapter IV: Results II

4.1 Overview

In this chapter, I further develop the observations presented in Chapter III by defining the contribution of different cell types to the actions of CNP in the cardiopulmonary circulation. The data presented herein describe parallel investigations that explored the development of PH in transgenic mouse strains with cell-restricted deletion of this peptide. Animals with endothelial- and cardiomyocyte- specific abrogation of CNP were utilised on the basis that this peptide is found in particularly high concentrations in vascular ECs (Stingo et al., 1992) and co-localises with its cognate receptors in the heart (Kim et al., 1999; Del Ry et al., 2011). Finally, PH was induced in mice with a global deletion of NPR-C, to elucidate the cognate receptor (NPR-B or NPR-C) underpinning the biological actions of CNP in the pulmonary vasculature and right heart. Global NPR-B KO mice are subject to dwarfism and early death (Tamura et al., 2004), limiting their use in the study of chronic cardiovascular diseases, such as PH.

4.2 Ablation of endothelial CNP accentuates experimental PH in male mice

Whilst loss of endothelial CNP had no effect on RVSP in NmOx animals of either sex (***Figure 22A - B; Supplementary Figure 5A***), male ecCNP$^{-/-}$ SuHx mice demonstrated significantly elevated RVSP versus WT controls (***Figure 22A; Supplementary Figure 5A***), mirroring the phenotype observed in gbCNP$^{-/-}$ animals. In fact, loss of endothelial CNP resulted in an even greater increase in RVSP (~7mmHg) than global loss of the peptide (~4 mmHg). Furthermore, the elevation of right heart afterload accentuated the development of RVH in these animals, indicated by a significantly increased RV/[LV+S] ratio (***Figure 24A; Supplementary Figure 5D***). In contrast to male mice, deletion of endothelial CNP had no impact on neither RVSP (***Figure 22B; Supplementary Figure 5A***) nor right heart weight (***Figure 24B; Supplementary Figure 5D***) in female SuHx animals.

In terms of vascular remodelling, SuHx mice had more than twice the number of muscularised small pulmonary arteries than NmOx controls; this morphological pathology was exacerbated in both male and female ecCNP$^{-/-}$ animals (***Figure 23A - D; Supplementary Figure 5C***). MABP was also significantly elevated in these mice following SuHx exposure, regardless of sex (***Figure 22C & D; Supplementary Figure 5B)***.

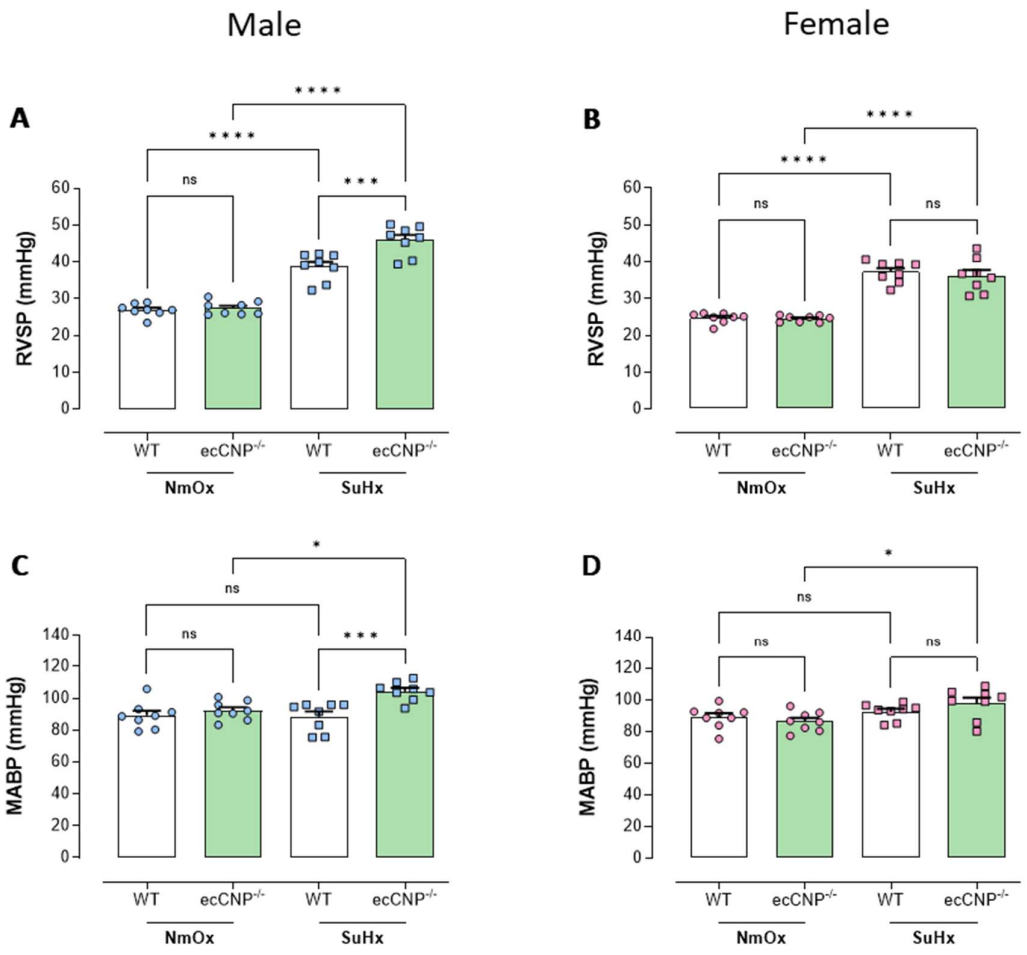

Figure 22: The effect of endothelial CNP deletion on cardiopulmonary and systemic arterial pressure in experimental PH

(A & B) Right ventricular systolic pressure (RVSP) and (*C & D*) mean arterial blood pressure (MABP) in normoxic (NmOx) and Sugen + hypoxia (SuHx) wildtype (WT) and endothelial-specific CNP knockout (ecCNP$^{-/-}$) mice. Data presented as mean ± *SEM*; symbols represent individual data points. Statistical analysis by one-way ANOVA with Šidák post hoc test. **P*<0.05, ****P*<0.001, *****P*<0.0001; *ns*, not significant (adjusted for multiplicity).

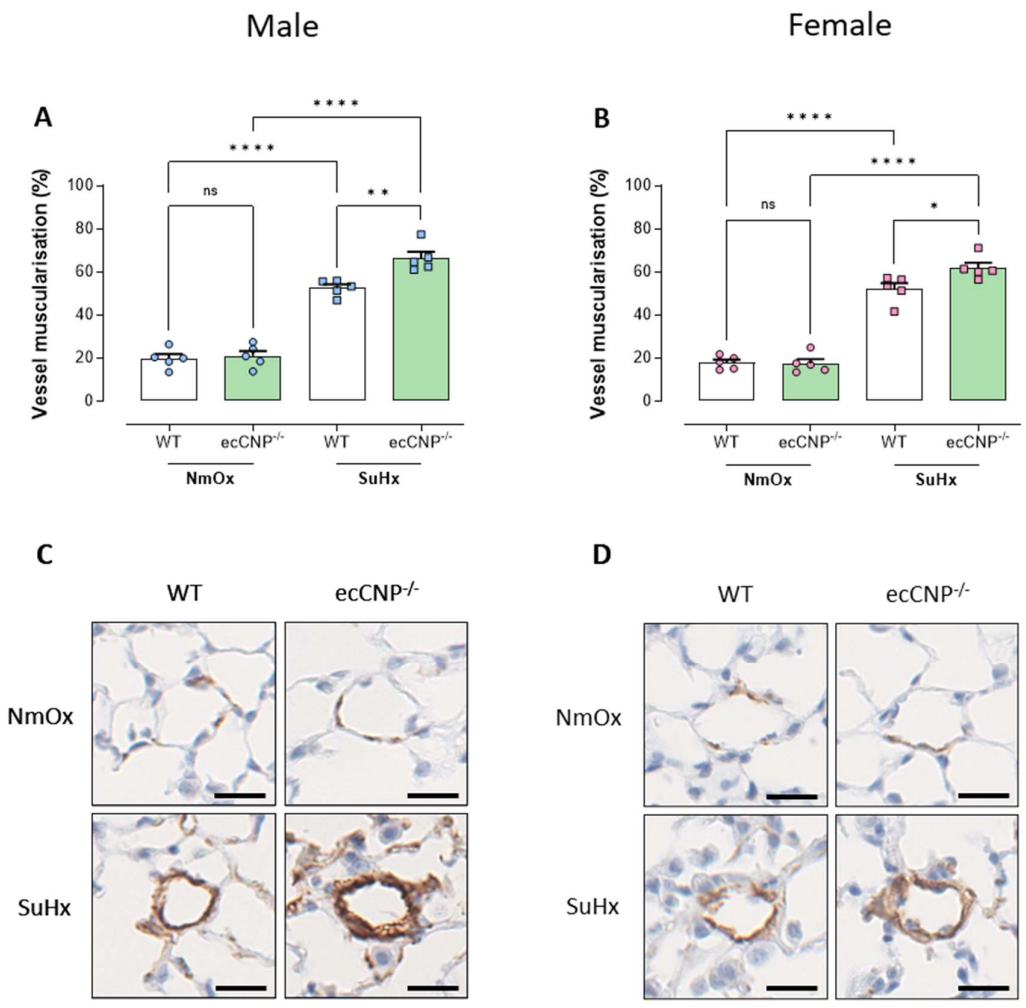

Figure 23: The effect of endothelial CNP deletion on pulmonary vascular remodelling in experimental PH

(A & *B*) Quantification of small (<80 μm in diameter) pulmonary vessel muscularisation in normoxic (NmOx) and Sugen + hypoxia (SuHx) wildtype (WT) and endothelial-specific CNP knockout (ecCNP$^{-/-}$) mice. (*C & D*) Representative images of lung sections stained for α-SMA (brown) and with haematoxylin (blue), demonstrating non-muscularised (staining ≤50% of circumference) and muscularised (staining ≥50% of circumference) pulmonary vessels at x20 magnification. Scale bar = 20 μm. Data presented as mean ± *SEM*; symbols represent individual data points. Statistical analysis by one-way ANOVA with Šidák post hoc test. *$P \leq 0.05$, **$P \leq 0.01$, ****$P \leq 0.0001$; *ns*, not significant (adjusted for multiplicity).

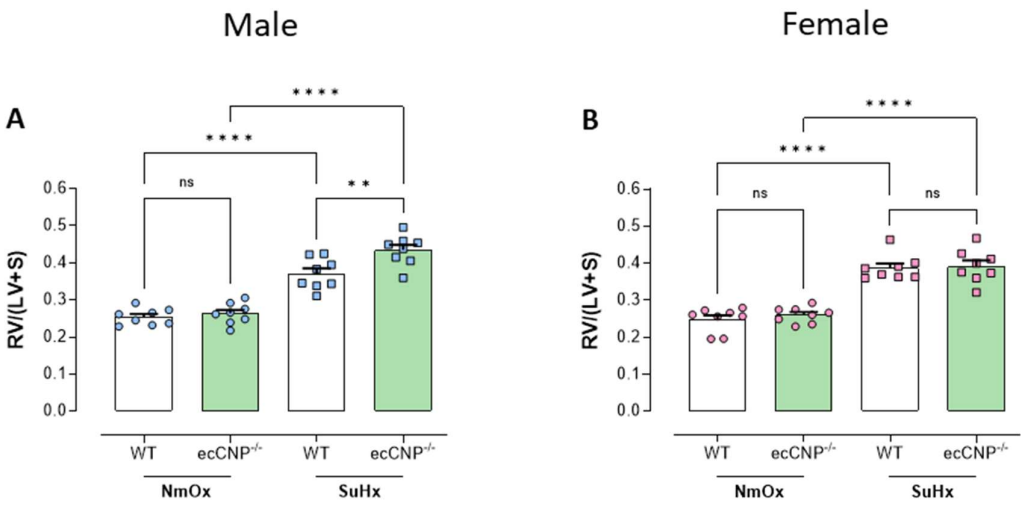

Figure 24: The effect of endothelial CNP deletion on RV hypertrophy following pressure overload

(A & B) Right ventricle to left ventricle plus septum (RV/(LV+S) in normoxic (NmOx) and Sugen + hypoxia (SuHx) wildtype (WT) and endothelial-specific CNP knockout (ecCNP$^{-/-}$) mice. Data presented as mean ± *SEM*; symbols represent individual data points. Statistical analysis by one-way ANOVA with Šidák post hoc test. **P*<0.05, ***P*<0.01, ****P*<0.001, *****P*<0.0001; *ns*, not significant (adjusted for multiplicity).

4.3 Loss of cardiomyocyte CNP does not alter experimental RVH

The phenotype observed in cmCNP$^{-/-}$ was consistent between male and female animals. In NmOx mice, loss of cardiomyocyte CNP had no effect on cardiopulmonary pressure. However, RVSP was significantly depressed in cmCNP$^{-/-}$ SuHx animals versus WT controls (***Figure 25A & B; Supplementary Figure 6A***). Right heart weight was unaltered in both NmOx and SuHx cmCNP$^{-/-}$ mice (***Figure 26A & B; Supplementary Figure 6C***). MABP was likewise unaffected by genotype (***Figure 25C & D; Supplementary Figure 6B***), though a modest but significant increase in MABP was observed in female WT SuHx animals versus WT NmOx mice.

The unexpected protective phenotype in cmCNP$^{-/-}$ animals was probed further by quantifying the mRNA expression of CNP in the RV of these mice. Surprisingly, the expression of CNP was significantly elevated in NmOx cmCNP$^{-/-}$ animals (***Figure 27A***), indicating that other cell types in the right heart enhance production of the peptide to compensate for the loss of cardiomyocyte derived CNP. Though WT and cmCNP$^{-/-}$ mice exhibited no significant difference in expression of the peptide following SuHx exposure (***Figure 27A***), the elevation of CNP expression at normoxia appeared to offset hypertrophic and fibrotic gene expression in the RV. Indeed, the expression of TGF-β1 and fibronectin expression were significantly reduced in cmCNP$^{-/-}$ SuHx mice, and the expression of CTGF and β-MHC also tended to be constrained (***Figure 27B - E***). Interestingly, the expression of SERCA2a, a modulator of cardiac contractility, was significantly upregulated in cmCNP$^{-/-}$ animals at baseline, but significantly depressed in these mice following SuHx exposure (***Figure 27F***).

To determine if the reduction of cardiopulmonary pressure following deletion of cardiomyocyte CNP was related to increased production of CNP by the right heart, pulmonary arterial remodelling was quantifying in female cmCNP$^{-/-}$ mice. Notably, the number of muscularised vessels was significantly tempered in cmCNP$^{-/-}$ animals versus WT controls (***Figure 28A & B***), consistent with a paracrine, vasoprotective action of cardiac-derived CNP.

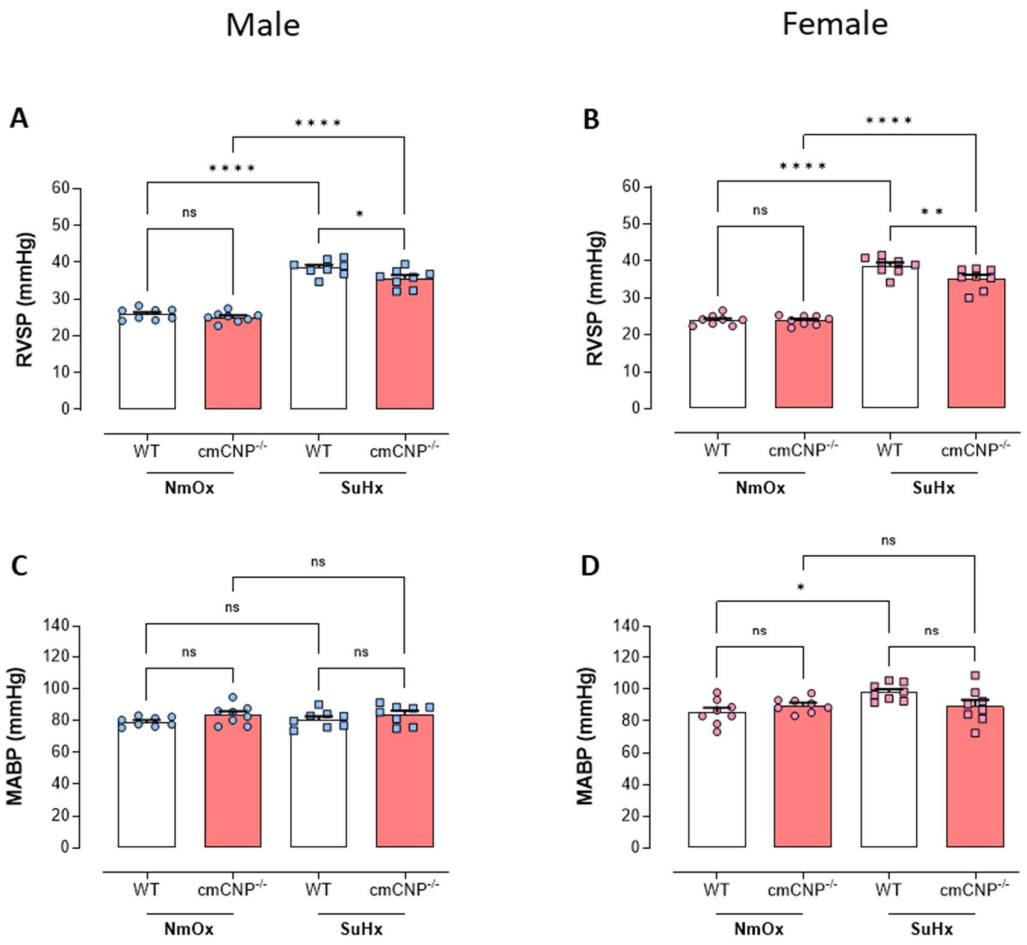

Figure 25: The effect of cardiomyocyte CNP deletion on cardiopulmonary and systemic arterial pressure in experimental PH

(*A & B*) Right ventricular systolic pressure (RVSP) and (*C & D*) mean arterial blood pressure (MABP) in normoxic (NmOx) and Sugen + hypoxia (SuHx) wildtype (WT) and cardiomyocyte-specific CNP knockout (cmCNP$^{-/-}$) mice. Data presented as mean ± *SEM*; symbols represent individual data points. *P<0.05, **P<0.01, ****P<0.0001; *ns*, not significant (adjusted for multiplicity).

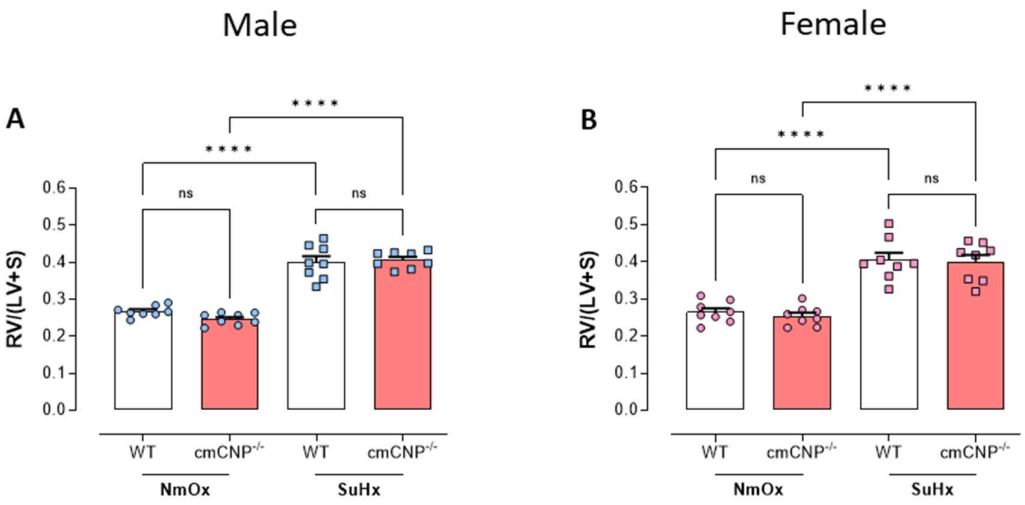

Figure 26: The effect of cardiomyocyte CNP deletion on RV hypertrophy following pressure overload

(*A & B*) Right ventricle to left ventricle plus septum; RV/(LV+S) in normoxic (NmOx) and Sugen + hypoxia (SuHx) wildtype (WT) and cardiomyocyte-specific CNP knockout (cmCNP$^{-/-}$) mice. Data presented as mean ± *SEM*; symbols represent individual data points. Statistical analysis by one-way ANOVA with Šidák post hoc test. ***P<0.01, ****P<0.0001; *ns*, not significant (adjusted for multiplicity).

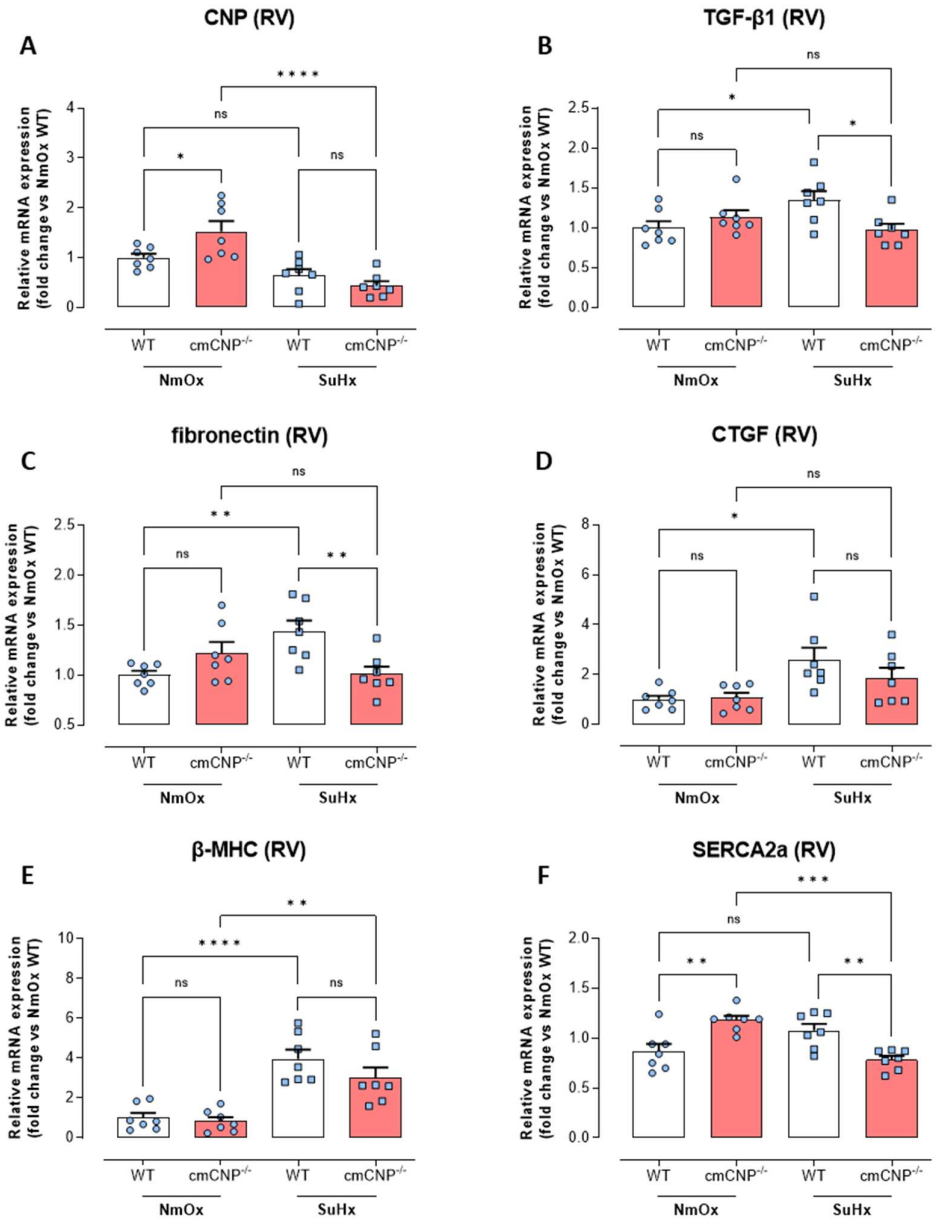

Figure 27: The effect of cardiomyocyte CNP depletion on remodelling-associated gene expression in the right heart of male mice following pressure overload

Right ventricular (RV) expression of (*A*) C-type natriuretic peptide (CNP), (*B*) transforming growth factor β1 (TGF-β1), (*C*) fibronectin, (*D*) connective tissue growth factor (CTGF), (E) β-myosin heavy chain (β-MHC) and (F) sarco/endoplasmic reticulum Ca^{2+}-ATPase (SERCA2a) mRNA in male normoxic (NmOx) and Sugen + hypoxia (SuHx) wildtype (WT) and cardiomyocyte-specific CNP knockout (cmCNP$^{-/-}$) mice. Data presented as mean ± *SEM*; symbols depict individual data points. Statistical analysis by one-way ANOVA with Šidák post hoc test. *$P \leq 0.05$, **$P \leq 0.01$, ***$P \leq 0.001$, ****$P \leq 0.0001$; *ns*, not significant (adjusted for multiplicity).

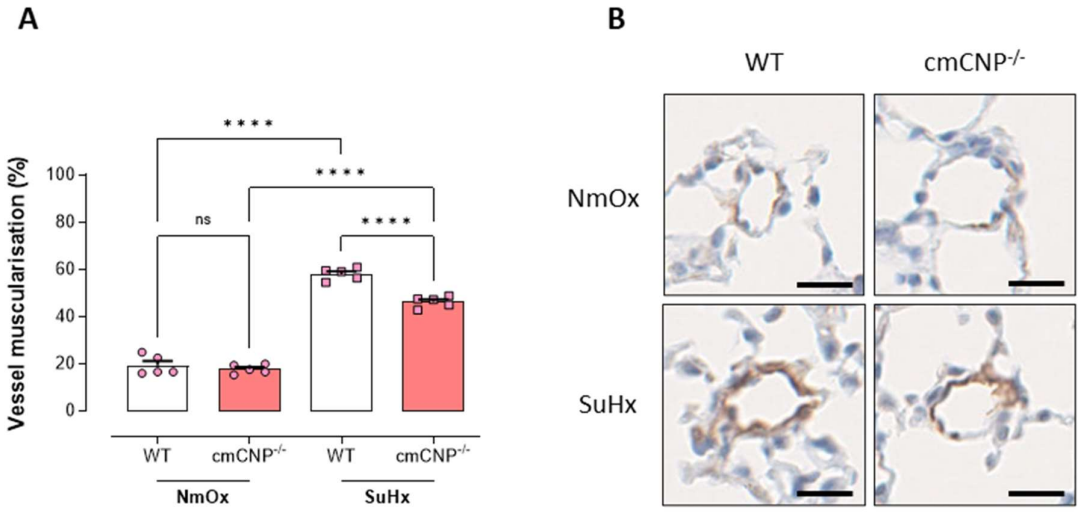

Figure 28: The effect of cardiomyocyte CNP depletion on pulmonary vascular remodelling in female mice with experimental PH

(*A*) Quantification of small (<80 μm in diameter) pulmonary vessel muscularisation in normoxic (NmOx) and Sugen + hypoxia (SuHx) wildtype (WT) and cardiomyocyte-specific CNP knockout (cmCNP$^{-/-}$) mice. (*B*) Representative images of lung sections stained for α-SMA (brown) and with haematoxylin (blue), demonstrating non-muscularised (staining ≤50% of circumference) and muscularised (staining ≥50% of circumference) pulmonary vessels at x20 magnification. Scale bar = 20 μm. Data presented as mean ± *SEM*; symbols represent individual data points. Statistical analysis by one-way ANOVA with Šidák post hoc test. ****$P \leq 0.0001$; *ns*, not significant (adjusted for multiplicity).

4.4 Global deletion of NPR-C exacerbates RVH and fibrosis in male SuHx mice

Having established CNP as a pivotal pathophysiological regulator of cardiopulmonary pressure, parallel investigations were conducted in global NPR-C$^{-/-}$ animals to ascertain which cognate receptor, NPR-B or NPR-C, underpins the detrimental effect(s) observed in male ecCNP$^{-/-}$ SuHx mice.

Global loss of NPR-C had no effect on RVSP (***Figure 29A; Supplementary Figure 7A***) nor pulmonary arterial muscularisation (***Figure 30A & C; Supplementary Figure 7C***) in male NmOx and SuHx animals, suggesting that regulation of pulmonary vascular pressure by endothelial CNP is independent of NPR-C. Furthermore, no significant changes were noted in MABP (***Figure 29C; Supplementary Figure 7B***). Whilst these data suggest that NPR-B is the major effector receptor for CNP in the pulmonary circulation, NPR-C deletion exacerbated the hypertrophic response of the RV to pressure overload, as demonstrated by a significant increase in RV/[LV+S] ratio (***Figure 31A; Supplementary Figure 7D***). Linked to this elevation of RV weight was a significant increase in the fibrotic burden of the ventricle (***Figure 32A & C; Supplementary Figure 7E***).

Mirroring the naïve phenotype observed in male mice, cardiopulmonary pressure was ostensibly identical in female NmOx NPR-C$^{-/-}$ animals and WT controls (***Figure 29B; Supplementary Figure 7A***). On the other hand, RVSP (***Figure 29B; Supplementary Figure 7A***) and pulmonary vascular remodelling (***Figure 30B & D; Supplementary Figure 7C***) were significantly reduced in female SuHx NPR-C$^{-/-}$ mice, suggesting that the loss of NPR-C signalling is offset by increased CNP bioavailability and NPR-B activation in these animals. Despite the easing of cardiopulmonary pressure overload, RV weight (***Figure 31B; Supplementary Figure 7D***) and fibrosis (***Figure 32B & D; Supplementary Figure 7E***) were unaltered. In addition, MABP was unchanged in female NPR-C$^{-/-}$ animals (***Figure 29D; Supplementary Figure 7B***).

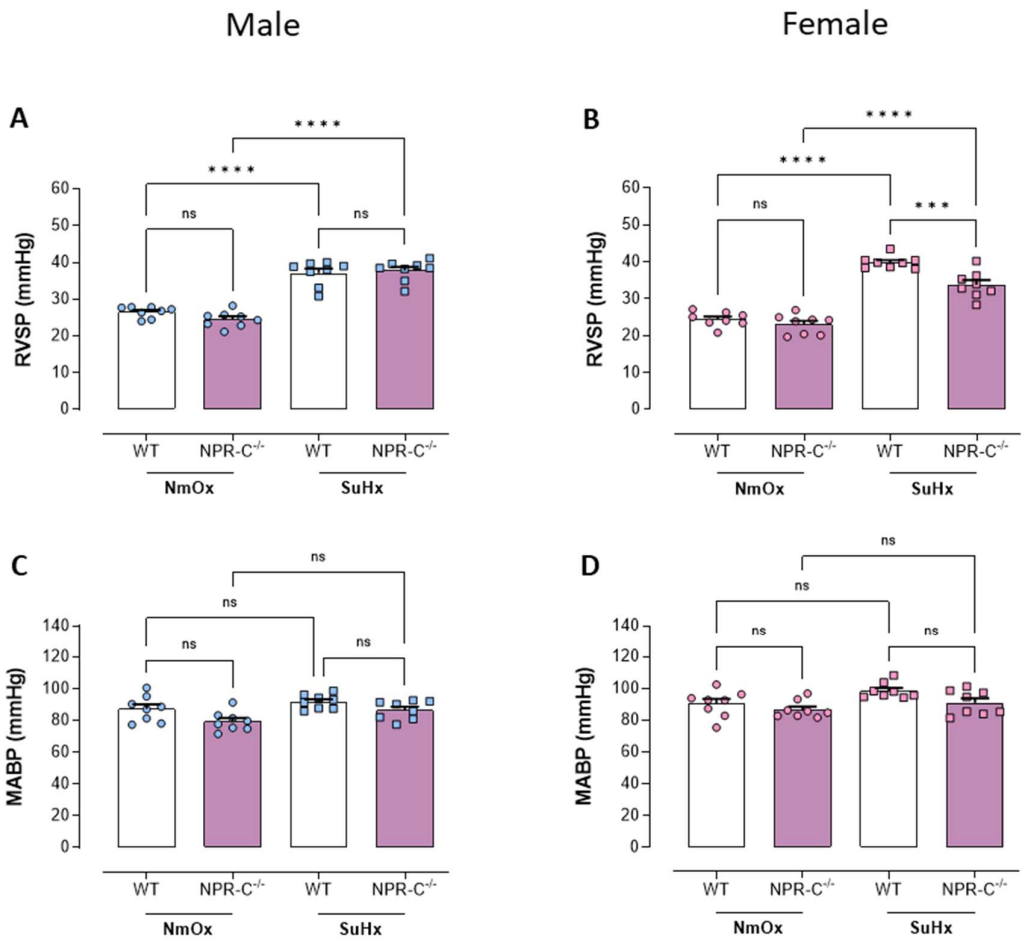

Figure 29: The effect of global NPR-C deletion on cardiopulmonary and systemic arterial pressure in experimental PH

(*A & B*) Right ventricular systolic pressure (RVSP) and (*C & D*) mean arterial blood pressure (MABP) in normoxic (NmOx) and Sugen + hypoxia (SuHx) wildtype (WT) and global NPR-C knockout (NPR-C$^{-/-}$) mice. Data presented as mean ± *SEM*; symbols represent individual data points. Statistical analysis by one-way ANOVA with Šidák post hoc test. ***$P \leq 0.001$, ****$P \leq 0.0001$; *ns*, not significant (adjusted for multiplicity).

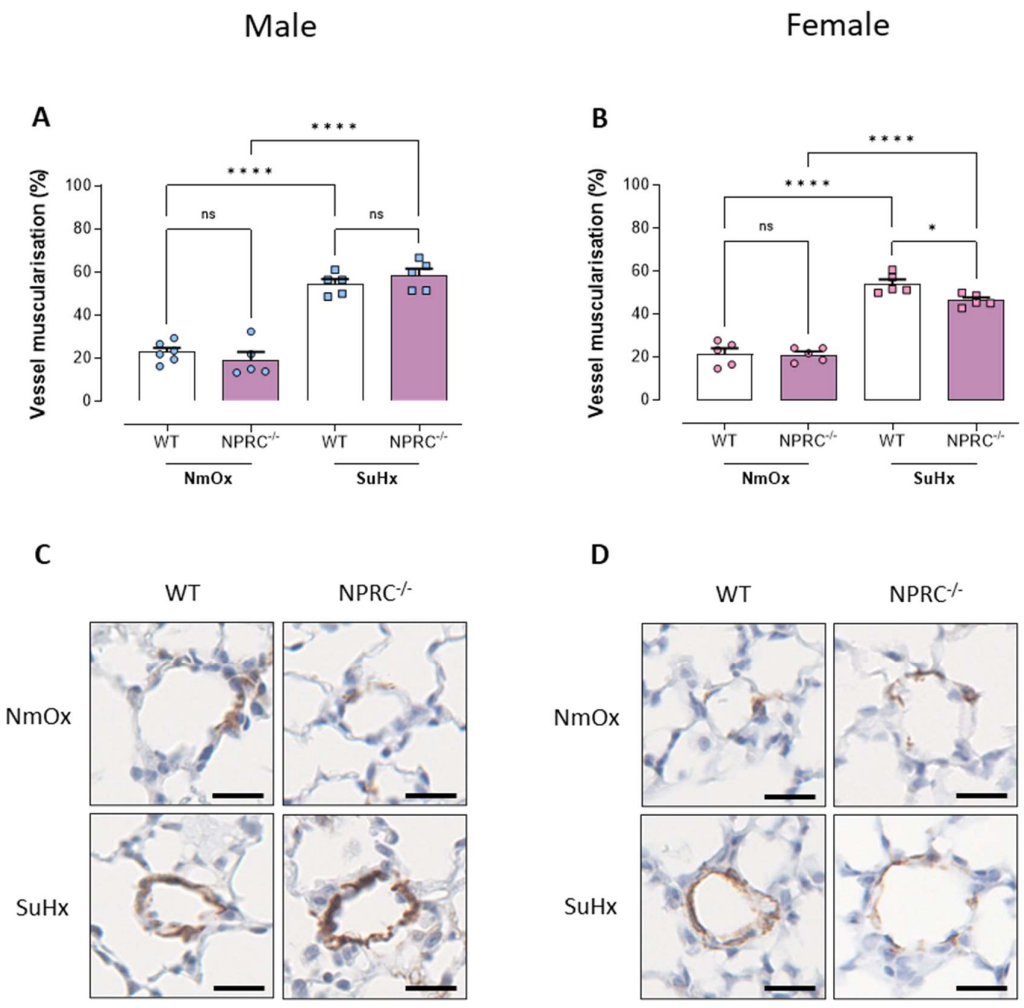

Figure 30: The effect of global NPR-C deletion on pulmonary vascular remodelling in experimental PH

(A & *B*) Quantification of small (<80 μm in diameter) pulmonary vessel muscularisation in normoxic (NmOx) and Sugen + hypoxia (SuHx) wildtype (WT) and global NPR-C knockout (NPR-C$^{-/-}$) mice. (*C & D*) Representative images of lung sections stained for α-SMA (brown) and with haematoxylin (blue), demonstrating non-muscularised (staining ≤50% of circumference) and muscularised (staining ≥50% of circumference) pulmonary vessels at x20 magnification. Scale bar = 20 μm. Data presented as mean ± *SEM*; symbols represent individual data points. Statistical analysis by one-way ANOVA with Šidák post hoc test. **P* ≤ 0.05, *****P* ≤ 0.0001; *ns*, not significant (adjusted for multiplicity).

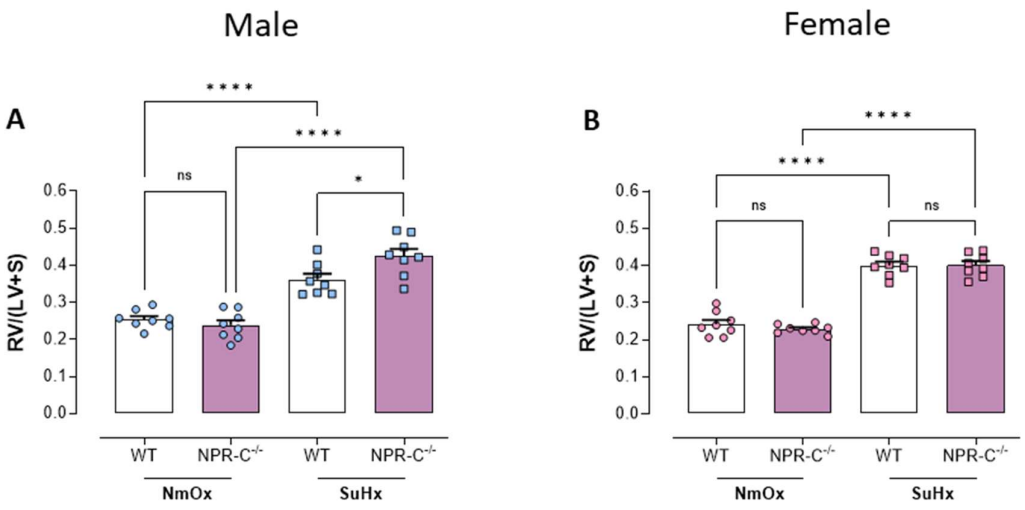

Figure 31: The effect of global NPR-C deletion on RV hypertrophy in experimental PH

(*A & B*) Right ventricle to left ventricle plus septum ratio; RV/(LV+S) in normoxic (NmOx) and Sugen + hypoxia (SuHx) wildtype (WT) and global NPR-C knockout (NPR-C$^{-/-}$) mice. Data presented as mean ± *SEM*; symbols represent individual data points. Statistical analysis by one-way ANOVA with Šidák post hoc test. *$P \leq 0.05$, ****$P \leq 0.0001$; *ns*, not significant (adjusted for multiplicity).

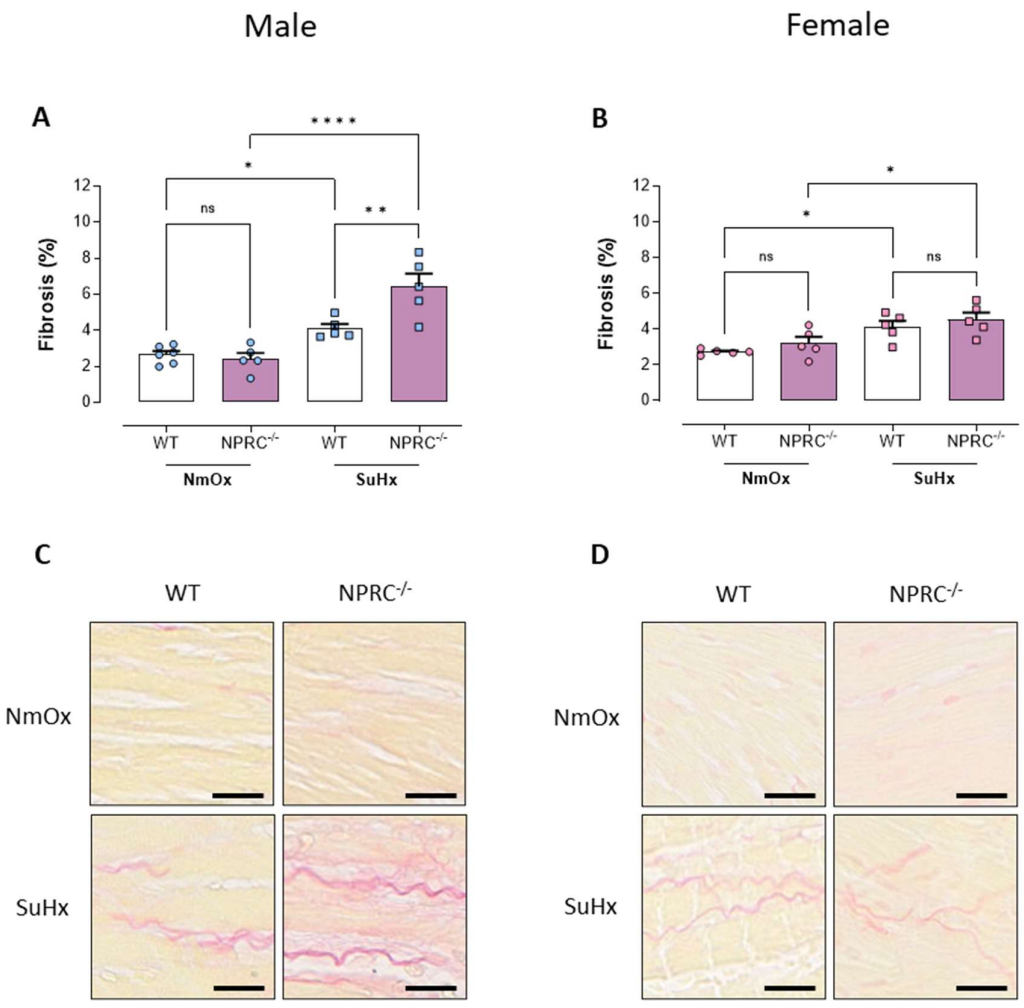

Figure 32: The effect of global NPR-C depletion on the development of RV fibrosis following pressure overload

(A & *B*) Quantification of right ventricular collagen deposition in normoxic (NmOx) and Sugen + hypoxia (SuHx) wildtype (WT) and global NPR-C knockout (NPR-C$^{-/-}$) mice. (*C & D*) Representative images of RV sections stained with picrosirius red stain at x20 magnification, with collagen shown in red. Scale bar = 20 µm. Data presented as mean ± *SEM*; symbols represent individual data points. Statistical analysis by one-way ANOVA with Šidák post hoc test. *$P \leq 0.05$, **$P \leq 0.01$, ****$P \leq 0.0001$; *ns*, not significant (adjusted for multiplicity).

Chapter V: Results III

5.1 Overview

The data presented thus far outline a protective role for endogenous CNP in the pathogenesis of PH and provide a clear rationale for pharmacologically targeting the signalling pathway of this peptide. Accordingly, the data contained within this chapter probe the therapeutic potential of exogenous peptide in the context of experimental PH. In a proof-of-concept study, CNP was delivered to male WT SuHx mice by subcutaneous osmotic minipump, at a fixed dose of 0.2 mg/kg/day (according to previous studies Bubb et al., 2019; Moyes et al., 2020). Peptide therapy was initiated 3 weeks after the onset of hypoxic exposure and then maintained for the remainder of the duration of the study. In addition, NPR-C$^{-/-}$ SuHx animals were also treated with CNP, to further corroborate the critical role of CNP/NPR-B signalling in pulmonary vascular homeostasis. In these experiments, echocardiography was used to track pathological changes in the cardiopulmonary system longitudinally, providing a more detailed picture of pulmonary haemodynamics and RV structure, and allowing insight into the functional status of the heart.

5.2 Exogenous CNP reverses established experimental PH via NPR-B-signalling

CNP infusion significantly lowered RVSP by an average of 6.43 ± 0.98 and 6.92 ± 1.02 mmHg in WT and NPR-C$^{-/-}$ mice, respectively. The preserved effect of CNP in NPR-C$^{-/-}$ animals substantiates the role of CNP/NPR-B signalling in the regulation of pulmonary vascular homeostasis (***Figure 33A***). Crucially, the absence of a concomitant (adverse) drop in MABP alludes to a degree of pulmonary selectivity (***Figure 33B***). Despite a robust reduction in RVSP, CNP administration did not significantly reverse RV remodelling in WT mice, though the easing of pressure overload tended to reduce RV/(LV+S) and significantly reduced RV fibrosis in NPR-C$^{-/-}$ animals (***Figure 33C & D***).

Circulating natriuretic peptide levels were also investigated in SuHx and CNP-treated animals. The plasma concentration of CNP trended towards lower levels in WT SuHx mice. As expected, plasma levels of the peptide were significantly elevated in CNP-treated SuHx animals versus non-treated SuHx mice (***Figure 34A & B***). Plasma levels of ANP were likewise investigated, Circulating ANP was not significantly altered in SuHx animals (***Figure 34C & D***); nonetheless, plasma levels of the peptide were significantly elevated in CNP-treated NPR-C$^{-/-}$ SuHx mice (***Figure 34D***).

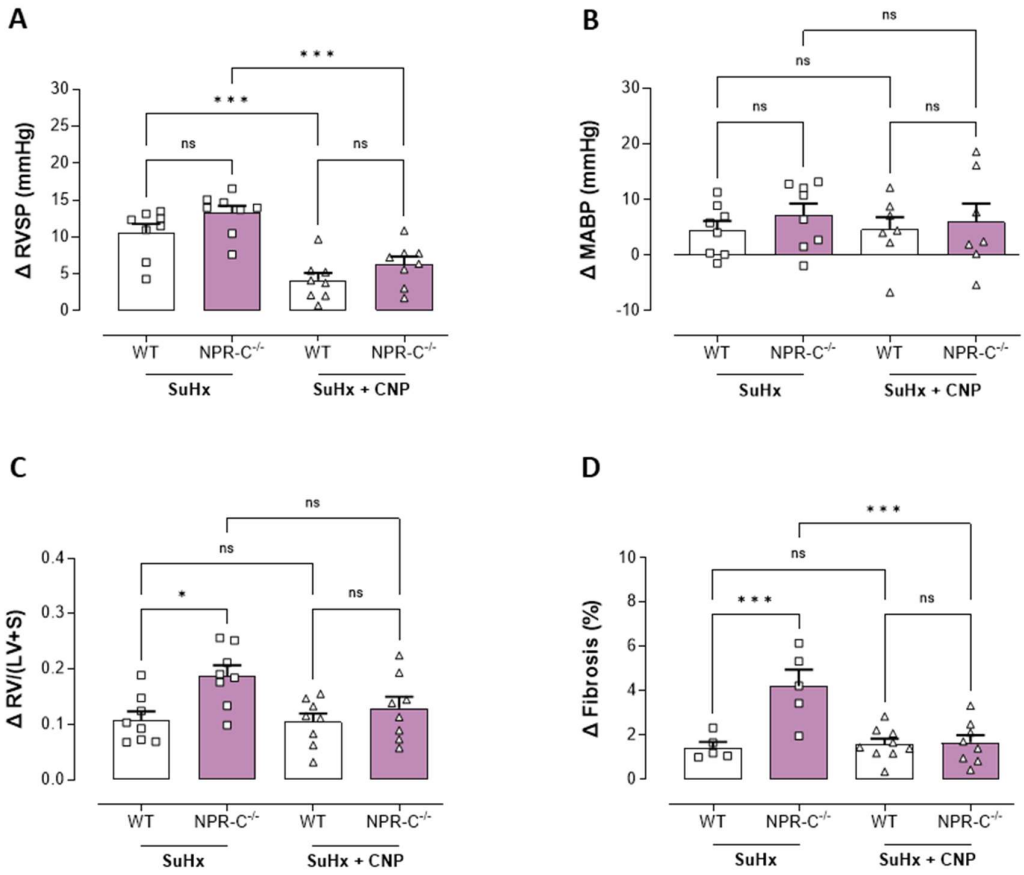

Figure 33: The effect of CNP infusion on cardiopulmonary pressure, systemic arterial pressure, RV hypertrophy, and RV fibrosis in male WT and NPR-C$^{-/-}$ mice with experimental PH

Change in (*A*) right ventricular systolic pressure (RVSP), (*B*) mean arterial blood pressure (MABP), (*C*) right ventricle to left ventricle plus septum ratio (RV/(LV+S), and (*D*) RV fibrosis in Sugen + hypoxia (SuHx) wildtype (WT) and global NPR-C knockout (NPR-C$^{-/-}$) mice treated with CNP. Peptide was delivered by osmotic minipump (0.2 mg/kg/day, s.c., initiated at 3w). Δ is change relative to normoxic control animals for the respective genotype. Data presented as mean ± *SEM*; symbols represent individual data points. Statistical analysis by one-way ANOVA with Šidák post hoc test. **P* ≤ 0.05, ***P* ≤ 0.01, ****P* ≤ 0.001; *ns*, not significant (adjusted for multiplicity).

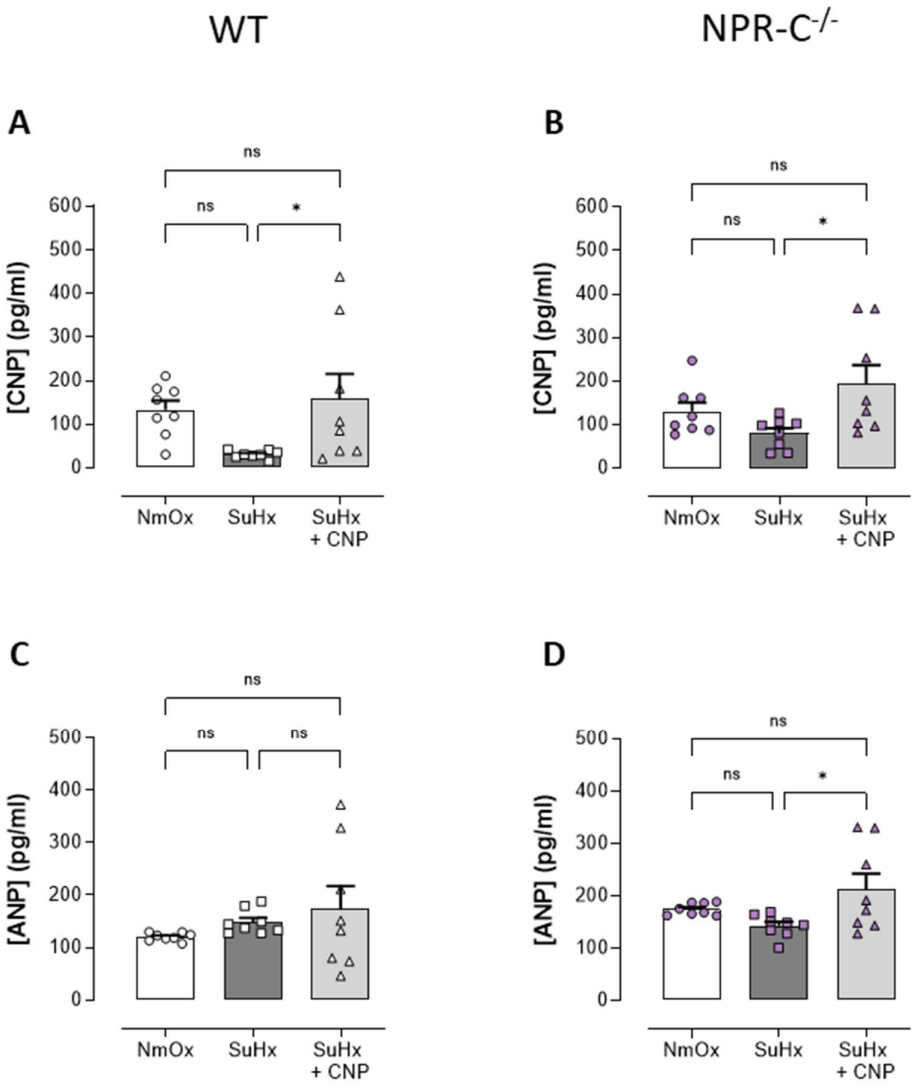

Figure 34: Plasma natriuretic peptide levels in male WT and NPR-C$^{-/-}$ mice with experimental PH

Concentration of (*A & B*) C-type natriuretic peptide (CNP), and (*C & D*) A-type natriuretic peptide (ANP) in the plasma of normoxic (NmOx) and Sugen + hypoxia (SuHx) wildtype (WT) and global NPR-C knockout (NPR-C$^{-/-}$) mice. CNP was delivered by osmotic minipump (0.2 mg/kg/day, s.c., initiated at 3w). Data presented as mean ± *SEM*; symbols represent individual data points. Statistical analysis by one-way ANOVA with Šidák post hoc test. *$P \leq 0.05$; *ns*, not significant (adjusted for multiplicity).

5.3 Pulmonary haemodynamics in CNP-treated WT and NPR-C$^{-/-}$ SuHx mice

In WT and NPR-C$^{-/-}$ mice, PAT (a non-invasive measure of pulmonary haemodynamics) was significantly decreased at 3w versus normoxia (i.e. baseline; ***Figure 35A & B***), indicative of a PH phenotype. Interestingly, PAT tended to be higher in NPR-C$^{-/-}$ mice compared to WT animals at normoxia and 3w and was significantly higher at 5w (***Table 20***). Furthermore, following SuHx exposure, NPR-C deletion prevented the reduction in pulmonary artery peak velocity observed in WT mice (***Figure 35C & D***). This may be attributed to the tendency towards lower baseline velocity in NPR-C$^{-/-}$ animals (***Table 20***), which may have masked any pathological changes. Taken together, these findings suggest that reduced CNP clearance (i.e. greater bioavailability) has a subtle protective effect on pulmonary haemodynamics, mediated by NPR-B, albeit with no impact on RVSP.

Following the 3w recording, 50% of mice were implanted with osmotic minipumps containing CNP. In non-treated animals, there was no further decrease in PAT between 3w and 5w (***Figure 35A & B***). In CNP-treated WT mice, PAT was elevated versus non-treated mice, commensurate with the decrease in RVSP presented earlier (***Figure 33A***). Indeed, this salutary effect was so pronounced that PAT was restored to NmOx values in some mice. Interestingly, this effect was abolished in NPR-C$^{-/-}$ mice (***Figure 35B***), despite the propensity of CNP to reduce RVSP in these animals. Still, PAT was not significantly different between CNP-treated WT and NPR-C$^{-/-}$ mice at 5w (***Table 20***), indicating a parity in the magnitude of benefit achieved by endogenous and exogenous CNP.

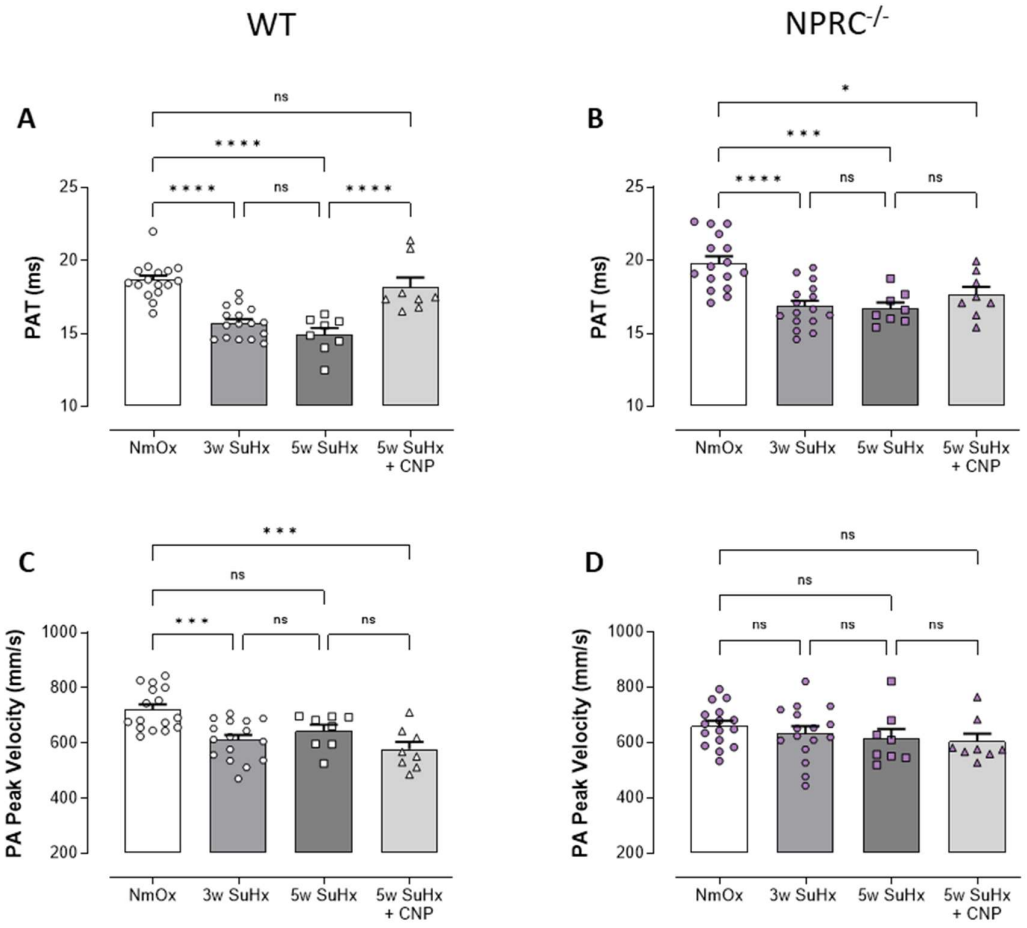

Figure 35: The effect of CNP infusion on pulmonary artery function in male WT and NPR-C$^{-/-}$ mice with experimental PH

(*A & B*) Pulmonary acceleration time (PAT) and (*C & D*) pulmonary artery (PA) peak velocity in normoxic (NmOx) and Sugen + hypoxia (SuHx) wildtype (WT) and global NPR-C knockout (NPR-C$^{-/-}$) mice. CNP was delivered by osmotic minipump (0.2 mg/kg/day, s.c., initiated at 3w). Data presented as mean ± *SEM*; symbols represent individual data points. Statistical analysis by one-way ANOVA with Šidák post hoc test. *$P \leq 0.05$, ***$P \leq 0.001$, ****$P \leq 0.0001$; *ns*, not significant (adjusted for multiplicity).

5.4 Cardiac function in CNP-treated WT and NPR-C$^{-/-}$ SuHx mice

RVH was also assessed by echocardiography. End-diastolic right ventricular free wall thickness (RVFWd) was comparable between WT and NPR-C$^{-/-}$ animals at normoxia (***Table 20***). Moreover, both genotypes demonstrated a progressive and significant increase in RVFWd at 3w and 5w (***Figure 36A & B***); mirroring the endpoint tissue weight presented in the previous chapter (***Figure 30A***), RVFWd was significantly higher in NPR-C$^{-/-}$ mice versus WT animals at 3w and trended towards greater thickness at 5w (***Table 20***). CNP infusion did not alter RVFWd in either genotype (***Figure 36A & B***).

The impact of RV remodelling on the functional status of the heart was also investigated. At normoxia, there was no effect of NPR-C depletion on TAPSE (a measure of RV systolic function; ***Table 20***). SuHx exposure resulted in a modest depression of TAPSE in both WT and NPR-C$^{-/-}$ animals, albeit with no significant difference in the magnitude of RV dysfunction, nor the propensity for reversal by CNP (***Figure 36C & D***). A similar pattern was noted for tricuspid valve peak velocity (***Figure 36E & F***), albeit with trends towards greater velocity in NPR-C$^{-/-}$ mice at baseline and following CNP treatment (***Table 20***).

Curiously, RV dysfunction was accompanied by augmented left ventricular ejection fraction (LVEF) in WT mice (***Figure 37A***). Conversely, LVEF was unaltered in NPR-C$^{-/-}$ animals (***Figure 37B***) and thus was significantly lower versus WT mice at 3w and 5w (***Table 21***). In the context of PH, increased LVEF may be a compensatory mechanism to ensure adequate perfusion of the systemic circulation in the face of diminished RV function and reduced venous return. Indeed, CO was maintained in WT mice following SuHx exposure (***Figure 36C***) but was significantly lower in NPR-C$^{-/-}$ animals. Intriguingly, CO trended towards improvement in NPR-C$^{-/-}$ mice following CNP infusion (***Figure 36D***), though LVEF was unaffected (***Figure 37B***). Neither NPR-C depletion (***Table 21***) nor SuHx exposure (***Figure 37E & F***) had any effect on HR.

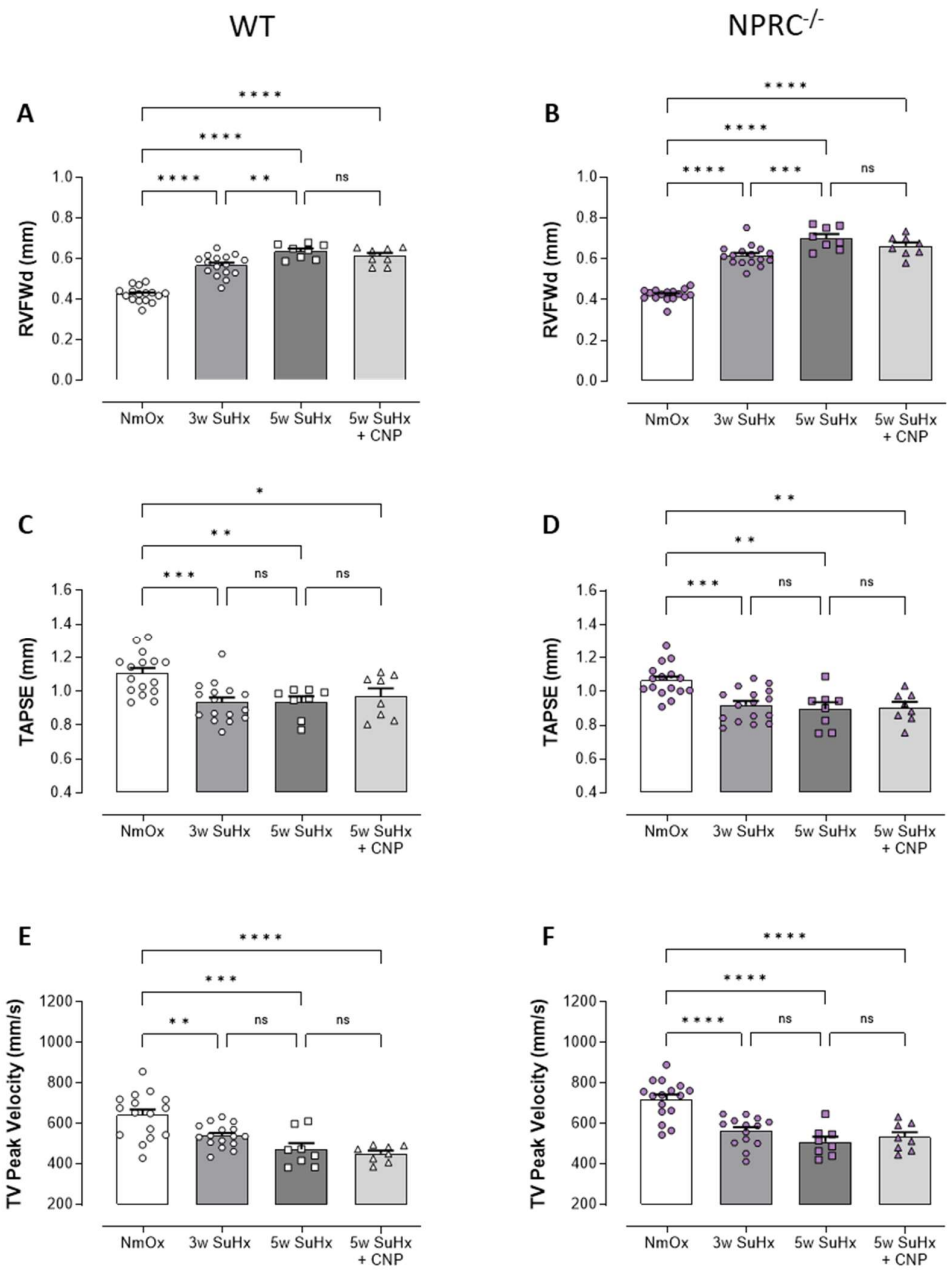

Figure 36: The effect of CNP infusion on cardiopulmonary structure and function in male WT and NPR-C$^{-/-}$ mice with experimental PH

(*A & B*) diastolic right ventricular free wall thickness (RVFWd), (*C & D*) tricuspid annular plane systolic excursion (TAPSE), and (*E & F*) tricuspid valve (TV) peak velocity in normoxic (NmOx) and Sugen + hypoxia (SuHx) wildtype (WT) and global NPR-C knockout (NPR-C$^{-/-}$) mice. CNP was delivered by osmotic minipump (0.2 mg/kg/day, s.c., initiated at 3w). Data presented as mean ± *SEM*; symbols represent individual data points. Statistical analysis by one-way ANOVA with Šidák post hoc test. *$P \leq 0.05$, **$P \leq 0.01$, ***$P \leq 0.001$, ****$P \leq 0.0001$; *ns*, not significant (adjusted for multiplicity).

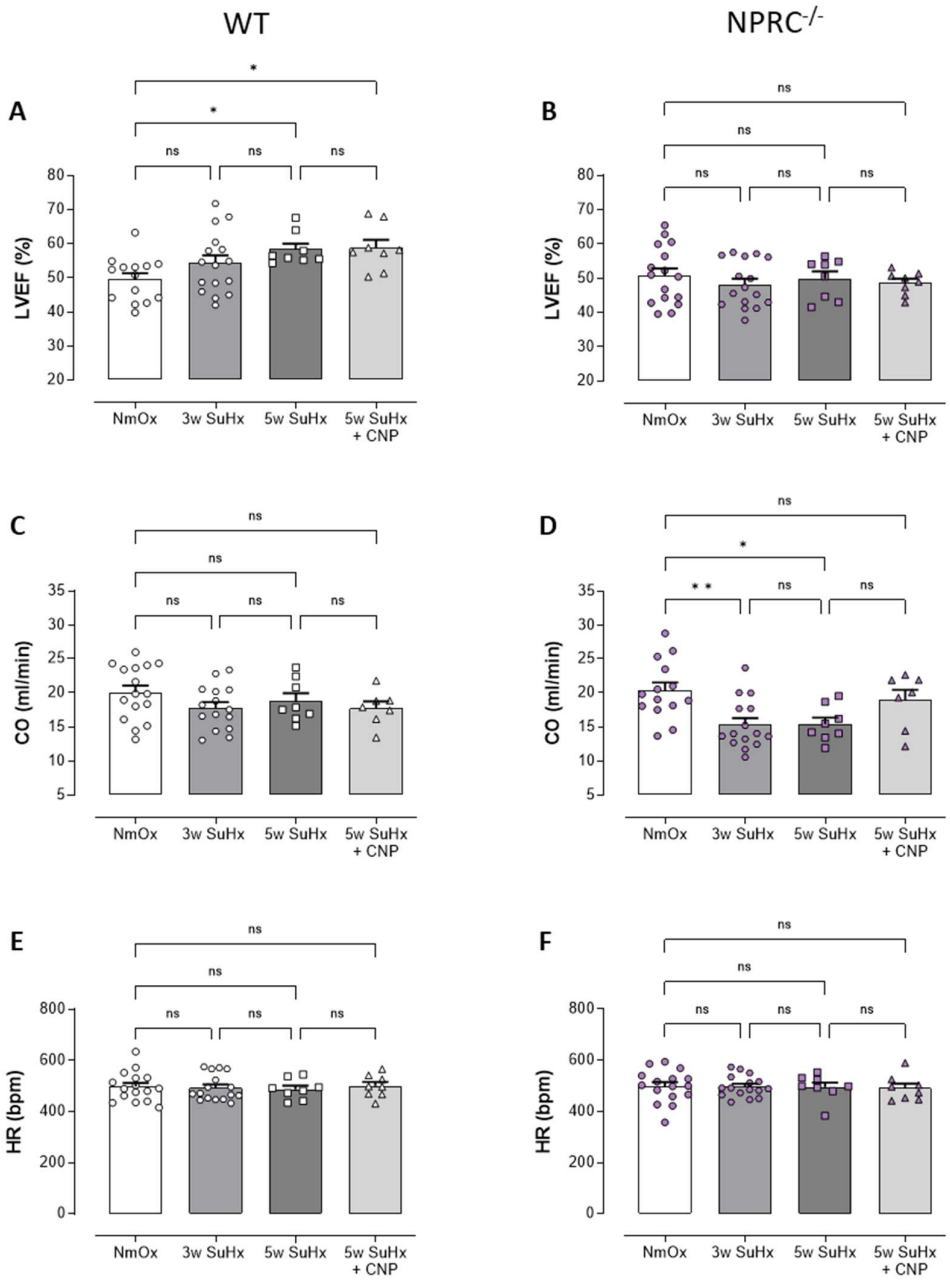

Figure 37: The effect of CNP infusion on global heart function in male WT and NPR-C$^{-/-}$ mice with experimental PH

(*A & B*) Left ventricular ejection fraction (LVEF), (*C & D*) cardiac output (CO), and (*E & F*) heart rate (HR) in normoxic (NmOx) and Sugen + hypoxia (SuHx) wildtype (WT) and global NPR-C knockout (NPR-C$^{-/-}$) mice. CNP was delivered by osmotic minipump (0.2 mg/kg/day, s.c., initiated at 3w). Data presented as mean ± *SEM*; symbols represent individual data points. Statistical analysis by one-way ANOVA with Šidák post hoc test. *$P \leq 0.05$, **$P \leq 0.01$; *ns*, not significant (adjusted for multiplicity).

Table 20: Cardiopulmonary function in NPR-C$^{-/-}$ mice

		WT	NPR-C$^{-/-}$	*P* Value
PAT (ms)	*NmOx*	18.66 ± 0.31	19.81 ± 0.46	0.18
	3w SuHx	15.72 ± 0.27	16.85 ± 0.37	0.08
	5w SuHx	14.94 ± 0.45	16.72 ± 0.39	0.04*
	5w SuHx + CNP	18.19 ± 0.65	17.63 ± 0.54	0.95
PA Peak Velocity (mm/s)	*NmOx*	721.07 ± 18.85	659.80 ± 18.40	0.10
	3w SuHx	611.24 ± 18.12	634.62 ± 24.53	0.91
	5w SuHx	643.98 ± 22.57	613.90 ± 35.00	0.93
	5w SuHx + CNP	578.06 ± 26.58	604.28 ± 27.93	0.94
RVFWd (mm)	*NmOx*	0.42 ± 0.01	0.42 ± 0.01	>0.99
	3w SuHx	0.57 ± 0.01	0.62 ± 0.01	0.04*
	5w SuHx	0.64 ± 0.01	0.70 ± 0.02	0.07
	5w SuHx + CNP	0.61 ± 0.02	0.66 ± 0.02	0.17
TAPSE (mm)	*NmOx*	1.11 ± 0.03	1.06 ± 0.02	0.75
	3w SuHx	0.93 ± 0.03	0.92 ± 0.02	>0.99
	5w SuHx	0.94 ± 0.03	0.90 ± 0.04	0.90
	5w SuHx + CNP	0.97 ± 0.05	0.91 ± 0.03	0.72
TV Peak Velocity (mm/s)	*NmOx*	641.82 ± 28.26	720.14 ± 23.74	0.16
	3w SuHx	539.76 ± 14.04	562.24 ± 19.44	0.83
	5w SuHx	472.32 ± 31.31	509.46 ± 25.74	0.85
	5w SuHx + CNP	452.10 ± 14.38	533.04 ± 24.33	0.06

PAT, pulmonary acceleration time; PA, pulmonary artery; RVFW, diastolic right ventricular free wall thickness; TAPSE, tricuspid annular plane systolic excursion; TV, tricuspid valve; ms, millisecond; mm, millimetre; s, second; NmOx, normoxic; w, week; SuHx, Sugen plus hypoxia. CNP was delivered by osmotic minipump (0.2 mg/kg/day, s.c., for 14 days) implanted after echocardiography on week 3. Data presented as mean ± *SEM*; *n*=8-16. Statistical analysis by two-way ANOVA with Šidák post hoc test (adjusted for multiplicity). *$P \leq 0.05$.

Table 21: Global heart function in NPR-C$^{-/-}$ mice

		WT	NPR-C$^{-/-}$	*P* Value
LVEF (%)	*NmOx*	49.61 ± 1.74	50.76 ± 2.10	0.99
	3w SuHx	54.33 ± 2.25	48.19 ± 1.70	0.14
	5w SuHx	58.34 ± 1.70	49.87 ± 2.09	0.03*
	5w SuHx + CNP	58.78 ± 2.37	48.68 ± 1.21	0.01*
CO (ml/min)	*NmOx*	20.02 ± 1.00	20.22 ± 1.15	>0.99
	3w SuHx	17.78 ± 0.83	15.34 ± 0.95	0.23
	5w SuHx	18.79 ± 1.09	15.43 ± 0.92	0.13
	5w SuHx + CNP	17.73 ± 0.97	18.89 ± 1.53	0.95
HR (bpm)	*NmOx*	497 ± 14	498 ± 16	>0.99
	3w SuHx	493 ± 13	497 ± 10	>0.99
	5w SuHx	487 ± 14	494 ± 18	>0.99
	5w SuHx + CNP	499 ± 16	491 ± 18	>0.99

LVEF, left ventricular ejection fraction; CO, cardiac output; HR, heart rate; ml, millilitre; min, minute; bpm, beats per minute; NmOx, normoxic; w, week; SuHx, Sugen plus hypoxia. CNP was delivered by osmotic minipump (0.2 mg/kg/day, s.c., for 14 days) implanted after echocardiography on week 3. Data presented as mean ± *SEM*; *n*=8-16. Statistical analysis by two-way ANOVA with Šidák post hoc test (adjusted for multiplicity). *$P \leq 0.05$.

5.5 CNP infusion tempers the expression of remodelling-associated genes

To gain insight into the molecular pathways underlying the therapeutic effect of CNP in the SuHx mouse model, the mRNA expression of BMPR2 (an established causal factor in human PH) and its downstream effectors (Smads) was investigated in the lungs of WT SuHx mice treated with CNP.

Akin to human PH, BMPR2 expression was significantly reduced in SuHx mice versus NmOx controls. Crucially, CNP administration boosted the expression of BMPR2 to a level commensurate with NmOx controls (***Figure 38A***). Smad3 expression was likewise significantly decreased in SuHx animals, an effect which was partially reversed by CNP infusion (***Figure 38B***). The transcription of Smad5 and Smad7 was also significantly upregulated in CNP-treated mice versus SuHx animals (***Figure 38C & D***). These changes are commensurate with a shift in balance from TGF-β to BMP signalling, promoting an anti-proliferative, anti-remodelling environment.

The expression of pro-hypertrophic and pro-fibrotic markers in the RV was also investigated. In SuHx animals, gene expression of the ventricular stress hormone, BNP, was increased versus NmOx controls (***Figure 39A***). Furthermore, TGF-β1, fibronectin and CTGF were similarly upregulated in the RV (***Figure 39B - D***); of these genes, CNP impacted the expression of CTGF alone, which was reduced to near-control levels.

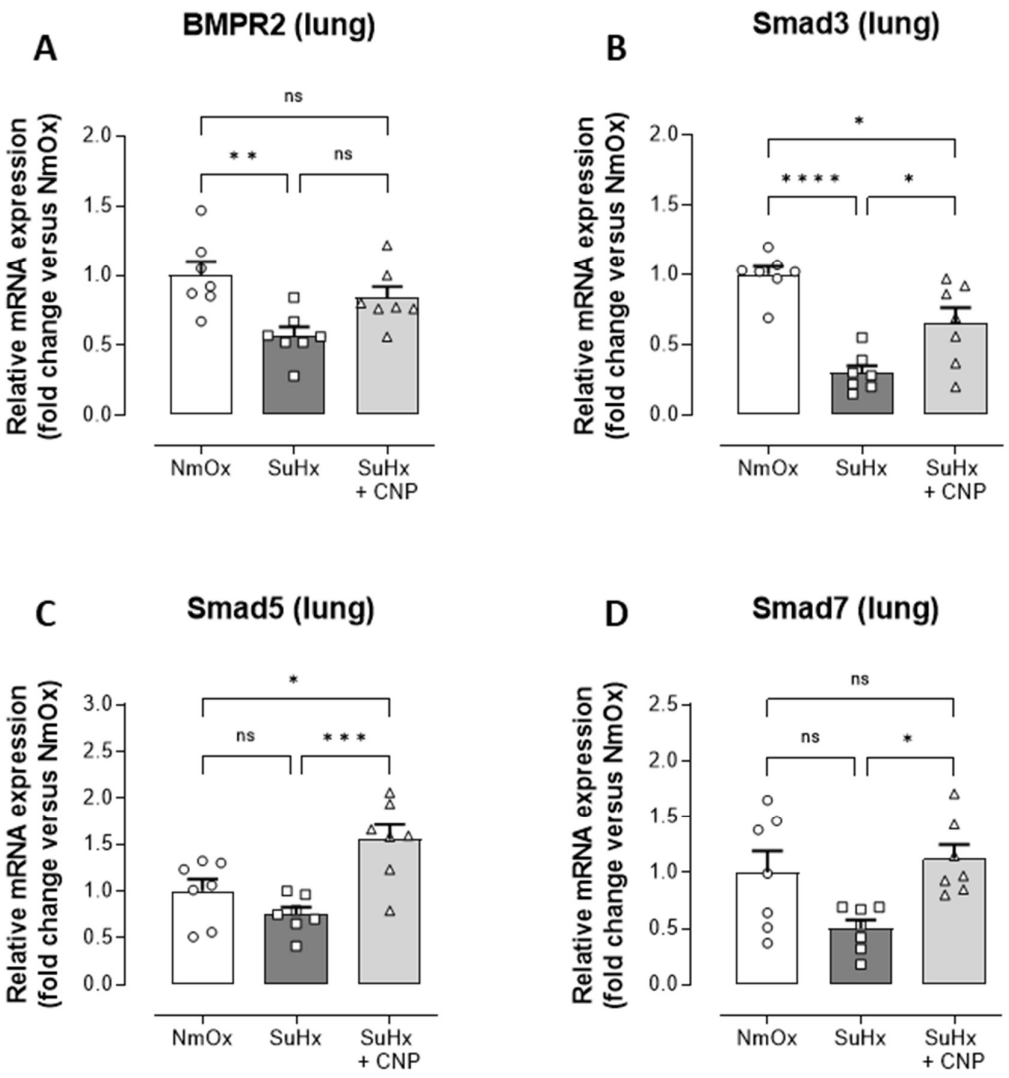

Figure 38: The effect of CNP infusion on remodelling-associated gene expression in the lungs of male WT mice with experimental PH

Pulmonary expression of (*A*) bone morphogenetic protein receptor type 2 (BMPR2), (*B*) suppressor of mothers against decapentaplegic 3 (Smad3), (*C*) Smad5, and (*D*) Smad7 mRNA in normoxic (NmOx) and Sugen + hypoxia (SuHx) wildtype (WT) mice. CNP was delivered by osmotic minipump (0.2 mg/kg/day, s.c., for 14 days). Data presented as mean ± *SEM*; symbols depict individual data points. Statistical analysis by one-way ANOVA with Šidák post hoc test. *$P \leq 0.05$, **$P \leq 0.01$, ***$P \leq 0.001$, ****$P \leq 0.0001$; *ns*, not significant (adjusted for multiplicity).

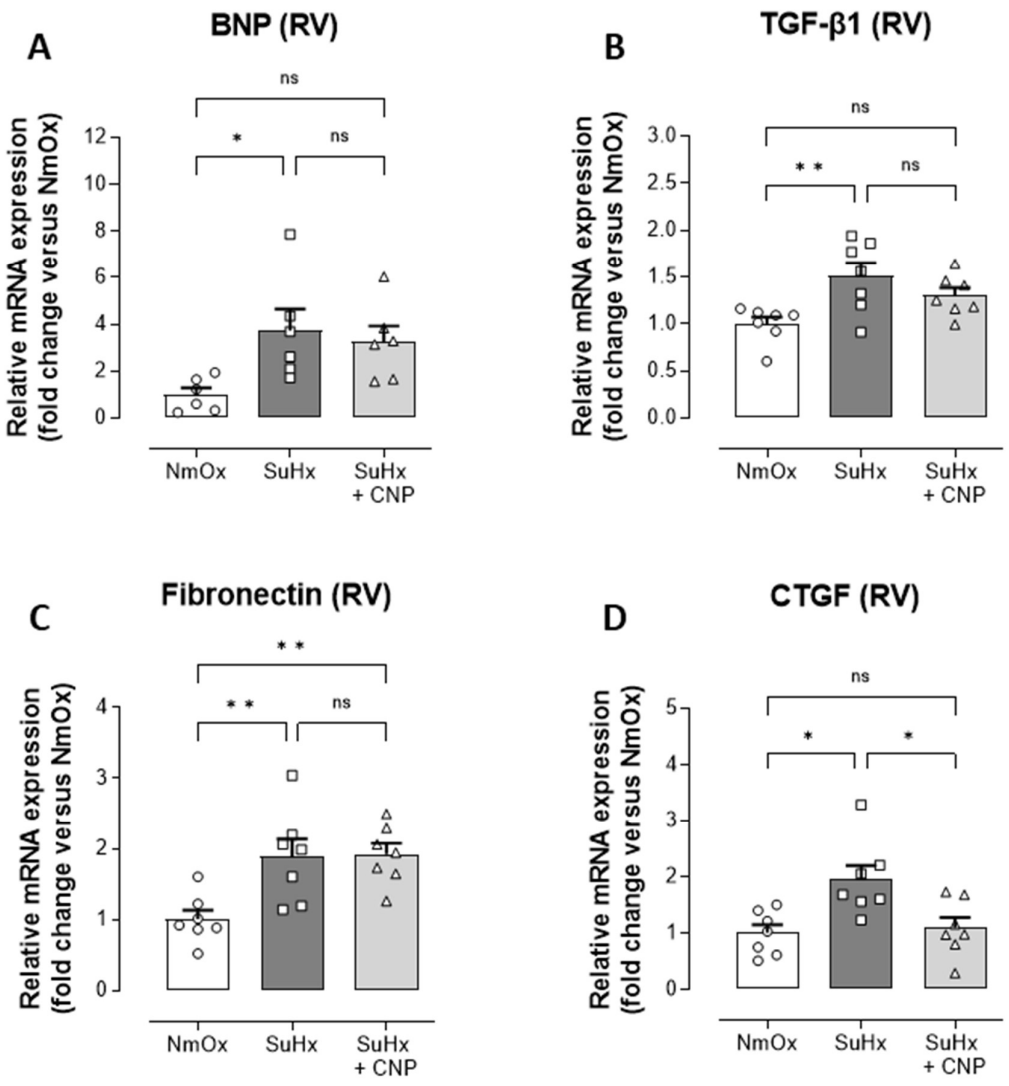

Figure 39: The effect of CNP infusion on remodelling-associated gene expression in the right heart of male WT mice with experimental PH

Right ventricular (RV) expression of (*A*) B-type natriuretic peptide (BNP), (*B*) transforming growth factor β (TGF-β), (*C*) fibronectin, and (*D*) connective tissue growth factor (CTGF) mRNA in normoxic (NmOx) and Sugen + hypoxia (SuHx) wildtype (WT) mice. CNP was delivered by osmotic minipump (0.2 mg/kg/day, s.c., for 14 days). Data presented as mean ± *SEM*; symbols depict individual data points. Statistical analysis by one-way ANOVA with Šidák post hoc test. *$P \leq 0.05$, **$P \leq 0.01$; *ns*, not significant (adjusted for multiplicity).

5.6 Principal findings

In WT SuHx mice the pulmonary mRNA expression of NPR-B and NPR-C is significantly reduced (***Table 22***), suggesting that PH is associated with deficient CNP signalling. Furthermore, the production of endogenous CNP by the endothelium protects against PH. The accentuated PH phenotype observed in ecCNP$^{-/-}$ (and gbCNP$^{-/-}$) mice was not replicated by the loss of NPR-C signalling (***Table 23***), and administration of CNP to both WT and NPR-C$^{-/-}$ mice reversed established PH (***Table 24***), indicating the importance of NPR-B signalling in CNP-mediated protection of the pulmonary circulation. Despite the absence of a pressure phenotype, male NPR-C$^{-/-}$ animals demonstrated an exacerbated hypertrophic and fibrotic response in the right heart, alluding to an import role of NPR-C in RV cardioprotection. In addition, deletion of cardiomyocyte CNP was unexpectedly compensated by increased expression of the peptide in other cardiac cell types. As a result, neither PH nor the subsequent RV remodelling were aggravated in cmCNP$^{-/-}$ mice. In clear disparity to male animals, deletion of CNP or NPR-C from female SuHx mice had either no impact on, or else diminished, the development of PH (***Table 23***).

Table 22: Summary of CNP/NPR expression data

		CNP	NPR-B	NPR-C
Lung	male	=	↓	↓
	female	=	↓	↓
RV	male	↓	↑	=
	female	=	=	=

RV, right ventricle.

Table 23: Summary of CNP/NPR-C knockout data

		RVSP	MABP	RV/(LV+S)
gbCNP$^{-/-}$	male	↑	=	=
	female	↓	=	=
ecCNP$^{-/-}$	male	↑↑	↑	↑
	female	=	↑	=
cmCNP$^{-/-}$	male	↓	=	=
	female	↓	=	=
NPR-C$^{-/-}$	male	=	=	↑
	female	↓	=	=

RVSP, right ventricular systolic pressure; MABP, mean arterial blood pressure; RV/(LV+S), right ventricle to left ventricle plus septum ratio; gbCNP$^{-/-}$, global CNP KO; ecCNP$^{-/-}$, endothelial-specific CNP KO; cmCNP$^{-/-}$, cardiomyocyte-specific CNP KO; NPR C$^{-/-}$, global NPR-C KO.

Table 24: Summary of CNP infusion data

	RVSP	MABP	RV/(LV+S)
WT	↓	=	=
NPR-C$^{-/-}$	↓	=	=

RVSP, right ventricular systolic pressure; MABP, mean arterial blood pressure; RV/(LV+S), right ventricle to left ventricle plus septum ratio; WT, wildtype; NPR C$^{-/-}$, global NPR-C KO.

Chapter VI: Discussion

6.1 Overview and key findings

PH is a debilitating and devastating disease driven by endothelial dysfunction, pulmonary vascular remodelling, and RV failure (Hoeper et al., 2016a; Humbert et al., 2019). Whilst targeted pharmacological and surgical treatments significantly improve outcomes in PAH and CTEPH, many patients still develop fatal right heart failure, even with optimal therapy (Pulido et al., 2013; McLaughlin et al., 2015; Sitbon et al., 2015). For other forms of PH, the only treatment is optimisation of the underlying disease (Rose-Jones et al., 2015). In the absence of a curative therapy, approximately 40% of PAH patients die within 5 years of diagnosis, rising to nearly 60% for CLD-PH (Badesch et al., 2010; Gall et al., 2017). Evidently, there is an urgent requirement for new therapies to address this unmet clinical need.

CNP is an endogenous homeostatic peptide that regulates numerous cardiovascular processes pertinent to the pathophysiology of PH, including EC function, VSMC proliferation and cardiac remodelling (Moyes and Hobbs, 2019). Furthermore, activation of NPR-B by the peptide enriches levels of cGMP within VSMC (Potter et al., 2006), a mechanism known to produce favourable effects in PH (Humbert et al., 2014). CNP has also been shown to constrain vascular and cardiac remodelling through the activation of a second receptor, NPR-C (Moyes et al., 2014, 2020). However, the pathophysiological role and therapeutic potential of CNP in the context of PH have yet to be fully explored. In accordance, this project was designed to test two hypotheses: firstly, that ‘genetic deletion of CNP worsens disease severity in experimental PH’ and secondly, that ‘administration of exogenous CNP alleviates experimental PH.’

Using a well-defined experimental model of PH (SuHx), it is demonstrated herein that the NPR-B and NPR-C genes are downregulated in the lungs as a consequence of the disease. Furthermore, male mice in which CNP is deleted exclusively from the endothelium exhibit an exaggerated response to SuHx exposure, characterised by enhanced cardiopulmonary pressure, pulmonary vascular remodelling, and RVH. This corroborates the idea that constitutive liberation of CNP from pulmonary ECs protects against PH; correspondingly, this study also reveals that intervention with exogenous peptide alleviates the established disease.

In contrast, genetic ablation of NPR-C does not alter the vascular response to SuHx exposure in male mice, positioning NPR-B as the major effector receptor for CNP in the pulmonary circulation. In further support of this notion, the current study determined that pharmacological activation of NPR-C is insufficient to relax isolated pulmonary arteries, and that the propensity for CNP to reverse established PH is unaltered in NPR-C$^{-/-}$ animals.

In the male murine RV, pathological hypertrophy is accompanied by reduced CNP gene expression and an increase in NPR-B mRNA levels. Whilst SuHx exposure does not alter NPR-C gene expression in the RV, global deletion of this gene accentuates the hypertrophic and fibrotic response of the right heart, alluding to an important role of NPR-C in RV cardioprotection. Paradoxically, loss of cardiomyocyte CNP reduces cardiopulmonary pressure and abrogates the expression of hypertrophic mediators/markers in the RV. This may be explained by an unexpected rise in CNP mRNA levels, possibly the result of an adaptive increase in expression of the peptide by other cardiac cells (e.g. ECs or fibroblasts). Despite easing pressure overload, two weeks of CNP infusion does not reverse the development of RV remodelling in WT animals. Finally, in clear disparity to male animals, deletion of CNP or NPR-C from female SuHx mice did not exacerbate the development of PH or RVH.

Together, these data substantiate a protective role for endogenous CNP signalling in the context of PH and suggest that administration of exogenous CNP (or molecules mimicking the bioactivity of the peptide) is a tangible therapeutic strategy for the treatment of this condition.

6.2 Cardiopulmonary CNP/NPR expression is altered in PH

From a pre-clinical perspective, the cardiopulmonary expression of the CNP signalling pathway has primarily been explored in the hypoxic rat model of PH. Exposure to chronic hypoxia (CH) reduces pulmonary levels of CNP without altering the quantity of mRNA transcripts (Klinger et al., 1998a), indicative of enhanced inactivation of the peptide, rather than diminished synthesis. This mechanism seems to be independent of receptor-based clearance, as expression of the NPR-C gene is suppressed in the lungs of rats exposed to CH (Li et al., 1995). Likewise, the activity of NEP within the lung is also constrained by hypoxia

(Carpenter and Stenmark, 2001; Wick et al., 2011), hinting at the involvement of a third, as yet unknown, clearance mechanism. These observations are in-line with the data presented herein; pulmonary expression of the CNP gene was unaltered in male and female SuHx mice, whilst the NPR-C gene was downregulated.

The process by which hypoxia constrains NPR-C expression has yet to be elucidated. As circulating CNP is elevated in CH rats (Klinger et al., 1998a), one possibility is that excessive receptor activation leads to homologous desensitisation of the receptor in these animals, as has been previously described in A10 (smooth muscle-like) cells following chronic ANP and $cANF^{4-23}$ treatment (Anand-Srivastava, 2000). NPR-B gene expression is also augmented in hypoxia-adapted rats (Li et al., 1995) and the subsequent enrichment of pulmonary cGMP levels (Jin et al., 1991) may impair the recovery of NPR-C expression (Kato et al., 1991, 1992). Whilst an eloquent theory, the failure of global ANP deletion to prevent hypoxia-induced NPR-C downregulation in the lung (Sun et al., 2000) suggests this phenomenon is independent of circulating natriuretic peptide levels. Similarly, the present study found that NPR-C gene expression was curtailed in the lungs of SuHx mice, despite a concomitant downregulation of NPR-B mRNA, and a trend towards lower plasma CNP.

An alternate theory is that NPR-C downregulation is an endogenous adaptive response intended to offset the development of PH by augmenting the bioactivity of natriuretic peptides (i.e. by reducing clearance). In rat PASMCs, a link between hypoxia, FGF-2 and PDGF upregulation, and NPR-C downregulation was identified (Sun et al., 2001). Consequently, NPR-C downregulation may act as 'brake' to limit the pathogenic effects of RTK activation. On the other hand, diminished NPR-C signalling may underly the detrimental effects of enhanced growth factor expression in the pulmonary vasculature.

Existing data on the expression of CNP and NPRs in the hypertrophied right heart is ambiguous. In male rats exposed to CH, CNP levels in the RV are unaltered, though levels of the peptide in the right atria are significantly depressed (Klinger et al., 1998a). In contrast, CNP-evoked cGMP production is decreased in the RV endocardium of male monocrotaline (MCT)-treated rats, indicative of NPR-B downregulation. A reduction in the availability of ^{125}I-labeled ANP binding sites is also evident, consistent with a fall in NPR-C (and/or NPR-A) expression

(Kim et al., 1999). NPR-C mRNA is likewise depleted in the hypertrophied RV myocardium of male rats with aortovenocaval fistula, though NPR-B is upregulated in this model (Brown et al., 1993). The results presented herein further obfuscate the matter, as in male SuHx animals, CNP gene expression was diminished, NPR-B was upregulated, and NPR-C expression was unchanged. Furthermore, expression of the both the peptide and NPRs was preserved in female SuHx mice. Taken together, these findings suggest that the CNP signalling pathway is differentially expressed in the hypertrophied RV depending on the species, sex, experimental model, and tissue (i.e. endocardium, myocardium or whole RV tissue) studied.

More recently, the expression of CNP has been investigated in patient cohorts. In subjects requiring cardiac catheterisation for cardiovascular disorders, PAP was found to independently predict plasma CNP (Palmer et al., 2009). Furthermore, in a study of subjects with PH (PAH, CLD-PH, and CTEPH), a tendency towards higher circulating NT-proCNP was observed but did not reach statistical significance. The same study did not find an association between circulating NT-proCNP and mPAP, though correlations with right atrial pressure (RAP) and renal function were noted (Kaiser et al., 2015). Whilst this study did not find evidence for a relationship between CNP and PH *per se*, the variability in age, gender, and renal function between groups may have influenced circulating natriuretic peptides levels, suggesting further investigation is warranted (Prickett and Espiner, 2020).

6.3 CNP regulates pulmonary vascular tone

The ability of exogenous CNP to relax the vasculature has been exhaustively researched *ex vivo* using isolated blood vessel preparations (Moyes and Hobbs, 2019). Indeed, CNP is an effective vasodilator in many different vascular beds, relaxing human resistance arteries with greater efficacy and potency than either ANP or BNP (Garcha and Hughes, 2006; Edvinsson et al., 2016). Furthermore, the role of endogenous CNP in the maintenance of systemic vascular tone has been elucidated *in vivo* by global and endothelial-specific deletion of the peptide, which elevates MABP and impairs vascular responses to endothelium-dependent vasodilators (Moyes et al., 2014; Nakao et al., 2017; Špiranec et al., 2018; Perez-

Ternero et al., 2022). However, comparatively less is known about the actions of the peptide in the pulmonary circulation.

In the present study, the effect of exogenous CNP on pulmonary vascular reactivity was investigated using isolated second order conduit pulmonary arteries. The peptide readily relaxed vessels from NmOx mice, corroborating previous work with rat proximal intralobular pulmonary arteries (Klinger et al., 1998a; Vang et al., 2010). Compared to CNP, cANF$^{4-23}$ was a relatively ineffective vasorelaxant, intimating that NPR-B primarily governs the vasodilator activity of the peptide in murine conduit pulmonary arteries. However, despite the propensity for exogenous peptide to relax pulmonary arteries, the data herein infers that endogenous CNP plays little role in the regulation of PVT in healthy individuals. Indeed, RVSP was unaltered in naïve ecCNP$^{-/-}$ animals (regardless of sex) despite a 50% reduction in pulmonary CNP mRNA (Moyes et al., 2014). Likewise, genetic deletion of NPR-C had no impact on RVSP in NmOx animals. This finding contests previous reports of a strikingly decrease in RVSP following cANF$^{4-23}$ infusion (Egom et al., 2017a) and of significantly elevated cardiopulmonary pressure in NPR-C$^{-/-}$ mice (Egom et al., 2017b). Still, as others have previously highlighted, a representative pressure trace in one of the referenced studies appears to show RAP (Agrawal and Hemnes, 2020). Indeed, the RVSP values reported in these studies (≥5 mmHg) fall far below the expected value of 20 - 30 mmHg for unchallenged WT mice (Ikeda et al., 2019), suggesting that technical differences in catheter placement account for these divergent observations.

The mechanism by which CNP elicits vasodilatation differs considerably depending on the species and vessel studied (Moyes and Hobbs, 2019). Prior investigations imply that CNP-mediated relaxation of conduit vessels is dependent on NPR-B activation and subsequent production of cGMP. Indeed, NPR-B blockade (with the dual NPR-A/B antagonist HS-142-1) inhibits the dilatory effect of CNP in rodent aortic rings and canine coronary arteries (Drewett et al., 1995; Wennberg et al., 1999; Madhani et al., 2003), and administration of cANF$^{4-23}$ does not relax the mouse aorta (Madhani et al., 2003). These findings dovetail nicely with the observations detailed herein.

As conductance vessels transition into the microcirculation, the contribution of NPR-C to vascular tone rises starkly. In fact, in resistance vessels, activation of

this receptor by CNP is posited to account for a major component of VSMC endothelium-derived hyperpolarisation (EDH) by ACh. Accordingly, the response to ACh is diminished in the mesenteric arteries of male gbCNP$^{-/-}$ mice, female ecCNP$^{-/-}$ mice, and NPR-C$^{-/-}$ animals (Moyes et al., 2014; Perez-Ternero et al., 2022), yet preserved in the same vessels from female smooth muscle-restricted NPR-B KO mice (Nakao et al., 2017). In addition, ACh-induced vasorelaxation is ablated by NPR-C antagonists and blockade of SK_{Ca}, IK_{Ca} or GIRKs (Villar et al., 2007). As such, it appears that opening of small and intermediate conductance calcium-sensitive potassium channels (SK_{Ca} and IK_{Ca}) on the endothelium triggers the release of CNP, which binds to NPR-C on VSMCs, resulting in the $G_{i/0}$ mediated activation of G-protein-gated inwardly rectifying potassium (GIRK) channels, K^+ efflux, and hyperpolarisation. The receptor mediating the effects of exogenous CNP in resistance vessels is less clear, as CNP-induced vasorelaxation is abolished in the mesenteric arteries of smooth muscle-restricted NPR-B KO mice (Nakao et al., 2017), yet the response of human mesenteric vessels to the peptide is blunted by the NPR-C antagonist M372049 (Moyes et al., 2014).

In addition to GIRKs, a study using human penile resistance arteries found that large conductance Ca^{2+}-activated K^+ channels (BK_{Ca}) contribute to CNP-evoked hyperpolarisation of VSMC and vasodilatation (Kun et al., 2008). In the pulmonary vasculature, BK_{Ca} current is largely confined to conduit artery VSMCs, with limited activity in microcirculatory VSMCs (Bonnet and Archer, 2007). Be this as it may, BK_{Ca} channel activation decreases PAP in isolated perfused rat lungs (Vang et al., 2010), suggesting an alternative mechanism is at play in resistance vessels. Indeed, Vang et al. demonstrated that CNP activates BK_{Ca} channels on the pulmonary microvascular endothelium, and subsequent endothelial hyperpolarisation stimulates eNOS, culminating in NO-mediated vasodilatation. In the context of PH, the vasoprotective actions of DHEA are thought to be mediated by BK_{Ca} channel activation (Peng et al., 1999; Bonnet et al., 2003). As DHEA has been shown to enhance CNP/NPR-B expression in certain tissues (Wang et al., 2018a; Zheng et al., 2022), one might speculate that its favourable effects in animal models of PH is intermediated via this signalling pathway.

Pulmonary arteries respond to alveolar hypoxia with HPV, a reflex response that preserves matching of regional perfusion and ventilation (Dunham-Snary et

al., 2017). CNP is ineffective at reversing acute HPV, both in unchallenged isolated perfused lungs and those preconditioned by CH exposure (Klinger et al., 1998a; Zhao et al., 1999). Paradoxically, the inability of exogenous CNP to modulate acute HPV may be advantageous from a therapeutic standpoint, as the maintenance of V/Q matching is vital in in patients with CLD-PH (Stolz et al., 2008; Blanco et al., 2010).

6.4 Endogenous CNP protects against PH

Whilst SuHx exposure suppresses pulmonary NPR expression, the present study found the vasorelaxant properties of CNP to be fully preserved in arteries isolated from male SuHx animals, verifying previous findings in proximal intrapulmonary arteries from hypoxia-adapted male rats (Klinger et al., 1998a). This implies that the exacerbation of cardiopulmonary pressure overload in male mice with endothelial-restricted deletion of CNP (and global deletion of the peptide) is primarily attributable to enhanced remodelling, rather than tempered vasodilatation. This paradigm is substantiated by an increase in the muscularisation of small pulmonary arteries in ecCNP$^{-/-}$ mice. Interestingly, endothelial-specific CNP ablation upregulates ET-1 in murine pulmonary vascular ECs, and circulating ET-1 is correspondingly increased (Nakao et al., 2017). In accordance, exogenous CNP inhibits the secretion of ET-1 by vascular ECs (Kohno et al., 1992). Given the pertinence of ET-1 to PH pathophysiology, it is plausible that a local increase in ET-1 production in the pulmonary arteries contributes to the accentuated PH phenotype observed in male ecCNP$^{-/-}$ mice.

In contrast to male animals, pulmonary vascular reactivity to CNP was moderately constrained in vessels isolated from female SuHx mice. Nonetheless, this dampened vascular reactivity to the peptide does not appear to contribute to the development of PH, as endothelial-specific (and global) deletion of CNP from female animals does not accentuate cardiopulmonary pressure overload (though pulmonary vascular remodelling is enhanced, in ecCNP$^{-/-}$ mice only). The abolition of CNP-mediated vasodilatation may be offset in female animals by compensatory changes in other vasoactive pathways. Indeed, as presented herein, the vasoconstrictive response to the α1-adrenoceptor agonist Phe is diminished in

female SuHx mice, and this blunting of sympathetic tone may offset any potential increase in cardiopulmonary pressure resulting from CNP deletion.

In contrast to CNP, the vasorelaxant response elicited by NPR-C activation is curtailed in arteries isolated from SuHx animals, in a sex-independent manner. As CNP and cANF$^{4-23}$ responses were mutually reduced in vessels isolated from female SuHx mice, it appears that NPR-C underlies the biological activity of CNP in female conduit pulmonary arteries, at least in part. As previously discussed, the vasorelaxant activity of the peptide in conduit arteries from other vascular beds is primarily attributed to NPR-B, yet there are reports that NPR-C can couple to eNOS in the rat aorta, resulting in NO production, and vasorelaxation (Caniffi et al., 2010, 2016). The findings presented herein run in contrast to a previous study demonstrating that acute cANF$^{4-23}$ infusion modestly reduces mPAP in hypoxia-adapted rats, but has no effect in NmOx animals (Jin et al., 1990). However, cANF$^{4-23}$ treatment elevated circulating ANP in this study, suggesting that competition for NPR-C binding sites resulted in reduced clearance of endogenous natriuretic peptides.

Notwithstanding the aforementioned findings, cardiopulmonary pressure and pulmonary vascular remodelling are not accentuated in NPR-C$^{-/-}$ mice, suggesting that suppression of NPR-C mediated vasorelaxation does not contribute to the development of PH. Furthermore, depletion of NPR-C did not recapitulate the pro-remodelling phenotype displayed by male ecCNP$^{-/-}$ mice, positioning NPR-B as the principal mediator of pulmonary vasoprotection. Curiously, the present study found that NPR-C deletion eases cardiopulmonary pressure overload and pulmonary vascular remodelling in female SuHx animals, possibly due to reduced CNP clearance in the pulmonary circulation, and increased activation of NPR-B.

The impact of CNP on vascular remodelling, wound healing, and repair is well-characterised. In models of vein graft and balloon angioplasty, the peptide concomitantly accelerates re-endothelialisation and inhibits VSMC proliferation, attenuating deleterious neointimal hyperplasia (Furuya et al., 1993; Ueno et al., 1997; Doi et al., 2001; Ohno et al., 2002; Schachner et al., 2004). Restoration of the endothelial barrier may bolster the direct anti-mitogenic effects of CNP on VSMCs by removing the influence of circulating growth factors and cytokines.

Furthermore, the peptide may also regulate ECM remodelling by antagonising the expression, release, and activation of several matrix-remodelling molecules, including MMPs (Krejci et al., 2005; Hu et al., 2013). By increasing iNOS expression and NO generation, CNP also dampens endothelial activation, shear-stress, and thrombosis (Qian et al., 2002).

Existing evidence suggests that the NPR mediating the anti-remodelling effects of CNP is dictated by the type of injury. Dovetailing with the results of the current study, the anti-remodelling actions of CNP in models of vein graft and balloon angioplasty have been linked to elevated cGMP production (Furuya et al., 1991, 1993; Doi et al., 2001). Indeed, by augmenting intracellular cGMP, CNP elicits a potent anti-mitogenic effect in VSMCs from control rats, in contrast, $cANF^{4-23}$ has no effect on the growth of these cells (Hutchinson et al., 1997). On the other hand, NPR-C downregulation contributes to the hyperproliferation of VSMCs from spontaneously hypertensive rats, by enhancing the expression of growth factors and cell cycle proteins. This hyperproliferative phenotype is reversed by NPR-C overexpression (Li and Anand-Srivastava, 2022) or $cANF^{4-23}$ treatment (Jain and Anand-Srivastava, 2018). Supporting these findings, mice lacking NPR-C (and endothelial-derived CNP) demonstrate slower wound healing and accentuated intimal hyperplasia following ischaemic vascular injury (Bubb et al., 2019). Accordingly, the proliferation of pulmonary microvascular ECs isolated from $NPR\text{-}C^{-/-}$ mice is reduced, whilst the proliferation of aortic VSMCs is augmented (Khambata et al., 2011). In addition, the pro- and anti-mitogenic effects of CNP on ECs and VSMCs, respectively, can be blocked by small molecule NPR-C antagonists and *Pertussis* toxin (a $G_{i/0}$ inhibitor; Cahill and Hassid, 1994; Khambata et al., 2011).

6.5 CNP protects against remodelling in the RV

Compared to ANP and BNP, basal cardiac expression of CNP is low in healthy subjects (Del Ry et al., 2011; Del Ry, 2013), suggesting that the peptide does not play a major role in regulating cardiac morphology or function. This paradigm was confirmed by the absence of a gross cardiac phenotype in naïve $cmCNP^{-/-}$ mice (Moyes et al., 2020), and as detailed herein, is further reinforced by the absence of altered RV morphology in these animals. Still, a large body of evidence implies

that the significance of CNP in the heart rises exponentially under pathological conditions. Plasma levels of the peptide increase in patients with heart failure (HF; Wei et al., 1993; Prickett et al., 2001; Wright et al., 2004; Del Ry et al., 2005, 2008b, 2008a), and are associated with cardiovascular comorbidities, LV dysfunction, and future cardiovascular risk in the general population (Sangaralingham et al., 2015). Moreover, plasma NT-proCNP levels correlate with severity in HFpEF patients, predicting hospitalisation and all-cause mortality (Lok et al., 2014). Critically, the concentration of CNP is significantly higher in the coronary vascular tree than in the systemic circulation of HF patients (Del Ry et al., 2006), implying that the source of the peptide is the heart itself. This observation is supported by studies showing that the expression of CNP is increased in the failing heart at the gene and protein levels (Wei et al., 1993; Del Ry et al., 2008a). Taken together, these findings allude to a cardioprotective role for the peptide in the context of heart disease.

Evidence to support this hypothesis is supplied by *in vitro* studies detailing the ability of the peptide to modulate cardiac remodelling. In isolated rat cardiomyocytes, exogenous CNP inhibits ET-1-induced hypertrophic responses, including GATA binding protein 4 (GATA4) and myocyte enhancer factor (MEF)-2 expression, CAMK II activity, ERK phosphorylation, and ANP secretion (Tokudome et al., 2004). Similarly, a further study found protective effects against Ang-II-induced [3H]phenylalanine incorporation (an *in vitro* marker of hypertrophy), with a related decrease in c-fos expression (Rosenkranz et al., 2003). In these studies, the anti-hypertrophic actions of the peptide were reproduced by 8-bromo-cyclic GMP (a cyclic GMP analogue), and abolished by a dual NPR-A/B antagonist and a PKG inhibitor (Rosenkranz et al., 2003; Tokudome et al., 2004), alluding to NPR-B dependency.

Beyond cardiomyocytes, CNP modulates the activity of cardiac fibroblasts with much greater potency than ANP or BNP (Horio et al., 2003). Moreover, it appears that these cells synthesise the peptide as a stress response to pathological insults. As previously demonstrated by Horio and colleagues, factors pertinent to the pathobiology of PH, including FGF-2, TGF-β and ET-1, stimulate rat cardiac fibroblasts to release CNP, which acts in an autocrine manner to reduce proliferation and ECM secretion (Horio et al., 2003). In addition, exogenous CNP

inhibits cardiac fibroblasts by attenuating differentiation (into myofibroblasts), migration, and the release of pro-fibrotic mediators (Sangaralingham et al., 2011; Ichiki et al., 2014; Li et al., 2015).

The advent of cell-specific transgenic animals with altered CNP expression has furthered understanding of its protective actions in the heart. Indeed, over-expression of the peptide in cardiomyocytes protects against LV hypertrophy in a murine model of myocardial infarction (MI; (Wang et al., 2007). More importantly, cmCNP$^{-/-}$ mice with pressure overload-induced HF exhibit elevated cardiomyocyte hypertrophy, augmented fibrosis, and greater systolic dysfunction. Interestingly, deletion of fibroblast-derived CNP, but not endothelial-derived CNP, recapitulates this phenotype (albeit without exaggerated cardiomyocyte hypertrophy; Moyes et al., 2020). Importantly, exogenous CNP has been shown to attenuate cardiac hypertrophy and fibrosis in models of MI and HF (Soeki et al., 2005; Izumiya et al., 2012; Moyes et al., 2020).

As described herein, the development of RV hypertrophy is unaltered in cmCNP$^{-/-}$ mice, though the expression of several pro-remodelling mediators is tempered. Whilst unexpected, this protective phenotype is outwardly explained by an upswing in CNP mRNA transcripts. As CNP mRNA expression is reduced by ~80% in isolated neonatal cmCNP$^{-/-}$ cardiomyocytes (Moyes et al., 2020), other cell types within the heart are likely responsible for this adaptive response. As outlined above, CNP secretion from activated fibroblasts constrains remodelling processes within the stressed myocardium. Still, endothelial-derived CNP may make a greater contribution to cardioprotection in the RV, particularly as the EC to cardiomyocyte ratio of the RV far exceeds that of the LV (Brutsaert, 2003). Surprisingly, the development of cardiopulmonary pressure overload was also eased in cmCNP$^{-/-}$ SuHx mice, presumably due to the adaptive upregulation of CNP. Indeed, pulmonary vascular remodelling was tempered in these animals, indicating a paracrine, vasoprotective action of cardiac-derived CNP. Still, the contribution of an autocrine pressure-modifying action on the heart cannot be ruled out.

Curiously, a similar effect seems to be at play in gbCNP$^{-/-}$ animals. The cardiopulmonary pressure reduction in female gbCNP$^{-/-}$ SuHx mice matches that of female cmCNP$^{-/-}$ animals (4 mmHg lower than WT), suggesting that the

deleterious effects of global CNP loss in the vasculature are offset by a compensatory cardioprotective response to cardiomyocyte CNP ablation. In further support of this notion, the pressure difference between male gbCNP$^{-/-}$ SuHx mice (4 mmHg increase versus WT) and male ecCNP$^{-/-}$ SuHx animals (7 mmHg increase versus WT) is equivalent to the pressure reduction observed in male cmCNP$^{-/-}$ SuHx mice (3 mmHg lower than WT). As such, it appears that a failsafe series of adaptive responses exist to protect the right heart if CNP signalling is disrupted. In gbCNP$^{-/-}$ mice, this response may involve upregulation of other cardioprotective molecules, such as ANP or BNP. Such an effect might explain why the exacerbation of cardiopulmonary pressure overload did not enhance RVH in male gbCNP$^{-/-}$ SuHx animals.

The roles of NPR-B and NPR-C in CNP-mediated cardioprotection have yet to be fully elucidated. Evidence from animal models suggests that endogenous NPR-B signalling is not involved in maladaptive remodelling of the heart, as the development of cardiac fibrosis unaltered in global- and cardiomyocyte-specific NPR-B KO animals (Michel et al., 2020; Moyes et al., 2020). On the other hand, transgenic rats expressing a dominant negative form of NPR-B exhibit a basal cardiac hypertrophy that can be exacerbated by infrarenal aortocaval shunt (chronic volume overload-induced HF). Still, the fibrotic burden and function of the heart is unaltered in these animals, inferring that NPR-B primarily governs adaptive cardiac remodelling (Langenickel et al., 2006).

In contrast, global ablation of the NPR-C gene potentiates cardiac hypertrophy, fibrosis, and functional decline following aortic banding, mirroring the severe HF phenotype observed in cmCNP$^{-/-}$ animals. In addition, CNP infusion reverses these changes in WT mice, but has no effect in NPR-C$^{-/-}$ animals (Moyes et al., 2020). These findings are supported by reports of baseline atrial fibrosis in NPR-C$^{-/-}$ mice (Egom et al., 2015), which can be enhanced by Ang II-induced pressure overload (Mackasey et al., 2018; Jansen et al., 2019). Though these studies position NPR-C signalling as an opponent of maladaptive cardiac remodelling, others have reported a protective effect of NPR-C deletion or blockade. Indeed, Rahmutula et al. demonstrate that crossing NPR-C$^{-/-}$ mice with animals that spontaneously develop atrial fibrosis (via TGFβ1 overexpression)

diminishes collagen deposition, consistent with reduced CNP clearance. Using a model of pressure overload-induced HF, the same study found that NPR-C deletion had no impact on LV hypertrophy or function (Rahmutula et al., 2019). Moreover, transgenic mice overexpressing osteocrin, a putative blocker of NPR-C, exhibited increased circulating ANP and CNP following MI, associated with reduced LV hypertrophy and fibrosis, and improved survival (Miyazaki et al., 2018).

As illustrated by the data presented herein, deletion of NPR-C from male mice accentuates the free wall thickness, weight, and fibrotic burden of the RV. Furthermore, despite a reduction in cardiopulmonary pressure and vascular remodelling, the development of RVH and fibrosis is unconstrained in female NPR-C$^{-/-}$ animals. Together, these observations suggest that NPR-C signalling modulates the hypertrophic response of the right heart. Activation of the receptor by ANP and/or BNP, both of which also protect against PH and the accompanying RVH *in vivo* (Jin et al., 1988; Klinger et al., 1993a, 1998b; Louzier et al., 2001), may also contribute to this protective effect.

Conflicting with these findings, cardiomyocyte-like (H9C2) cells overexpressing NPR-C demonstrate increased size and expression of hypertrophic genes. Furthermore, the receptor is upregulated in the hypertrophic RV of mice with obesity-induced HFpEF (Agrawal et al., 2019). NPR-C overexpression may favour clearance over signalling, negating the protective effects of CNP in the heart, and explaining these divergent observations. Evidently, the key to unlocking the therapeutic potential of CNP in the heart will be deciphering the factors governing the transition between NPR-C signalling and clearance, and how the balance of these seemingly opposing processes changes under pathological conditions.

6.6 CNP/NPR-C modulate cardiac function in PH

The present study found that cardiomyocyte-specific deletion of CNP is accompanied by significant alterations in SERCA2a expression. In healthy hearts, a moderate increase in SERCA2a expression is associated with maintained or improved contractility and relaxation, due to accelerated Ca^{2+} cycling within cardiomyocytes (He et al., 1997; Baker et al., 1998; Zhang et al., 2012). Paradoxically, stark rises in SERCA2a expression may in fact depress contractility

due to 'futile' Ca^{2+} cycling, whereby immediate reuptake diminishes $[Ca^{2+}]_{cyt}$ before contraction can occur (Teucher et al., 2004). On the other hand, SERCA2a downregulation is considered characteristic of a failing heart (Baker et al., 1998; Del Monte et al., 1999), as the resultant fall in sarcoplasmic reticulum (SR) Ca^{2+} uptake precipitates contractile dysfunction via reduced Ca^{2+} cycling, whilst the increase in diastolic $[Ca^{2+}]_{cyt}$ impairs cardiac relaxation (Zhihao et al., 2020).

Several previous studies have shown that CNP exerts negative inotropic response and positive lusitropic responses in the heart (Brusq et al., 1999; Pierkes et al., 2002; Moltzau et al., 2013, 2014). Curiously, the negative inotropic effect of the peptide can be blocked by pharmacological inhibition or cardiomyocyte-specific inactivation of the SERCA2 gene (Moltzau et al., 2013). Evidence suggests that CNP signalling results in phosphorylation and inhibition of phospholamban (PLB), a negative regulator of SERCA2a. Subsequent overactivity of the pump reduces the activation of contractile myofilaments by sequestering cytosolic Ca^{2+} in the SR (Pierkes et al., 2002; Moltzau et al., 2013, 2014; Manfra et al., 2022). Phosphorylation of troponin I (TnI), a protein that regulates Ca^{2+}-mediated interactions between actin and myosin, is also thought to contribute to the negative inotropic actions of the peptide (Moltzau et al., 2013, 2014; Manfra et al., 2022). CNP-mediated reductions in cardiac contractility can be replicated with 8-bromo-cyclic GMP (Brusq et al., 1999) and are sensitive to PKG inhibition (Moltzau et al., 2013), indicative of a reliance on NPR-B activation. Of interest, it has recently been demonstrated that the peptide elicits a local increase in cGMP concentration proximal to TnI and PLB (Manfra et al., 2022). Interestingly, BNP does not increase cGMP levels in this region (Moltzau et al., 2014), explaining why it does not share the negative inotropic properties of CNP.

In contrast to the above, there is some evidence that CNP evokes a positive inotropic response in the heart. These observations have predominantly been made in isolated canine heart preparations (Beaulieu et al., 1997; Hirose et al., 1998), though there is a report of CNP-evoked positive inotropy in the mouse heart, attributed to PKG-mediated phosphorylation of PLB and greater uptake of Ca^{2+} into the SR, creating a larger pool of Ca^{2+} available for contraction (Wollert et al., 2003).

As detailed herein, SERCA2a mRNA levels in the RV are augmented in parallel with increased CNP mRNA levels in NmOx cmCNP$^{-/-}$ animals. Even so, the

RVSP of these mice is commensurate with WT animals, suggesting contractility is not adversely impacted. Rather than being a pathological mechanism, upregulation of the SERCA2a gene may be an adaptive response to maintain cardiac function in the face of increased SERCA2a phosphorylation. Indeed, CNP mRNA levels fall sharply with decreased in SERCA2a expression in SuHx-challenged cmCNP$^{-/-}$ mice.

Basal cardiac function was unaltered in unchallenged NPR-C$^{-/-}$ mice. Similarly, TAPSE and tricuspid valve velocity were reduced in equal measure by SuHx exposure, indicating that the exacerbation of RV remodelling in these animals did not compromise RV function. On the other hand, CO (measured from the LV) was reduced in NPR-C$^{-/-}$ animals, and a compensatory increase in the LVEF of WT mice was absent. As such, it appears that NPR-C signalling maintains LV function in the face of RV pressure overload.

6.7 Cardiopulmonary sex differences in CNP signalling

The current study also uncovered a sex difference with regards to the impact of deficient CNP signalling on the development of PH. Specifically, a pulmonary hypertensive phenotype was observed in male gbCNP$^{-/-}$ and ecCNP$^{-/-}$ mice, whereas cardiopulmonary pressure was lowered or unaltered in female gbCNP$^{-/-}$ and ecCNP$^{-/-}$ animals, respectively. A sexual dimorphism in the consequences of global NPR-C deletion was also noted; the development of PH was unaffected in male NPR-C$^{-/-}$ mice, yet RVH and fibrosis were exacerbated, while female NPR-C$^{-/-}$ animals exhibited a pulmonary hypotensive phenotype, with no change in RV remodelling. A sex difference was also apparent in the RV of WT animals with PH; CNP mRNA transcripts were depreciated in male animals only. Given that male sex is linked to poorer RV function and worse survival in PH (Jacobs et al., 2014), one might speculate that females are better able to harness the cardioprotective effects of NPR-C in the right heart.

A sex disparity in the modulation of systemic blood pressure by endothelium derived CNP was previously described. As female ecCNP$^{-/-}$ and NPR-C$^{-/-}$ mice exhibit systemic hypertension, it is postulated that females maintain MABP through endothelial CNP release and activation of NPR-C (Moyes et al., 2014; Nakao et al., 2017). In contrast, male ecCNP$^{-/-}$ animals are normotensive, whilst male NPR-

$C^{-/-}$ animals are hypotensive (Moyes et al., 2014), consistent with reduced CNP clearance. As male sex is associated with a strong bias towards NO as an endothelium-derived relaxing factor (Scotland et al., 2005), it is hypothesised that males compensate for the loss of CNP during development by upregulating the NO pathway. This would also explain why global deletion of CNP from adolescent male mice unmasks a phenotype of systemic hypertension (Perez-Ternero et al., 2022).

Curiously, the present study found MABP to be unaltered in NmOx gbCNP$^{-/-}$, ecCNP$^{-/-}$ and NPR-C$^{-/-}$ animals of either sex, though deletion of endothelial CNP resulted in sex-independent systemic hypertension in SuHx mice. Whilst these findings are at odds with those of the previously described studies, the methodology used to measure MABP was considerably different. Indeed, the studies of Moyes et al. and Perez-Ternero et al. primarily assessed MABP in conscious telemetered animals, yet the current study relied on carotid artery cannulation in mice under anaesthesia, which exerts a depressive effect on the cardiovascular system (Constantinides et al., 2011). In addition, a growing body of evidence suggests that the CNP/NPR-C axis dampens sympathetic drive, particularly in the context of HR and blood pressure regulation (Rose et al., 2004; Anand-Srivastava, 2010; Buttgereit et al., 2016), effects which would be tempered or lost with depression of the CNS. Finally, though Moyes et al. also measured carotid artery pressure in anaesthetised mice (Moyes et al., 2014), the present study had the added variable of right heart catheterisation and jugular vein occlusion prior to MABP measurement, precluding direct comparisons.

The relationship between CNP and sex hormones has yet to be explored in animal or human studies. Be this as it may, there is some evidence that CNP expression and activity are linked to sex. Though plasma CNP is unaffected by sex (Prickett et al., 2013; Sangaralingham et al., 2015), plasma NT-proCNP is higher in men than women (Palmer et al., 2009; Prickett et al., 2013). In addition, following MI, increased NT-proCNP is associated with higher all-cause mortality in females only (Mark et al., 2021). However, these findings must be interpreted with caution, as alterations in plasma CNP and/or NT-proCNP may reflect other demographics influenced by sex (e.g. body fat percentage; Perez-Ternero et al., 2022), rather than direct actions of sex hormones. Also, GWAS studies linking NPR-C gene

variants with hypertension did not find a disparity between sexes (Ehret et al., 2011).

6.8 The therapeutic potential of CNP in PH

In the present study, two weeks of CNP infusion reduced cardiopulmonary pressure and improved pulmonary haemodynamics in mice with established PH. This beneficial pharmacodynamic profile was maintained in NPR-C$^{-/-}$ SuHx mice, alluding to a dependency on NPR-B. Crucially, the absence of altered MABP confirmed these beneficial effects were achieved using a subpressor dose of the peptide. Indeed, treated mice demonstrated increased pulmonary expression of BMPR2, which restrains PAEC and PASMC growth in the healthy lung (Yang et al., 2005; Upton et al., 2009; Rol et al., 2018) but is downregulated in PH (Morrell, 2006). As such, it appears that CNP offsets the development of this condition by shifting the environment of the pulmonary circulation from a state of pro-remodelling to a state of relative quiescence.

Switching focus to downstream effectors of BMPR2, overactive Smad2/3 signalling is thought to be a key pathogenic mechanism in the pulmonary vasculature of PH patients (Morrell, 2006). This effect has been primarily attributed to increased levels of phosphorylated (p)-Smad2/3 relative to total (t)-Smad2/3, though emerging evidence suggests that prolonged exposure to TGF-β also results in downregulation of the Smad3 gene (Yanagisawa et al., 1998; Zabini et al., 2018), which may also have pathogenic consequences. Smad3 mRNA levels are reduced in multiple animal models of PH (Zakrzewicz et al., 2007; Zabini et al., 2018; Sanada et al., 2021) and in lung tissue from patients with PAH (Richter et al., 2004; Zabini et al., 2018), consistent with the data presented herein. Furthermore, silencing of Smad3 in HPASMCs and HPAECs leads to enhanced proliferative and migratory responses (Zabini et al., 2018). Whilst the impact of CNP treatment on the ratio of p-Smad2/3 to t-Smad2/3 was not investigated in the current study, previous studies using riociguat and sildenafil have also positioned cGMP as an inhibitor of Smad2/Smad3 phosphorylation (Gong et al., 2014; Rai et al., 2018).

RNA sequencing analysis of whole-blood samples from PAH patients detected an association between lower Smad5 expression and disease susceptibility (Rhodes et al., 2020). Interestingly, CNP has previously shown to

synergise with osteogenic protein-1 to enhance phosphorylation of Smad5 in cultured osteoblastic cells (Yeh et al., 2006). The present study indicates that Smad5 levels are not significantly downregulated the SuHx mouse model, yet CNP treatment starkly upregulates pulmonary Smad5 mRNA transcripts, which may have contributed to the reversal of PH.

A promiscuous regulator, Smad7 modulates TGF-β, activin and BMP signalling by forming stable interactions with activated receptors, preventing binding and activation of pathway-restricted Smad family members (Souchelnytskyi et al., 1998; Ishisaki et al., 1999). Whilst Smad7 expression in PH patients has not been reported to date (Rol et al., 2018), reduced expressed is noted in related conditions, including COPD (Zandvoort et al., 2006) and SSc (Zhu et al., 2012). Moreover, transcription of this Smad is decreased in the lungs of MCT rats (Morty et al., 2007; Sanada et al., 2021), suggesting a contribution to enhanced TGF-β signalling. As demonstrated herein, SuHx exposure was associated with a clear trend towards reduced Smad7 gene expression, which was reversed by CNP treatment. In animal models, Smad7 gene transfer attenuates vascular remodelling (Mallawaarachchi et al., 2005), cardiac remodelling (Wei et al., 2013), and lung fibrosis (Nakao et al., 1999). As such, the anti-remodelling effects of Smad7 may have contributed to the efficaciousness of CNP in the present study.

Despite a robust reduction in cardiopulmonary pressure, two weeks of CNP infusion does not reverse the development of RVH in WT SuHx mice. Still, this intervention was able to restore the RV expression of CTGF to near-control levels in WT animals, suggesting a longer duration infusion may be necessary to harness the full benefits of the cardioprotective actions of CNP in the right heart. That said, in NPR-C$^{-/-}$ mice, CNP treatment significantly decreases RV fibrosis, tends to lower RV weight, and improves CO, suggesting the exaggerated RV remodelling observed in these animals is more amenable to reversal with afterload reduction. Contrasting with previous reports, the current study found that exogenous CNP did not alter the contractility of either the RV or LV, as neither TAPSE nor LVEF was altered in CNP-treated mice.

Conflicting results have emerged from previous investigations of the therapeutic potential of CNP in animal models of PH. In MCT rats, prophylactic or

interventional infusion of the peptide reduces RVSP, pulmonary arterial medial thickening, and RVH, ultimately improving survival. In this model, the beneficial effects of CNP are linked to regeneration of the pulmonary endothelium, driven by enhanced expression of Ki-67 and eNOS. Monocytic infiltration of the alveolar spaces is also reduced in these rats (Itoh et al., 2004), raising the possibility that CNP reduces the inflammatory component of PH. In accordance, ecCNP$^{-/-}$ and NPR-C$^{-/-}$ mice exhibit leukocyte hyper-reactivity (Moyes et al., 2014), which may have contributed to the adverse phenotypes observed in these mice in the present study. Likewise, the beneficial effects of CNP infusion detailed herein may also be partially underpinned by a dampening of inflammation. This dovetails with the ability of the peptide to temper IL-1β secretion and reduce inflammatory infiltrates (macrophages, neutrophils, and lymphocytes) in the lungs of mice with pulmonary fibrosis, ultimately reducing collagen deposition and improving survival (Murakami et al., 2004). In addition, CNP overexpression in fibroblasts attenuates pulmonary fibrosis by suppressing TGF-β signalling and myofibroblast differentiation (Kimura et al., 2016). As such, CNP may be of particular benefit in PH associated with inflammatory parenchymal lung diseases, including pulmonary fibrosis.

In stark contrast to the findings of Itoh et al., CNP infusion does not reduce RVSP, vascular remodelling, or RVH in SuHx rats (Casserly et al., 2011). This discrepancy may be underpinned by the different inciting stimuli used to induce PH. Indeed, proliferative endothelial obstructions resembling the occlusive plexiform lesions characteristic of PAH are a key pathological feature of the SuHx rat model but are absent in MCT rats (and SuHx mice). Beyond its ability to promote re-endothelialisation, CNP has potent angiogenic effects (Yamahara et al., 2003) attributed to NPR-C activation (Bubb et al., 2019). As such, when PH is primarily driven by EC apoptosis and VSMC proliferation, the peptide may support restoration of the endothelial barrier and regrowth of lost peripheral vessels. However, when EC apoptosis is followed by aberrant proliferation of apoptosis-resistant EC clones (i.e. PAH), NPR-C signalling may become pathogenic. Indeed, Casserly et al. report a trend towards an increased burden of occluded microvessels in the lungs of CNP-treated SuHx rats (Casserly et al., 2011), which may limit the efficacy of CNP. Clearly, the actions of the peptide in this model require further investigation.

Receptor downregulation may also have constrained the efficacy of CNP in the study of Casserly et al. As highlighted by the present study, CNP ameliorates PH primarily through activation of NPR-B (at least in male mice). However, Casserly et al. found that CNP infusion markedly downregulated NPR-B at the protein level (Casserly et al., 2011). This observation is consistent with previous reports of decreased NPR-B gene expression in rat VSMCs following chronic CNP exposure (Rahmutula and Gardner, 2005). Still, Itoh et al. were able to demonstrate a considerable therapeutic effect with a longer duration infusion (5 weeks versus 3 weeks) of a threefold lower dose (18 µg/day versus 54 µg/day), suggesting that NPR-B downregulation can avoided by adjustment of the dosing regimen.

Selective enhancement of NPR-B signalling may be a more appropriate strategy in severe PH. Expression of a constitutively active NPR-B mutant decreases RVSP, medial wall thickness, and the number of occlusive lesions in the lungs of SuHx rats. Transduction of HPASMCs from PAH patients with the same mutant attenuates proliferation (Nawa et al., 2016).

6.9 CNP therapeutic agents

The findings presented hitherto offer an early hint of the clinical potential of targeting CNP signalling in PH. However, direct use of the peptide as a therapeutic agent is precluded by major pitfalls, including a short plasma half-life and a lack of oral bioavailability (Baliga et al., 2011).

One approach that circumvents these issues is boosting endogenous CNP levels by blocking NEP-mediated degradation (Northridge et al., 1989). A vast wealth of data indicates that NEP inhibitors attenuate the development of hypoxic PH by boosting the activity of endogenous natriuretic peptides (Winter et al., 1991; Klinger et al., 1993b; Thompson et al., 1994). In concert, NEP KO mice are protected against hypoxia-induced pulmonary oedema (Irwin et al., 2005). As discussed previously, NEP inhibition synergises with PDE5 inhibition to favourable effect in hypoxia-adapted rats (Baliga et al., 2008), fibrosis-associated PH (Baliga et al., 2014), and PAH patients (Hobbs et al., 2019). Intriguingly, despite being the preferred substrate for NEP (Watanabe et al., 1997), plasma CNP was unaltered by NEP blockade in the aforementioned clinical trial (Hobbs et al., 2019). Still, as

highlighted by the authors, circulating CNP levels may not be representative of local tissue concentrations, which is pertinent considering the peptide has predominantly localised effects. Alternatively, the beneficial effects observed in this trial may be attributed to ANP and/or BNP, which are also substrates for NEP (Kenny and Stephenson, 1988; Soleilhac et al., 1992; Thompson et al., 1994; Watanabe et al., 1997). This notion is supported by the loss of synergy between PDE5 and NEP inhibition in NPR-A KO mice (Baliga et al., 2014). It should be noted that NEP also metabolises ET-1, which may limit the efficacy of NEP inhibitors (Whyteside and Turner, 2008).

Beyond PH, NEP inhibitors have been explored extensively in the realm of HF, due to their ability to ability to promote natriuresis and diuresis, and inhibit the RAAS system (Richards et al., 1990; Rademaker et al., 1996). Though monotherapy with a NEP inhibitor does not hold significant advantages over conventional ACE inhibitors (O'Connor et al., 1999; Packer et al., 2002), a dual angiotensin-receptor blocker (ARB)/NEP inhibitor (sacubitril/valsartan; LCZ696) was found to elicit greater reductions in plasma NT-proBNP and left atrial size than an ARB in HFrEF patients (Solomon et al., 2012). Sacubitril/valsartan was also superior to ACE inhibition in regards to symptom relief, easing the rate of disease progression, and reducing the risk of hospitalisation and death (McMurray et al., 2014; Packer et al., 2015), resulting in FDA approval for the treatment of HFrEF (marketed as Entresto). Recently, sacubitril/valsartan was reported to reduce mPAP and alleviate pulmonary vascular and RV remodelling in experimental PH models, through a combination of RAAS inhibition and CNP/NPR-B/cGMP potentiation (Liu et al., 2021). However, these haemodynamic and structural changes were not accompanied by improvement in RV function, which the authors attributed to the treatment duration. The effect of sacubitril/valsartan on RV function will require further investigation in pre-clinical models and may set the groundwork for repurposing Entresto for the treatment of RV dysfunction.

The challenges associated with employing the natriuretic peptides as therapeutics have led to the advent of synthetic 'designer' peptides. *Dendroaspis* natriuretic peptide (DNP) was first isolated from the venom of the green mamba (*Dendroaspis angusticeps*; Schweitz et al., 1992). Cenderitide (CD-NP) is a fusion protein of CNP and DNP and displays powerful vasodilatory, anti-fibrotic,

natriuretic, and diuretic effects *in vivo* (Lisy et al., 2008; Martin et al., 2012). A major advantage of this peptide is that it can be delivered subcutaneously (Ichiki et al., 2020) due to reduced susceptibility to NEP (Dickey and Potter, 2011). Cenderitide was well-tolerated in Phase 1 trials; Phase 2 studies provided an early indication of favourable effects on renal function in HF patients (Costello-Boerrigter et al., 2011; Neutel et al., 2012; Kawakami et al., 2018), setting the foundation for large-scale Phase 3 clinical trials. Cenderitide has yet to be investigated in the context of PH and RV failure.

Vosoritide (BMN111) is a CNP analogue with structural modifications that facilitate subcutaneous delivery (Lorget et al., 2012). Compared to the native peptide, vosoritide demonstrates superior resistance to NEP degradation *in vitro*, and a greatly extended serum half-life when delivered intravenously or subcutaneously *in vivo* (Wendt et al., 2015). Following a series of successful clinical trials, (Savarirayan et al., 2019, 2021a, 2021b) vosoritide was granted approval in the EU and USA as a therapeutic agent for achondroplasia (Savarirayan et al., 2022). Like vosoritide, TransCon CNP is a synthetic analogue in development for achondroplasia. This novel prodrug consists of a CNP molecule conjugated to a polyethylene glycol carrier molecule via a cleavable linker, facilitating sustained release of the peptide with weekly subcutaneous administration. *In vivo*, the conjugated peptide has a considerably longer serum half-life than vosoritide, and, by avoiding high peak CNP levels, improved hemodynamic tolerability (Breinholt et al., 2019). The results of a recent first-in-human trial indicate that TransCon CNP is well-tolerated in healthy adults (Breinholt et al., 2022). Whilst neither of these peptides have yet been investigated in the realms of cardiovascular disease, their potential applications certainly warrant investigation.

Orally available small molecule drugs targeting CNP signalling are an even more attractive prospect than designer peptides. The data presented herein suggest that a dual NPR-B/NPR-C agonist would exert protective effects in both the pulmonary vasculature and RV, for maximal clinical benefit. Such a molecule remains a therapeutic ideal, yet endeavours to develop small molecules that target these receptors are beginning to bear fruit. The most promising effort to date (in the context of PH) are novel NPR-C agonists (Conole et al., 2019), which have

vasorelaxant properties in the rat aorta and mesenteric artery (Smith et al., 2022). Small molecule NPR-B antagonists have also been developed and are proposed as a novel therapy for HF, on the basis of their ability to dampen the facilitatory effect of CNP on detrimental catecholamine-mediated positive inotropic and chronotropic responses in the failing heart (Bach et al., 2014). The results of the current study do not support such an approach in the management of PH, yet the aforementioned study does at least provide proof-of-principle that NPR-B can be successfully targeted with small molecules.

6.10 Limitations of the present study, and future work

One pitfall of the present study is the exclusive use of second order conduit arteries (right and left main pulmonary arteries) to investigate pulmonary vascular reactivity. Resistance vessels (small pulmonary arteries and arterioles) are the major site of PVR and an important regulator of blood pressure (Ventetuolo and Klinger, 2014). However, in the mouse lung, resistance arteries (fourth order vessels, or higher) branch extensively and are deeply embedded in the parenchyma (Wenceslau et al., 2021), such that only a short length of artery (approximately 200 μm) is accessible (Ko et al., 2010; Wenceslau et al., 2021). As discussed previously, NPR-C signalling is believed to play a much larger role in governing the tone of resistance vessels than conduit arteries (Moyes and Hobbs, 2019). Consequently, the current study may have underestimated the overall vasoreactivity of this signalling pathway *in vitro*. Nonetheless, as NPR-C$^{-/-}$ mice do not exhibit a pulmonary hypertensive phenotype *in vivo*, the overall conclusions of this study remain the same.

A further drawback of the present study is that whole lung mRNA analysis may not detect confined changes in the pulmonary vasculature due to the influence of parenchymal cells. Furthermore, a lack of suitable antibodies prevented the characterisation of CNP, NPR-B and NPR-C protein levels. Whilst the mRNA expression of a gene tends to predict protein expression (Schwanhüusser et al., 2011; Koussounadis et al., 2015; Edfors et al., 2016), post-transcriptional modifications (e.g. splicing) may alter the efficiency of translation (Maier et al., 2009; Vogel and Marcotte, 2012). Furthermore, the *in vivo* half-life of proteins can

vary considerably; some experience rapid post-translational degradation whilst others are incredibly stable (Greenbaum et al., 2003; Schwanhüusser et al., 2011). As such, in some cases final protein expression does not correlate with the abundance of mRNA transcripts. Work is underway in the Hobbs lab to characterise antibodies for CNP and NPR-C, and future experiments will aim to characterise the expression and localisation of CNP/NPR proteins in the lung using immunoblotting and immunohistochemistry. Likewise, a vital future step will be the use of immunoblotting to explore the influence of CNP on Smad phosphorylation in the lung, to confirm the anti-proliferative, anti-remodelling effects on BMP signalling already demonstrated at the mRNA level.

A notable limitation for histological analyses requiring visual scoring or quantification by an analyst is their subjective nature, which is further amplified when limited fields of view are selected for analysis (Schipke et al., 2017). In the present study, steps were undertaken to mitigate analyst bias. For each set of lungs analysed for pulmonary vessel muscularisation, one random field of view from each of the five lobes was selected for analysis, which was conducted with the analyst blind to the genetic background and treatment of the tissue being scored. Furthermore, when assessing RV fibrosis, a cross section of the entire RV was examined, eliminating 'field of view' bias. In addition, a more objective, semi-automated computer-aided analysis was employed (though analyst bias could not be eliminated entirely due to the need to manually set a colour threshold). Threshold analysis may also result in the inclusion of non-collagen structures and/or the exclusion of subtle collagen deposits (Schipke et al., 2017). Still, other commonly employed approaches to assess fibrosis also have limitations. For example, the hydroxyproline assay necessitates that tissue samples are homogenised, which precludes differentiation between different morphological patterns of fibrosis (i.e. perivascular versus interstitial; de Jong et al., 2012).

6.11 Limitations of the SuHx mouse model

The link between hypoxia and PH has been long established in communities living at high altitude (Arias-Stella and Saldana, 1963) and in patients with CLD (Zhao, 2010). From an experimental standpoint, the exposure of rodents to CH is the most common approach to study PH. Mice exposed to CH (10% O_2) exhibit increased

RVSP, muscularisation of the precapillary arterioles, and RVH (Gomez-Arroyo et al., 2012). Despite hypoxic exposure on a scale exceeding that of the human disease, the rodent phenotype is modest (Maarman et al., 2013), and reversible upon return to normoxic conditions (Voelkel and Tuder, 2000).

To recreate the more severe pathology of human PH (particularly PAH), CH is often combined with administration of the VEGFR-2 antagonist, Sugen. In rats, this combination produces severe and progressive pulmonary vascular remodelling that cannot be reversed, even by a return to normoxia (Taraseviciene Stewart et al., 2001). In fact, a return to normoxic conditions is demarcated by the progressive development of complex 'angio-obliterative' vascular lesions comparable to the plexiform lesions seen in PAH patients (Abe et al., 2010; Vitali et al., 2014). It is thought that blockade of VEGFR-2, which under normal conditions promotes EC survival, leads to selective death of PAECs (Voelkel et al., 2002), thereby enriching a subpopulation of apoptosis-resistant, hyper-proliferative ECs (Sakao et al., 2005). SuHx rats also demonstrate maladaptive RV remodelling, demarcated by RVH, functional decline and, RV dilation (Bogaard et al., 2009b, 2010).

Naturally, attempts have been made to recreate the SuHx model in mice, which are more amenable to genetic modification, and thus remain a key tool to understand the distinct role(s) of pathway of interest in the pathobiology of PH. In regards to RVSP and RVH, concomitant Sugen administration induces a more profound phenotype in mice than CH alone (Ciuclan et al., 2011; Vitali et al., 2014). In the present study, SuHx animals demonstrated many pathological alterations consistent with human PH, including elevated RVSP, haemodynamic alterations, pulmonary vascular remodelling, increased RV weight and thickness, and cardiac dysfunction. Still, this model is not without drawbacks, namely the absence of disturbed pulmonary endothelial architecture and RV failure (Vitali et al., 2014; Wang et al., 2018b). In addition, arteriolar muscularisation remains reversible upon return to normoxic conditions (Ciuclan et al., 2011). As such, this model is more reminiscent of CLD-PH than PAH.

Despite these limitations, the current study employed the SuHx mouse model due to a lack of suitable alternatives compatible with transgenic mice. Indeed, attempts have been made to establish a murine MCT model, but the

resulting pathology is more reminiscent of acute lung injury than PH (Goto et al., 2002; Dumitrascu et al., 2008). Mice administered bleomycin develop PH secondary to pulmonary fibrosis, but acute mortality (Hemnes et al., 2008) and spontaneous fibrosis resolution (Jarman et al., 2014) limit the use of this model. As such, whilst the reliance on a single experimental model is acknowledged as a shortcoming of the present study, it is one that could not be mitigated. An important follow-up to the present study would be to examine the impact of CNP infusion on the development of PH in SuHx rats, with a focus on titrating the peptide dose to avoid efficacy-limiting NPR-B downregulation and adverse angio-proliferative effects.

Another drawback of the current study is that potential direct cardioprotective effects of CNP could not be distinguished from PVR-driven afterload modification, due to the functional coupling of the RV and pulmonary vasculature. In future studies, this issue could be circumvented through the use of the pulmonary artery banding (PAB) model, which involves mechanical constriction of the pulmonary trunk to 'fix' RV afterload in an elevated state, nullifying coupling to the pulmonary vasculature (Guihaire et al., 2013). The main advantage of this model is that RV remodelling and the potential for reversal can be studied in the absence of pulmonary vascular remodelling, also avoiding the potential confounding effects of hypoxia, VEGF inhibition and MCT toxicity on the heart (Borgdorff et al., 2015). PAB is an extremely versatile model; by changing the diameter of constriction, severity can be altered as desired, from adaptive RVH to decompensated RV failure (Andersen et al., 2018). Whilst MCT and SuHx rats develop RV failure, the functional coupling of the heart and vasculature still poses an issue when investigating cardiac-targeted therapies (Andersen et al., 2018). As such, the PAB model would be well placed for a future investigation into the effects of CNP on RV function and failure.

6.12 Limitations of echocardiography

The gold standard for the assessment of PH in rodents is quantification of RVSP (Zimmer et al., 1988; Wauthy et al., 2004; Gaynor et al., 2005), which in the absence of pulmonary stenosis is equivalent to pulmonary artery systolic pressure (Thibault et al., 2010). However, right heart catheterisation is a terminal procedure

in mice, which precludes longitudinal study. In the clinic, transthoracic echocardiography is used extensively for PH screening and is the only non-invasive method for estimating PAP and monitoring RV structure and function following diagnosis (McLaughlin et al., 2009; Bossone et al., 2013). From a pre-clinical perspective, echocardiography permits baseline assessment and serial evaluation of cardiovascular function in the same individual, and thus is ideally suited for mapping disease progression and the response to therapeutic interventions.

Pulmonary acceleration time (the interval between the onset of pulmonary flow and peak velocity) has been proposed as an alternative index to estimate PAP in the absence of tricuspid regurgitation (Thibault et al., 2010). Shorter PATs correlate with elevated PAP in humans (Isobe et al., 1986) and with elevated RVSP in rodents (Jones et al., 2002; Thibault et al., 2010; Zhu et al., 2019). Furthermore, the feasibility of measuring pulmonary artery peak velocity has been demonstrated in a murine model of pulmonary artery occlusion (Cheng et al., 2014).

Despite extensive application in the realm of LV structure and function, murine right heart echocardiography remains in its infancy (Koskenvuo et al., 2010; Thibault et al., 2010). This is primarily due to the technical difficulty associated with the crescent shape, thin walls, and retrosternal location of the RV (Karas and Kizer, 2012; Cheng et al., 2014). The spatial and temporal resolution achievable by echocardiography instrumentation has improved the accessibility of RV imaging (Scherrer-Crosbie and Thibault, 2008; Cheng et al., 2014), but some clinically relevant parameters cannot be reliably assessed in rodents due to physiological differences with humans. Indeed, the velocity of tricuspid valve regurgitant jets is often used as a surrogate for PAP in the clinic (Rudski et al., 2010), yet these jets are only evident in mice with very severely elevated PAP (Kohut et al., 2016). Furthermore, true alignment of PW Doppler flow for the small size of regurgitant jets that occur in rodents remains a technical challenge (Thibault et al., 2010). Clinical assessment of RV diastolic function involves assessment of tricuspid inflow using PW Doppler to determine the ratio of the early filling (E) wave and the late diastolic filling (A) wave peak velocities (E/A ratio; Rudski et al., 2010). Unfortunately, this assessment is precluded in mice by the rapid HR, which causes the E and A waves to fuse (Egemnazarov et al., 2015; Kohut et al., 2016).

Still, other echocardiographic parameters of RV structure and function can be reliably measured in mice. RVFW correlates with RV weight in murine models of PH (Maron et al., 2007; Zhu et al., 2019). In addition, due to the unique contractile pattern of the RV, systolic function can be assessed by TAPSE, which quantifies systolic base-to-apex shortening (Hardziyenka et al., 2006) and correlates with prognosis and other parameters of RV function, in the clinic (Forfia et al., 2006; Kohut et al., 2016) and in animal models of PH (Toldo et al., 2011; Brittain et al., 2013; Vitali et al., 2014; Kohut et al., 2016; Zhu et al., 2019). Furthermore, the present study demonstrates the feasibility of measuring tricuspid valve velocity to assess the efficiency of blood flow through the right heart.

6.13 Conclusions

In sum, this study provides *in vitro* and *in vivo* evidence of the protective effects of endogenous CNP signalling against PH and RV remodelling (summarised in **Figure 40**). Endothelial-specific deletion of the peptide accentuates cardiopulmonary pressure overload, pulmonary vascular remodelling and RVH. The potential deleterious effects of cardiomyocyte restricted CNP deletion are offset by increased expression of the CNP gene by other cell types in the heart. Whilst the negative pathological profile of ecCNP$^{-/-}$ mice is not reflected by global deletion of NPR-C, RV remodelling is nonetheless exacerbated, underscoring a cardioprotective role for this receptor in the right heart. Notably, the detrimental consequences of CNP and NPR-C deletion are predominantly associated with male sex. Administration of the exogenous peptide to WT animals with established PH eases cardiopulmonary pressure overload and alters the pulmonary gene expression of BMPR2 and downstream Smad signalling molecules to favour quiescence over proliferation. This beneficial pharmacodynamic profile is maintained in NPR-C$^{-/-}$ mice, indicating that akin to endogenous CNP, the therapeutic effects of the exogenous peptide in the pulmonary vasculature are primarily mediated by activation of NPR-B. All in all, these results suggest that CNP, and its downstream receptors, are potential disease-modifying targets in the treatment of PH.

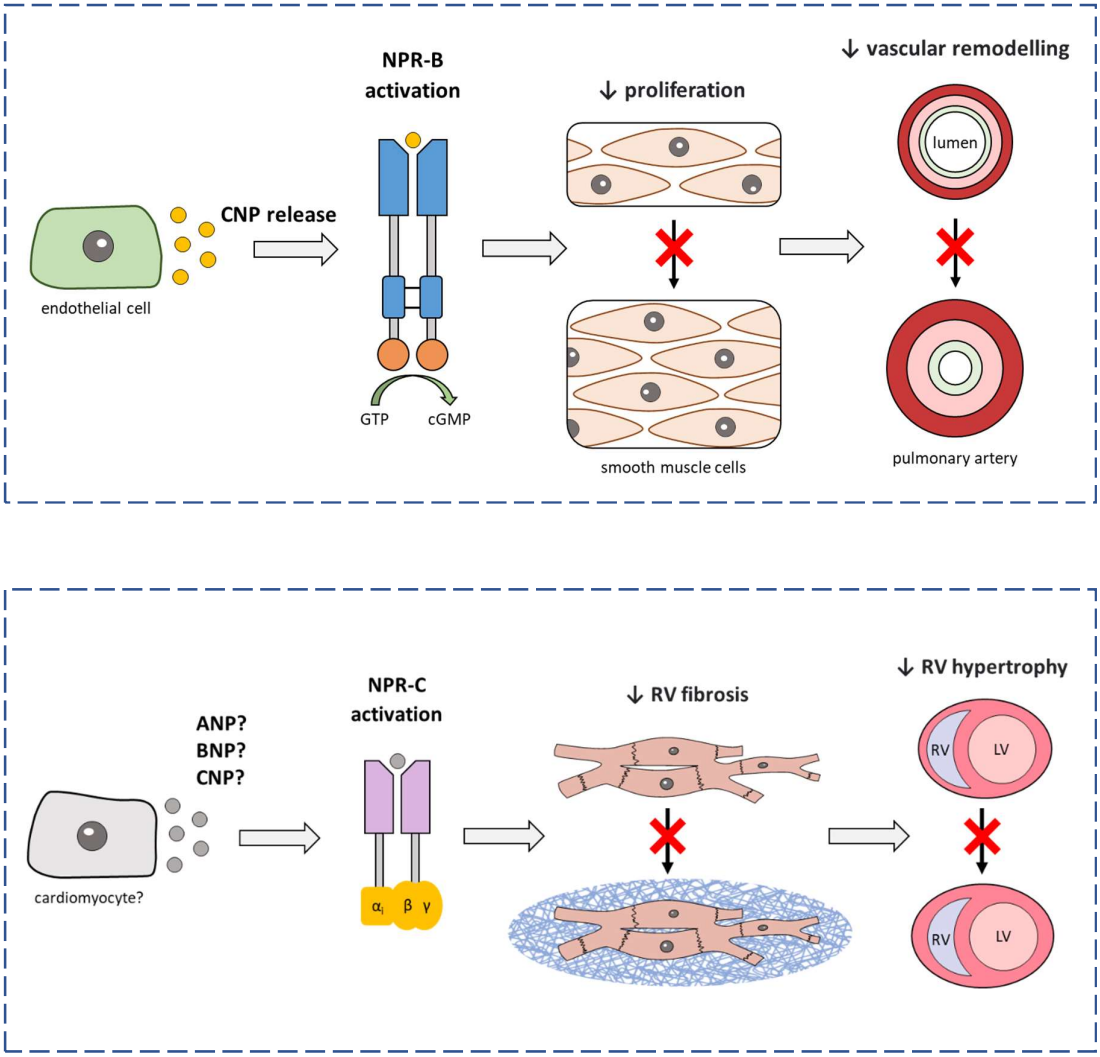

Figure 40: Summary of key findings

Protective actions of signalling pathways activated by CNP in the pulmonary circulation (*upper panel*) and the RV (*lower panel*). In the vasculature, constitutive release of CNP by endothelial cells activates NPR-B to inhibit smooth muscle cell growth and protect against vascular remodelling. In the heart, activation of NPR-C by an unidentified molecule (or molecules; likely cardiomyocyte-derived natriuretic peptides) attenuates hypertrophy by easing the development and progression of fibrotic remodelling.

Bibliography

Abe, K., Toba, M., Alzoubi, A., Ito, M., Fagan, K.A., Cool, C.D., et al. (2010). Formation of plexiform lesions in experimental severe pulmonary arterial hypertension. Circulation *121*: 2747–2754.

Abraham, W.T., Adams, K.F., Fonarow, G.C., Costanzo, M.R., Berkowitz, R.L., Lejemtel, T.H., et al. (2005). In-hospital mortality in patients with acute decompensated heart failure requiring intravenous vasoactive medications: An analysis from the Acute Decompensated Heart Failure National Registry (ADHERE). J. Am. Coll. Cardiol. *46*: 57–64.

Achcar, R.O.D., Yung, G.L., Saffer, H., Cool, C.D., Voelkel, N.F., and Yi, E.S. (2006). Morphologic changes in explanted lungs after prostacyclin therapy for pulmonary hypertension. Eur. J. Med. Res. *11*: 203–207.

Agard, C., Rolli-Derkinderen, M., Dumas-de-La-Roque, E., Rio, M., Sagan, C., Savineau, J.P., et al. (2009). Protective role of the antidiabetic drug metformin against chronic experimental pulmonary hypertension. Br. J. Pharmacol. *158*: 1285–1294.

Agnew, C., Ayaz, P., Kashima, R., Loving, H.S., Ghatpande, P., Kung, J.E., et al. (2021). Structural basis for ALK2/BMPR2 receptor complex signaling through kinase domain oligomerization. Nat. Commun. *12*:.

Agrawal, A., Verma, I., Shah, V., Agarwal, A., and Sikachi, R.R. (2016). Cardiac manifestations of idiopathic pulmonary fibrosis. Intractable Rare Dis. Res.

Agrawal, V., Fortune, N., Yu, S., Fuentes, J., Shi, F., Nichols, D., et al. (2019). Natriuretic peptide receptor C contributes to disproportionate right ventricular hypertrophy in a rodent model of obesity-induced heart failure with preserved ejection fraction with pulmonary hypertension. Pulm. Circ. *9*:.

Agrawal, V., and Hemnes, A.R. (2020). Authors' reply: role of natriuretic peptide receptor C signalling in obesity-induced heart failure with preserved ejection fraction with pulmonary hypertension. Pulm. Circ. *10*:.

Ahmed, S.M.U., Luo, L., Namani, A., Wang, X.J., and Tang, X. (2017). Nrf2 signaling pathway: Pivotal roles in inflammation. Biochim. Biophys. Acta - Mol. Basis Dis. *1863*: 585–597.

Al-Qazazi, R., Lima, P.D.A., Prisco, S.Z., Potus, F., Dasgupta, A., Chen, K.-H., et al. (2022). Macrophage-NLRP3 Activation Promotes Right Ventricle Failure in Pulmonary Arterial Hypertension. Am. J. Respir. Crit. Care Med.

Alastalo, T.P., Li, M., Jesus Perez, V. De, Pham, D., Sawada, H., Wang, J.K., et al. (2011). Disruption of PPARγ/β-catenin-mediated regulation of apelin impairs BMP-induced mouse and human pulmonary arterial EC survival. J. Clin. Invest. *121*: 3735–3746.

Alzoubi, A., Toba, M., Abe, K., O'Neill, K.D., Rocic, P., Fagan, K.A., et al. (2013). Dehydroepiandrosterone restores right ventricular structure and function in rats with severe pulmonary arterial hypertension. Am. J. Physiol. - Hear. Circ. Physiol. *304*:.

Anand-Srivastava, M.B. (2000). Downregulation of atrial natriuretic peptide ANP-C receptor is associated with alterations in G-protein expression in A10 smooth muscle cells. Biochemistry *39*: 6503–6513.

Anand-Srivastava, M.B. (2005). Natriuretic peptide receptor-C signaling and regulation. Peptides *26*: 1044–1059.

Anand-Srivastava, M.B. (2010). Modulation of Gi Proteins in Hypertension: Role of Angiotensin II and Oxidative Stress. Curr. Cardiol. Rev. *6*: 298–308.

Anand-Srivastava, M.B., Sehl, P.D., and Lowe, D.G. (1996). Cytoplasmic domain of natriuretic peptide receptor-C inhibits adenylyl cyclase. Involvement of a pertussis toxin-sensitive G protein. J. Biol. Chem. *271*: 19324–19329.

Andersen, S., Schultz, J.G., Andersen, A., Ringgaard, S., Nielsen, J.M., Holmboe, S., et al. (2014). Effects of bisoprolol and losartan treatment in the hypertrophic and failing right heart. J. Card. Fail. *20*: 864–873.

Andersen, S., Schultz, J.G., Holmboe, S., Axelsen, J.B., Hansen, M.S., Lyhne, M.D., et al. (2018). A pulmonary trunk banding model of pressure overload induced

right ventricular hypertrophy and failure. J. Vis. Exp. *2018*: e58050.

Anwar, A., Li, M., Frid, M.G., Kumar, B., Gerasimovskaya, E. V., Riddle, S.R., et al. (2012). Osteopontin is an endogenous modulator of the constitutively activated phenotype of pulmonary adventitial fibroblasts in hypoxic pulmonary hypertension. Am. J. Physiol. - Lung Cell. Mol. Physiol. *303*:.

Arciniegas, E., Frid, M.G., Douglas, I.S., and Stenmark, K.R. (2007). Perspectives on endothelial-to-mesenchymal transition: Potential contribution to vascular remodeling in chronic pulmonary hypertension. Am. J. Physiol. - Lung Cell. Mol. Physiol. *293*:.

Arias-Stella, J., and Saldana, M. (1963). The Terminal Portion of the Pulmonary Arterial Tree in People Native To High Altitudes. Circulation *28*: 915–925.

Atkinson, C., Stewart, S., Upton, P.D., Machado, R., Thomson, J.R., Trembath, R.C., et al. (2002). Primary pulmonary hypertension is associated with reduced pulmonary vascular expression of type II bone morphogenetic protein receptor. Circulation *105*: 1672–1678.

Austin, E.D., and Loyd, J.E. (2014). The genetics of pulmonary arterial hypertension. Circ. Res. *115*: 189–200.

Bach, T., Bergholtz, S., Riise, J., Qvigstad, E., Skomedal, T., Osnes, J.B., et al. (2014). Identification of small molecule NPR-B antagonists by high throughput screening - Potential use in heart failure. Naunyn. Schmiedebergs. Arch. Pharmacol. *387*: 5–14.

Badagliacca, R., Poscia, R., Pezzuto, B., Papa, S., Reali, M., Pesce, F., et al. (2018a). Prognostic relevance of right heart reverse remodeling in idiopathic pulmonary arterial hypertension. J. Hear. Lung Transplant. *37*: 195–205.

Badagliacca, R., Raina, A., Ghio, S., D'Alto, M., Confalonieri, M., Correale, M., et al. (2018b). Influence of various therapeutic strategies on right ventricular morphology, function and hemodynamics in pulmonary arterial hypertension. J. Hear. Lung Transplant. *37*: 365–375.

Badesch, D., MD, F., Raskob, G., Elliott, C., Greg MD, F., Krichman, A., et al.

(2010). Pulmonary Arterial Hypertension: Baseline Characteristics From the REVEAL Registry. Chest *137*: 376–387.

Baird, G.L., Archer-Chicko, C., Barr, R.G., Bluemke, D.A., Foderaro, A.E., Fritz, J.S., et al. (2018). Lower DHEA-S levels predict disease and worse outcomes in post-menopausal women with idiopathic, connective tissue disease- And congenital heart disease associated pulmonary arterial hypertension. Eur. Respir. J. *51*:.

Baird, G.L., Walsh, T., Aliotta, J., Allahua, M., Andrew, R., Bourjeily, G., et al. (2021). Insights from the menstrual cycle in pulmonary arterial hypertension. Ann. Am. Thorac. Soc. *18*: 218–228.

Baker, D.L., Hashimoto, K., Grupp, I.L., Ji, Y., Reed, T., Loukianov, E., et al. (1998). Targeted overexpression of the sarcoplasmic reticulum Ca2+-ATPase increases cardiac contractility in transgenic mouse hearts. Circ. Res. *83*: 1205–1214.

Baliga, R.S., MacAllister, R.J., and Hobbs, A.J. (2011). New perspectives for the treatment of pulmonary hypertension. Br. J. Pharmacol. *163*: 125–140.

Baliga, R.S., Scotton, C.J., Trinder, S.L., Chambers, R.C., MacAllister, R.J., and Hobbs, A.J. (2014). Intrinsic defence capacity and therapeutic potential of natriuretic peptides in pulmonary hypertension associated with lung fibrosis. Br. J. Pharmacol. *171*: 3463–3475.

Baliga, R.S., Zhao, L., Madhani, M., Lopez-Torondel, B., Visintin, C., Selwood, D., et al. (2008). Synergy between natriuretic peptides and phosphodiesterase 5 inhibitors ameliorates pulmonary arterial hypertension. Am. J. Respir. Crit. Care Med. *178*: 861–869.

Baňasová, A., Maxová, H., Hampl, V., Vízek, M., Povýšilová, V., Novotná, J., et al. (2008). Prevention of mast cell degranulation by disodium cromoglycate attenuates the development of hypoxic pulmonary hypertension in rats exposed to chronic hypoxia. Respiration *76*: 102–107.

Bandyopadhyay, D., Bajaj, N.S., Zein, J., Minai, O.A., and Dweik, R.A. (2015). Outcomes of β-blocker use in pulmonary arterial hypertension: A propensity-

matched analysis. Eur. Respir. J. *46*: 750–760.

Banks, D.A., Pretorius, G.V.D., Kerr, K.M., and Manecke, G.R. (2014). Pulmonary endarterectomy: Part I. Pathophysiology, clinical manifestations, and diagnostic evaluation of chronic thromboembolic pulmonary hypertension. Semin. Cardiothorac. Vasc. Anesth. *18*: 319–330.

Barberà, J.A. (2013). Mechanisms of development of chronic obstructive pulmonary disease-associated pulmonary hypertension. Pulm. Circ. *3*: 160–164.

Barberà, J.A., Peinado, V.I., Santos, S., Ramirez, J., Roca, J., and Rodriguez-Roisin, R. (2001). Reduced expression of endothelial nitric oxide synthase in pulmonary arteries of smokers. Am. J. Respir. Crit. Care Med. *164*: 709–713.

Barnes, P.J., and Liu, S.F. (1995). Regulation of pulmonary vascular tone. Pharmacol. Rev.

Barst, R.J., Rubin, L.J., Long, W.A., Mcgoon, M.D., Rich, S., Badesch, D.B., et al. (1996). A comparison of continuous intravenous epoprostenol (prostacyclin) with conventional therapy for primary pulmonary hypertension. N. Engl. J. Med. *334*: 296–300.

Bartelds, B., Loon, R.L.E. Van, Mohaupt, S., Wijnberg, H., Dickinson, M.G., Boersma, B., et al. (2012). Mast cell inhibition improves pulmonary vascular remodeling in pulmonary hypertension. Chest *141*: 651–660.

Bauer, M., Wilkens, H., Langer, F., Schneider, S.O., Lausberg, H., and Schäfers, H.J. (2002). Selective upregulation of endothelin B receptor gene expression in severe pulmonary hypertension. Circulation *105*: 1034–1036.

Bauer, P.M., Buga, G.M., and Ignarro, L.J. (2001). Role of p42/p44 mitogen-activated-protein kinase and p21waf1/cip1 in the regulation of vascular smooth muscle cell proliferation by nitric oxide. Proc. Natl. Acad. Sci. U. S. A. *98*: 12802–12807.

Beaulieu, P., Cardinal, R., Page, P., Francoeur, F., Tremblay, J., and Lambert, C. (1997). Positive chronotropic and inotropic effects of C-type natriuretic peptide in dogs. Am. J. Physiol. *273*:.

Benson, L., Brittain, E.L., Pugh, M.E., Austin, E.D., Fox, K., Wheeler, L., et al. (2014). Impact of diabetes on survival and right ventricular compensation in pulmonary arterial hypertension. Pulm. Circ. *4*: 311–318.

Benza, R.L., Miller, D.P., Barst, R.J., Badesch, D.B., Frost, A.E., and McGoon, M.D. (2012). An evaluation of long-term survival from time of diagnosis in pulmonary arterial hypertension from the reveal registry. Chest *142*: 448–456.

Berman, M., Hardman, G., Sharples, L., Pepke-Zaba, J., Sheares, K., Tsuia, S., et al. (2012). Pulmonary endarterectomy: Outcomes in patients aged >70. Eur. J. Cardio-Thoracic Surg. *41*:.

Bernard, J., and Yi, E.S. (2007). Pulmonary thromboendarterectomy: a clinicopathologic study of 200 consecutive pulmonary thromboendarterectomy cases in one institution. Hum. Pathol. *38*: 871–877.

Bertero, T., Oldham, W.M., Cottrill, K.A., Pisano, S., Vanderpool, R.R., Yu, Q., et al. (2016). Vascular stiffness mechanoactivates YAP/TAZ-dependent glutaminolysis to drive pulmonary hypertension. J. Clin. Invest. *126*: 3313–3335.

Blanco, I., Gimeno, E., Munoz, P.A., Pizarro, S., Gistau, C., Rodriguez-Roisin, R., et al. (2010). Hemodynamic and gas exchange effects of sildenafil in patients with chronic obstructive pulmonary disease and pulmonary hypertension. Am. J. Respir. Crit. Care Med. *181*: 270–278.

Boehm, M., Kojonazarov, B., Ghofrani, H.A., Grimminger, F., Weissmann, N., Liles, J.T., et al. (2015). Effects of apoptosis signal- regulating kinase 1 (ASK1) inhibition in experimental pressure overload-induced right ventricular dysfunction. PA4913.

Bogaard, H.J., Abe, K., Noordegmaf, A.V., and Voelkel, N.F. (2009a). The right ventricle under pressure. Chest *135*: 794–804.

Bogaard, H.J., Natarajan, R., Henderson, S.C., Long, C.S., Kraskauskas, D., Smithson, L., et al. (2009b). Chronic pulmonary artery pressure elevation is insufficient to explain right heart failure. Circulation *120*: 1951–1960.

Bogaard, H.J., Natarajan, R., Mizuno, S., Abbate, A., Chang, P.J., Chau, V.Q., et al. (2010). Adrenergic receptor blockade reverses right heart remodeling and

dysfunction in pulmonary hypertensive rats. Am. J. Respir. Crit. Care Med. *182*: 652–660.

Bonelli, M., Savitskaya, A., Steiner, C.-W., Rath, E., Smolen, J.S., and Scheinecker, C. (2009). Phenotypic and Functional Analysis of CD4 + CD25 − Foxp3 + T Cells in Patients with Systemic Lupus Erythematosus . J. Immunol. *182*: 1689–1695.

Bonnet, S., and Archer, S.L. (2007). Potassium channel diversity in the pulmonary arteries and pulmonary veins: Implications for regulation of the pulmonary vasculature in health and during pulmonary hypertension. Pharmacol. Ther. *115*: 56–69.

Bonnet, S., Dumas-de-La-Roque, E., Bégueret, H., Marthan, R., Fayon, M., Santos, P. Dos, et al. (2003). Dehydroepiandrosterone (DHEA) prevents and reverses chronic hypoxic pulmonary hypertension. Proc. Natl. Acad. Sci. U. S. A. *100*: 9488–9493.

Bonnet, S., Michelakis, E.D., Porter, C.J., Andrade-Navarro, M.A., Thébaud, B., Bonnet, S., et al. (2006). An Abnormal mitochondrial-hypoxia inducible factor-1α-Kv channel pathway disrupts oxygen sensing and triggers pulmonary arterial hypertension in fawn hooded rats: Similarities to human pulmonary arterial hypertension. Circulation *113*: 2630–2641.

Bordenave, J., Tu, L., Berrebeh, N., Thuillet, R., Cumont, A., Vely, B. Le, et al. (2020). Lineage tracing reveals the dynamic contribution of pericytes to the blood vessel remodeling in pulmonary hypertension. Arterioscler. Thromb. Vasc. Biol. 766–782.

Borgdorff, M.A., Bartelds, B., Dickinson, M.G., Steendijk, P., and Berger, R.M.F. (2013). A cornerstone of heart failure treatment is not effective in experimental right ventricular failure. Int. J. Cardiol. *169*: 183–189.

Borgdorff, M.A.J., Dickinson, M.G., Berger, R.M.F., and Bartelds, B. (2015). Right ventricular failure due to chronic pressure load: What have we learned in animal models since the NIH working group statement? Heart Fail. Rev. *20*: 475–491.

Bossone, E., D'Andrea, A., D'Alto, M., Citro, R., Argiento, P., Ferrara, F., et al. (2013). Echocardiography in pulmonary arterial hypertension: From diagnosis to prognosis. J. Am. Soc. Echocardiogr. *26*: 1–14.

Botney, M.D., Liptay, M.J., Kaiser, L.R., Cooper, J.D., Parks, W.C., and Mecham, R.P. (1993). Active collagen synthesis by pulmonary arteries in human primary pulmonary hypertension. Am. J. Pathol. *143*: 121–129.

Boulanger, C., and Luscher, T.F. (1990). Release of endothelin from the porcine aorta. Inhibition of endothelium-derived nitric oxide. J. Clin. Invest. *85*: 587–590.

Bowers, R., Cool, C., Murphy, R.C., Tuder, R.M., Hopken, M.W., Flores, S.C., et al. (2004). Oxidative Stress in Severe Pulmonary Hypertension. Am. J. Respir. Crit. Care Med. *169*: 764–769.

Brash, L., Barnes, G.D., Brewis, M.J., Church, A.C., Gibbs, S.J., Howard, L.S.G.E., et al. (2018). Short-Term Hemodynamic Effects of Apelin in Patients With Pulmonary Arterial Hypertension. JACC Basic to Transl. Sci. *3*: 176–186.

Breinholt, V.M., Mygind, P.H., Christoffersen, E.D., Zhang, Y., Ota, S., Will Charlton, R., et al. (2022). Phase 1 safety, tolerability, pharmacokinetics and pharmacodynamics results of a long-acting C-type natriuretic peptide prodrug, TransCon CNP. Br. J. Clin. Pharmacol.

Breinholt, V.M., Rasmussen, C.E., Mygind, P.H., Kjelgaard-Hansen, M., Faltinger, F., Bernhard, A., et al. (2019). Transcon CNP, a sustained-release C-type natriuretic peptide prodrug, a potentially safe and efficacious new therapeutic modality for the treatment of comorbidities associated with fibroblast growth factor receptor 3-related skeletal dysplasias. J. Pharmacol. Exp. Ther. *370*: 459–471.

Bristow, M.R., Ginsburg, R., and Harrison, D.C. (1982). Histamine and the human heart: The other receptor system. Am. J. Cardiol. *49*: 249–251.

Brittain, E., Penner, N.L., West, J., and Hemnes, A. (2013). Echocardiographic assessment of the right heart in mice. J. Vis. Exp.

Brittain, E.L., Niswender, K., Agrawal, V., Chen, X., Fan, R., Pugh, M.E., et al. (2020). Mechanistic phase II clinical trial of metformin in pulmonary arterial

hypertension. J. Am. Heart Assoc. *9*:.

Brown, J., Chen, Q., and Hong, G. (1997). An autocrine system for C-type natriuretic peptide within rat carotid neointima during arterial repair. Am. J. Physiol. - Hear. Circ. Physiol. *272*:.

Brown, J., and Zuo, Z. (1994). Receptor proteins and biological effects of C-type natriuretic peptides in the renal glomerulus of the rat. Am. J. Physiol. - Regul. Integr. Comp. Physiol. *266*:.

Brown, L.A., Nunez, D.J.R., and Wilkins, M.R. (1993). Differential regulation of natriuretic peptide receptor messenger RNAs during the development of cardiac hypertrophy in the rat. J. Clin. Invest. *92*: 2702–2712.

Brusq, J.M., Mayoux, E., Guigui, L., and Kirilovsky, J. (1999). Effects of C-type natriuretic peptide on rat cardiac contractility. Br. J. Pharmacol. *128*: 206–212.

Brutsaert, D.L. (2003). Cardiac endothelial-myocardial signaling: Its role in cardiac growth, contractile performance, and rhythmicity. Physiol. Rev. *83*: 59–115.

Bubb, K.J., Aubdool, A.A., Moyes, A.J., Lewis, S., Drayton, J.P., Tang, O., et al. (2019). Endothelial C-Type Natriuretic Peptide Is a Critical Regulator of Angiogenesis and Vascular Remodeling. Circulation *139*: 1612–1628.

Bubb, K.J., Trinder, S.L., Baliga, R.S., Patel, J., Clapp, L.H., MacAllister, R.J., et al. (2014). Inhibition of phosphodiesterase 2 augments cGMP and cAMP signaling to ameliorate pulmonary hypertension. Circulation *130*: 496–507.

Budas, G.R., Boehm, M., Kojonazarov, B., Viswanathan, G., Tian, X., Veeroju, S., et al. (2018). ASK1 inhibition halts disease progression in preclinical models of pulmonary arterial hypertension. Am. J. Respir. Crit. Care Med. *197*: 373–385.

Budhiraja, R., Tuder, R.M., and Hassoun, P.M. (2004). Endothelial Dysfunction in Pulmonary Hypertension. Circulation *109*: 159–165.

Bueltmann, M., Kong, X., Mertens, M., Yin, N., Yin, J., Liu, Z., et al. (2009). Inhaled milrinone attenuates experimental acute lung injury. Intensive Care Med. *35*: 171–178.

Buttgereit, J., Shanks, J., Li, D., Hao, G., Athwal, A., Langenickel, T.H., et al. (2016). C-type natriuretic peptide and natriuretic peptide receptor B signalling inhibits cardiac sympathetic neurotransmission and autonomic function. Cardiovasc. Res. *112*: 637–644.

Cahill, P.A., and Hassid, A. (1994). ANF-C-receptor-mediated inhibition of aortic smooth muscle cell proliferation and thymidine kinase activity. Am. J. Physiol. - Regul. Integr. Comp. Physiol. *266*: R194-203.

Campen, J.S.J.A. Van, Boer, K. De, Veerdonk, M.C. Van De, Bruggen, C.E.E. Van Der, Allaart, C.P., Raijmakers, P.G., et al. (2016). Bisoprolol in idiopathic pulmonary arterial hypertension: An explorative study. Eur. Respir. J. *48*: 787–796.

Campo, A., Mathai, S.C., Pavec, J. Le, Zaiman, A.L., Hummers, L.K., Boyce, D., et al. (2011). Outcomes of hospitalisation for right heart failure in pulmonary arterial hypertension. Eur. Respir. J. *38*: 359–367.

Caniffi, C., Cerniello, F.M., Gobetto, M.N., Sueiro, M.L., Costa, M.A., and Arranz, C. (2016). Vascular tone regulation induced by C-Type natriuretic peptide: Differences in endothelium-dependent and -independent mechanisms involved in normotensive and spontaneously hypertensive rats. PLoS One *11*: e0167817.

Caniffi, C., Elesgaray, R., Gironacci, M., Arranz, C., and Costa, M.Á. (2010). C-type natriuretic peptide effects on cardiovascular nitric oxide system in spontaneously hypertensive rats. Peptides *31*: 1309–1318.

Cannon, J.E., Su, L., Kiely, D.G., Page, K., Toshner, M., Swietlik, E., et al. (2016). Dynamic risk stratification of patient long-term outcome after pulmonary Endarterectomy: Results from the United Kingdom national cohort. Circulation *133*: 1761–1771.

Carpenter, D., Keller, L., Palacios, M., Rurka, J., Crizer, K., Pack, T., et al. (2019). Once Daily Oral Dosing of Rodatristat Ethyl (Rvt-1201) Achieves Reductions in Serotonin Biosynthesis Comparable To Those Associated With Reversal of Vascular Remodeling in Pah Animal Models. Chest *156*: A1175–A1176.

Carpenter, T.C., and Stenmark, K.R. (2001). Hypoxia decreases lung neprilysin

expression and increases pulmonary vascular leak. Am. J. Physiol. - Lung Cell. Mol. Physiol. *281*:.

Cassady, S., and Ramani, G. V. (2020). Right Heart Failure in Pulmonary Hypertension. Cardiol. Clin. *38*: 243–255.

Casserly, B., Mazer, J.M., Vang, A., Harrington, E.O., Klinger, J.R., Rounds, S., et al. (2011). C-type natriuretic peptide does not attenuate the development of pulmonary hypertension caused by hypoxia and VEGF receptor blockade. Life Sci. *89*: 460–466.

Celermajer, D.S., Dollery, C., Burch, M., and Deanfield, J.E. (1994). Role of endothelium in the maintenance of low pulmonary vascular tone in normal children. Circulation *89*: 2041–2044.

Chandra, S.M., Razavi, H., Kim, J., Agrawal, R., Kundu, R.K., Jesus Perez, V. De, et al. (2011). Disruption of the apelin-APJ system worsens hypoxia-induced pulmonary hypertension. Arterioscler. Thromb. Vasc. Biol. *31*: 814–820.

Charles, C.J., Espiner, E.A., Nicholls, M.G., Richards, A.M., Yandle, T.G., Protter, A., et al. (1996). Clearance receptors and endopeptidase 24.11: Equal role in natriuretic peptide metabolism in conscious sheep. Am. J. Physiol. - Regul. Integr. Comp. Physiol. *271*:.

Chelladurai, P., Seeger, W., and Pullamsetti, S.S. (2012). Matrix metalloproteinases and their inhibitors in pulmonary hypertension. Eur. Respir. J. *40*: 766–782.

Chemla, D., Lau, E.M.T., Papelier, Y., Attal, P., and Hervé, P. (2015). Pulmonary vascular resistance and compliance relationship in pulmonary hypertension. Eur. Respir. J. *46*: 1178–1189.

Cheng, H.W., Fisch, S., Cheng, S., Bauer, M., Ngoy, S., Qiu, Y., et al. (2014). Assessment of right ventricular structure and function in mouse model of pulmonary artery constriction by transthoracic echocardiography. J. Vis. Exp. e51041.

Christman, B.W., Mcpherson, C.D., Newman, J.H., King, G.A., Bernard, G.R.,

Groves, B.M., et al. (1992). An Imbalance between the Excretion of Thromboxane and Prostacyclin Metabolites in Pulmonary Hypertension. N. Engl. J. Med. *327*: 70–75.

Chun, H.J., and Yu, P.B. (2015). Elafin in Pulmonary Arterial Hypertension beyond Targeting Elastases. Am. J. Respir. Crit. Care Med. *191*: 1217–1219.

Chun, T.H., Itoh, H., Ogawa, Y., Tamura, N., Takaya, K., Igaki, T., et al. (1997). Shear stress augments expression of C-type natriuretic peptide and adrenomedullin. Hypertension *29*: 1296–1302.

Chusho, H., Tamura, N., Ogawa, Y., Yasoda, A., Suda, M., Miyazawa, T., et al. (2001). Dwarfism and early death in mice lacking C-type natriuretic peptide. Proc. Natl. Acad. Sci. U. S. A. *98*: 4016–4021.

Ciuclan, L., Bonneau, O., Hussey, M., Duggan, N., Holmes, A.M., Good, R., et al. (2011). A novel murine model of severe pulmonary arterial hypertension. Am. J. Respir. Crit. Care Med. *184*: 1171–1182.

Clapp, L.H., Finney, P., Turcato, S., Tran, S., Rubin, L.J., and Tinker, A. (2002). Differential effects of stable prostacyclin analogs on smooth muscle proliferation and cyclic AMP generation in human pulmonary artery. Am. J. Respir. Cell Mol. Biol. *26*: 194–201.

Cohen, D., Koh, G.Y., Nikonova, L.N., Porter, J.G., and Maack, T. (1996). Molecular determinants of the clearance function of type C receptors of natriuretic peptides. J. Biol. Chem. *271*: 9863–9869.

Condon, D.F., Agarwal, S., Chakraborty, A., Auer, N., Vazquez, R., Patel, H., et al. (2022). Novel Mechanisms Targeted by Drug Trials in Pulmonary Arterial Hypertension. Chest *161*: 1060–1072.

Conole, D., Myers, S.H., Mota, F., Hobbs, A.J., and Selwood, D.L. (2019). Biophysical screening methods for extracellular domain peptide receptors, application to natriuretic peptide receptor C ligands. Chem. Biol. Drug Des. *93*: 1011–1020.

Constantinides, C., Mean, R., and Janssen, B.J. (2011). Effects of isoflurane

anesthesia on the cardiovascular function of the C57BL/6 mouse. ILAR J. *52*: e21–e31.

Cool, C.D., Kuebler, W.M., Bogaard, H.J., Spiekerkoetter, E., Nicolls, M.R., and Voelkel, N.F. (2020). The hallmarks of severe pulmonary arterial hypertension: The cancer hypothesis-Ten years later. Am. J. Physiol. - Lung Cell. Mol. Physiol. *318*: L1115–L1130.

Cool, C.D., Stewart, J.S., Werahera, P., Miller, G.J., Williams, R.L., Voelkel, N.F., et al. (1999). Three-dimensional reconstruction of pulmonary arteries in plexiform pulmonary hypertension using cell-specific markers: Evidence for a dynamic and heterogeneous process of pulmonary endothelial cell growth. Am. J. Pathol. *155*: 411–419.

Corkish, M.E., Devine, L.T., Clarke, M.M., Murray, B.P., and Rose-Jones, L.J. (2019). Rates of hospitalization associated with the use of aldosterone receptor antagonists in patients with pulmonary arterial hypertension. Pulm. Circ. *9*:.

Costello-Boerrigter, L.C., Schirger, J.A., Miller, W.L., Boerrigter, G., Chen, H.H., Kempf, R., et al. (2011). Cenderitide (CD-NP), a novel peptide designed to activate both guanylyl cyclase B and A, activates the second messenger cGMP, suppresses aldosterone, and preserves GFR without reducing blood pressure in a proof-of-concept study in patients with chronic he. BMC Pharmacol. *11*:.

Cotroneo, E., Ashek, A., Wang, L., Wharton, J., Dubois, O., Bozorgi, S., et al. (2015). Iron homeostasis and pulmonary hypertension: Iron deficiency leads to pulmonary vascular remodeling in the rat. Circ. Res. *116*: 1680–1690.

Cracowski, J.L., Cracowski, C., Bessard, G., Pepin, J.L., Bessard, J., Schwebel, C., et al. (2001). Increased lipid peroxidation in patients with pulmonary hypertension. Am. J. Respir. Crit. Care Med. *164*: 1038–1042.

Croix, C.M.S., and Steinhorn, R.H. (2016). New thoughts about the origin of plexiform lesions. Am. J. Respir. Crit. Care Med. *193*: 484–485.

Crosswhite, P., and Sun, Z. (2010). Nitric oxide, oxidative stress and inflammation in pulmonary arterial hypertension. J. Hypertens. *28*: 201–212.

D'Alto, M., Badagliacca, R., Argiento, P., Romeo, E., Farro, A., Papa, S., et al. (2020). Risk Reduction and Right Heart Reverse Remodeling by Upfront Triple Combination Therapy in Pulmonary Arterial Hypertension. Chest *157*: 376–383.

D'Souza, S.P., Davis, M., and Baxter, G.F. (2004). Autocrine and paracrine actions of natriuretic peptides in the heart. Pharmacol. Ther. *101*: 113–129.

Dahal, B.K., Kosanovic, D., Kaulen, C., Cornitescu, T., Savai, R., Hoffmann, J., et al. (2011). Involvement of mast cells in monocrotaline-induced pulmonary hypertension in rats. Respir. Res. *12*:.

Dao, H.H., Bouvet, C., Moreau, S., Beaucage, P., Larivière, R., Servant, M.J., et al. (2006). Endothelin is a dose-dependent trophic factor and a mitogen in small arteries in vivo. Cardiovasc. Res. *71*: 61–68.

Dasgupta, A., Bowman, L., D'Arsigny, C.L., and Archer, S.L. (2015). Soluble guanylate cyclase: A new therapeutic target for pulmonary arterial hypertension and chronic thromboembolic pulmonary hypertension. Clin. Pharmacol. Ther. *97*: 88–102.

Davie, N., Haleen, S.J., Upton, P.D., Polak, J.M., Yacoub, M.H., Morrell, N.W., et al. (2002). ETA and ETB receptors modulate the proliferation of human pulmonary artery smooth muscle cells. Am. J. Respir. Crit. Care Med. *165*: 398–405.

Dean, A., Nilsen, M., Loughlin, L., Salt, I.P., and MacLean, M.R. (2016). Metformin Reverses Development of Pulmonary Hypertension via Aromatase Inhibition. Hypertension *68*: 446–454.

Delcroix, M., Lang, I., Pepke-Zaba, J., Jansa, P., D'Armini, A.M., Snijder, R., et al. (2016). Long-Term Outcome of Patients with Chronic Thromboembolic Pulmonary Hypertension : Results from an International Prospective Registry. Circulation *133*: 859–871.

Denver, N., Homer, N.Z.M., Andrew, R., Harvey, K.Y., Morrell, N., Austin, E.D., et al. (2020). Estrogen metabolites in a small cohort of patients with idiopathic pulmonary arterial hypertension. Pulm. Circ. *10*:.

Dickey, D.M., and Potter, L.R. (2011). Dendroaspis natriuretic peptide and the

designer natriuretic peptide, CD-NP, are resistant to proteolytic inactivation. J. Mol. Cell. Cardiol. *51*: 67–71.

Diebold, I., Hennigs, J.K., Miyagawa, K., Li, C.G., Nickel, N.P., Kaschwich, M., et al. (2015). BMPR2 preserves mitochondrial function and DNA during reoxygenation to promote endothelial cell survival and reverse pulmonary hypertension. Cell Metab. *21*: 596–608.

Dignam, J.P., Scott, T.E., Kemp-Harper, B.K., and Hobbs, A.J. (2022). Animal models of pulmonary hypertension: Getting to the heart of the problem. Br. J. Pharmacol. *179*: 811–837.

Dimitroulas, T., Giannakoulas, G., Sfetsios, T., Karvounis, H., Dimitroula, H., Koliakos, G., et al. (2008). Asymmetrical dimethylarginine in systemic sclerosis-related pulmonary arterial hypertension. Rheumatology *47*: 1682–1685.

Docherty, C.K., Nilsen, M., and MacLean, M.R. (2019). Influence of 2-Methoxyestradiol and Sex on Hypoxia-Induced Pulmonary Hypertension and Hypoxia-Inducible Factor-1-α. J. Am. Heart Assoc. *8*:.

Doi, K., Ikeda, T., Itoh, H., Ueyama, K., Hosoda, K., Ogawa, Y., et al. (2001). C-type natriuretic peptide induces redifferentiation of vascular smooth muscle cells with accelerated reendothelialization. Arterioscler. Thromb. Vasc. Biol. *21*: 930–936.

Doi, K., Itoh, H., Komatsu, Y., Igaki, T., Chun, T.H., Takaya, K., et al. (1996). Vascular endothelial growth factor suppresses C-type natriuretic peptide secretion. Hypertension *27*: 811–815.

Donati, B., Lorenzini, E., and Ciarrocchi, A. (2018). BRD4 and Cancer: Going beyond transcriptional regulation. Mol. Cancer *17*:.

Dorfmüller, P., Günther, S., Ghigna, M.R., Montpréville, V.T. De, Boulate, D., Paul, J.F., et al. (2014). Microvascular disease in chronic thromboembolic pulmonary hypertension: A role for pulmonary veins and systemic vasculature. Eur. Respir. J. *44*: 1275–1288.

Dorfmüller, P., Humbert, M., Perros, F., Sanchez, O., Simonneau, G., Müller, K.M.,

et al. (2007). Fibrous remodeling of the pulmonary venous system in pulmonary arterial hypertension associated with connective tissue diseases. Hum. Pathol. *38*: 893–902.

Dorfmüller, P., Zarka, V., Durand-Gasselin, I., Monti, G., Balabanian, K., Garcia, G., et al. (2002). Chemokine RANTES in severe pulmonary arterial hypertension. Am. J. Respir. Crit. Care Med. *165*: 534–539.

Douwes, J.M., Roofthooft, M.T.R., Bartelds, B., Talsma, M.D., Hillege, H.L., and Berger, R.M.F. (2013). Pulsatile haemodynamic parameters are predictors of survival in paediatric pulmonary arterial hypertension. Int. J. Cardiol. *168*: 1370–1377.

Drewett, J.G., Fendly, B.M., Garbers, D.L., and Lowe, D.G. (1995). Natriuretic peptide receptor-B (guanylyl cyclase-B) mediates C-type natriuretic peptide relaxation of precontracted rat aorta. J. Biol. Chem. *270*: 4668–4674.

Duluc, L., Ahmetaj-Shala, B., Mitchell, J., Abdul-Salam, V.B., Mahomed, A.S., Aldabbous, L., et al. (2017). Tipifarnib prevents development of hypoxia-induced pulmonary hypertension. Cardiovasc. Res. *113*: 276–287.

Dumas de La Roque, E., Savineau, J.P., Metivier, A.C., Billes, M.A., Kraemer, J.P., Doutreleau, S., et al. (2012). Dehydroepiandrosterone (DHEA) improves pulmonary hypertension in chronic obstructive pulmonary disease (COPD): A pilot study. Ann. Endocrinol. (Paris). *73*: 20–25.

Dumitrascu, R., Koebrich, S., Dony, E., Weissmann, N., Savai, R., Pullamsetti, S.S., et al. (2008). Characterization of a murine model of monocrotaline pyrrole-induced acute lung injury. BMC Pulm. Med. *8*: 25.

Dunham-Snary, K.J., Wu, D., Sykes, E.A., Thakrar, A., Parlow, L.R.G., Mewburn, J.D., et al. (2017). Hypoxic Pulmonary Vasoconstriction: From Molecular Mechanisms to Medicine. Chest *151*: 181–192.

Eddahibi, S., and Adnot, S. (2001). Anorexigen-induced pulmonary hypertension and the serotonin (5-HT) hypothesis: Lessons for the future in pathogenesis. Respir. Res. *3*:.

Edfors, F., Danielsson, F., Hallström, B.M., Käll, L., Lundberg, E., Pontén, F., et al. (2016). Gene-specific correlation of RNA and protein levels in human cells and tissues . Mol. Syst. Biol. *12*: 883.

Edvinsson, M.L., Ahnstedt, H., Edvinsson, L., and Andersson, S.E. (2016). Characterization of Relaxant Responses to Natriuretic Peptides in the Human Microcirculation In Vitro and In Vivo. Microcirculation *23*: 438–446.

Edwards, B.S., Zimmerman, R.S., Schwab, T.R., Heublein, D.M., and Burnett, J.C. (1988). Atrial stretch, not pressure, is the principal determinant controlling the acute release of atrial natriuretic factor. Circ. Res. *62*: 191–195.

Egemnazarov, B., Schmidt, A., Crnkovic, S., Sydykov, A., Nagy, B.M., Kovacs, G., et al. (2015). Pressure Overload Creates Right Ventricular Diastolic Dysfunction in a Mouse Model: Assessment by Echocardiography. J. Am. Soc. Echocardiogr. *28*: 828–843.

Egom, E.E., Feridooni, T., Pharithi, R.B., Khan, B., Shiwani, H.A., Maher, V., et al. (2017a). A natriuretic peptides clearance receptor's agonist reduces pulmonary artery pressures and enhances cardiac performance in preclinical models: New hope for patients with pulmonary hypertension due to left ventricular heart failure. Biomed. Pharmacother. *93*: 1144–1150.

Egom, E.E., Vella, K., Hua, R., Jansen, H.J., Moghtadaei, M., Polina, I., et al. (2015). Impaired sinoatrial node function and increased susceptibility to atrial fibrillation in mice lacking natriuretic peptide receptor C. J. Physiol. *593*: 1127–1146.

Egom, E.E.A., Feridooni, T., Pharithi, R.B., Khan, B., Shiwani, H.A., Maher, V., et al. (2017b). New insights and new hope for pulmonary arterial hypertension: Natriuretic peptides clearance receptor as a novel therapeutic target for a complex disease. Int. J. Physiol. Pathophysiol. Pharmacol. *9*: 112–118.

Ehret, G.B., Munroe, P.B., Rice, K.M., Bochud, M., Johnson, A.D., Chasman, D.I., et al. (2011). Genetic variants in novel pathways influence blood pressure and cardiovascular disease risk. Nature *478*: 103–109.

Escribano-Subias, P., Blanco, I., López-Meseguer, M., Lopez-Guarch, C.J., Roman, A., Morales, P., et al. (2012). Survival in pulmonary hypertension in Spain: Insights from the Spanish registry. Eur. Respir. J. *40*: 596–603.

Estrada, K.D., and Chesler, N.C. (2009). Collagen-related gene and protein expression changes in the lung in response to chronic hypoxia. Biomech. Model. Mechanobiol. *8*: 263–272.

Fadel, E., Mercier, O., Mussot, S., Leroy-Ladurie, F., Cerrina, J., Chapelier, A., et al. (2010). Long-term outcome of double-lung and heart-lung transplantation for pulmonary hypertension: A comparative retrospective study of 219 patients. Eur. J. Cardio-Thoracic Surg. *38*: 277–284.

Falcão-Pires, I., Gonçalves, N., Henriques-Coelho, T., Moreira-Gonçalves, D., Roncon-Albuquerque, R., and Leite-Moreira, A.F. (2009). Apelin decreases myocardial injury and improves right ventricular function in monocrotaline-induced pulmonary hypertension. Am. J. Physiol. - Hear. Circ. Physiol. *296*:.

Falcetti, E., Hall, S.M., Phillips, P.G., Patel, J., Morrell, N.W., Haworth, S.G., et al. (2010). Smooth muscle proliferation and role of the prostacyclin (IP) receptor in idiopathic pulmonary arterial hypertension. Am. J. Respir. Crit. Care Med. *182*: 1161–1170.

Fang, Y.H., Piao, L., Hong, Z., Toth, P.T., Marsboom, G., Bache-Wiig, P., et al. (2012). Therapeutic inhibition of fatty acid oxidation in right ventricular hypertrophy: Exploiting Randle's cycle. J. Mol. Med. *90*: 31–43.

Farha, S., Saygin, D., Park, M.M., Cheong, H.I., Asosingh, K., Comhair, S.A., et al. (2017). Pulmonary arterial hypertension treatment with carvedilol for heart failure: a randomized controlled trial. JCI Insight *2*:.

Farha, S., Sharp, J., Asosingh, K., Park, M., Comhair, S.A.A., Wilson Tang, W.H., et al. (2012). Mast cell number, phenotype, and function in human pulmonary arterial hypertension. Pulm. Circ. *2*: 220–228.

Fayyaz, A.U., Edwards, W.D., Maleszewski, J.J., Konik, E.A., DuBrock, H.M., Borlaug, B.A., et al. (2018). Global pulmonary vascular remodeling in pulmonary

hypertension associated with heart failure and preserved or reduced ejection fraction. Circulation *137*: 1796–1810.

Feen, D.E. Van Der, Berger, R.M.F., and Bartelds, B. (2019a). Converging paths of pulmonary arterial hypertension and cellular senescence. Am. J. Respir. Cell Mol. Biol. *61*: 11–20.

Feen, D.E. Van Der, Kurakula, K., Tremblay, E., Boucherat, O., Bossers, G.P.L., Szulcek, R., et al. (2019b). Multicenter preclinical validation of BET inhibition for the treatment of pulmonary arterial hypertension. Am. J. Respir. Crit. Care Med. *200*: 910–920.

Finch, K.T., Stratton, E.A., and Farber, H.W. (2016). Ranolazine for the treatment of pulmonary hypertension associated with heart failure with preserved ejection fraction: A pilot study. J. Hear. Lung Transplant. *35*: 1370–1373.

Folino, A., Montarolo, P.G., Samaja, M., and Rastaldo, R. (2015). Effects of apelin on the cardiovascular system. Heart Fail. Rev. *20*: 505–518.

Forfia, P.R., Fisher, M.R., Mathai, S.C., Housten-Harris, T., Hemnes, A.R., Borlaug, B.A., et al. (2006). Tricuspid annular displacement predicts survival in pulmonary hypertension. Am. J. Respir. Crit. Care Med. *174*: 1034–1041.

Frantz, R.P., Benza, R.L., Channick, R.N., Chin, K., Howard, L.S., McLaughlin, V. V., et al. (2021). TORREY, a Phase 2 study to evaluate the efficacy and safety of inhaled seralutinib for the treatment of pulmonary arterial hypertension. Pulm. Circ. *11*:.

Frid, M.G., Brunetti, J.A., Burke, D.L., Carpenter, T.C., Davie, N.J., Reeves, J.T., et al. (2006). Hypoxia-induced pulmonary vascular remodeling requires recruitment of circulating mesenchymal precursors of a monocyte/macrophage lineage. Am. J. Pathol. *168*: 659–669.

Friedberg, M.K., and Redington, A.N. (2014). Right versus left ventricular failure: Differences, similarities, and interactions. Circulation *129*: 1033–1044.

Fritts, H.W., Harris, P., Clauss, R.H., Odell, J.E., and Cournand, A. (1958). The effect of acetylcholine on the human pulmonary circulation under normal and

hypoxic conditions. J. Clin. Invest. *37*: 99–110.

Frump, A.L., Albrecht, M., Yakubov, B., Breuils-Bonnet, S., Nadeau, V., Tremblay, E., et al. (2021). 17β-estradiol and estrogen receptor α protect right ventricular function in pulmonary hypertension via BMPR2 and apelin. J. Clin. Invest. *131*:.

Fu, S., Ping, P., Wang, F., and Luo, L. (2018). Synthesis, secretion, function, metabolism and application of natriuretic peptides in heart failure. J. Biol. Eng. *12*:.

Fukumoto, Y., Yamada, N., Matsubara, H., Mizoguchi, M., Uchino, K., Yao, A., et al. (2013). Double-blind, placebo-controlled clinical trial with a rho-kinase inhibitor in pulmonary arterial hypertension; a pilot efficacy trial. Circ. J. *77*: 2619–2625.

Fukuroda, T., Fujikawa, T., Ozaki, S., Ishikawa, K., Yano, M., and Nishikibe, M. (1994). Clearance of circulating endothelin-1 by etb receptors in rats. Biochem. Biophys. Res. Commun. *199*: 1461–1465.

Furuya, M., Aisaka, K., Miyazaki, T., Honbou, N., Kawashima, K., Ohno, T., et al. (1993). C-type natriuretic peptide inhibits intimal thickening after vascular injury. Biochem. Biophys. Res. Commun. *193*: 248–253.

Furuya, M., Yoshida, M., Hayashi, Y., Ohnuma, N., Minamino, N., Kangawa, K., et al. (1991). C-Type natriuretic peptide is a growth inhibitor of rat vascular smooth muscle cells. Biochem. Biophys. Res. Commun. *177*: 927–931.

Galambos, C., Sims-Lucas, S., Abman, S.H., and Cool, C.D. (2016). Intrapulmonary bronchopulmonary anastomoses and plexiform lesions in idiopathic pulmonary arterial hypertension. Am. J. Respir. Crit. Care Med. *193*: 574–576.

Galiè, N., Channick, R.N., Frantz, R.P., Grünig, E., Jing, Z.C., Moiseeva, O., et al. (2019). Risk stratification and medical therapy of pulmonary arterial hypertension. Eur. Respir. J. *53*:.

Galiè, N., Humbert, M., Vachiery, J.L., Gibbs, S., Lang, I., Torbicki, A., et al. (2016). 2015 ESC/ERS Guidelines for the diagnosis and treatment of pulmonary hypertension. Eur. Heart J. *37*: 67–119.

Galié, N., Manes, A., and Branzi, A. (2004). The endothelin system in pulmonary

arterial hypertension. Cardiovasc. Res. *61*: 227–237.

Gall, H., Felix, J.F., Schneck, F.K., Milger, K., Sommer, N., Voswinckel, R., et al. (2017). The Giessen Pulmonary Hypertension Registry: Survival in pulmonary hypertension subgroups. J. Hear. Lung Transplant. *36*: 957–967.

Gambaryan, N., Perros, F., Montani, D., Cohen-Kaminsky, S., Mazmanian, M., Renaud, J.F., et al. (2011). Targeting of c-kit+ haematopoietic progenitor cells prevents hypoxic pulmonary hypertension. Eur. Respir. J. *37*: 1392–1399.

Gan, C.T.J., Lankhaar, J.W., Marcus, J.T., Westerhof, N., Marques, K.M., Bronzwaer, J.G.F., et al. (2006). Impaired left ventricular filling due to right-to-left ventricular interaction in patients with pulmonary arterial hypertension. Am. J. Physiol. - Hear. Circ. Physiol. *290*:.

Garbers, D.L., Koesling, D., and Schultz, G. (1994). Guanylyl cyclase receptors. Mol. Biol. Cell *5*: 1–5.

Garcha, R.S., and Hughes, A.D. (2006). CNP, but not ANP or BNP, relax human isolated subcutaneous resistance arteries by an action involving cyclic GMP and BKCa channels. JRAAS - J. Renin-Angiotensin-Aldosterone Syst. *7*: 87–91.

Gardner, D.G., Chen, S., Glenn, D.J., and Grigsby, C.L. (2007). Molecular biology of the natriuretic peptide system: Implications for physiology and hypertension. Hypertension *49*: 419–426.

Gaynor, S.L., Maniar, H.S., Bloch, J.B., Steendijk, P., and Moon, M.R. (2005). Right atrial and ventricular adaptation to chronic right ventricular pressure overload. Circulation *112*: I212-8.

Geiger, R., Berger, R.M.F., Hess, J., Bogers, A.J.J.C., Sharma, H.S., and Mooi, W.J. (2000). Enhanced expression of vascular endothelial growth factor in pulmonary plexogenic arteriopathy due to congenital heart disease. J. Pathol. *191*: 202–207.

Ghigna, M.R., Guignabert, C., Montani, D., Girerd, B., Jaïs, X., Savale, L., et al. (2016). BMPR2 mutation status influences bronchial vascular changes in pulmonary arterial hypertension. Eur. Respir. J. *48*: 1668–1681.

Ghio, S., Fortuni, F., Capettini, A.C., Scelsi, L., Greco, A., Vullo, E., et al. (2021). Iron deficiency in pulmonary arterial hypertension: prevalence and potential usefulness of oral supplementation. Acta Cardiol. *76*: 162–167.

Ghio, S., Schirinzi, S., and Pica, S. (2015). Pulmonary arterial compliance: How and why should we measure it? Glob. Cardiol. Sci. Pract. *2015*: 58.

Ghofrani, H.A., Al-Hiti, H., Vonk-Noordegraaf, A., Behr, J., Neurohr, C., Jansa, P., et al. (2012). Proof-Of-Concept Study To Investigate The Efficacy, Hemodynamics And Tolerability Of Terguride Vs. Placebo In Subjects With Pulmonary Arterial Hypertension: Results Of A Double Blind, Randomised, Prospective Phase IIa Study. A2496–A2496.

Ghofrani, H.A., D'Armini, A.M., Grimminger, F., Hoeper, M.M., Jansa, P., Kim, N.H., et al. (2013). Riociguat for the treatment of chronic thromboembolic pulmonary hypertension. N. Engl. J. Med. *369*: 319–329.

Giaid, A., and Saleh, D. (1995). Reduced expression of endothelial nitric oxide synthase in the lungs of patients with pulmonary hypertension. N. Engl. J. Med. *333*: 214–221.

Giaid, A., Yanagisawa, M., Langleben, D., Michel, R.P., Levy, R., Shennib, H., et al. (1993). Expression of Endothelin-1 in the Lungs of Patients with Pulmonary Hypertension. N. Engl. J. Med. *328*: 1732–1739.

Girgis, R.E., Champion, H.C., Diette, G.B., Johns, R.A., Permutt, S., and Sylvester, J.T. (2005). Decreased exhaled nitric oxide in pulmonary arterial hypertension: Response to Bosentan therapy. Am. J. Respir. Crit. Care Med. *172*: 352–357.

Gkaliagkousi, E., and Ferro, A. (2011). Nitric oxide signalling in the regulation of cardiovascular and platelet function. Front. Biosci. *16*: 1873–1897.

Goldenberg, N.M., and Kuebler, W.M. (2015). Endothelial cell regulation of pulmonary vascular tone, inflammation, and coagulation. Compr. Physiol. *5*: 531–559.

Gomberg-Maitland, M., Schilz, R., Mediratta, A., Addetia, K., Coslet, S., Thomeas, V., et al. (2015). Phase i safety study of ranolazine in pulmonary arterial

hypertension. Pulm. Circ. *5*: 691–700.

Gomez-Arroyo, J., Saleem, S.J., Mizuno, S., Syed, A.A., Bogaard, H.J., Abbate, A., et al. (2012). A brief overview of mouse models of pulmonary arterial hypertension: Problems and prospects. Am. J. Physiol. - Lung Cell. Mol. Physiol. *302*: L977-91.

Gomez-Puerto, M.C., Iyengar, P.V., García de Vinuesa, A., Dijke, P. ten, and Sanchez-Duffhues, G. (2019). Bone morphogenetic protein receptor signal transduction in human disease. J. Pathol. *247*: 9–20.

Goncharov, D.A., Goncharova, E.A., Tofovic, S.P., Hu, J., Baust, J.J., Pena, A.Z., et al. (2018). Metformin therapy for pulmonary hypertension associated with heart failure with preserved ejection fraction versus pulmonary arterial hypertension. Am. J. Respir. Crit. Care Med. *198*: 681–684.

Goncharov, D.A., Kudryashova, T. V., Ziai, H., Ihida-Stansbury, K., Delisser, H., Krymskaya, V.P., et al. (2014). Mammalian target of rapamycin complex 2 (mTORC2) coordinates pulmonary artery smooth muscle cell metabolism, proliferation, and survival in pulmonary arterial hypertension. Circulation *129*: 864–874.

Gong, W., Yan, M., Chen, J., Chaugai, S., Chen, C., and Wang, D. (2014). Chronic inhibition of cyclic guanosine monophosphate-specific phosphodiesterase 5 prevented cardiac fibrosis through inhibition of transforming growth factor β-induced Smad signaling. Front. Med. *8*: 445–455.

Gorenflo, M., Zheng, C., Werle, E., Fiehn, W., and Ulmer, H.E. (2001). Plasma levels of asymmetrical dimethyl-L-arginine in patients with congenital heart disease and pulmonary hypertension. J. Cardiovasc. Pharmacol. *37*: 489–492.

Goto, J., Ishikawa, K., Kawamura, K., Watanabe, Y., Matumoto, H., Sugawara, D., et al. (2002). Heme oxygenase-1 reduces murine monocrotaline-induced pulmonary inflammatory responses and resultant right ventricular overload. Antioxidants Redox Signal. *4*: 563–568.

Goudie, A.R., Lipworth, B.J., Hopkinson, P.J., Wei, L., and Struthers, A.D. (2014).

Tadalafil in patients with chronic obstructive pulmonary disease: A randomised, double-blind, parallel-group, placebo-controlled trial. Lancet Respir. Med. *2*: 293–300.

Gräf, S., Haimel, M., Bleda, M., Hadinnapola, C., Southgate, L., Li, W., et al. (2018). Identification of rare sequence variation underlying heritable pulmonary arterial hypertension. Nat. Commun. *9*: 1416.

Greenbaum, D., Colangelo, C., Williams, K., and Gerstein, M. (2003). Comparing protein abundance and mRNA expression levels on a genomic scale. Genome Biol. *4*:.

Grinnan, D., Trankle, C., Andruska, A., Bloom, B., and Spiekerkoetter, E. (2019). Drug repositioning in pulmonary arterial hypertension: challenges and opportunities. Pulm. Circ. *9*:.

Groeneveldt, J.A., Man, F.S. De, and Westerhof, B.E. (2019). The right treatment for the right ventricle. Curr. Opin. Pulm. Med. *25*: 410–417.

Guarini, G., Huqi, A., Morrone, D., Capozza, P.F.G., and Marzilli, M. (2018). Trimetazidine and other metabolic modifiers. Eur. Cardiol. Rev. *13*: 104–111.

Guihaire, J., Bogaard, H., Flécher, E., Noly, P.E., Mercier, O., Haddad, F., et al. (2013). Experimental models of right heart failure: A window for translational research in pulmonary hypertension. Semin. Respir. Crit. Care Med. *34*: 689–699.

Guo, Y., Liu, X., Zhang, Y., Qiu, H., Ouyang, F., and He, Y. (2020). 3-Bromopyruvate ameliorates pulmonary arterial hypertension by improving mitochondrial metabolism. Life Sci. *256*:.

Gupta, M.P. (2007). Factors controlling cardiac myosin-isoform shift during hypertrophy and heart failure. J. Mol. Cell. Cardiol. *43*: 388–403.

Hamada, H., Terai, M., Kimura, H., Hirano, K., Oana, S., and Niimi, H. (1999). Increased expression of mast cell chymase in the lungs of patients with congenital heart disease associated with early pulmonary vascular disease. Am. J. Respir. Crit. Care Med. *160*: 1303–1308.

Hampl, V., Bíbová, J., Povýšiloá, V., and Herget, J. (2003).

Dehydroepiandrosterone sulphate reduces chronic hypoxic pulmonary hypertension in rats. Eur. Respir. J. *21*: 862–865.

Han, Y., Forfia, P.R., Vaidya, A., Mazurek, J.A., Park, M.H., Ramani, G., et al. (2018). Rationale and design of the ranolazine PH–RV study: a multicentred randomised and placebo-controlled study of ranolazine to improve RV function in patients with non-group 2 pulmonary hypertension. Open Hear. *5*: e000736.

Hardziyenka, M., Campian, M.E., Rianne de Bruin-Bon, H.A.C.M., Michel, M.C., and Tan, H.L. (2006). Sequence of Echocardiographic Changes During Development of Right Ventricular Failure in Rat. J. Am. Soc. Echocardiogr. *19*: 1272–1279.

Hashimoto, Y., Nakao, K., Hama, N., Imura, H., Mori, S., Yamaguchi, M., et al. (1994). Clearance Mechanisms of Atrial and Brain Natriuretic Peptides in Rats. Pharm. Res. An Off. J. Am. Assoc. Pharm. Sci. *11*: 60–64.

Hatano, S., and Strasser, T. (1975). Primary pulmonary hypertension. Report on a WHO meeting. Who,Geneva *29*: 371.

Hawwa, N., and Menon, V. (2013). Ranolazine: Clinical applications and therapeutic basis. Am. J. Cardiovasc. Drugs *13*: 5–16.

Hayakawa, R., Hayakawa, T., Takeda, K., and Ichijo, H. (2012). Therapeutic targets in the ASK1-dependent stress signaling pathways. Proc. Japan Acad. Ser. B Phys. Biol. Sci. *88*: 434–453.

He, H., Giordano, F.J., Hilal-Dandan, R., Choi, D.J., Rockman, H.A., McDonough, P.M., et al. (1997). Overexpression of the rat sarcoplasmic reticulum Ca2+ ATPase gene in the heart of transgenic mice accelerates calcium transients and cardiac relaxation. J. Clin. Invest. *100*: 380–389.

He, X. lin, Dukkipati, A., and Garcia, K.C. (2006). Structural Determinants of Natriuretic Peptide Receptor Specificity and Degeneracy. J. Mol. Biol. *361*: 698–714.

Heath, D., and Yacoub, M. (1991). Lung mast cells in plexogenic pulmonary arteriopathy. J. Clin. Pathol. *44*: 1003–1006.

Hemnes, A.R., Brittain, E.L., Trammell, A.W., Fessel, J.P., Austin, E.D., Penner, N., et al. (2014). Evidence for right ventricular lipotoxicity in heritable pulmonary arterial hypertension. Am. J. Respir. Crit. Care Med. *189*: 325–334.

Hemnes, A.R., Luther, J.M., Rhodes, C.J., Burgess, J.P., Carlson, J., Fan, R., et al. (2019). Human PAH is characterized by a pattern of lipid-related insulin resistance. JCI Insight *4*:.

Hemnes, A.R., Rathinasabapathy, A., Austin, E.A., Brittain, E.L., Carrier, E.J., Chen, X., et al. (2018). A potential therapeutic role for angiotensin-converting enzyme 2 in human pulmonary arterial hypertension. Eur. Respir. J. *51*:.

Hemnes, A.R., Zaiman, A., and Champion, H.C. (2008). PDE5A inhibition attenuates bleomycin-induced pulmonary fibrosis and pulmonary hypertension through inhibition of ROS generation and RhoA/Rho kinase activation. Am. J. Physiol. - Lung Cell. Mol. Physiol. *294*:.

Henning, R.J., and Sawmiller, D.R. (2001). Vasoactive intestinal peptide: Cardiovascular effects. Cardiovasc. Res. *49*: 27–37.

Hirata, M., Chang, C.H., and Murad, F. (1989). Stimulatory effects of atrial natriuretic factor on phosphoinositide hydrolysis in cultured bovine aortic smooth muscle cells. BBA - Mol. Cell Res. *1010*: 346–351.

Hirata, Y., Emori, T., Eguchi, S., Kanno, K., Imai, T., Ohta, K., et al. (1993). Endothelin receptor subtype B mediates synthesis of nitric oxide by cultured bovine endothelial cells. J. Clin. Invest. *91*: 1367–1373.

Hiress, M. Le, Tu, L., Ricard, N., Phan, C., Thuillet, R., Fadel, E., et al. (2015). Proinflammatory signature of the dysfunctional endothelium in pulmonary hypertension role of the macrophage migration inhibitory factor/CD74 complex. Am. J. Respir. Crit. Care Med. *192*: 983–997.

Hirose, M., Furukawa, Y., Kurogouchi, F., Nakajima, K., Miyashita, Y., and Chiba, S. (1998). C-type natriuretic peptide increases myocardial contractility and sinus rate mediated by guanylyl cyclase-linked natriuretic peptide receptors in isolated, blood-perfused dog heart preparations. J. Pharmacol. Exp. Ther. *286*: 70–76.

Hobbs, A., Foster, P., Prescott, C., Scotland, R., and Ahluwalia, A. (2004). Natriuretic peptide receptor-C regulates coronary blood flow and prevents myocardial ischemia/reperfusion injury: Novel cardioprotective role for endothelium-derived C-type natriuretic peptide. Circulation *110*: 1231–1235.

Hobbs, A.J., Moyes, A.J., Baliga, R.S., Ghedia, D., Ochiel, R., Sylvestre, Y., et al. (2019). Neprilysin inhibition for pulmonary arterial hypertension: a randomized, double-blind, placebo-controlled, proof-of-concept trial. Br. J. Pharmacol.

Hoeper, M.M., Apitz, C., Grünig, E., Halank, M., Ewert, R., Kaemmerer, H., et al. (2018). Targeted therapy of pulmonary arterial hypertension: Updated recommendations from the Cologne Consensus Conference 2018. Int. J. Cardiol. *272*: 37–45.

Hoeper, M.M., Barst, R.J., Bourge, R.C., Feldman, J., Frost, A.E., Galié, N., et al. (2013a). Imatinib mesylate as add-on therapy for pulmonary arterial hypertension: Results of the randomized IMPRES study. Circulation *127*: 1128–1138.

Hoeper, M.M., Bogaard, H.J., Condliffe, R., Frantz, R., Khanna, D., Kurzyna, M., et al. (2013b). Definitions and diagnosis of pulmonary hypertension. J. Am. Coll. Cardiol. *62*: D42-50.

Hoeper, M.M., Humbert, M., Souza, R., Idrees, M., Kawut, S.M., Sliwa-Hahnle, K., et al. (2016a). A global view of pulmonary hypertension. Lancet Respir. Med. *4*: 306–322.

Hoeper, M.M., McLaughlin, V. V., Dalaan, A.M.A., Satoh, T., and Galiè, N. (2016b). Treatment of pulmonary hypertension. Lancet Respir. Med. *4*: 323–336.

Hoffmann, J., Marsh, L.M., Pieper, M., Stacher, E., Ghanim, B., Kovacs, G., et al. (2015a). Biomarkers in lung diseases: From pathogenesis to prediction to new therapiescompartment-specific expression of collagens and their processing enzymes in intrapulmonary arteries of IPAH patients. Am. J. Physiol. - Lung Cell. Mol. Physiol. *308*: L1002–L1013.

Hoffmann, J., Marsh, L.M., Pieper, M., Stacher, E., Ghanim, B., Kovacs, G., et al. (2015b). Compartment-specific expression of collagens and their processing

enzymes in intrapulmonary arteries of IPAH patients. Am. J. Physiol. Cell. Mol. Physiol. *308*: L1002–L1013.

Hogan, B.L.M. (1996). Bone morphogenetic proteins: Multifunctional regulators of vertebrate development. Genes Dev. *10*: 1580–1594.

Holmström, K.M., Baird, L., Zhang, Y., Hargreaves, I., Chalasani, A., Land, J.M., et al. (2013). Nrf2 impacts cellular bioenergetics by controlling substrate availability for mitochondrial respiration. Biol. Open *2*: 761–770.

Hood, K.Y., Montezano, A.C., Harvey, A.P., Nilsen, M., Maclean, M.R., and Touyz, R.M. (2016). Nicotinamide adenine dinucleotide phosphate oxidase-mediated redox signaling and vascular remodeling by 16α-hydroxyestrone in human pulmonary artery cells. Hypertension *68*: 796–808.

Hopkins, W.E., Ochoa, L.L., Richardson, G.W., and Trulock, E.P. (1996). Comparison of the hemodynamics and survival of adults with severe primary pulmonary hypertension or Eisenmenger syndrome. J. Hear. Lung Transplant. *15*: 100–105.

Horio, T., Tokudome, T., Maki, T., Yoshihara, F., Suga, S.I., Nishikimi, T., et al. (2003). Gene expression, secretion, and autocrine action of C-type natriuretic peptide in cultured adult rat cardiac fibroblasts. Endocrinology *144*: 2279–2284.

Houssaini, A., Abid, S., Mouraret, N., Wan, F., Rideau, D., Saker, M., et al. (2013). Rapamycin reverses pulmonary artery smooth muscle cell proliferation in pulmonary hypertension. Am. J. Respir. Cell Mol. Biol. *48*: 568–577.

Howard, L.S. (2011). Prognostic factors in pulmonary arterial hypertension: Assessing the course of the disease. Eur. Respir. Rev. *20*: 236–242.

Howard, L.S.G.E., He, J., Watson, G.M.J., Huang, L., Wharton, J., Luo, Q., et al. (2021). Supplementation with iron in pulmonary arterial hypertension two randomized crossover trials. Ann. Am. Thorac. Soc. *18*: 981–988.

Hu, P., Wang, J., Zhao, X.Q., Hu, B., Lu, L., and Qin, Y.H. (2013). Overexpressed C-type natriuretic peptide serves as an early compensatory response to counteract extracellular matrix remodeling in unilateral ureteral obstruction rats. Mol. Biol.

Rep. *40*: 1429–1441.

Huang, H., Zhang, P., Wang, Z., Tang, F., and Jiang, Z. (2011). Activation of endothelin-1 receptor signaling pathways is associated with neointima formation, neoangiogenesis and irreversible pulmonary artery hypertension in patients with congenital heart disease. Circ. J. *75*: 1463–1471.

Huertas, A., Guignabert, C., Barberà, J.A., Bärtsch, P., Bhattacharya, J., Bhattacharya, S., et al. (2018). Pulmonary vascular endothelium: The orchestra conductor in respiratory diseases. Eur. Respir. J. *51*:.

Humbert, M., Guignabert, C., Bonnet, S., Dorfmüller, P., Klinger, J.R., Nicolls, M.R., et al. (2019). Pathology and pathobiology of pulmonary hypertension: state of the art and research perspectives. Eur. Respir. J. *53*:.

Humbert, M., Lau, E.M.T., Montani, D., Jaïs, X., Sitbon, O., and Simonneau, G. (2014). Advances in therapeutic interventions for patients with pulmonary arterial hypertension. Circulation *130*: 2189–2208.

Humbert, M., McLaughlin, V., Gibbs, J.S.R., Gomberg-Maitland, M., Hoeper, M.M., Preston, I.R., et al. (2021). Sotatercept for the Treatment of Pulmonary Arterial Hypertension. N. Engl. J. Med. *384*: 1204–1215.

Humbert, M., Montani, D., Perros, F., Dorfmüller, P., Adnot, S., and Eddahibi, S. (2008). Endothelial cell dysfunction and cross talk between endothelium and smooth muscle cells in pulmonary arterial hypertension. Vascul. Pharmacol. *49*: 113–118.

Humbert, M., Monti, G., Brenot, F., Sitbon, O., Portier, A., Grangeot-Keros, L., et al. (1995). Increased interleukin-1 and interleukin-6 serum concentrations in severe primary pulmonary hypertension. Am. J. Respir. Crit. Care Med. *151*: 1628–1631.

Humbert, M., Monti, G., Fartoukh, M., Magnan, A., Brenot, F., Rain, B., et al. (1998). Platelet-derived growth factor expression in primary pulmonary hypertension: Comparison of HIV seropositive and HIV seronegative patients. Eur. Respir. J. *11*: 554–559.

Humbert, M., Morrell, N.W., Archer, S.L., Stenmark, K.R., MacLean, M.R., Lang, I.M., et al. (2004). Cellular and molecular pathobiology of pulmonary arterial hypertension. J. Am. Coll. Cardiol. *43*: S13–S24.

Humbert, M.J.C., Sitbon, O., Chaouat, A., Bertocchi, M., Habib, G., Gressin, V., et al. (2010). Survival In Patients With Idiopathic, Familial, And Anorexigen-associated Pulmonary Arterial Hypertension In The Modern Management Era. A4812–A4812.

Hunt, P.J., Richards, A.M., Espiner, E.A., Nicholls, M.G., and Yandle, T.G. (1994). Bioactivity and metabolism of C-type natriuretic peptide in normal man. J. Clin. Endocrinol. Metab. *78*: 1428–1435.

Hunter, K.S., Lee, P.F., Lanning, C.J., Ivy, D.D., Kirby, K.S., Claussen, L.R., et al. (2008). Pulmonary vascular input impedance is a combined measure of pulmonary vascular resistance and stiffness and predicts clinical outcomes better than pulmonary vascular resistance alone in pediatric patients with pulmonary hypertension. Am. Heart J. *155*: 166–174.

Hutchinson, H.G., Trindade, P.T., Cunanan, D.B., Wu, C.F., and Pratt, R.E. (1997). Mechanisms of natriuretic-peptide-induced growth inhibition of vascular smooth muscle cells. Cardiovasc. Res. *35*: 158–167.

Hynes, R.O. (1992). Integrins: Versatility, modulation, and signaling in cell adhesion. Cell *69*: 11–25.

Ichiki, T., Schirger, J., Wanek, J.R., Scott, C., Sangaralingham, J., Chen, H.H., et al. (2020). Cenderitide: a Novel Therapeutic To Increase Endogenous Cardiac Natriuretic Peptides in Heart Failure. J. Am. Coll. Cardiol. *75*: 788.

Ichiki, T., Schirger, J.A., Huntley, B.K., Brozovich, F. V., Maleszewski, J.J., Sandberg, S.M., et al. (2014). Cardiac fibrosis in end-stage human heart failure and the cardiac natriuretic peptide guanylyl cyclase system: Regulation and therapeutic implications. J. Mol. Cell. Cardiol. *75*: 199–205.

Iino, M., Dymarkowski, S., Chaothawee, L., Delcroix, M., and Bogaert, J. (2008). Time course of reversed cardiac remodeling after pulmonary endarterectomy in

patients with chronic pulmonary thromboembolism. Eur. Radiol. *18*: 792–799.

Ikeda, K.T., Hale, P.T., Pauciulo, M.W., Dasgupta, N., Pastura, P.A., Cras, T.D. Le, et al. (2019). Hypoxia-induced pulmonary hypertension in different mouse strains: Relation to transcriptome. Am. J. Respir. Cell Mol. Biol. *60*: 106–116.

Ikeda, S., Satoh, K., Kikuchi, N., Miyata, S., Suzuki, K., Omura, J., et al. (2014). Crucial role of rho-kinase in pressure overload-induced right ventricular hypertrophy and dysfunction in mice. Arterioscler. Thromb. Vasc. Biol. *34*: 1260–1271.

Inoue, K., Sakamoto, T., Yuge, S., Iwatani, H., Yamagami, S., Tsutsumi, M., et al. (2005). Structural and functional evolution of three cardiac natriuretic peptides. Mol. Biol. Evol. *22*: 2428–2434.

Irodova, N.L., Lankin, V.Z., Konovalova, G.K., Kochetov, A.G., and Chazova, I.E. (2002). Oxidative stress in patients with primary pulmonary hypertension. Bull. Exp. Biol. Med. *133*: 580–582.

Irwin, D.C., Patot, M.T. Van, Tucker, A., and Bowen, R. (2005). Neutral endopeptidase null mice are less susceptible to high altitude-induced pulmonary vascular leak. High Alt. Med. Biol. *6*: 311–319.

Ishisaki, A., Yamato, K., Hashimoto, S., Nakao, A., Tamaki, K., Nonaka, K., et al. (1999). Differential inhibition of Smad6 and Smad7 on bone morphogenetic protein- and activin-mediated growth arrest and apoptosis in B cells. J. Biol. Chem. *274*: 13637–13642.

Isobe, M., Yazaki, Y., Takaku, F., Koizumi, K., Hara, K., Tsuneyoshi, H., et al. (1986). Prediction of pulmonary arterial pressure in adults by pulsed doppler echocardiography. Am. J. Cardiol. *57*: 316–321.

Itoh, T., Nagaya, N., Murakami, S., Fujii, T., Iwase, T., Ishibashi-Ueda, H., et al. (2004). C-type natriuretic peptide ameliorates monocrotaline-induced pulmonary hypertension in rats. Am. J. Respir. Crit. Care Med. *170*: 1204–1211.

Izikki, M., Guignabert, C., Fadel, E., Humbert, M., Tu, L., Zadigue, P., et al. (2009). Endothelial-derived FGF2 contributes to the progression of pulmonary

hypertension in humans and rodents. J. Clin. Invest. *119*: 512–523.

Izumiya, Y., Araki, S., Usuku, H., Rokutanda, T., Hanatani, S., and Ogawa, H. (2012). Chronic C-type natriuretic peptide infusion attenuates angiotensin II-induced myocardial superoxide production and cardiac remodeling. Int. J. Vasc. Med. *2012*:.

Jacobs, W., Veerdonk, M.C. Van De, Trip, P., Man, F. De, Heymans, M.W., Marcus, J.T., et al. (2014). The Right Ventricle Explains Sex Differences in Survival in Idiopathic Pulmonary Arterial Hypertension. Chest *145*: 1230–1236.

Jain, A., and Anand-Srivastava, M.B. (2018). Natriuretic peptide receptor-C-mediated attenuation of vascular smooth muscle cell hypertrophy involves Gqα/PLCβ1 proteins and ROS-associated signaling. Pharmacol. Res. Perspect. *6*:.

Jansen, H.J., Mackasey, M., Moghtadaei, M., Liu, Y., Kaur, J., Egom, E.E., et al. (2019). NPR-C (Natriuretic Peptide Receptor-C) Modulates the Progression of Angiotensin II-Mediated Atrial Fibrillation and Atrial Remodeling in Mice. Circ. Arrhythm. Electrophysiol. *12*: e006863.

Jarman, E.R., Khambata, V.S., Ye, L.Y., Cheung, K., Thomas, M., Duggan, N., et al. (2014). A translational preclinical model of interstitial pulmonary fibrosis and pulmonary hypertension: Mechanistic pathways driving disease pathophysiology. Physiol. Rep. *2*:.

Jaubert, J., Jaubert, F., Martin, N., Washburn, L.L., Lee, B.K., Eicher, E.M., et al. (1999). Three new allelic mouse mutations that cause skeletal overgrowth involve the natriuretic peptide receptor C gene (Npr3). Proc. Natl. Acad. Sci. U. S. A. *96*: 10278–10283.

Jenkins, D. (2015). Pulmonary endarterectomy: The potentially curative treatment for patients with chronic thromboembolic pulmonary hypertension. Eur. Respir. Rev. *24*: 263–271.

Jin, H., Chen, Y.F., Yang, R.H., Jackson, R.M., and Oparil, S. (1990). Atrial natriuretic peptide clearance receptor agonist lowers pulmonary pressure in

hypoxic rats. J. Appl. Physiol. *68*: 2413–2418.

Jin, H., Yang, R.H., Chen, Y.F., Jackson, R.M., Itoh, H., Mukoyama, M., et al. (1991). Atrial natriuretic peptide in acute hypoxia-induced pulmonary hypertension in rats. J. Appl. Physiol. *71*: 807–814.

Jin, H.K., Yang, R.H., Chen, Y.F., Jackson, R.M., and Oparil, S. (1988). Chronic infusion of atrial natriuretic peptide prevents pulmonary hypertension in hypoxia-adapted rats. Trans. Assoc. Am. Physicians *101*: 185–192.

Jones, J.E., Mendes, L., Audrey Rudd, M., Russo, G., Loscalzo, J., and Zhang, Y.Y. (2002). Serial noninvasive assessment of progressive pulmonary hypertension in a rat model. Am. J. Physiol. - Hear. Circ. Physiol. *283*: H364-71.

Jones, P.L., Cowan, K.N., and Rabinovitch, M. (1997). Tenascin-C, proliferation and subendothelial fibronectin in progressive pulmonary vascular disease. Am. J. Pathol. *150*: 1349–1360.

Jones, P.L., and Rabinovitch, M. (1996). Tenascin-C is induced with progressive pulmonary vascular disease in rats and is functionally related to increased smooth muscle cell proliferation. Circ. Res. *79*: 1131–1142.

Jong, S. de, Veen, T.A.B. van, Bakker, J.M.T. de, and Rijen, H.V.M. Van (2012). Monitoring cardiac fibrosis: A technical challenge. Netherlands Hear. J. *20*: 44–48.

Jonigk, D., Golpon, H., Bockmeyer, C.L., Maegel, L., Hoeper, M.M., Gottlieb, J., et al. (2011). Plexiform lesions in pulmonary arterial hypertension: Composition, architecture, and microenvironment. Am. J. Pathol. *179*: 167–179.

Joshi, S.R., Liu, J., Pearsall, R.S., Li, G., and Kumar, R. (2019). ACTRIIA-Fc (Sotatercept) Reverses Pulmonary Vascular Remodeling to Attenuate Pulmonary Arterial Hypertension (PAH) by Rebalancing TGF-b/BMP Signaling in a Preclinical Model. Am. J. Respir. Crit. Care Med. *199*: A4395–A4395.

Kaiser, R., Grotemeyer, K., Lepper, P., Stokes, C., Bals, R., and Wilkens, H. (2015). Associations of circulating natriuretic peptides with haemodynamics in precapillary pulmonary hypertension. Respir. Med. *109*: 1213–1223.

Kamiyama, M., Utsunomiya, K., Taniguchi, K., Yokota, T., Kurata, H., Tajima, N.,

et al. (2003). Contribution of Rho A and Rho kinase to platelet-derived growth factor-BB-induced proliferation of vascular smooth muscle cells. J. Atheroscler. Thromb. *10*: 117–123.

Karas, M.G., and Kizer, J.R. (2012). Echocardiographic assessment of the right ventricle and associated hemodynamics. Prog. Cardiovasc. Dis. *55*: 144–160.

Kasimir, M.T., Seebacher, G., Jaksch, P., Winkler, G., Schmid, K., Marta, G.M., et al. (2004). Reverse cardiac remodelling in patients with primary pulmonary hypertension after isolated lung transplantation. Eur. J. Cardio-Thoracic Surg. *26*: 776–781.

Kasmi, K.C. El, Pugliese, S.C., Riddle, S.R., Poth, J.M., Anderson, A.L., Frid, M.G., et al. (2014). Adventitial Fibroblasts Induce a Distinct Proinflammatory/Profibrotic Macrophage Phenotype in Pulmonary Hypertension. J. Immunol. *193*: 597–609.

Kato, J., Lanier-Smith, K.L., and Currie, M.G. (1991). Cyclic GMP down-regulates atrial natriuretic peptide receptors on cultured vascular endothelial cells. J. Biol. Chem. *266*: 14681–14685.

Kato, J., Oehlenschlager, W.F., Newman, W.H., and Currie, M.G. (1992). Inhibition of endothelial cell clearance of atrial natriuretic peptide by cyclic GMP treatment. Biochem. Biophys. Res. Commun. *182*: 420–424.

Kawakami, R., Lee, C.Y.W., Scott, C., Bailey, K.R., Schirger, J.A., Chen, H.H., et al. (2018). A Human Study to Evaluate Safety, Tolerability, and Cyclic GMP Activating Properties of Cenderitide in Subjects With Stable Chronic Heart Failure. Clin. Pharmacol. Ther. *104*: 546–552.

Kawut, S.M., Archer-Chicko, C.L., DeMichele, A., Fritz, J.S., Klinger, J.R., Ky, B., et al. (2017). Anastrozole in pulmonary arterial hypertension: A randomized, double-blind, placebo-controlled trial. Am. J. Respir. Crit. Care Med. *195*: 360–368.

Kawut, S.M., Bagiella, E., Lederer, D.J., Shimbo, D., Horn, E.M., Roberts, K.E., et al. (2011). Randomized clinical trial of aspirin and simvastatin for pulmonary arterial hypertension: ASA-STAT. Circulation *123*: 2985–2993.

Kawut, S.M., Pinder, D., Al-Naamani, N., Mccormick, A., Palevsky, H.I., Fritz, J., et

al. (2019). Fulvestrant for the treatment of pulmonary arterial hypertension. Ann. Am. Thorac. Soc. *16*: 1456–1459.

Keegan, A., Morecroft, I., Smillie, D., Hicks, M.N., and MacLean, M.R. (2001). Contribution of the 5-HT1B receptor to hypoxia-induced pulmonary hypertension: Converging evidence using 5-HT1B-receptor knockout mice and the 5-HT1B/1D-receptor antagonist GR127935. Circ. Res. *89*: 1231–1239.

Kelland, N.F., Kuc, R.E., McLean, D.L., Azfer, A., Bagnall, A.J., Gray, G.A., et al. (2010). Endothelial cell-specific ETB receptor knockout: Autoradiographic and histological characterisation and crucial role in the clearance of endothelin-1. Can. J. Physiol. Pharmacol. *88*: 644–651.

Kelsall, C.J., Chester, A.H., Sarathchandra, P., and Singer, D.R.J. (2006). Expression and localization of C-type natriuretic peptide in human vascular smooth muscle cells. Vascul. Pharmacol. *45*: 368–373.

Kenny, A.J., Bourne, A., and Ingram, J. (1993). Hydrolysis of human and pig brain natriuretic peptides, urodilatin, C-type natriuretic peptide and some C-receptor ligands by endopeptidase-24.11. Biochem. J. *291*: 83–88.

Kenny, A.J., and Stephenson, S.L. (1988). Role of endopeptidase-24.11 in the inactivation of atrial natriuretic peptide. FEBS Lett. *232*: 1–8.

Kerr, M.A., and Kenny, A.J. (1974). The purification and specificity of a neutral endopeptidase from rabbit kidney brush border. Biochem. J. *137*: 477–488.

Khambata, R.S., Panayiotou, C.M., and Hobbs, A.J. (2011). Natriuretic peptide receptor-3 underpins the disparate regulation of endothelial and vascular smooth muscle cell proliferation by C-type natriuretic peptide. Br. J. Pharmacol. *164*: 584–597.

Khan, S.S., Cuttica, M.J., Beussink-Nelson, L., Kozyleva, A., Sanchez, C., Mkrdichian, H., et al. (2015). Effects of ranolazine on exercise capacity, right ventricular indices, and hemodynamic characteristics in pulmonary arterial hypertension: A pilot study. Pulm. Circ. *5*: 547–556.

Kibbe, M.R., Li, J., Nie, S., Watkins, S.C., Lizonova, A., Kovesdi, I., et al. (2000).

Inducible nitric oxide synthase (iNOS) expression upregulates p21 and inhibits vascular smooth muscle cell proliferation through p42/44 mitogen-activated protein kinase activation and independent of p53 and cyclic guanosine monophosphate. J. Vasc. Surg. *31*: 1214–1228.

Kielstein, J.T., Bode-Böger, S.M., Hesse, G., Martens-Lobenhoffer, J., Takacs, A., Fliser, D., et al. (2005). Asymmetrical dimethylarginine in idiopathic pulmonary arterial hypertension. Arterioscler. Thromb. Vasc. Biol. *25*: 1414–1418.

Kim, N.H. (2016). Group 4 Pulmonary Hypertension: Chronic Thromboembolic Pulmonary Hypertension: Epidemiology, Pathophysiology, and Treatment. Cardiol. Clin. *34*: 435–441.

Kim, N.H., Delcroix, M., Jenkins, D.P., Channick, R., Dartevelle, P., Jansa, P., et al. (2013). Chronic thromboembolic pulmonary hypertension. J. Am. Coll. Cardiol. *62*: D92-9.

Kim, S.Z.S.H., Cho, K.W., and Kim, S.Z.S.H. (1999). Modulation of endocardial natriuretic peptide receptors in right ventricular hypertrophy. Am. J. Physiol. - Hear. Circ. Physiol. *277*: H2280-9.

Kimura, K., Ieda, M., Kanazawa, H., Yagi, T., Tsunoda, M., Ninomiya, S.I., et al. (2007). Cardiac sympathetic rejuvenation: A link between nerve function and cardiac hypertrophy. Circ. Res. *100*: 1755–1764.

Kimura, T., Nojiri, T., Hino, J., Hosoda, H., Miura, K., Shintani, Y., et al. (2016). C-type natriuretic peptide ameliorates pulmonary fibrosis by acting on lung fibroblasts in mice. Respir. Res. *17*: 19.

Kjellström, B., Nisell, M., Kylhammar, D., Bartfay, S.E., Ivarsson, B., Rådegran, G., et al. (2019). Erratum: Sex-specific differences and survival in patients with idiopathic pulmonary arterial hypertension 2008-2016 (ERJ Open Res, (2019), 5). ERJ Open Res. *5*:.

Klein, M., Schermuly, R.T., Ellinghaus, P., Milting, H., Riedl, B., Nikolova, S., et al. (2008). Combined tyrosine and serine/threonine kinase inhibition by sorafenib prevents progression of experimental pulmonary hypertension and myocardial

remodeling. Circulation *118*: 2081–2090.

Klinger, J.R., Petit, R.D., Curtin, L.A., Warburton, R.R., Wrenn, D.S., Steinhelper, M.E., et al. (1993a). Cardiopulmonary responses to chronic hypoxia in transgenic mice that overexpress ANP. J. Appl. Physiol. *75*: 198–205.

Klinger, J.R., Petit, R.D., Warburton, R.R., Wrenn, D.S., Arnal, F., and Hill, N.S. (1993b). Neutral endopeptidase inhibition attenuates development of hypoxic pulmonary hypertension in rats. J. Appl. Physiol. *75*: 1615–1623.

Klinger, J.R., Siddiq, F.M., Swift, R.A., Jackson, C., Pietras, L., Warburton, R.R., et al. (1998a). C-type natriuretic peptide expression and pulmonary vasodilation in hypoxia-adapted rats. Am. J. Physiol. - Lung Cell. Mol. Physiol. *275*: L645-52.

Klinger, J.R., Warburton, R.R., Pietras, L., and Hill, N.S. (1998b). Brain natriuretic peptide inhibits hypoxic pulmonary hypertension in rats. J. Appl. Physiol. *84*: 1646–1652.

Klinger, J.R., Warburton, R.R., Pietras, L., Oliver, P., Fox, J., Smithies, O., et al. (2002). Targeted disruption of the gene for natriuretic peptide receptor-A worsens hypoxia-induced cardiac hypertrophy. Am. J. Physiol. - Hear. Circ. Physiol. *282*:.

Ko, E.A., Song, M.Y., Donthamsetty, R., Makino, A., and Yuan, J.X.J. (2010). Tension measurement in isolated rat and mouse pulmonary artery. Drug Discov. Today Dis. Model. *7*: 123–130.

Kohno, M., Horio, T., Yokokawa, K., Kurihara, N., and Takeda, T. (1992). C-type natriuretic peptide inhibits thrombin- and angiotensin II-stimulated endothelin release via cyclic guanosine 3', 5'-monophosphate. Hypertension *19*: 320–325.

Kohut, A., Patel, N., and Singh, H. (2016). Comprehensive echocardiographic assessment of the right ventricle in murine models. J. Cardiovasc. Ultrasound *24*: 229–238.

Koller, K.J., Lowe, D.G., Bennett, G.L., Minamino, N., Kangawa, K., Matsuo, H., et al. (1991). Selective activation of the B natriuretic peptide receptor by C-type natriuretic peptide (CNP). Science (80-.). *252*: 120–123.

Komatsu, Y., Chusho, H., Tamura, N., Yasoda, A., Miyazawa, T., Suda, M., et al.

(2002). Significance of C-type natriuretic peptide (CNP) in endochondral ossification: Analysis of CNP knockout mice. J. Bone Miner. Metab. *20*: 331–336.

Kone, B.C. (2001). Molecular biology of natriuretic peptides and nitric oxide synthases. Cardiovasc. Res. *51*: 429–441.

Koskenvuo, J.W., Mirsky, R., Zhang, Y., Angeli, F.S., Jahn, S., Alastalo, T.P., et al. (2010). A comparison of echocardiography to invasive measurement in the evaluation of pulmonary arterial hypertension in a rat model. Int. J. Cardiovasc. Imaging *26*: 509–518.

Koussounadis, A., Langdon, S.P., Um, I.H., Harrison, D.J., and Smith, V.A. (2015). Relationship between differentially expressed mRNA and mRNA-protein correlations in a xenograft model system. Sci. Rep. *5*:.

Krasuski, R.A., Hart, S.A., Smith, B., Wang, A., Harrison, J.K., and Bashore, T.M. (2011). Association of anemia and long-term survival in patients with pulmonary hypertension. Int. J. Cardiol. *150*: 291–295.

Krejci, P., Masri, B., Fontaine, V., Mekikian, P.B., Weis, M.A., Prats, H., et al. (2005). Interaction of fibroblast growth factor and C-natriuretic peptide signaling in regulation of chondrocyte proliferation and extracellular matrix homeostasis. J. Cell Sci. *118*: 5089–5100.

Krietsch, J., Caron, M.C., Gagné, J.P., Ethier, C., Vignard, J., Vincent, M., et al. (2012). PARP activation regulates the RNA-binding protein NONO in the DNA damage response to DNA double-strand breaks. Nucleic Acids Res. *40*: 10287–10301.

Krymskaya, V.P., Snow, J., Cesarone, G., Khavin, I., Goncharov, D.A., Lim, P.N., et al. (2011). mTOR is required for pulmonary arterial vascular smooth muscle cell proliferation under chronic hypoxia. FASEB J. *25*: 1922–1933.

Kudryashova, T. V., Goncharov, D.A., Pena, A., Kelly, N., Vanderpool, R., Baust, J., et al. (2016). HIPPO-integrin-linked kinase cross-talk controls self-sustaining proliferation and survival in pulmonary hypertension. Am. J. Respir. Crit. Care Med. *194*: 866–877.

Kuhn, M. (2004). Molecular physiology of natriuretic peptide signalling. Basic Res. Cardiol. *99*: 76–82.

Kun, A., Kiraly, I., Pataricza, J., Marton, Z., Krassoi, I., Varro, A., et al. (2008). C-Type natriuretic peptide hyperpolarizes and relaxes human penile resistance arteries. J. Sex. Med. *5*: 1114–1125.

Lahm, T., Albrecht, M., Fisher, A.J., Selej, M., Patel, N.G., Brown, J.A., et al. (2012). 17β-Estradiol attenuates hypoxic pulmonary hypertension via estrogen receptor-mediated effects. Am. J. Respir. Crit. Care Med. *185*: 965–980.

Lahm, T., Frump, A.L., Albrecht, M.E., Fisher, A.J., Cook, T.G., Jones, T.J., et al. (2016). 17β-Estradiol mediates superior adaptation of right ventricular function to acute strenuous exercise in female rats with severe pulmonary hypertension. Am. J. Physiol. - Lung Cell. Mol. Physiol. *311*: L375–L388.

Lakhal-Littleton, S., Crosby, A., Frise, M.C., Mohammad, G., Carr, C.A., Loick, P.A.M., et al. (2019). Intracellular iron deficiency in pulmonary arterial smooth muscle cells induces pulmonary arterial hypertension in mice. Proc. Natl. Acad. Sci. U. S. A. *116*: 13122–13130.

Lal, H., Woodward, B., and Williams, K.I. (1996). Investigation of the contributions of nitric oxide and prostaglandins to the actions of endothelins and sarafotoxin 6c in rat isolated perfused lungs. Br. J. Pharmacol. *118*: 1931–1938.

Lammers, S., Scott, D., Hunter, K., Tan, W., Shandas, R., and Stenmark, K.R. (2012). Mechanics and function of the pulmonary vasculature: Implications for pulmonary vascular disease and right ventricular function. Compr. Physiol. *2*: 295–319.

Landburg, P.P., Teerlink, T., Beers, E.J. Van, Muskiet, F.A.J., Kappers-Klunne, M.C., Esser, J.W.J. Van, et al. (2008). Association of asymmetric dimethylarginine with sickle cell disease-related pulmonary hypertension. Haematologica *93*: 1410–1412.

Lang, I.M., Dorfmüller, P., and Noordegraaf, A.V. (2016). The pathobiology of chronic thromboembolic pulmonary hypertension. Ann. Am. Thorac. Soc. *13*:

S215–S221.

Langenickel, T.H., Buttgereit, J., Pagel-Langenickel, I., Lindner, M., Monti, J., Beuerlein, K., et al. (2006). Cardiac hypertrophy in transgenic rats expressing a dominant-negative mutant of the natriuretic peptide receptor B. Proc. Natl. Acad. Sci. U. S. A. *103*: 4735–4740.

Lannan, K.L., Phipps, R.P., and White, R.J. (2014). Thrombosis, platelets, microparticles and PAH: More than a clot. Drug Discov. Today *19*: 1230–1235.

Launay, J.M., Hervé, P., Peoc'h, K., Tournois, C., Callebert, J., Nebigil, C.G., et al. (2002). Function of the serotonin 5-hydroxytryptamine 2B receptor in pulmonary hypertension. Nat. Med. *8*: 1129–1135.

Laursen, J.B., Somers, M., Kurz, S., McCann, L., Warnholtz, A., Freeman, B.A., et al. (2001). Endothelial regulation of vasomotion in ApoE-deficient mice: Implications for interactions between peroxynitrite and tetrahydrobiopterin. Circulation *103*: 1282–1288.

Lavoie, J.R., Ormiston, M.L., Perez-Iratxeta, C., Courtman, D.W., Jiang, B., Ferrer, E., et al. (2014). Proteomic analysis implicates translationally controlled tumor protein as a novel mediator of occlusive vascular remodeling in pulmonary arterial hypertension. Circulation *129*: 2125–2135.

Lazarus, H., Denning, J., Kamau-Kelley, W., Wring, S., Palacios, M., and Humbert, M. (2021). ELEVATE 2: A multicenter study of rodatristat ethyl in patients with WHO Group 1 pulmonary arterial hypertension (PAH). PA1919.

Leary, P.J., Barr, R.G., Bluemke, D.A., Bristow, M.R., Kronmal, R.A., Lima, J.A., et al. (2014). H2 receptor antagonists and right ventricular morphology: The MESA right ventricle study. Ann. Am. Thorac. Soc. *11*: 1379–1386.

Leary, P.J., Hess, E., Barón, A.E., Branch, K.R., Choudhary, G., Hough, C.L., et al. (2018). H2 Receptor Antagonist Use and Mortality in Pulmonary Hypertension: Insight from the VA-CART Program. Am. J. Respir. Crit. Care Med. *197*: 1638–1641.

Lee, J.Y., Michael Francis, C., Bauer, N.N., Gassman, N.R., and Stevens, T.

(2020). A cancer amidst us: The plexiform lesion in pulmonary arterial hypertension. Am. J. Physiol. - Lung Cell. Mol. Physiol. *318*: L1142–L1144.

Lee, S. Do, Shroyer, K.R., Markham, N.E., Cool, C.D., Voelkel, N.F., and Tuder, R.M. (1998). Monoclonal endothelial cell proliferation is present in primary but not secondary pulmonary hypertension. J. Clin. Invest. *101*: 927–934.

Lehners, M., Dobrowinski, H., Feil, S., and Feil, R. (2018). cGMP Signaling and Vascular Smooth Muscle Cell Plasticity. J. Cardiovasc. Dev. Dis. *5*: 20.

Leitman, D.C., Andresen, J.W., Kuno, T., Kamisaki, Y., Chang, J.K., and Murad, F. (1986). Identification of multiple binding sites for atrial natriuretic factor by affinity cross-linking in cultured endothelial cells. J. Biol. Chem. *261*: 11650–11655.

Lepetit, H., Eddahibi, S., Fadel, E., Frisdal, E., Munaut, C., Noel, A., et al. (2005). Smooth muscle cell matrix metalloproteinases in idiopathic pulmonary arterial hypertension. Eur. Respir. J. *25*: 834–842.

Lewis, R.A., Durrington, C., Condliffe, R., and Kiely, D.G. (2020). BNP/NT-probnp in pulmonary arterial hypertension: Time for point-of-care testing? Eur. Respir. Rev. *29*:.

Li, H., Oparil, S., Qing Cheng Meng, Elton, T.S., and Chen, Y.F. (1995). Selective downregulation of ANP-clearance-receptor gene expression in lung of rats adapted to hypoxia. Am. J. Physiol. - Lung Cell. Mol. Physiol. *268*: L328-35.

Li, M., Riddle, S., Zhang, H., D'Alessandro, A., Flockton, A., Serkova, N.J., et al. (2016). Metabolic Reprogramming Regulates the Proliferative and Inflammatory Phenotype of Adventitial Fibroblasts in Pulmonary Hypertension Through the Transcriptional Corepressor C-Terminal Binding Protein-1. Circulation *134*: 1105–1121.

Li, N., Luo, W., Juhong, Z., Yang, J., Wang, H., Zhou, L., et al. (2010). Associations between genetic variations in the FURIN gene and hypertension. BMC Med. Genet. *11*:.

Li, Y., and Anand-Srivastava, M. (2022). Downregulation of Natriuretic Peptide Receptor-C in Vascular Smooth Muscle Cells from Spontaneously Hypertensive

Rats Contributes to Vascular Remodeling. SSRN Electron. J.

Li, Z.Q., Liu, Y.L., Li, G., Li, B., Liu, Y., Li, X.F., et al. (2015). Inhibitory effects of C.type natriuretic peptide on the differentiation of cardiac fibroblasts, and secretion of monocyte chemoattractant protein-1 and plasminogen activator inhibitor-1. Mol. Med. Rep. *11*: 159–165.

Liao, S., Li, D., Hui, Z., McLachlan, C.S., and Zhang, Y. (2018). Metformin added to bosentan therapy in patients with pulmonary arterial hypertension associated with congenital heart defects: A pilot study. ERJ Open Res. *4*:.

Lin, S., and Du, L. (2020). The therapeutic potential of BRD4 in cardiovascular disease. Hypertens. Res. *43*: 1006–1014.

Lisy, O., Huntley, B.K., McCormick, D.J., Kurlansky, P.A., and Burnett, J.C. (2008). Design, Synthesis, and Actions of a Novel Chimeric Natriuretic Peptide: CD-NP. J. Am. Coll. Cardiol. *52*: 60–68.

Liu, C.P., Dai, Z.K., Huang, C.H., Yeh, J.L., Wu, B.N., Wu, J.R., et al. (2014). Endothelial nitric oxide synthase-enhancing G-protein coupled receptor antagonist inhibits pulmonary artery hypertension by endothelin-1-dependent and endothelin-1-independent pathways in a monocrotaline model. Kaohsiung J. Med. Sci. *30*: 267–278.

Liu, H., Liu, Z. -y., and Guan, Q. (2007). Oral sildenafil prevents and reverses the development of pulmonary hypertension in monocrotaline-treated rats. Interact. Cardiovasc. Thorac. Surg. *6*: 608–613.

Liu, P., Gu, Y., Luo, J., Ye, P., Zheng, Y., Yu, W., et al. (2019). Inhibition of Src activation reverses pulmonary vascular remodeling in experimental pulmonary arterial hypertension via Akt/mTOR/HIF-1<alpha> signaling pathway. Exp. Cell Res. *380*: 36–46.

Liu, S.F., and Barnes, P.J. (1994). Role of Endothelium in the Control of Pulmonary Vascular Tone. Endothelium *2*: 11–33.

Liu, S.Y., Wang, Y., Lu, S., Hu, J., Zeng, X.H., Liu, W.H., et al. (2021). Sacubitril/valsartan treatment relieved the progression of established pulmonary

hypertension in rat model and its mechanism. Life Sci. *266*:.

Liu, Y., Ren, W., Warburton, R., Toksoz, D., and Fanburg, B.L. (2009). Serotonin induces Rho/ROCK-dependent activation of Smads 1/5/8 in pulmonary artery smooth muscle cells. FASEB J. *23*: 2299–2306.

Llis, E., Evin, R.L., Avid, D., Ardner, G.G., Illis, W., and Amson, K.S. (1998). Mechanisms of disease natriuretic peptides. N Engl J Med 321–328.

Lo, C.C.W., Moosavi, S.M., and Bubb, K.J. (2018). The regulation of pulmonary vascular tone by neuropeptides and the implications for pulmonary hypertension. Front. Physiol. *9*:.

Lok, D.J., Klip, Ij.T., Voors, A.A., Lok, S.I., Bruggink-André De La Porte, P.W., Hillege, H.L., et al. (2014). Prognostic value of N-terminal pro C-type natriuretic peptide in heart failure patients with preserved and reduced ejection fraction. Eur. J. Heart Fail. *16*: 958–966.

Long, L., Crosby, A., Yang, X., Southwood, M., Upton, P.D., Kim, D.K., et al. (2009). Altered bone morphogenetic protein and transforming growth factor-β signaling in rat models of pulmonary hypertension. Potential for activin receptor-like kinase-5 inhibition in prevention and progression of disease. Circulation *119*: 566–576.

Lordan, J.L., and Corris, P.A. (2011). Pulmonary arterial hypertension and lung transplantation. Expert Rev. Respir. Med. *5*: 441–454.

Lorget, F., Kaci, N., Peng, J., Benoist-Lasselin, C., Mugniery, E., Oppeneer, T., et al. (2012). Evaluation of the therapeutic potential of a CNP analog in a Fgfr3 mouse model recapitulating achondroplasia. Am. J. Hum. Genet. *91*: 1108–1114.

Lorusso, D., Tripodi, E., Maltese, G., Lepori, S., Sabatucci, I., Bogani, G., et al. (2018). Spotlight on olaparib in the treatment of BRCA-mutated ovarian cancer: Design, development and place in therapy. Drug Des. Devel. Ther. *12*: 1501–1509.

Louzier, V., Eddahibi, S., Raffestin, B., Déprez, I., Adam, M., Levame, M., et al. (2001). Adenovirus-mediated atrial natriuretic protein expression in the lung protects rats from hypoxia-induced pulmonary hypertension. Hum. Gene Ther. *12*:

503–513.

Lowe, D.G., Klisak, I., Sparkes, R.S., Mohandas, T., and Goeddel, D. V. (1990). Chromosomal distribution of three members of the human natriuretic peptide receptor/guanylyl cyclase gene family. Genomics *8*: 304–312.

Lowes, B.D., Minobe, W., Abraham, W.T., Rizeq, M.N., Bohlmeyer, T.J., Quaife, R.A., et al. (1997). Changes in gene expression in the intact human heart: Downregulation of α-myosin heavy chain in hypertrophied, failing ventricular myocardium. J. Clin. Invest. *100*: 2315–2324.

Lumsden, N.G., Khambata, R.S., and Hobbs, A.J. (2011). C-type Natriuretic Peptide (CNP): Cardiovascular Roles and Potential as a Therapeutic Target. Curr. Pharm. Des. *16*: 4080–4088.

Maack, T. (1992). Receptors of Atrial Natriuretic Factor. Annu. Rev. Physiol. *54*: 11–27.

Maack, T., Suzuki, M., Almeida, F.A., Nussenzveig, D., Scarborough, R.M., Mcenroe, G.A., et al. (1987). Physiological role of silent receptors of atrial natriuretic factor. Science (80-.). *238*: 675–678.

Maarman, G., Lecour, S., Butrous, G., Thienemann, F., and Sliwa, K. (2013). A comprehensive review: The evolution of animal models in pulmonary hypertension research; are we there yet? Pulm. Circ. *3*: 739–756.

Mackasey, M., Egom, E.E., Jansen, H.J., Hua, R., Moghtadaei, M., Liu, Y., et al. (2018). Natriuretic Peptide Receptor-C Protects Against Angiotensin II-Mediated Sinoatrial Node Disease in Mice. JACC Basic to Transl. Sci. *3*: 824–843.

MacLean, M. (Mandy) R. (2018). The serotonin hypothesis in pulmonary hypertension revisited: targets for novel therapies (2017 Grover Conference Series). Pulm. Circ. *8*:.

MacLean, M.R., Herve, P., Eddahibi, S., and Adnot, S. (2000). 5-Hydroxytryptamine and the pulmonary circulation: Receptors, transporters and relevance to pulmonary arterial hypertension. Br. J. Pharmacol. *131*: 161–168.

Madani, M.M., Auger, W.R., Pretorius, V., Sakakibara, N., Kerr, K.M., Kim, N.H.,

et al. (2012). Pulmonary endarterectomy: Recent changes in a single institution's experience of more than 2,700 patients. Ann. Thorac. Surg. *94*: 97–103.

Madhani, M., Scotland, R.S., MacAllister, R.J., and Hobbs, A.J. (2003). Vascular natriuretic peptide receptor-linked particulate guanylate cyclases are modulated by nitric oxide-cyclic GMP signalling. Br. J. Pharmacol. *139*: 1289–1296.

Magliano, M., Isenberg, D.A., and Hillson, J. (2002). Pulmonary hypertension in autoimmune rheumatic diseases: Where are we now? Arthritis Rheum. *46*: 1997–2009.

Mahapatra, S., Nishimura, R.A., Oh, J.K., and McGoon, M.D. (2006a). The Prognostic Value of Pulmonary Vascular Capacitance Determined by Doppler Echocardiography in Patients with Pulmonary Arterial Hypertension. J. Am. Soc. Echocardiogr. *19*: 1045–1050.

Mahapatra, S., Nishimura, R.A., Sorajja, P., Cha, S., and McGoon, M.D. (2006b). Relationship of pulmonary arterial capacitance and mortality in idiopathic pulmonary arterial hypertension. J. Am. Coll. Cardiol.

Maier, T., Güell, M., and Serrano, L. (2009). Correlation of mRNA and protein in complex biological samples. FEBS Lett. *583*: 3966–3973.

Mair, K.M., Gaw, R., and MacLean, M.R. (2020). Obesity, estrogens and adipose tissue dysfunction – implications for pulmonary arterial hypertension. Pulm. Circ. *10*:.

Mair, K.M., MacLean, M.R., Morecroft, I., Dempsie, Y., and Palmer, T.M. (2008). Novel interactions between the 5-HT transporter, 5-HT 1B receptors and Rho kinase in vivo and in pulmonary fibroblasts. Br. J. Pharmacol. *155*: 606–616.

Mair, K.M., Wright, A.F., Duggan, N., Rowlands, D.J., Hussey, M.J., Roberts, S., et al. (2014). Sex-dependent influence of endogenous estrogen in pulmonary hypertension. Am. J. Respir. Crit. Care Med. *190*: 456–467.

Majka, S.M., Skokan, M., Wheeler, L., Harral, J., Gladson, S., Burnham, E., et al. (2008). Evidence for cell fusion is absent in vascular lesions associated with pulmonary arterial hypertension. Am. J. Physiol. - Lung Cell. Mol. Physiol. *295*:.

Malenfant, S., Neyron, A.S., Paulin, R., Potus, F., Meloche, J., Provencher, S., et al. (2013). Signal transduction in the development of pulmonary arterial hypertension. Pulm. Circ. *3*: 278–293.

Mallawaarachchi, C.M., Weissberg, P.L., and Siow, R.C.M. (2005). Smad7 gene transfer attenuates adventitial cell migration and vascular remodeling after balloon injury. Arterioscler. Thromb. Vasc. Biol. *25*: 1383–1387.

Man, F.S. De, Tu, L., Handoko, M.L., Rain, S., Ruiter, G., François, C., et al. (2012). Dysregulated renin-angiotensin-aldosterone system contributes to pulmonary arterial hypertension. Am. J. Respir. Crit. Care Med. *186*: 780–789.

Manders, E., Bogaard, H.J., Handoko, M.L., Veerdonk, M.C. Van De, Keogh, A., Westerhof, N., et al. (2014). Contractile dysfunction of left ventricular cardiomyocytes in patients with pulmonary arterial hypertension. J. Am. Coll. Cardiol. *64*: 28–37.

Manfra, O., Calamera, G., Froese, A., Arunthavarajah, D., Surdo, N.C., Meier, S., et al. (2022). CNP regulates cardiac contractility and increases cGMP near both SERCA and TnI: difference from BNP visualized by targeted cGMP biosensors. Cardiovasc. Res. *118*: 1506–1519.

Mangiafico, S., Costello-Boerrigter, L.C., Andersen, I.A., Cataliotti, A., and Burnett, J.C. (2013). Neutral endopeptidase inhibition and the natriuretic peptide system: An evolving strategy in cardiovascular therapeutics. Eur. Heart J. *34*: 886–893.

Mann, D.L. (2004). Basic mechanisms of left ventricular remodeling: the contribution of wall stress. J. Card. Fail. *10*:.

Mark, P.D., Frydland, M., Helgestad, O.K.L., Holmvang, L., Møller, J.E., Johansson, P.I., et al. (2021). Sex-specific mortality prediction by pro-C-type natriuretic peptide measurement in a prospective cohort of patients with ST-elevation myocardial infarction. BMJ Open *11*:.

Maron, B.A., and Leopold, J.A. (2015). Emerging concepts in the molecular basis of pulmonary arterial hypertension: Part II: Neurohormonal signaling contributes to the pulmonary vascular and right ventricular pathophenotype of pulmonary arterial

hypertension. Circulation *131*: 2079–2091.

Maron, B.A., Waxman, A.B., Opotowsky, A.R., Gillies, H., Blair, C., Aghamohammadzadeh, R., et al. (2013). Effectiveness of spironolactone plus ambrisentan for treatment of pulmonary arterial hypertension (from the [ARIES] Study 1 and 2 Trials). Am. J. Cardiol. *112*: 720–725.

Maron, B.A., Zhang, Y.Y., White, K., Chan, S.Y., Handy, D.E., Mahoney, C.E., et al. (2012). Aldosterone inactivates the endothelin-B receptor via a cysteinyl thiol redox switch to decrease pulmonary endothelial nitric oxide levels and modulate pulmonary arterial hypertension. Circulation *126*: 963–974.

Maron, M.S., Hauser, T.H., Dubrow, E., Horst, T.A., Kissinger, K. V., Udelson, J.E., et al. (2007). Right Ventricular Involvement in Hypertrophic Cardiomyopathy. Am. J. Cardiol. *100*: 1293–1298.

Marsboom, G., Toth, P.T., Ryan, J.J., Hong, Z., Wu, X., Fang, Y.H., et al. (2012). Dynamin-related protein 1-mediated mitochondrial mitotic fission permits hyperproliferation of vascular smooth muscle cells and offers a novel therapeutic target in pulmonary hypertension. Circ. Res. *110*: 1484–1497.

Martin, F.L., Sangaralingham, S.J., Huntley, B.K., McKie, P.M., Ichiki, T., Chen, H.H., et al. (2012). CD-NP: A Novel Engineered Dual Guanylyl Cyclase Activator with Anti-Fibrotic Actions in the Heart. PLoS One *7*: e52422.

Masri, F.A., Anand-Apte, B., Vasanji, A., Xu, W., Goggans, T., Drazba, J., et al. (2005). Definitive Evidence of Fundamental and Inherent Alteration in the Phenotype of Primary Pulmonary Hypertension Endothelial Cells in Angiogenesis. Chest *128*: 571S.

Matsukawa, M., Grzesik, W.J., Takahashi, N., Pandey, K.N., Pang, S., Yamauchi, M., et al. (1999). The natriuretic peptide clearance receptor locally modulates the physiological effects of the natriuretic peptide system. Proc. Natl. Acad. Sci. U. S. A. *96*: 7403–7408.

Matsusaka, S., and Wakabayashi, I. (2005). 5-Hydroxytryptamine augments migration of human aortic smooth muscle cells through activation of RhoA and

ERK. Biochem. Biophys. Res. Commun. *337*: 916–921.

Mauritz, G.J., Vonk-Noordegraaf, A., Kind, T., Surie, S., Kloek, J.J., Bresser, P., et al. (2012). Pulmonary endarterectomy normalizes interventricular dyssynchrony and right ventricular systolic wall stress. J. Cardiovasc. Magn. Reson. *14*:.

Mayer, E., Jenkins, D., Lindner, J., D'Armini, A., Kloek, J., Meyns, B., et al. (2011). Surgical management and outcome of patients with chronic thromboembolic pulmonary hypertension: Results from an international prospective registry. J. Thorac. Cardiovasc. Surg. *141*: 702–710.

McGoon, M.D., and Miller, D.P. (2012). REVEAL: A contemporary US pulmonary arterial hypertension registry. Eur. Respir. Rev. *21*: 8–18.

McGrath, M.F., Kuroski De Bold, M.L., and Bold, A.J. De (2005). The endocrine function of the heart. Trends Endocrinol. Metab. *16*: 469–477.

McLaughlin, V., Channick, R.N., Ghofrani, H.A., Lemarié, J.C., Naeije, R., Packer, M., et al. (2015). Bosentan added to sildenafil therapy in patients with pulmonary arterial hypertension. Eur. Respir. J. *46*: 405–413.

McLaughlin, V. V., Archer, S.L., Badesch, D.B., Barst, R.J., Farber, H.W., Lindner, J.R., et al. (2009). A report of the american college of cardiology foundation task force on expert consensus documents and the american heart association. Circulation *119*: 2250–2294.

McMurray, J.J.V., Packer, M., Desai, A.S., Gong, J., Lefkowitz, M.P., Rizkala, A.R., et al. (2014). Angiotensin-neprilysin inhibition versus enalapril in heart failure. N. Engl. J. Med. *371*: 993–1004.

Medarametla, V., Festin, S., Sugarragchaa, C., Eng, A., Naqwi, A., Wiedmann, T., et al. (2014). Pk10453, a nonselective platelet-derived growth factor receptor inhibitor, prevents the progression of pulmonary arterial hypertension. Pulm. Circ. *4*: 82–102.

Meloche, J., Pflieger, A., Vaillancourt, M., Paulin, R., Potus, F., Zervopoulos, S., et al. (2014). Role for DNA damage signaling in pulmonary arterial hypertension. Circulation *129*: 786–797.

Meloche, J., Potus, F., Vaillancourt, M., Bourgeois, A., Johnson, I., Deschamps, L., et al. (2015). Bromodomain-containing protein 4: The epigenetic origin of pulmonary arterial hypertension. Circ. Res. *117*: 525–535.

Mendonça, M.C., Koles, N., Doi, S.Q., and Sellitti, D.F. (2010). Transforming growth factor-β 1 regulation of C-type natriuretic peptide expression in human vascular smooth muscle cells: Dependence on TSC22D1. Am. J. Physiol. - Hear. Circ. Physiol. *299*:.

Meo, S. Di, Reed, T.T., Venditti, P., and Victor, V.M. (2016). Role of ROS and RNS Sources in Physiological and Pathological Conditions. Oxid. Med. Cell. Longev. *2016*:.

Michel, K., Herwig, M., Werner, F., Spes, K.Š., Abeßer, M., Schuh, K., et al. (2020). C-type natriuretic peptide moderates titin-based cardiomyocyte stiffness. JCI Insight *5*:.

Michelakis, E.D., Gurtu, V., Webster, L., Barnes, G., Watson, G., Howard, L., et al. (2017). Inhibition of pyruvate dehydrogenase kinase improves pulmonary arterial hypertension in genetically susceptible patients. Sci. Transl. Med. *9*:.

Migneault, A., Sauvageau, S., Villeneuve, L., Thorin, E., Fournier, A., Leblanc, N., et al. (2005). Chronically elevated endothelin levels reduce pulmonary vascular reactivity to nitric oxide. Am. J. Respir. Crit. Care Med. *171*: 506–513.

Minami, M., Arita, T., Iwasaki, H., Muta, T., Aoki, T., Aoki, K., et al. (2017). Comparative analysis of pulmonary hypertension in patients treated with imatinib, nilotinib and dasatinib. Br. J. Haematol. *177*: 578–587.

Minamino, N., Makino, Y., Tateyama, H., Kangawa, K., and Matsuo, H. (1991). Characterization of immunoreactive human C-type natriuretic peptide in brain and heart. Biochem. Biophys. Res. Commun. *179*: 535–542.

Misono, K.S. (2002). Natriuretic peptide receptor: Structure and signaling. Mol. Cell. Biochem. *230*: 49–60.

Misono, K.S., Philo, J.S., Arakawa, T., Ogata, C.M., Qiu, Y., Ogawa, H., et al. (2011). Structure, signaling mechanism and regulation of the natriuretic peptide

receptor guanylate cyclase. FEBS J. *278*: 1818–1829.

Mitani, Y., Ueda, M., Maruyama, K., Shimpo, H., Kojima, A., Matsumura, M., et al. (1999). Mast cell chymase in pulmonary hypertension. Thorax *54*: 88–90.

Mitchell, J.A., Ali, F., Bailey, L., Moreno, L., and Harrington, L.S. (2008). Role of nitric oxide and prostacyclin as vasoactive hormones released by the endothelium. Exp. Physiol. *93*: 141–147.

Miyazaki, T., Otani, K., Chiba, A., Nishimura, H., Tokudome, T., Takano-Watanabe, H., et al. (2018). A new secretory peptide of natriuretic peptide family, osteocrin, suppresses the progression of congestive heart failure after myocardial infarction. Circ. Res. *122*: 742–751.

Miyazawa, T., Ogawa, Y., Chusho, H., Yasoda, A., Tamura, N., Komatsu, Y., et al. (2002). Cyclic GMP-dependent protein kinase II plays a critical role in C-type natriuretic peptide-mediated endochondral ossification. Endocrinology *143*: 3604–3610.

Moltzau, L.R., Aronsen, J.M., Meier, S., Nguyen, C.H.T., Hougen, K., Ørstavik, et al. (2013). SERCA2 activity is involved in the CNP-mediated functional responses in failing rat myocardium. Br. J. Pharmacol. *170*: 366–379.

Moltzau, L.R., Aronsen, J.M., Meier, S., Skogestad, J., Ørstavik, Ø., Lothe, G.B., et al. (2014). Different compartmentation of responses to brain natriuretic peptide and c-type natriuretic peptide in failing rat ventricle. J. Pharmacol. Exp. Ther. *350*: 681–690.

Moncada, S., Higgs, E.A., and Vane, J.R. (1977). Human Arterial and Venous Tissues Generate Prostacyclin (Prostaglandin X), a Potent Inhibitor of Platelet Aggregation. Lancet *309*: 18–21.

Montani, D., Chaumais, M.C., Guignabert, C., Günther, S., Girerd, B., Jaïs, X., et al. (2014). Targeted therapies in pulmonary arterial hypertension. Pharmacol. Ther. *141*: 172–191.

Montani, D., Perros, F., Gambaryan, N., Girerd, B., Dorfmuller, P., Price, L.C., et al. (2011). C-kit-positive cells accumulate in remodeled vessels of idiopathic

pulmonary arterial hypertension. Am. J. Respir. Crit. Care Med. *184*: 116–123.

Montani, D., Savale, L., Natali, D., Jaïs, X., Herve, P., Garcia, G., et al. (2010). Long-term response to calcium-channel blockers in non-idiopathic pulmonary arterial hypertension. Eur. Heart J. *31*: 1898–1907.

Monte, F. Del, Harding, S.E., Schmidt, U., Matsui, T., Kang, Z. Bin, Dec, G.W., et al. (1999). Restoration of contractile function in isolated cardiomyocytes from failing human hearts by gene transfer of SERCA2a. Circulation *100*: 2308–2311.

Morecroft, I., Loughlin, L., Nilsen, M., Colston, J., Dempsie, Y., Sheward, J., et al. (2005). Functional interactions between 5-hydroxytryptamine receptors and the serotonin transporter in pulmonary arteries. J. Pharmacol. Exp. Ther. *313*: 539–548.

Morgado, M., Cairrão, E., Santos-Silva, A.J., and Verde, I. (2012). Cyclic nucleotide-dependent relaxation pathways in vascular smooth muscle. Cell. Mol. Life Sci. *69*: 247–266.

Morrell, N.W. (2006). Pulmonary hypertension due to BMPR2 mutation: A new paradigm for tissue remodeling? Proc. Am. Thorac. Soc. *3*: 680–686.

Morris, H., Denver, N., Gaw, R., Labazi, H., Mair, K., and MacLean, M.R. (2021). Sex Differences in Pulmonary Hypertension. Clin. Chest Med. *42*: 217–228.

Morty, R.E., Nejman, B., Kwapiszewska, G., Hecker, M., Zakrzewicz, A., Kouri, F.M., et al. (2007). Dysregulated bone morphogenetic protein signaling in monocrotaline-induced pulmonary arterial hypertension. Arterioscler. Thromb. Vasc. Biol. *27*: 1072–1078.

Moser, K.M., and Bloor, C.M. (1993). Pulmonary vascular lesions occurring in patients with chronic major vessel thromboembolic pulmonary hypertension. Chest *103*: 685–692.

Moyes, A.J., Chu, S.M., Aubdool, A.A., Dukinfield, M.S., Margulies, K.B., Bedi, K.C., et al. (2020). C-type natriuretic peptide co-ordinates cardiac structure and function. Eur. Heart J. *41*: 1006–1020.

Moyes, A.J., and Hobbs, A.J. (2019). C-type natriuretic peptide: A multifaceted

paracrine regulator in the heart and vasculature. Int. J. Mol. Sci. *20*:.

Moyes, A.J., Khambata, R.S., Villar, I., Bubb, K.J., Baliga, R.S., Lumsden, N.G., et al. (2014). Endothelial C-type natriuretic peptide maintains vascular homeostasis. J. Clin. Invest. *124*: 4039–4051.

Murakami, S., Nagaya, N., Itoh, T., Fujii, T., Iwase, T., Hamada, K., et al. (2004). C-type natriuretic peptide attenuates bleomycin-induced pulmonary fibrosis in mice. Am. J. Physiol. - Lung Cell. Mol. Physiol. *287*: L1172-7.

Murray, F., MacLean, M.R., and Pyne, N.J. (2002). Increased expression of the cGMP-inhibited cAMP-specific (PDE3) and cGMP binding cGMP-specific (PDE5) phosphodiesterases in models of pulmonary hypertension. Br. J. Pharmacol. *137*: 1187–1194.

Murthy, K.S., and Makhlouf, G.M. (1999). Identification of the G protein-activating domain of the natriuretic peptide clearance receptor (NPR-C). J. Biol. Chem. *274*: 17587–17592.

Murthy, K.S., Teng, B.Q., Zhou, H., Jin, J.G., Grider, J.R., and Makhlouf, G.M. (2000). G(i)-1/G(i)-2-dependent signaling by single-transmembrane natriuretic peptide clearance receptor. Am. J. Physiol. - Gastrointest. Liver Physiol. *278*: G974-80.

Nagendran, J., Archer, S.L., Soliman, D., Gurtu, V., Moudgil, R., Haromy, A., et al. (2007). Phosphodiesterase type 5 is highly expressed in the hypertrophied human right ventricle, and acute inhibition of phosphodiesterase type 5 improves contractility. Circulation *116*: 238–248.

Nakao, A., Fujii, M., Matsumura, R., Kumano, K., Saito, Y., Miyazono, K., et al. (1999). Transient gene transfer and expression of Smad7 prevents bleomycin-induced lung fibrosis in mice. J. Clin. Invest. *104*: 5–11.

Nakao, K.K., Kuwahara, K., Nishikimi, T., Nakagawa, Y., Kinoshita, H., Minami, T., et al. (2017). Endothelium-Derived C-Type Natriuretic Peptide Contributes to Blood Pressure Regulation by Maintaining Endothelial Integrity. Hypertension *69*: 286–296.

Nathan, S.D., Barbera, J.A., Gaine, S.P., Harari, S., Martinez, F.J., Olschewski, H., et al. (2019). Pulmonary hypertension in chronic lung disease and hypoxia. Eur. Respir. J. *53*:.

Nawa, N., Ishida, H., Katsuragi, S., Baden, H., Takahashi, K., Higeno, R., et al. (2016). Constitutively active form of natriuretic peptide receptor 2 ameliorates experimental pulmonary arterial hypertension. Mol. Ther. - Methods Clin. Dev. *3*: 16044.

Nazario, B., Hu, R.M., Pedram, A., Prins, B., and Levin, E.R. (1995). Atrial and brain natriuretic peptides stimulate the production and secretion of C-type natriuretic peptide from bovine aortic endothelial cells. J. Clin. Invest. *95*: 1151–1157.

Neutel, J., Rolston, W., Maddock, S., Goldsmith, S., Koren, M., Bill, V.A., et al. (2012). Initial Experience With Subcutaneous Infusion of Cenderitide in Patients With Chronic Heart Failure. J. Am. Coll. Cardiol. *59*: E1037.

Nickel, N.P., Spiekerkoetter, E., Gu, M., Li, C.G., Li, H., Kaschwich, M., et al. (2015). Elafin reverses pulmonary hypertension via caveolin-1-dependent bone morphogenetic protein signaling. Am. J. Respir. Crit. Care Med. *191*: 1273–1286.

Nogueira-Ferreira, R., Ferreira, R., and Henriques-Coelho, T. (2014). Cellular interplay in pulmonary arterial hypertension: Implications for new therapies. Biochim. Biophys. Acta - Mol. Cell Res. *1843*: 885–893.

Northridge, D.B., Alabaster, C.T., Connell, J.M.C., Dilly, S.G., Lever, A.F., Jardine, A.G., et al. (1989). Effects of Uk 69 578: a Novel Atriopeptidase Inhibitor. Lancet *334*: 591–593.

Nunes, K.P., Rigsby, C.S., and Webb, R.C. (2010). RhoA/Rho-kinase and vascular diseases: What is the link? Cell. Mol. Life Sci. *67*: 3823–3836.

Nussenzveig, D.R., Lewicki, J.A., and Maack, T. (1990). Cellular mechanisms of the clearance function of type C receptors of atrial natriuretic factor. J. Biol. Chem. *265*: 20952–20958.

O'Connor, C.M., Gattis, W.A., Gheorghiade, M., Granger, C.B., Gilbert, J.,

McKenney, J.M., et al. (1999). A randomized trial of ecadotril versus placebo in patients with mild to moderate heart failure: The U.S. Ecadotril Pilot Safety Study. Am. Heart J. *138*: 1140–1148.

Ogawa, A., Firth, A.L., Yao, W., Madani, M.M., Kerr, K.M., Auger, W.R., et al. (2009). Inhibition of mTOR attenuates store-operated Ca2+ entry in cells from endarterectomized tissues of patients with chronic thromboembolic pulmonary hypertension. Am. J. Physiol. - Lung Cell. Mol. Physiol. *297*:.

Ogawa, H., Qiu, Y., Ogata, C.M., and Misono, K.S. (2004). Crystal structure of hormone-bound atrial natriuretic peptide receptor extracellular domain. Rotation mechanism for transmembrane signal transduction. J. Biol. Chem. *279*: 28625–28631.

Ogawa, Y., Itoh, H., Yoshitake, Y., Inoue, M., Yoshimasa, T., Serikawa, T., et al. (1994). Molecular cloning and chromosomal assignment of the mouse C-Type natriuretic peptide (CNP) gene (NPPC): Comparison with the human CNP gene (NPPC). Genomics *24*: 383–387.

Ohno, N., Itoh, H., Ikeda, T., Ueyama, K., Yamahara, K., Doi, K., et al. (2002). Accelerated reendothelialization with suppressed thrombogenic property and neointimal hyperplasia of rabbit jugular vein grafts by adenovirus-mediated gene transfer of C-type natriuretic peptide. Circulation *105*: 1623–1626.

Okada, M., Harada, T., Kikuzuki, R., Yamawaki, H., and Hara, Y. (2009). Effects of telmisartan on right ventricular remodeling induced by monocrotaline in rats. J. Pharmacol. Sci. *111*: 193–200.

Olsson, K.M., Fuge, J., Brod, T., Kamp, J.C., Schmitto, J., Kempf, T., et al. (2020). Oral iron supplementation with ferric maltol in patients with pulmonary hypertension. Eur. Respir. J. *56*:.

Ono, K., Mannami, T., Baba, S., Tomoike, H., Suga, S.I., and Iwai, N. (2002). A single-nucleotide polymorphism in C-type natriuretic peptide gene may be associated with hypertension. Hypertens. Res. *25*: 727–730.

Oudiz, R.J., Meyer, C., Chin, M., Feldman, J., Goldsberry, A., Mcconnell, J.W., et

al. (2017). Results Of Interim Analysis Of The Efficacy And Safety Of Bardoxolone Methyl In Patients With Pulmonary Arterial Hypertension Associated With Connective Tissue Disease (ctd) (the Lariat Study). C106. MONEY DON'T MATTER TONIGHT Pulm. Hypertens. ASSESSMENT, Progn. Treat. *10*:.

Overbeek, M.J., Lankhaar, J.W., Westerhof, N., Voskuyl, A.E., Boonstra, A., Bronzwaer, J.G.F., et al. (2008a). Right ventricular contractility in systemic sclerosis-associated and idiopathic pulmonary arterial hypertension. Eur. Respir. J. *31*: 1160–1166.

Overbeek, M.J., Vonk, M.C., Boonstra, A., Voskuyl, A.E., Vonk-Noordegraaf, A., Smit, E.F., et al. (2008b). Pulmonary arterial hypertension in limited cutaneous systemic sclerosis: A distinctive vasculopathy. Eur. Respir. J. *34*: 371–379.

Packer, M., Califf, R.M., Konstam, M.A., Krum, H., McMurray, J.J., Rouleau, J.L., et al. (2002). Comparison of omapatrilat and enalapril in patients with chronic heart failure: The omapatrilat versus enalapril randomized trial of utility in reducing events (OVERTURE). Circulation *106*: 920–926.

Packer, M., McMurray, J.J.V., Desai, A.S., Gong, J., Lefkowitz, M.P., Rizkala, A.R., et al. (2015). Angiotensin receptor neprilysin inhibition compared with enalapril on the risk of clinical progression in surviving patients with heart failure. Circulation *131*: 54–61.

Paddenberg, R., Stieger, P., Lilien, A.L. von, Faulhammer, P., Goldenberg, A., Tillmanns, H.H., et al. (2007). Rapamycin attenuates hypoxia-induced pulmonary vascular remodeling and right ventricular hypertrophy in mice. Respir. Res. *8*:.

Pagano, M., and Anand-Srivastava, M.B. (2001). Cytoplasmic Domain of Natriuretic Peptide Receptor C Constitutes G i Activator Sequences That Inhibit Adenylyl Cyclase Activity. J. Biol. Chem. *276*: 22064–22070.

Pak, O., Scheibe, S., Esfandiary, A., Gierhardt, M., Sydykov, A., Logan, A., et al. (2018). Impact of the mitochondria-targeted antioxidant MitoQ on hypoxia-induced pulmonary hypertension. Eur. Respir. J. *51*:.

Palmer, S.C., Prickett, T.C.R., Espiner, E.A., Yandle, T.G., and Richards, A.M.

(2009). Regional release and clearance of C-type natriuretic peptides in the human circulation and relation to cardiac function. Hypertension *54*: 612–618.

Paralkar, V., Pearson, P., Mason, J.W., Li, S.-X., Curry, S., Aiello, R., et al. (2017). Kar5585 a first-in-class oral tryptophan hydroxylase 1 (TPH1) inhibitor as a novel candidate for the treatment of pulmonary arterial hypertension. Am. J. Respir. Crit. Care Med. *195*:.

Paulin, R., Meloche, J., Jacob, M.H., Bisserier, M., Courboulin, A., and Bonnet, S. (2011). Dehydroepiandrosterone inhibits the Src/STAT3 constitutive activation in pulmonary arterial hypertension. Am. J. Physiol. - Hear. Circ. Physiol. *301*:.

Paulin, R., and Michelakis, E.D. (2014). The metabolic theory of pulmonary arterial hypertension. Circ. Res. *115*: 148–164.

Peng, W., Hoidal, J.R., and Farrukh, I.S. (1999). Role of a novel KCa opener in regulating K+ channels of hypoxic human pulmonary vascular cells. Am. J. Respir. Cell Mol. Biol. *20*: 737–745.

Pepke-Zaba, J., Delcroix, M., Lang, I., Mayer, E., Jansa, P., Ambroz, D., et al. (2011). Chronic thromboembolic pulmonary hypertension (CTEPH): Results from an international prospective registry. Circulation *124*: 1973–1981.

Pereira, N.L., Redfield, M.M., Scott, C., Tosakulwong, N., Olson, T.M., Bailey, K.R., et al. (2014). A functional genetic variant (N521D) in natriuretic peptide receptor 3 is associated with diastolic dysfunction: The prevalence of asymptomatic ventricular dysfunction study. PLoS One *9*:.

Perez-Ternero, C., Aubdool, A.A., Makwana, R., Sanger, G.J., Stimson, R.H., Chan, L.F., et al. (2022). C-type natriuretic peptide is a pivotal regulator of metabolic homeostasis. Proc. Natl. Acad. Sci. U. S. A. *119*:.

Perros, F., Dorfmüller, P., Montani, D., Hammad, H., Waelput, W., Girerd, B., et al. (2012). Pulmonary lymphoid neogenesis in idiopathic pulmonary arterial hypertension. Am. J. Respir. Crit. Care Med. *185*: 311–321.

Perros, F., Günther, S., Ranchoux, B., Godinas, L., Antigny, F., Chaumais, M.C., et al. (2015). Mitomycin-induced pulmonary veno-occlusive disease: Evidence

from human disease and animal models. Circulation *132*: 834–847.

Perros, F., Montani, D., Dorfmüller, P., Durand-Gasselin, I., Tcherakian, C., Pavec, J. Le, et al. (2008). Platelet-derived growth factor expression and function in idiopathic pulmonary arterial hypertension. Am. J. Respir. Crit. Care Med. *178*: 81–88.

Perros, F., Sentenac, P., Boulate, D., Manaud, G., Kotsimbos, T., Lecerf, F., et al. (2019). Smooth Muscle Phenotype in Idiopathic Pulmonary Hypertension: Hyper-Proliferative but not Cancerous. Int. J. Mol. Sci. *20*:.

Petkov, V., Mosgoeller, W., Ziesche, R., Raderer, M., Stiebellehner, L., Vonbank, K., et al. (2003). Vasoactive intestinal peptide as a new drug for treatment of primary pulmonary hypertension. J. Clin. Invest. *111*: 1339–1346.

Pfeffer, M.A., Lopes, A.A., Maeda, N.Y., and Gon[ccedil]alves, R.C. (2000). Endothelial cell dysfunction correlates differentially with survival in primary and secondary pulmonary hypertension. Am. Heart J. *139*: 0618–0623.

Piao, L., Fang, Y.H., Cadete, V.J.J., Wietholt, C., Urboniene, D., Toth, P.T., et al. (2010). The inhibition of pyruvate dehydrogenase kinase improves impaired cardiac function and electrical remodeling in two models of right ventricular hypertrophy: Resuscitating the hibernating right ventricle. J. Mol. Med. *88*: 47–60.

Pierkes, M., Gambaryan, S., Bokník, P., Lohmann, S.M., Schmitz, W., Potthast, R., et al. (2002). Increased effects of C-type natriuretic peptide on cardiac ventricular contractility and relaxation in guanylyl cyclase A-deficient mice. Cardiovasc. Res. *53*: 852–861.

Pietra, G.G., Capron, F., Stewart, S., Leone, O., Humbert, M., Robbins, I.M., et al. (2004). Pathologic assessment of vasculopathies in pulmonary hypertension. J. Am. Coll. Cardiol. *43*: S25–S32.

Pistelli, M., Mora, A. Della, Ballatore, Z., and Berardi, R. (2018). Aromatase inhibitors in premenopausal women with breast cancer: The state of the art and future prospects. Curr. Oncol. *25*: e168–e175.

Pogoriler, J.E., Rich, S., Archer, S.L., and Husain, A.N. (2012). Persistence of

complex vascular lesions despite prolonged prostacyclin therapy of pulmonary arterial hypertension. Histopathology *61*: 597–609.

Poiani, G.J., Tozzi, C.A., Yohn, S.E., Pierce, R.A., Belsky, S.A., Berg, R.A., et al. (1990). Collagen and elastin metabolism in hypertensive pulmonary arteries of rats. Circ. Res. *66*: 968–978.

Pollock, D.M., Keith, T.L., and Highsmith, R.F. (1995). Endothelin receptors and calcium signaling 1 . FASEB J. *9*: 1196–1204.

Porter, J.G., Arfsten, A., Fuller, F., Miller, J.A., Gregory, L.C., and Lewicki, J.A. (1990). Isolation and functional expression of the human atrial natriuretic peptide clearance receptor cDNA. Biochem. Biophys. Res. Commun. *171*: 796–803.

Potter, L.R. (1998). Phosphorylation-dependent regulation of the guanylyl cyclase-linked Natriuretic Peptide Receptor B: Dephosphorylation is a mechanism of desensitization. Biochemistry *37*: 2422–2429.

Potter, L.R. (2011). Natriuretic peptide metabolism, clearance and degradation. FEBS J. *278*: 1808–1817.

Potter, L.R., Abbey-Hosch, S., and Dickey, D.M. (2006). Natriuretic peptides, their receptors, and cyclic guanosine monophosphate-dependent signaling functions. Endocr. Rev. *27*: 47–72.

Potter, L.R., and Hunter, T. (1998). Identification and characterization of the major phosphorylation sites of the B-type natriuretic peptide receptor. J. Biol. Chem. *273*: 15533–15539.

Potter, L.R., and Hunter, T. (2000). Activation of protein kinase C stimulates the dephosphorylation of natriuretic peptide receptor-B at a single serine residue a possible mechanism of heterologous desensitization. J. Biol. Chem. *275*: 31099–31106.

Potter, L.R., Yoder, A.R., Flora, D.R., Antos, L.K., and Dickey, D.M. (2009). Natriuretic peptides: Their structures, receptors, physiologic functions and therapeutic applications. Handb. Exp. Pharmacol. *191*: 341–366.

Potthast, R., Abbey-Hosch, S.E., Antos, L.K., Marchant, J.S., Kuhn, M., and Potter,

L.R. (2004). Calcium-dependent dephosphorylation mediates the hyperosmotic and lysophosphatidic acid-dependent inhibition of natriuretic peptide receptor-B/guanylyl cyclase-B. J. Biol. Chem. *279*: 48513–48519.

Preston, I.R., Sagliani, K.D., Warburton, R.R., Hill, N.S., Fanburg, B.L., and Jaffe, I.Z. (2013). Mineralocorticoid receptor antagonism attenuates experimental pulmonary hypertension. Am. J. Physiol. - Lung Cell. Mol. Physiol. *304*:.

Prickett, T.C., and Espiner, E.A. (2020). Circulating products of C-type natriuretic peptide and links with organ function in health and disease. Peptides *132*:.

Prickett, T.C.R., Olney, R.C., Cameron, V.A., Ellis, M.J., Richards, A.M., and Espiner, E.A. (2013). Impact of age, phenotype and cardio-renal function on plasma C-type and B-type natriuretic peptide forms in an adult population. Clin. Endocrinol. (Oxf). *78*: 783–789.

Prickett, T.C.R., Yandle, T.G., Nicholls, M.G., Espiner, E.A., and Richards, A.M. (2001). Identification of amino-terminal pro-C-type natriuretic peptide in human plasma. Biochem. Biophys. Res. Commun. *286*: 513–517.

Prins, K.W., Weir, E.K., Archer, S.L., Markowitz, J., Rose, L., Pritzker, M., et al. (2016). Pulmonary pulse wave transit time is associated with right ventricular–pulmonary artery coupling in pulmonary arterial hypertension. Pulm. Circ. *6*: 576–585.

Provencher, S., Potus, F., Blais-Lecours, P., Bernard, S., Martineau, S., Breuils-Bonnet, S., et al. (2022). BET Protein Inhibition for Pulmonary Arterial Hypertension: A Pilot Clinical Trial. Am. J. Respir. Crit. Care Med. *205*: 1357–1360.

Pulido, T., Adzerikho, I., Channick, R.N., Delcroix, M., Galiè, N., Ghofrani, H.A., et al. (2013). Macitentan and morbidity and mortality in pulmonary arterial hypertension. N. Engl. J. Med. *369*: 809–818.

Pullamsetti, S., Kiss, L., Ghofrani, H.A., Voswinckel, R., Haredza, P., Klepetko, W., et al. (2005). Increased levels and reduced catabolism of asymmetric and symmetric dimethylarginines in pulmonary hypertension. FASEB J. *19*: 1175–1177.

Pullamsetti, S.S., Schermuly, R., Ghofrani, A., Weissmann, N., Grimminger, F., and Seeger, W. (2014). Novel and emerging therapies for pulmonary hypertension. Am. J. Respir. Crit. Care Med. *189*: 394–400.

Qian, J.Y., Haruno, A., Asada, Y., Nishida, T., Saito, Y., Matsuda, T., et al. (2002). Local expression of C-type natriuretic peptide suppresses inflammation, eliminates shear stress-induced thrombosis, and prevents neointima formation through enhanced nitric oxide production in rabbit injured carotid arteries. Circ. Res. *91*: 1063–1069.

Rabinovitch, M. (2012). Molecular pathogenesis of pulmonary arterial hypertension. J. Clin. Invest. *122*: 4306–4313.

Rabinovitch, M., Bothwell, T., Hayakawa, B.N., Williams, W.G., Trusler, G.A., Rowe, R.D., et al. (1986). Pulmonary artery endothelial abnormalities in patients with congenital heart defects and pulmonary hypertension. A correlation of light with scanning electron microscopy and transmission electron microscopy. Lab. Investig. *55*: 632–653.

Rabinovitch, M., Guignabert, C., Humbert, M., and Nicolls, M.R. (2014). Inflammation and immunity in the pathogenesis of pulmonary arterial hypertension. Circ. Res. *115*: 165–175.

Rademaker, M.T., Charles, C.J., Espiner, E.A., Nicholls, M.G., Richards, A.M., and Kosoglou, T. (1996). Neutral endopeptidase inhibition: Augmented atrial and brain natriuretic peptide, haemodynamic and natriuretic responses in ovine heart failure. Clin. Sci. *91*: 283–291.

Radstake, T.R.D.J., Bon, L. van, Broen, J., Wenink, M., Santegoets, K., Deng, Y., et al. (2009). Increased frequency and compromised function of T regulatory cells in systemic sclerosis (SSc) is related to a diminished CD69 and TGFβ expression. PLoS One *4*:.

Rahmutula, D., and Gardner, D.G. (2005). C-type natriuretic peptide down-regulates expression of its cognate receptor in rat aortic smooth muscle cells. Endocrinology *146*: 4968–4974.

Rahmutula, D., Nakayama, T., Soma, M., Kosuge, K., Aoi, N., Izumi, Y., et al. (2002). Structure and polymorphisms of the human natriuretic peptide receptor C gene. Endocrine *17*: 85–90.

Rahmutula, D., Zhang, H., Wilson, E.E., and Olgin, J.E. (2019). Absence of natriuretic peptide clearance receptor attenuates TGF-β1-induced selective atrial fibrosis and atrial fibrillation. Cardiovasc. Res. *115*: 357–372.

Rai, N., Veeroju, S., Schymura, Y., Janssen, W., Wietelmann, A., Kojonazarov, B., et al. (2018). Effect of Riociguat and Sildenafil on Right Heart Remodeling and Function in Pressure Overload Induced Model of Pulmonary Arterial Banding. Biomed Res. Int. *2018*:.

Rai, P.R., Cool, C.D., King, J.A.C., Stevens, T., Burns, N., Winn, R.A., et al. (2008). The cancer paradigm of severe pulmonary arterial hypertension. Am. J. Respir. Crit. Care Med. *178*: 558–564.

Ranchoux, B., Günther, S., Quarck, R., Chaumais, M.C., Dorfmüller, P., Antigny, F., et al. (2015). Chemotherapy-induced pulmonary hypertension: Role of alkylating agents. Am. J. Pathol. *185*: 356–371.

Ratre, P., Mishra, K., Dubey, A., Vyas, A., Jain, A., and Thareja, S. (2020). Aromatase Inhibitors for the Treatment of Breast Cancer: A Journey from the Scratch. Anticancer. Agents Med. Chem. *20*: 1994–2004.

Redout, E.M., Toorn, A. Van Der, Zuidwijk, M.J., Kolk, C.W.A. Van De, Echteld, C.J.A. Van, Musters, R.J.P., et al. (2010). Antioxidant treatment attenuates pulmonary arterial hypertension-induced heart failure. Am. J. Physiol. - Hear. Circ. Physiol. *298*:.

Redout, E.M., Wagner, M.J., Zuidwijk, M.J., Boer, C., Musters, R.J.P., Hardeveld, C. van, et al. (2007). Right-ventricular failure is associated with increased mitochondrial complex II activity and production of reactive oxygen species. Cardiovasc. Res. *75*: 770–781.

Reesink, H.J., Marcus, J.T., Tulevski, I.I., Jamieson, S., Kloek, J.J., Noordegraaf, A.V., et al. (2007). Reverse right ventricular remodeling after pulmonary

endarterectomy in patients with chronic thromboembolic pulmonary hypertension: Utility of magnetic resonance imaging to demonstrate restoration of the right ventricle. J. Thorac. Cardiovasc. Surg. *133*: 58–64.

Reis, G.S., Augusto, V.S., Silveira, A.P.C., Jordão, A.A., Baddini-Martinez, J., Poli Neto, O., et al. (2013). Oxidative-stress biomarkers in patients with pulmonary hypertension. Pulm. Circ. *3*: 856–861.

Ren, X., Johns, R.A., and Gao, W.D. (2019). Right heart in pulmonary hypertension: from adaptation to failure. Pulm. Circ. *9*:.

Rhodes, C.J., Ghataorhe, P., Wharton, J., Rue-Albrecht, K.C., Hadinnapola, C., Watson, G., et al. (2017). Plasma Metabolomics Implicates Modified Transfer RNAs and Altered Bioenergetics in the Outcomes of Pulmonary Arterial Hypertension. Circulation *135*: 460–475.

Rhodes, C.J., Howard, L.S., Busbridge, M., Ashby, D., Kondili, E., Gibbs, J.S.R., et al. (2011). Iron deficiency and raised hepcidin in idiopathic pulmonary arterial hypertension. J. Am. Coll. Cardiol. *58*: 300–309.

Rhodes, C.J., Otero-Núñez, P., Wharton, J., Swietlik, E.M., Kariotis, S., Harbaum, L., et al. (2020). Whole-blood RNA profiles associated with pulmonary arterial hypertension and clinical outcome. Am. J. Respir. Crit. Care Med. *202*: 586–594.

Ricard, N., Tu, L., Hiress, M. Le, Huertas, A., Phan, C., Thuillet, R., et al. (2014). Increased pericyte coverage mediated by endothelial-derived fibroblast growth factor-2 and interleukin-6 is a source of smooth muscle-like cells in pulmonary hypertension. Circulation *129*: 1586–1597.

Rich, S., Kaufmann, E., and Levy, P.S. (1992). The Effect of High Doses of Calcium-Channel Blockers on Survival in Primary Pulmonary Hypertension. N. Engl. J. Med. *327*: 76–81.

Richards, M., Espiner, E., Frampton, C., Ikram, H., Yandle, T., Sopwith, M., et al. (1990). Inhibition of endopeptidase EC 24.11 in humans: Renal and endocrine effects. Hypertension.

Richter, A., Yeager, M.E., Zaiman, A., Cool, C.D., Voelkel, N.F., and Tuder, R.M.

(2004). Impaired transforming growth factor-β signaling in idiopathic pulmonary arterial hypertension. Am. J. Respir. Crit. Care Med. *170*: 1340–1348.

Rocchetti, M., Sala, L., Rizzetto, R., Irene Staszewsky, L., Alemanni, M., Zambelli, V., et al. (2014). Ranolazine prevents INaL enhancement and blunts myocardial remodelling in a model of pulmonary hypertension. Cardiovasc. Res. *104*: 37–48.

Rol, N., Kurakula, K.B., Happé, C., Bogaard, H.J., and Goumans, M.J. (2018). TGF-β and BMPR2 signaling in PAH: Two black sheep in one family. Int. J. Mol. Sci. *19*:.

Rose-Jones, L., Mclaughlin, V., L.J., R.-J., and V.V., M. (2015). Pulmonary hypertension: Types and treatments. Curr. Cardiol. Rev. *11*: 73–79.

Rose, R.A., Lomax, A.E., Kondo, C.S., Anand-Srivastava, M.B., and Giles, W.R. (2004). Effects of C-type natriuretic peptide on ionic currents in mouse sinoatrial node: A role for the NPR-C receptor. Am. J. Physiol. - Hear. Circ. Physiol. *286*:.

Rosenberg, H.G., Williams, W.G., Trusler, G.A., Higa, T., and Rabinovitch, M. (1987). Structural composition of central pulmonary arteries: Growth potential after surgical shunts. J. Thorac. Cardiovasc. Surg. *94*: 498–503.

Rosenkranz, A.C., Woods, R.L., Dusting, G.J., and Ritchie, R.H. (2003). Antihypertrophic actions of the natriuretic peptides in adult rat cardiomyocytes: Importance of cyclic GMP. Cardiovasc. Res. *57*: 515–522.

Rosenkranz, S., Feldman, J., McLaughlin, V. V., Rischard, F., Lange, T.J., White, R.J., et al. (2022). Selonsertib in adults with pulmonary arterial hypertension (ARROW): a randomised, double-blind, placebo-controlled, phase 2 trial. Lancet Respir. Med. *10*: 35–46.

Ross, R.S., Pham, C., Shai, S.Y., Goldhaber, J.I., Fenczik, C., Glembotski, C.C., et al. (1998). β Integrins participate in the hypertrophic response of rat ventricular myocytes. Circ. Res. *82*: 1160–1172.

Rubens, C., Ewert, R., Halank, M., Wensel, R., Orzechowski, H.D., Schultheiss, H.P., et al. (2001). Big endothelin-1 and endothelin-1 plasma levels are correlated with the severity of primary pulmonary hypertension. Chest *120*: 1562–1569.

Rudski, L.G., Lai, W.W., Afilalo, J., Hua, L., Handschumacher, M.D., Chandrasekaran, K., et al. (2010). Guidelines for the Echocardiographic Assessment of the Right Heart in Adults: A Report from the American Society of Echocardiography. Endorsed by the European Association of Echocardiography, a registered branch of the European Society of Cardiology, and . J. Am. Soc. Echocardiogr. *23*: 685–713.

Ruffenach, G., Chabot, S., Tanguay, V.F., Courboulin, A., Boucherat, O., Potus, F., et al. (2016). Role for runt-related transcription factor 2 in proliferative and calcified vascular lesions in pulmonary arterial hypertension. Am. J. Respir. Crit. Care Med. *194*: 1273–1285.

Ruiter, G., Manders, E., Happé, C.M., Schalij, I., Groepenhoff, H., Howard, L.S., et al. (2015). Intravenous iron therapy in patients with idiopathic pulmonary arterial hypertension and iron deficiency. Pulm. Circ. *5*: 466–472.

Ruwhof, C., and Laarse, A. Van Der (2000). Mechanical stress-induced cardiac hypertrophy: Mechanisms and signal transduction pathways. Cardiovasc. Res. *47*: 23–37.

Ry, S. Del (2013). C-type natriuretic peptide: A new cardiac mediator. Peptides *40*: 93–98.

Ry, S. Del, Cabiati, M., and Clerico, A. (2013). Recent advances on natriuretic peptide system: New promising therapeutic targets for the treatment of heart failure. Pharmacol. Res. *76*: 190–198.

Ry, S. Del, Cabiati, M., Lionetti, V., Emdin, M., Recchia, F.A., and Giannessi, D. (2008a). Expression of C-type natriuretic peptide and of its receptor NPR-B in normal and failing heart. Peptides *29*: 2208–2215.

Ry, S. Del, Cabiati, M., Vozzi, F., Battolla, B., Caselli, C., Forini, F., et al. (2011). Expression of C-type natriuretic peptide and its receptor NPR-B in cardiomyocytes. Peptides *32*: 1713–1718.

Ry, S. Del, Maltinti, M., Cabiati, M., Emdin, M., Giannessi, D., and Morales, M.A. (2008b). C-type natriuretic peptide and its relation to non-invasive indices of left

ventricular function in patients with chronic heart failure. Peptides *29*: 79–82.

Ry, S. Del, Maltinti, M., Piacenti, M., Passino, C., Emdin, M., and Giannessi, D. (2006). Cardiac production of C-type natriuretic peptide in heart failure. J. Cardiovasc. Med. *7*: 397–399.

Ry, S. Del, Passino, C., Maltinti, M., Emdin, M., and Giannessi, D. (2005). C-type natriuretic peptide plasma levels increase in patients with chronic heart failure as a function of clinical severity. Eur. J. Heart Fail. *7*: 1145–1148.

Ryan, J.J., and Archer, S.L. (2014). The right ventricle in pulmonary arterial hypertension: Disorders of metabolism, angiogenesis and adrenergic signaling in right ventricular failure. Circ. Res. *115*: 176–188.

Ryan, J.J., and Archer, S.L. (2015). Emerging concepts in the molecular basis of pulmonary arterial hypertension. Part I: Metabolic plasticity and mitochondrial dynamics in the pulmonary circulation and right ventricle in pulmonary arterial hypertension. Circulation *131*: 1691–1702.

Said, S.I. (2012). Vasoactive intestinal peptide in pulmonary arterial hypertension. Am. J. Respir. Crit. Care Med. *185*: 786.

Said, S.I., Hamidi, S.A., Dickman, K.G., Szema, A.M., Lyubsky, S., Lin, R.Z., et al. (2007). Moderate pulmonary arterial hypertension in male mice lacking the vasoactive intestinal peptide gene. Circulation *115*: 1260–1268.

Sakao, S., Taraseviciene-Stewart, L., Lee, J.D., Wood, K., Cool, C.D., and Voelkel, N.F. (2005). Initial apoptosis is followed by increased proliferation of apoptosis-resistant endothelial cells. FASEB J. *19*: 1178–1180.

Sakao, S., Tatsumi, K., and Voelkel, N.F. (2009). Endothelial cells and pulmonary arterial hypertension: Apoptosis, proliferation, interaction and transdifferentiation. Respir. Res. *10*:.

Saker, M., Lipskaia, L., Marcos, E., Abid, S., Parpaleix, A., Houssaini, A., et al. (2016). Osteopontin, a key mediator expressed by senescent pulmonary vascular cells in pulmonary hypertension. Arterioscler. Thromb. Vasc. Biol. *36*: 1879–1890.

Sakti Muliawan, H., Widyantoro, B., Soerarso, R., Hersunarti, N., Sahara, E.,

Atmadikoesoemah, C.A., et al. (2020). P194 Trimetazidine preserves right ventricular function on pulmonary arterial hypertension patients in national cardiovascular center harapan kita hospital indonesia. Eur. Heart J. *41*:.

Sanada, T.J., Sun, X.Q., Happé, C., Guignabert, C., Tu, L., Schalij, I., et al. (2021). Altered tgfβ/smad signaling in human and rat models of pulmonary hypertension: An old target needs attention. Cells *10*: 1–13.

Sanchez, O., Marcos, E., Perros, F., Fadel, E., Tu, L., Humbert, M., et al. (2007). Role of endothelium-derived CC chemokine ligand 2 in idiopathic pulmonary arterial hypertension. Am. J. Respir. Crit. Care Med. *176*: 1041–1047.

Sanchez, O., Sitbon, O., Jaï'S, X., Simonneau, G., and Humbert, M. (2006). Immunosuppressive therapy in connective tissue diseases-associated pulmonary arterial hypertension. Chest *130*: 182–189.

Sangaralingham, S.J., Huntley, B.K., Martin, F.L., McKie, P.M., Bellavia, D., Ichiki, T., et al. (2011). The aging heart, myocardial fibrosis, and its relationship to circulating C-type natriuretic peptide. Hypertension *57*: 201–207.

Sangaralingham, S.J., McKie, P.M., Ichiki, T., Scott, C.G., Heublein, D.M., Chen, H.H., et al. (2015). Circulating C-Type Natriuretic Peptide and Its Relationship to Cardiovascular Disease in the General Population. Hypertension *65*: 1187–1194.

Santamore, W.P., Lynch, P.R., Heckman, J.L., Bove, A.A., and Meier, G.D. (1976). Left ventricular effects on right ventricular developed pressure. J. Appl. Physiol. *41*: 925–930.

Sanz, J., Sánchez-Quintana, D., Bossone, E., Bogaard, H.J., and Naeije, R. (2019). Anatomy, Function, and Dysfunction of the Right Ventricle: JACC State-of-the-Art Review. J. Am. Coll. Cardiol. *73*: 1463–1482.

Sauvageau, S., Thorin, E., Caron, A., and Dupuis, J. (2007). Endothelin-1-induced pulmonary vasoreactivity is regulated by ET A and ETB receptor interactions. J. Vasc. Res. *44*: 375–381.

Savarirayan, R., Baratela, W., Butt, T., Cormier-Daire, V., Irving, M., Miller, B.S., et al. (2022). Literature review and expert opinion on the impact of achondroplasia

on medical complications and health-related quality of life and expectations for long-term impact of vosoritide: a modified Delphi study. Orphanet J. Rare Dis. *17*:.

Savarirayan, R., Irving, M., Bacino, C.A., Bostwick, B., Charrow, J., Cormier-Daire, V., et al. (2019). C-Type Natriuretic Peptide Analogue Therapy in Children with Achondroplasia. N. Engl. J. Med. *381*: 25–35.

Savarirayan, R., Tofts, L., Irving, M., Wilcox, W.R., Bacino, C.A., Hoover-Fong, J., et al. (2021a). Once-daily, subcutaneous vosoritide therapy in children with achondroplasia: a randomised, double-blind, phase 3, placebo-controlled, multicentre trial. Yearb. Paediatr. Endocrinol.

Savarirayan, R., Tofts, L., Irving, M., Wilcox, W.R., Bacino, C.A., Hoover-Fong, J., et al. (2021b). Safe and persistent growth-promoting effects of vosoritide in children with achondroplasia: 2-year results from an open-label, phase 3 extension study. Genet. Med. *23*: 2443–2447.

Savoie, P., Champlain, J. de, and Anand-Srivastava, M.B. (1995). C-type natriuretic peptide and brain natriuretic peptide inhibit adenylyl cyclase activity: interaction with ANF-R2/ANP-C receptors. FEBS Lett. *370*: 6–10.

Saxton, R.A., and Sabatini, D.M. (2017). mTOR Signaling in Growth, Metabolism, and Disease. Cell *169*: 361–371.

Schachner, T., Zou, Y., Oberhuber, A., Mairinger, T., Tzankov, A., Laufer, G., et al. (2004). Perivascular application of C-type natriuretic peptide attenuates neointimal hyperplasia in experimental vein grafts. Eur. J. Cardio-Thoracic Surg. *25*: 585–590.

Schermuly, R.T., Dony, E., Ghofrani, H.A., Pullamsetti, S., Savai, R., Roth, M., et al. (2005). Reversal of experimental pulmonary hypertension by PDGF inhibition. J. Clin. Invest. *115*: 2811–2821.

Schermuly, R.T., Ghofrani, H.A., Wilkins, M.R., and Grimminger, F. (2011). Mechanisms of disease: Pulmonary arterial hypertension. Nat. Rev. Cardiol. *8*: 443–455.

Schermuly, R.T., Kreisselmeier, K.P., Ghofrani, H.A., Samidurai, A., Pullamsetti, S., Weissmann, N., et al. (2004). Antiremodeling Effects of Iloprost and the Dual-

Selective Phosphodiesterase 3/4 Inhibitor Tolafentrine in Chronic Experimental Pulmonary Hypertension. Circ. Res. *94*: 1101–1108.

Schermuly, R.T., Stasch, J.P., Pullamsetti, S.S., Middendorff, R., Müller, D., Schlüter, K.D., et al. (2008). Expression and function of soluble guanylate cyclase in pulmonary arterial hypertension. Eur. Respir. J. *32*: 881–891.

Scherrer-Crosbie, M., and Thibault, H.B. (2008). Echocardiography in Translational Research: Of Mice and Men. J. Am. Soc. Echocardiogr. *21*: 1083–1092.

Schipke, J., Brandenberger, C., Rajces, A., Manninger, M., Alogna, A., Post, H., et al. (2017). Assessment of cardiac fibrosis: A morphometric method comparison for collagen quantification. J. Appl. Physiol. *122*: 1019–1030.

Schlossmann, J., Feil, R., and Hofmann, F. (2005). Insights into cGMP signalling derived from cGMP kinase knockout mice. Front. Biosci. *10*: 1279–1289.

Schulz, S. (2005). C-type natriuretic peptide and guanylyl cyclase B receptor. Peptides *26*: 1024–1034.

Schwanhüusser, B., Busse, D., Li, N., Dittmar, G., Schuchhardt, J., Wolf, J., et al. (2011). Global quantification of mammalian gene expression control. Nature *473*: 337–342.

Schweitz, H., Vigne, P., Moinier, D., Frelin, C., and Lazdunski, M. (1992). A new member of the natriuretic peptide family is present in the venom of the Green Mamba (Dendroaspis angusticeps). J. Biol. Chem. *267*: 13928–13932.

Scotland, R.S., Cohen, M., Foster, P., Lovell, M., Mathur, A., Ahluwalia, A., et al. (2005). C-type natriuretic peptide inhibits leukocyte recruitment and platelet-leukocyte interactions via suppression of P-selectin expression. Proc. Natl. Acad. Sci. U. S. A. *102*: 14452–14457.

Scott, T.E., Kemp-Harper, B.K., and Hobbs, A.J. (2019). Inflammasomes: a novel therapeutic target in pulmonary hypertension? Br. J. Pharmacol. *176*: 1880–1896.

Scott, T.E., Qin, C.X., Drummond, G.R., Hobbs, A.J., and Kemp-Harper, B.K. (2021). Innovative Anti-Inflammatory and Pro-resolving Strategies for Pulmonary

Hypertension: High Blood Pressure Research Council of Australia Award 2019. Hypertension 1168–1184.

Seo, B., Oemar, B.S., Siebenmann, R., Segesser, L. Von, and Luscher, T.F. (1994). Both ET(A) and ET(B) receptors mediate contraction to endothelin-1 in human blood vessels. Circulation *89*: 1203–1208.

Shapiro, S., Traiger, G.L., Turner, M., McGoon, M.D., Wason, P., and Barst, R.J. (2012). Sex differences in the diagnosis, treatment, and outcome of patients with pulmonary arterial hypertension enrolled in the registry to evaluate early and long-term pulmonary arterial hypertension disease management. Chest *141*: 363–373.

Sharp, J., Farha, S., Park, M.M., Comhair, S.A., Lundgrin, E.L., Tang, W.H.W., et al. (2014). Coenzyme Q supplementation in pulmonary arterial hypertension. Redox Biol. *2*: 884–891.

Sheikh, A.Q., Lighthouse, J.K., and Greif, D.M. (2014). Recapitulation of developing artery muscularization in pulmonary hypertension. Cell Rep. *6*: 809–817.

Sheikh, A.Q., Misra, A., Rosas, I.O., Adams, R.H., and Greif, D.M. (2015). Smooth muscle cell progenitors are primed to muscularize in pulmonary hypertension. Sci. Transl. Med. *7*:.

Shenoy, V., Qi, Y., Katovich, M.J., and Raizada, M.K. (2011). ACE2, a promising therapeutic target for pulmonary hypertension. Curr. Opin. Pharmacol. *11*: 150–155.

Shimoda, L.A., and Laurie, S.S. (2013). Vascular remodeling in pulmonary hypertension. J. Mol. Med. *91*: 297–309.

Shyy, J.Y.J., and Chien, S. (1997). Role of integrins in cellular responses to mechanical stress and adhesion. Curr. Opin. Cell Biol. *9*: 707–713.

Simon, M., Gomberg-Maitland, M., Oudiz, R.J., Machado, R., Rischard, F., Elinoff, J.M., et al. (2019). Severe Pulmonary Arterial Hypertension Treated with ABI-009, nab-Sirolimus, an mTOR Inhibitor. J. Hear. Lung Transplant. *38*: S487.

Simon, M.A., Hanrott, K., Budd, D.C., Torres, F., Grünig, E., Escribano-Subias, P.,

et al. (2022). An open-label, dose-escalation study to evaluate the safety, tolerability, pharmacokinetics, and pharmacodynamics of single doses of GSK2586881 in participants with pulmonary arterial hypertension. Pulm. Circ. *12*:.

Simonneau, G., D'Armini, A.M., Ghofrani, H.A., Grimminger, F., Jansa, P., Kim, N.H., et al. (2016). Predictors of long-term outcomes in patients treated with riociguat for chronic thromboembolic pulmonary hypertension: Data from the CHEST-2 open-label, randomised, long-term extension trial. Lancet Respir. Med. *4*: 372–380.

Simonneau, G., Montani, D., Celermajer, D.S., Denton, C.P., Gatzoulis, M.A., Krowka, M., et al. (2019). Haemodynamic definitions and updated clinical classification of pulmonary hypertension. Eur. Respir. J. *53*:.

Simonneau, G., Torbicki, A., Dorfmüller, P., and Kim, N. (2017). The pathophysiology of chronic thromboembolic pulmonary hypertension. Eur. Respir. Rev. *26*:.

Sitbon, O., Channick, R., Chin, K.M., Frey, A., Gaine, S., Galiè, N., et al. (2015). Selexipag for the treatment of pulmonary arterial hypertension. N. Engl. J. Med. *373*: 2522–2533.

Sitbon, O., Gomberg-Maitland, M., Granton, J., Lewis, M.I., Mathai, S.C., Rainisio, M., et al. (2019). Clinical trial design and new therapies for pulmonary arterial hypertension. Eur. Respir. J. *53*:.

Sitbon, O., Humbert, M., Jaïs, X., Ioos, V., Hamid, A.M., Provencher, S., et al. (2005). Long-term response to calcium channel blockers in idiopathic pulmonary arterial hypertension. Circulation *111*: 3105–3111.

Sitbon, O., and Vonk Noordegraaf, A. (2017). Epoprostenol and pulmonary arterial hypertension: 20 years of clinical experience. Eur. Respir. Rev. *26*:.

Skoro-Sajer, N., Mittermayer, F., Panzenboeck, A., Bonderman, D., Sadushi, R., Hitsch, R., et al. (2007). Asymmetric dimethylarginine is increased in chronic thromboembolic pulmonary hypertension. Am. J. Respir. Crit. Care Med. *176*: 1154–1160.

Skride, A., Sablinskis, K., Lejnieks, A., Rudzitis, A., and Lang, I. (2018). Characteristics and survival data from Latvian pulmonary hypertension registry: comparison of prospective pulmonary hypertension registries in Europe. Pulm. Circ. *8*:.

Smith, R.J., Perez-Ternero, C., Conole, D., Martin, C., Myers, S.H., Hobbs, A.J., et al. (2022). A Series of Substituted Bis-Aminotriazines Are Activators of the Natriuretic Peptide Receptor C. J. Med. Chem. *65*: 5495–5513.

Sodimu, A., Bartolome, S., Igenoza, O.P., and Chin, K.M. (2020). Hemodynamic effects of fluoxetine in pulmonary arterial hypertension: an open label pilot study. Pulm. Circ. *10*:.

Soeki, T., Kishimoto, I., Okumura, H., Tokudome, T., Horio, T., Mori, K., et al. (2005). C-type natriuretic peptide, a novel antifibrotic and antihypertrophic agent, prevents cardiac remodeling after myocardial infarction. J. Am. Coll. Cardiol. *45*: 608–616.

Soleilhac, J.M., Lucas, E., Beaumont, A., Turcaud, S., Michel, J.B., Ficheux, D., et al. (1992). A 94-kDa protein, identified as neutral endopeptidase-24.11, can inactivate atrial natriuretic peptide in the vascular endothelium. Mol. Pharmacol. *41*: 609–614.

Solomon, S.D., Zile, M., Pieske, B., Voors, A., Shah, A., Kraigher-Krainer, E., et al. (2012). The angiotensin receptor neprilysin inhibitor LCZ696 in heart failure with preserved ejection fraction: A phase 2 double-blind randomised controlled trial. Lancet *380*: 1387–1395.

Sommer, N., Ghofrani, H.A., Pak, O., Bonnet, S., Provencher, S., Sitbon, O., et al. (2021). Current and future treatments of pulmonary arterial hypertension. Br. J. Pharmacol. *178*: 6–30.

Soon, E., Holmes, A.M., Treacy, C.M., Doughty, N.J., Southgate, L., MacHado, R.D., et al. (2010). Elevated levels of inflammatory cytokines predict survival in idiopathic and familial pulmonary arterial hypertension. Circulation *122*: 920–927.

Souchelnytskyi, S., Nakayama, T., Nakao, A., Morén, A., Heldin, C.H., Christian,

J.L., et al. (1998). Physical and functional interaction of murine and Xenopus Smad7 with bone morphogenetic protein receptors and transforming growth factor-β receptors. J. Biol. Chem. *273*: 25364–25370.

Speich, R., Jenni, R., Opravil, M., Pfab, M., and Russi, E.W. (1991). Primary pulmonary hypertension in HIV infection. Chest *100*: 1268–1271.

Spiekerkoetter, E., Sung, Y.K., Sudheendra, D., Bill, M., Aldred, M.A., Veerdonk, M.C. Van De, et al. (2015). Low-dose FK506 (Tacrolimus) in end-stage pulmonary arterial hypertension. Am. J. Respir. Crit. Care Med. *192*: 254–257.

Spiekerkoetter, E., Sung, Y.K., Sudheendra, D., Scott, V., Rosario, P. Del, Bill, M., et al. (2017). Randomised placebo-controlled safety and tolerability trial of FK506 (tacrolimus) for pulmonary arterial hypertension. Eur. Respir. J. *50*: 1–12.

Spiekerkoetter, E., Tian, X., Cai, J., Hopper, R.K., Sudheendra, D., Li, C.G., et al. (2013). FK506 activates BMPR2, rescues endothelial dysfunction, and reverses pulmonary hypertension. J. Clin. Invest. *123*: 3600–3613.

Špiranec, K., Chen, W., Werner, F.K.A., Nikolaev, V.O., Naruke, T., Werner, F.K.A., et al. (2018). Endothelial C-type natriuretic peptide acts on pericytes to regulate microcirculatory flow and blood pressure. Circulation *138*: 494–508.

Stacher, E., Graham, B.B., Hunt, J.M., Gandjeva, A., Groshong, S.D., McLaughlin, V. V., et al. (2012). Modern age pathology of pulmonary arterial hypertension. Am. J. Respir. Crit. Care Med. *186*: 261–272.

Stamler, J.S., Loh, E., Roddy, M.A., Currie, K.E., and Creager, M.A. (1994). Nitric oxide regulates basal systemic and pulmonary vascular resistance in healthy humans. Circulation.

Stenmark, K.R., Davie, N., Frid, M., Gerasimovskaya, E., and Das, M. (2006). Role of the adventitia in pulmonary vascular remodeling. Physiology *21*: 134–145.

Stenmark, K.R., Frid, M.G., Graham, B.B., and Tuder, R.M. (2018). Dynamic and diverse changes in the functional properties of vascular smooth muscle cells in pulmonary hypertension. Cardiovasc. Res. *114*: 551–564.

Stenmark, K.R., Frid, M.G., Yeager, M., Li, M., Riddle, S., McKinsey, T., et al.

(2012). Targeting the adventitial microenvironment in pulmonary hypertension: A potential approach to therapy that considers epigenetic change. Pulm. Circ. *2*: 3–14.

Stenmark, K.R., Meyrick, B., Galie, N., Mooi, W.J., and McMurtry, I.F. (2009). Animal models of pulmonary arterial hypertension: The hope for etiological discovery and pharmacological cure. Am. J. Physiol. - Lung Cell. Mol. Physiol. *297*:.

Stenmark, K.R., Nozik-Grayck, E., Gerasimovskaya, E., Anwar, A., Li, M., Riddle, S., et al. (2011). The Adventitia: Essential Role in Pulmonary Vascular Remodeling. Compr. Physiol. *1*: 141–161.

Stenmark, K.R., Yeager, M.E., Kasmi, K.C. El, Nozik-Grayck, E., Gerasimovskaya, E. V., Li, M., et al. (2013). The Adventitia: Essential Regulator of Vascular Wall Structure and Function. Annu. Rev. Physiol. *75*: 23–47.

Steudel, W., Ichinose, F., Huang, P.L., Hurford, W.E., Jones, R.C., Bevan, J.A., et al. (1997). Pulmonary vasoconstriction and hypertension in mice with targeted disruption of the endothelial nitric oxide synthase (NOS 3) gene. Circ. Res. *81*: 34–41.

Stevens, G.R., Garcia-Alvarez, A., Sahni, S., Garcia, M.J., Fuster, V., and Sanz, J. (2012). RV dysfunction in pulmonary hypertension is independently related to pulmonary artery stiffness. JACC Cardiovasc. Imaging *5*: 378–387.

Stingo, A.J., Clavell, A.L., Heublein, D.M., Wei, C.M., Pittelkow, M.R., and Burnett, J.C. (1992). Presence of C-type natriuretic peptide in cultured human endothelial cells and plasma. Am. J. Physiol. - Hear. Circ. Physiol. *263*:.

Stolz, D., Rasch, H., Linka, A., Valentino, M. Di, Meyer, A., Brutsche, M., et al. (2008). A randomised, controlled trial of bosentan in severe COPD. Eur. Respir. J. *32*: 619–628.

Sudoh, T., Minamino, N., Kangawa, K., and Matsuo, H. (1990). C-Type natriuretic peptide (CNP): A new member of natriuretic peptide family identified in porcine brain. Biochem. Biophys. Res. Commun. *168*: 863–870.

Suga, S.I., Itoh, H., Komatsu, Y., Ogawa, Y., Hama, N., Yoshimasa, T., et al. (1993). Cytokine-induced C-type natriuretic peptide (CNP) secretion from vascular endothelial cells--evidence for CNP as a novel autocrine/paracrine regulator from endothelial cells. Endocrinology *133*: 3038–3041.

Suga, S.I., Nakao, K., Hosoda, K., Mukoyama, M., Ogawa, Y., Shirakami, G., et al. (1992a). Receptor selectivity of natriuretic peptide family, atrial natriuretic peptide, brain natriuretic peptide, and c-type natriuretic peptide. Endocrinology *130*: 229–239.

Suga, S.I., Nakao, K., Itoh, H., Komatsu, Y., Ogawa, Y., Hama, N., et al. (1992b). Endothelial production of C-type natriuretic peptide and its marked augmentation by transforming growth factor-β. Possible existence of 'vascular natriuretic peptide system'. J. Clin. Invest. *90*: 1145–1149.

Sugiyama, S., Kugiyama, K., Matsumura, T., Suga, S.I., Itoh, H., Nakao, K., et al. (1995). Lipoproteins regulate C-type natriuretic peptide secretion from cultured vascular endothelial cells. Arterioscler. Thromb. Vasc. Biol. *15*: 1968–1974.

Sun, J.Z., Chen, S.J., Li, G., and Chen, Y.F. (2000). Hypoxia reduces atrial natriuretic peptide clearance receptor gene expression in ANP knockout mice. Am. J. Physiol. - Lung Cell. Mol. Physiol. *279*:.

Sun, J.Z., Oparil, S., Lucchesi, P., Thompson, J.A., and Chen, Y.F. (2001). Tyrosine kinase receptor activation inhibits NPR-C in lung arterial smooth muscle cells. Am. J. Physiol. - Lung Cell. Mol. Physiol. *281*:.

Surie, S., Bouma, B.J., Bruin-Bon, R.A.H., Hardziyenka, M., Kloek, J.J., Plas, M.N. Van Der, et al. (2011). Time course of restoration of systolic and diastolic right ventricular function after pulmonary endarterectomy for chronic thromboembolic pulmonary hypertension. Am. Heart J. *161*: 1046–1052.

Sutendra, G., Bonnet, S., Rochefort, G., Haromy, A., Folmes, K.D., Lopaschuk, G.D., et al. (2010). Fatty acid oxidation and malonyl-CoA decarboxylase in the vascular remodeling of pulmonary hypertension. Sci. Transl. Med. *2*:.

Sutendra, G., Dromparis, P., Paulin, R., Zervopoulos, S., Haromy, A., Nagendran,

J., et al. (2013). A metabolic remodeling in right ventricular hypertrophy is associated with decreased angiogenesis and a transition from a compensated to a decompensated state in pulmonary hypertension. J. Mol. Med. *91*: 1315–1327.

Sztrymf, B., Souza, R., Bertoletti, L., Jaïs, X., Sitbon, O., Price, L.C., et al. (2010). Prognostic factors of acute heart failure in patients with pulmonary arterial hypertension. Eur. Respir. J. *35*: 1286–1293.

Takahashi, H., Goto, N., Kojima, Y., Tsuda, Y., Morio, Y., Muramatsu, M., et al. (2006). Downregulation of type II bone morphogenetic protein receptor in hypoxic pulmonary hypertension. Am. J. Physiol. - Lung Cell. Mol. Physiol. *290*:.

Takei, Y. (2001). Does the natriuretic peptide system exist throughout the animal and plant kingdom? Comp. Biochem. Physiol. - B Biochem. Mol. Biol. *129*: 559–573.

Tamura, N., Doolittle, L.K., Hammer, R.E., Shelton, J.M., Richardson, J.A., and Garbers, D.L. (2004). Critical roles of the guanylyl cyclase B receptor in endochondral ossification and development of female reproductive organs. Proc. Natl. Acad. Sci. U. S. A. *101*: 17300–17305.

Tamura, N., and Garbers, D.L. (2003). Regulation of the guanylyl cyclase-B receptor by alternative splicing. J. Biol. Chem. *278*: 48880–48889.

Tan, R., You, Q., Yu, D., Xiao, C., Adu-Amankwaah, J., Cui, J., et al. (2022). Novel hub genes associated with pulmonary artery remodeling in pulmonary hypertension. Front. Cardiovasc. Med. *9*:.

Taraseviciene-Stewart, L., Kasahara, Y., Alger, L., Hirth, P., Mahon, G.M., Waltenberger, J., et al. (2001). Inhibition of the VEGF receptor 2 combined with chronic hypoxia causes cell death-dependent pulmonary endothelial cell proliferation and severe pulmonary hypertension. FASEB J. *15*: 427–438.

Tawaragi, Y., Fuchimura, K., Tanaka, S., Minamino, N., Kangawa, K., and Matsuo, H. (1991). Gene and precursor structures of human C-type natriuretic peptide. Biochem. Biophys. Res. Commun. *175*: 645–651.

Teucher, N., Prestle, J., Seidler, T., Currie, S., Elliott, E.B., Reynolds, D.F., et al.

(2004). Excessive sarcoplasmic/endoplasmic reticulum Ca2+-ATPase expression causes increased sarcoplasmic reticulum Ca2+ uptake but decreases myocyte shortening. Circulation *110*: 3553–3559.

Thenappan, T., Chan, S.Y., and Weir, E.K. (2018a). Role of extracellular matrix in the pathogenesis of pulmonary arterial hypertension. Am. J. Physiol. - Hear. Circ. Physiol. *315*: H1322–H1331.

Thenappan, T., Ormiston, M.L., Ryan, J.J., and Archer, S.L. (2018b). Pulmonary arterial hypertension: Pathogenesis and clinical management. BMJ *360*:.

Thenappan, T., Prins, K.W., Pritzker, M.R., Scandurra, J., Volmers, K., and Weir, E.K. (2016). The critical role of pulmonary arterial compliance in pulmonary hypertension. Ann. Am. Thorac. Soc. *13*: 276–284.

Thenappan, T., Roy, S.S., Duval, S., Glassner-Kolmin, C., and Gomberg-Maitland, M. (2014). β-blocker therapy is not associated with adverse outcomes in patients with pulmonary arterial hypertension: a propensity score analysis. Circ. Hear. Fail. *7*: 903–910.

Thibault, H.B., Kurtz, B., Raher, M.J., Shaik, R.S., Waxman, A., Derumeaux, G., et al. (2010). Noninvasive assessment of murine pulmonary arterial pressure validation and application to models of pulmonary hypertension. Circ. Cardiovasc. Imaging *3*: 157–163.

Thompson, J.S., Sheedy, W., and Morice, A.H. (1994). Neutral endopeptidase (NEP) inhibition in rats with established pulmonary hypertension secondary to chronic hypoxia. Br. J. Pharmacol. *113*: 1121–1126.

Thompson, K., and Rabinovitch, M. (1996). Exogenous leukocyte and endogenous elastases can mediate mitogenic activity in pulmonary artery smooth muscle cells by release of extracellular matrix-bound basic fibroblast growth factor. J. Cell. Physiol. *166*: 495–505.

Tilton, R.G., Munsch, C.L., Sherwood, S.J., Chen, S.J., Chen, Y.F., Wu, C., et al. (2000). Attenuation of pulmonary vascular hypertension and cardiac hypertrophy with sitaxsentan sodium, an orally active ET(A) receptor antagonist. Pulm.

Pharmacol. Ther. *13*: 87–97.

Tio, D., Leter, E., Boerrigter, B., Boonstra, A., Vonk-Noordegraaf, A., and Bogaard, H.J. (2013). Risk Factors for Hemoptysis in Idiopathic and Hereditary Pulmonary Arterial Hypertension. PLoS One *8*:.

Todorovich-Hunter, L., Dodo, H., Ye, C., McCready, L., Keeley, F.W., and Rabinovitch, M. (1992). Increased pulmonary artery elastolytic activity in adult rats with monocrotaline-induced progressive hypertensive pulmonary vascular disease compared with infant rats with nonprogressive disease. Am. Rev. Respir. Dis. *146*: 213–223.

Todorovich-Hunter, L., Johnson, D.J., Ranger, P., Keeley, F.W., and Rabinovitch, M. (1988). Altered elastin and collagen synthesis associated with progressive pulmonary hypertension induced by monocrotaline. A biochemical and ultrastructural study. Lab. Investig. *58*: 184–195.

Togashi, K., Kameya, T., Kurosawa, T., Hasegawa, N., and Kawakami, M. (1992). Concentrations and molecular forms of C-type natriuretic peptide in brain and cerebrospinal fluid. Clin. Chem. *38*: 2136–2139.

Tokudome, T., Horio, T., Soeki, T., Mori, K., Kishimoto, I., Suga, S.I., et al. (2004). Inhibitory effect of C-type natriuretic peptide (CNP) on cultured cardiac myocyte hypertrophy: Interference between CNP and endothelin-1 signaling pathways. Endocrinology *145*: 2131–2140.

Toldo, S., Bogaard, H.J., Tassell, B.W. van, Mezzaroma, E., Seropian, I.M., Robati, R., et al. (2011). Right ventricular dysfunction following acute myocardial infarction in the absence of pulmonary hypertension in the mouse. PLoS One *6*: e18102.

Toshner, M., Church, C., Harbaum, L., Rhodes, C., Villar Moreschi, S.S., Liley, J., et al. (2022). Mendelian randomisation and experimental medicine approaches to interleukin-6 as a drug target in pulmonary arterial hypertension. Eur. Respir. J. *59*:.

Toshner, M., Spiekerkoetter, E., Bogaard, H., Hansmann, G., Nikkho, S., and Prins, K.W. (2020). Repurposing of medications for pulmonary arterial

hypertension. Pulm. Circ. *10*:.

Tournier, A., Wahl, D., Chaouat, A., Max, J.P., Regnault, V., Lecompte, T., et al. (2010). Calibrated automated thrombography demonstrates hypercoagulability in patients with idiopathic pulmonary arterial hypertension. Thromb. Res. *126*:.

Traish, A.M., Kang, H.P., Saad, F., and Guay, A.T. (2011). Dehydroepiandrosterone (DHEA)-A precursor steroid or an active hormone in human physiology (CME). J. Sex. Med. *8*: 2960–2982.

Trankle, C.R., Canada, J.M., Kadariya, D., Markley, R., Chazal, H.M. De, Pinson, J., et al. (2019). IL-1 blockade reduces inflammation in pulmonary arterial hypertension and right ventricular failure: A single-arm, open-label, phase Ib/II pilot study. Am. J. Respir. Crit. Care Med. *199*: 381–384.

Tual, L., Morel, O.E., Favret, F., Fouillit, M., Guernier, C., Buvry, A., et al. (2006). Carvedilol inhibits right ventricular hypertrophy induced by chronic hypobaric hypoxia. Pflugers Arch. Eur. J. Physiol. *452*: 371–379.

Tuder, R.M. (2009). Pathology of pulmonary arterial hypertension. Semin. Respir. Crit. Care Med. *30*: 376–385.

Tuder, R.M. (2017). Pulmonary vascular remodeling in pulmonary hypertension. Cell Tissue Res.

Tuder, R.M., Archer, S.L., Dorfmüller, P., Erzurum, S.C., Guignabert, C., Michelakis, E., et al. (2013). Relevant issues in the pathology and pathobiology of pulmonary hypertension. J. Am. Coll. Cardiol. *62*: D4-12.

Tuder, R.M., Chacon, M., Alger, L., Wang, J., Taraseviciene-Stewart, L., Kasahara, Y., et al. (2001). Expression of angiogenesis-related molecules in plexiform lesions in severe pulmonary hypertension: evidence for a process of disordered angiogenesis. J. Pathol. *195*: 367–374.

Tuder, R.M., Cool, C.D., Geraci, M.W., Wang, J., Abman, S.H., Wright, L., et al. (1999). Prostacyclin synthase expression is decreased in lungs from patients with severe pulmonary hypertension. Am. J. Respir. Crit. Care Med. *159*: 1925–1932.

Tuder, R.M., Marecki, J.C., Richter, A., Fijalkowska, I., and Flores, S. (2007).

Pathology of Pulmonary Hypertension. Clin. Chest Med. *28*: 23–42.

Ueno, H., Haruno, A., Morisaki, N., Furuya, M., Kangawa, K., Takeshita, A., et al. (1997). Local expression of C-type natriuretic peptide markedly suppresses neointimal formation in rat injured arteries through an autocrine/paracrine loop. Circulation *96*: 2272–2279.

Upton, P.D., Davies, R.J., Trembath, R.C., and Morrell, N.W. (2009). Bone morphogenetic protein (BMP)and activin type II receptors balance BMP9 signals mediated by activin receptor-like kinase-1 in human pulmonary artery endothelial cells. J. Biol. Chem. *284*: 15794–15804.

Vachiéry, J.L., Tedford, R.J., Rosenkranz, S., Palazzini, M., Lang, I., Guazzi, M., et al. (2019). Pulmonary hypertension due to left heart disease. Eur. Respir. J. *53*:.

Vane, J.R. (1971). Inhibition of prostaglandin synthesis as a mechanism of action for aspirin-like drugs. Nat. New Biol. *231*: 232–235.

Vang, A., Mazer, J., Casserly, B., and Choudhary, G. (2010). Activation of endothelial BKCa channels causes pulmonary vasodilation. Vascul. Pharmacol. *53*: 122–129.

Veerdonk, M.C. van de, Bogaard, H.J., and Voelkel, N.F. (2016). The right ventricle and pulmonary hypertension. Heart Fail. Rev. *21*: 259–271.

Veerdonk, M.C. Van de, Huis In T Veld, A.E., Marcus, J.T., Westerhof, N., Heymans, M.W., Bogaard, H.J., et al. (2017). Upfront combination therapy reduces right ventricular volumes in pulmonary arterial hypertension. Eur. Respir. J. *49*:.

Veerdonk, M.C. Van De, Kind, T., Marcus, J.T., Mauritz, G.J., Heymans, M.W., Bogaard, H.J., et al. (2011). Progressive right ventricular dysfunction in patients with pulmonary arterial hypertension responding to therapy. J. Am. Coll. Cardiol. *58*: 2511–2519.

Ventetuolo, C.E., Baird, G.L., Graham Barr, R., Bluemke, D.A., Fritz, J.S., Hill, N.S., et al. (2016). Higher estradiol and lower dehydroepiandrosterone-sulfate levels are associated with pulmonary arterial hypertension in men. Am. J. Respir. Crit. Care Med. *193*: 1168–1175.

Ventetuolo, C.E., and Klinger, J.R. (2014). Management of acute right ventricular failure in the intensive care unit. Ann. Am. Thorac. Soc. *11*: 811–822.

Viethen, T., Gerhardt, F., Dumitrescu, D., Knoop-Busch, S., Freyhaus, H. Ten, Rudolph, T.K., et al. (2014). Ferric carboxymaltose improves exercise capacity and quality of life in patients with pulmonary arterial hypertension and iron deficiency: A pilot study. Int. J. Cardiol. *175*: 233–239.

Villar, I.C., Panayiotou, C.M., Sheraz, A., Madhani, M., Scotland, R.S., Nobles, M., et al. (2007). Definitive role for natriuretic peptide receptor-C in mediating the vasorelaxant activity of C-type natriuretic peptide and endothelium-derived hyperpolarising factor. Cardiovasc. Res. *74*: 515–525.

Viray, M.C., Bonno, E.L., Gabrielle, N.D., Maron, B.A., Atkins, J., Amoroso, N.S., et al. (2020). Role of Pulmonary Artery Wedge Pressure Saturation during Right Heart Catheterization: A Prospective Study. Circ. Hear. Fail. 660–662.

Vitali, S.H., Hansmann, G., Rose, C., Fernandez-Gonzalez, A., Scheid, A., Mitsialis, S.A., et al. (2014). The Sugen 5416/hypoxia mouse model of pulmonary hypertension revisited: Long-term follow-up. Pulm. Circ. *4*: 619–629.

Voelkel, N.F., Cool, C., Taraceviene-Stewart, L., Geraci, M.W., Yeager, M., Bull, T., et al. (2002). Janus face of vascular endothelial growth factor: The obligatory survival factor for lung vascular endothelium controls precapillary artery remodeling in severe pulmonary hypertension. Crit. Care Med. *30*:.

Voelkel, N.F., Gomez-Arroyo, J., Abbate, A., Bogaard, H.J., and Nicolls, M.R. (2012). Pathobiology of pulmonary arterial hypertension and right ventricular failure. Eur. Respir. J. *40*: 1555–1565.

Voelkel, N.F., and Tuder, R.M. (2000). Hypoxia-induced pulmonary vascular remodeling: A model for what human disease? J. Clin. Invest. *106*: 733–738.

Vogel, C., and Marcotte, E.M. (2012). Insights into the regulation of protein abundance from proteomic and transcriptomic analyses. Nat. Rev. Genet. *13*: 227–232.

Volpe, M., Carnovali, M., and Mastromarino, V. (2016). The natriuretic peptides

system in the pathophysiology of heart failure: From molecular basis to treatment. Clin. Sci. *130*: 57–77.

Vonk-Noordegraaf, A., Haddad, F., Chin, K.M., Forfia, P.R., Kawut, S.M., Lumens, J., et al. (2013). Right heart adaptation to pulmonary arterial hypertension: Physiology and pathobiology. J. Am. Coll. Cardiol. *62*:.

Vonk-Noordegraaf, A., Westerhof, B.E., and Westerhof, N. (2017). The Relationship Between the Right Ventricle and its Load in Pulmonary Hypertension. J. Am. Coll. Cardiol. *69*: 236–243.

Vonk-Noordegraaf, A., Wolferen, S.A. van, Marcus, J.T., Boonstra, A., Postmus, P.E., Peeters, J.W.L., et al. (2005). Noninvasive assessment and monitoring of the pulmonary circulation. Eur. Respir. J. *25*: 758–766.

Vonk Noordegraaf, A., Chin, K.M., Haddad, F., Hassoun, P.M., Hemnes, A.R., Hopkins, S.R., et al. (2019). Pathophysiology of the right ventricle and of the pulmonary circulation in pulmonary hypertension: an update. Eur. Respir. J. *53*:.

Vonk Noordegraaf, A., and Galiè, N. (2011). The role of the right ventricle in pulmonary arterial hypertension. Eur. Respir. Rev. *20*: 243–253.

Walsh, T.P., Baird, G.L., Atalay, M.K., Agarwal, S., Arcuri, D., Klinger, J.R., et al. (2021). Experimental design of the Effects of Dehydroepiandrosterone in Pulmonary Hypertension (EDIPHY) trial. Pulm. Circ. *11*:.

Wang, A.P., Li, X.H., Yang, Y.M., Li, W.Q., Zhang, W., Hu, C.P., et al. (2015). A critical role of the mTOR/eIF2α pathway in hypoxia-induced pulmonary hypertension. PLoS One *10*:.

Wang, A.P., Yang, F., Tian, Y., Su, J.H., Gu, Q., Chen, W., et al. (2021). Pulmonary Artery Smooth Muscle Cell Senescence Promotes the Proliferation of PASMCs by Paracrine IL-6 in Hypoxia-Induced Pulmonary Hypertension. Front. Physiol. *12*:.

Wang, H.L., Dong, X., Zhang, X.H., and Xing, J. (2001). 5-HT1B receptor augmented 5-HT vasoconstrictor response of pulmonary artery in monocrotaline-induced pulmonary hypertensive rats. Acta Pharmacol. Sin. *22*: 269–273.

Wang, X., Shults, N. V., and Suzuki, Y.J. (2017a). Oxidative pro-ling of the failing

right heart in rats with pulmonary hypertension. PLoS One *12*:.

Wang, X., Wang, H., Liu, W., Zhang, Z., Zhang, Y., Zhang, W., et al. (2018a). High level of C-type natriuretic peptide induced by hyperandrogen-mediated anovulation in polycystic ovary syndrome mice. Clin. Sci. *132*: 759–776.

Wang, X.Y., Mo, D., Tian, W., Liu, X.X., Zhou, Y.G., Sun, Y., et al. (2019). Inhibition of RhoA/ROCK signaling pathway ameliorates hypoxic pulmonary hypertension via HIF-1α-dependent functional TRPC channels. Toxicol. Appl. Pharmacol. *369*: 60–72.

Wang, Y., Waard, M.C. de, Sterner-Kock, A., Stepan, H., Schultheiss, H.P., Duncker, D.J., et al. (2007). Cardiomyocyte-restricted over-expression of C-type natriuretic peptide prevents cardiac hypertrophy induced by myocardial infarction in mice. Eur. J. Heart Fail. *9*: 548–557.

Wang, Z., and Chesler, N.C. (2011). Pulmonary vascular wall stiffness: An important contributor to the increased right ventricular afterload with pulmonary hypertension. Pulm. Circ. *1*: 212–223.

Wang, Z., and Chesler, N.C. (2012). Role of collagen content and cross-linking in large pulmonary arterial stiffening after chronic hypoxia. Biomech. Model. Mechanobiol. *11*: 279–289.

Wang, Z., Lakes, R.S., Eickhoff, J.C., and Chesler, N.C. (2013). Effects of collagen deposition on passive and active mechanical properties of large pulmonary arteries in hypoxic pulmonary hypertension. Biomech. Model. Mechanobiol. *12*: 1115–1125.

Wang, Z., Patel, J.R., Schreier, D.A., Hacker, T.A., Moss, R.L., and Chesler, N.C. (2018b). Organ-level right ventricular dysfunction with preserved Frank-Starling mechanism in a mouse model of pulmonary arterial hypertension. J. Appl. Physiol. *124*: 1244–1253.

Wang, Z., Schreier, D.A., Abid, H., Hacker, T.A., and Chesler, N.C. (2017b). Pulmonary vascular collagen content, not cross-linking, contributes to right ventricular pulsatile afterload and overload in early pulmonary hypertension. J.

Appl. Physiol. *122*: 253–263.

Warburg, O. (1956). On the origin of cancer cells. Science (80-.). *123*: 309–314.

Watanabe, Y., Nakajima, K., Shimamori, Y., and Fujimoto, Y. (1997). Comparison of the hydrolysis of the three types of natriuretic peptides by human kidney neutral endopeptidase 24.11. Biochem. Mol. Med. *61*: 47–51.

Wauthy, P., Pagnamenta, A., Vassalli, F., Naeije, R., and Brimioulle, S. (2004). Right ventricular adaptation to pulmonary hypertension: An interspecies comparison. Am. J. Physiol. - Hear. Circ. Physiol. *286*: H1441-7.

Weatherald, J., Humbert, M., Guignabert, C., and Montani, D. (2017). Response to the article “Sorafenib as a potential strategy for refractory pulmonary arterial hypertension”. Pulm. Pharmacol. Ther. *45*: 11–12.

Wei, C.M., Heublein, D.M., Perrella, M.A., Lerman, A., Rodeheffer, R.J., McGregor, C.G.A., et al. (1993). Natriuretic peptide system in human heart failure. Circulation *88*: 1004–1009.

Wei, L.H., Huang, X.R., Zhang, Y., Li, Y.Q., Chen, H.Y., Yan, B.P., et al. (2013). Smad7 inhibits angiotensin II-induced hypertensive cardiac remodelling. Cardiovasc. Res. *99*: 665–673.

Wenceslau, C.F., McCarthy, C.G., Earley, S., England, S.K., Filosa, J.A., Goulopoulou, S., et al. (2021). Guidelines for the measurement of vascular function and structure in isolated arteries and veins. Am. J. Physiol. - Hear. Circ. Physiol. *321*: H77–H111.

Wendt, D.J., Dvorak-Ewell, M., Bullens, S., Lorget, F., Bell, S.M., Peng, J., et al. (2015). Neutral endopeptidase-resistant C-Type natriuretic peptide variant represents a new therapeutic approach for treatment of fibroblast growth factor receptor 3-related dwarfism. J. Pharmacol. Exp. Ther. *353*: 132–149.

Wennberg, P.W., Miller, V.M., Rabelink, T., and Burnett, J.C. (1999). Further attenuation of endothelium-dependent relaxation imparted by natriuretic peptide receptor antagonism. Am. J. Physiol. - Hear. Circ. Physiol. *277*:.

Wharton, J., Davie, N., Upton, P.D., Yacoub, M.H., Polak, J.M., and Morrell, N.W.

(2000). Prostacyclin analogues differentially inhibit growth of distal and proximal human pulmonary artery smooth muscle cells. Circulation *102*: 3130–3136.

White, K., Johansen, A.K., Nilsen, M., Ciuclan, L., Wallace, E., Paton, L., et al. (2012). Activity of the estrogen-metabolizing enzyme cytochrome P450 1B1 influences the development of pulmonary arterial hypertension. Circulation *126*: 1087–1098.

Whyteside, A.R., and Turner, A.J. (2008). Human neprilysin-2 (NEP2) and NEP display distinct subcellular localisations and substrate preferences. FEBS Lett. *582*: 2382–2386.

Wick, M.J., Buesing, E.J., Wehling, C.A., Loomis, Z.L., Cool, C.D., Zamora, M.R., et al. (2011). Decreased neprilysin and pulmonary vascular remodeling in chronic obstructive pulmonary disease. Am. J. Respir. Crit. Care Med. *183*: 330–340.

Wilkins, M.R., Paul, G.A., Strange, J.W., Tunariu, N., Gin-Sing, W., Banya, W.A., et al. (2005). Sildenafil versus Endothelin Receptor Antagonist for Pulmonary Hypertension (SERAPH) study. Am. J. Respir. Crit. Care Med. *171*: 1292–1297.

Wilson, J.L., Yu, J., Taylor, L., and Polgar, P. (2015). Hyperplastic growth of pulmonary artery smooth muscle cells from subjects with pulmonary arterial hypertension is activated through JNK and p38 MAPK. PLoS One *10*:.

Wilson, K.S., Buist, H., Suveizdyte, K., Liles, J.T., Budas, G.R., Hughes, C., et al. (2020). Apoptosis signal-regulating kinase 1 inhibition in in vivo and in vitro models of pulmonary hypertension. Pulm. Circ. *10*:.

Winter, R.J.D., Zhao, L., Krausz, T., and Hughes, J.M.B. (1991). Neutral endopeptidase 24.11 inhibition reduces pulmonary vascular remodeling in rats exposed to chronic hypoxia. Am. Rev. Respir. Dis. *144*: 1342–1346.

Wojciak-Stothard, B., Zhao, L., Oliver, E., Dubois, O., Wu, Y., Kardassis, D., et al. (2012). Role of RhoB in the regulation of pulmonary endothelial and smooth muscle cell responses to hypoxia. Circ. Res. *110*: 1423–1434.

Wollert, K.C., Yurukova, S., Kilic, A., Begrow, F., Fiedler, B., Gambaryan, S., et al. (2003). Increased effects of C-type natriuretic peptide on contractility and calcium

regulation in murine hearts overexpressing cyclic GMP-dependent protein kinase I. Br. J. Pharmacol. *140*: 1227–1236.

Wright, A.F., Ewart, M.A., Mair, K., Nilsen, M., Dempsie, Y., Loughlin, L., et al. (2015). Oestrogen receptor alpha in pulmonary hypertension. Cardiovasc. Res. *106*: 206–216.

Wright, R.S., Wei, C. ming, Kim, C.H., Kinoshita, M., Matsuda, Y., Aarhus, L.L., et al. (1996). C-type natriuretic peptide-mediated coronary vasodilation: Role of the coronary nitric oxide and particulate guanylate cyclase systems. J. Am. Coll. Cardiol. *28*: 1031–1038.

Wright, S.P., Prickett, T.C.R., Doughty, R.N., Frampton, C., Gamble, G.D., Yandle, T.G., et al. (2004). Amino-Terminal Pro-C-Type Natriuretic Peptide in Heart Failure. Hypertension *43*: 94–100.

Wu, C., Wu, F., Pan, J., Morser, J., and Wu, Q. (2003). Furin-mediated processing of pro-C-type natriuretic peptide. J. Biol. Chem. *278*: 25847–25852.

Wu, F., Yao, W., Yang, J., Zhang, M., Xu, Y., Hao, Y., et al. (2017). Protective effects of aloperin on monocroline-induced pulmonary hypertension via regulation of Rho A/Rho kinsase pathway in rats. Biomed. Pharmacother. *95*: 1161–1168.

Wu, Y., Feng, W., Zhang, H., Li, S., Wang, D., Pan, X., et al. (2012). Ca 2+-regulatory proteins in cardiomyocytes from the right ventricle in children with congenital heart disease. J. Transl. Med. *10*:.

Xu, W., Koeck, T., Lara, A.R., Neumann, D., DiFilippo, F.P., Koo, M., et al. (2007). Alterations of cellular bioenergetics in pulmonary artery endothelial cells. Proc. Natl. Acad. Sci. U. S. A. *104*: 1342–1347.

Yamahara, K., Itoh, H., Chun, T.H., Ogawa, Y., Yamashita, J., Sawada, N., et al. (2003). Significance and therapeutic potential of the natriuretic peptides/cGMP/cGMP-dependent protein kinase pathway in vascular regeneration. Proc. Natl. Acad. Sci. U. S. A. *100*: 3404–3409.

Yamakami, T., Taguchi, O., Gabazza, E.C., Yoshida, M., Kobayashi, T., Kobayashi, H., et al. (1997). Arterial endothelin-1 level in pulmonary emphysema

and interstitial lung disease. Relation with pulmonary hypertension during exercise. Eur. Respir. J. *10*: 2055–2060.

Yanagisawa, K., Osada, H., Masuda, A., Kondo, M., Saito, T., Yatabe, Y., et al. (1998). Induction of apoptosis by Smad3 and down-regulation of Smad3 expression in response to TGF-β in human normal lung epithelial cells. Oncogene *17*: 1743–1747.

Yang, P., Read, C., Kuc, R.E., Buonincontri, G., Southwood, M., Torella, R., et al. (2017). Elabela/toddler is an endogenous agonist of the apelin APJ receptor in the adult cardiovascular system, and exogenous administration of the peptide compensates for the downregulation of its expression in pulmonary arterial hypertension. Circulation *135*: 1160–1173.

Yang, X., Long, L., Southwood, M., Rudarakanchana, N., Upton, P.D., Jeffery, T.K., et al. (2005). Dysfunctional Smad signaling contributes to abnormal smooth muscle cell proliferation in familial pulmonary arterial hypertension. Circ. Res. *96*: 1053–1063.

Yaoita, N., Satoh, K., and Shimokawa, H. (2016). Novel Therapeutic Targets of Pulmonary Hypertension. Arterioscler. Thromb. Vasc. Biol. *36*: e97–e102.

Yeager, M.E., Frid, M.G., and Stenmark, K.R. (2011). Progenitor cells in pulmonary vascular remodeling. Pulm. Circ. *1*: 3–16.

Yeager, M.E., Halley, G.R., Golpon, H.A., Voelkel, N.F., and Tuder, R.M. (2001). Microsatellite instability of endothelial cell growth and apoptosis genes within plexiform lesions in primary pulmonary hypertension. Circ. Res. *88*:.

Yeh, L.C.C., Zavala, M.C., and Lee, J.C. (2006). C-type natriuretic peptide enhances osteogenic protein-1-induced osteoblastic cell differentiation via smad5 phosphorylation. J. Cell. Biochem. *97*: 494–500.

Yin, N., Kaestle, S., Yin, J., Hentschel, T., Pries, A.R., Kuppe, H., et al. (2009). Inhaled nitric oxide versus aerosolized iloprost for the treatment of pulmonary hypertension with left heart disease. Crit. Care Med. *37*: 980–986.

Yu, Y., Sweeney, M., Zhang, S., Platoshyn, O., Landsberg, J., Rothman, A., et al.

(2003). PDGF stimulates pulmonary vascular smooth muscle cell proliferation by upregulating TRPC6 expression. Am. J. Physiol. - Cell Physiol. *284*:.

Yuan, K., Agarwal, S., Chakraborty, A., Condon, D.F., Patel, H., Zhang, S., et al. (2021). Lung Pericytes in Pulmonary Vascular Physiology and Pathophysiology. Compr. Physiol. *11*: 2227–2247.

Yuan, K., Shamskhou, E.A., Orcholski, M.E., Nathan, A., Reddy, S., Honda, H., et al. (2019). Loss of Endothelium-Derived Wnt5a Is Associated with Reduced Pericyte Recruitment and Small Vessel Loss in Pulmonary Arterial Hypertension. Circulation *139*: 1710–1724.

Yuan, K., Shao, N.Y., Hennigs, J.K., Discipulo, M., Orcholski, M.E., Shamskhou, E., et al. (2016). Increased Pyruvate Dehydrogenase Kinase 4 Expression in Lung Pericytes Is Associated with Reduced Endothelial-Pericyte Interactions and Small Vessel Loss in Pulmonary Arterial Hypertension. Am. J. Pathol. *186*: 2500–2514.

Yung, L.M., Yang, P., Joshi, S., Augur, Z.M., Kim, S.S.J., Bocobo, G.A., et al. (2020). ACTRIIA-Fc rebalances activin/GDF versus BMP signaling in pulmonary hypertension. Sci. Transl. Med. *12*:.

Zabini, D., Granton, E., Hu, Y., Miranda, M.Z., Weichelt, U., Bonnet, S.B., et al. (2018). Loss of SMAD3 Promotes Vascular Remodeling in Pulmonary Arterial Hypertension via MRTF Disinhibition. Am. J. Respir. Crit. Care Med. *197*: 244–260.

Zaidi, S.H.E., You, X.M., Ciura, S., Husain, M., and Rabinovitch, M. (2002). Overexpression of the serine elastase inhibitor elafin protects transgenic mice from hypoxic pulmonary hypertension. Circulation *105*: 516–521.

Zakrzewicz, A., Kourl, F.M., Nejman, B., Kwapiszewska, G., Hecker, M., Sandu, R., et al. (2007). The transforming growth factor-β/Smad2,3 signalling axis is impaired in experimental pulmonary hypertension. Eur. Respir. J. *29*: 1094–1104.

Zamanian, R.T., Badesch, D., Chung, L., Domsic, R.T., Medsger, T., Pinckney, A., et al. (2021). Safety and efficacy of B-cell depletion with rituximab for the treatment of systemic sclerosis–associated pulmonary arterial hypertension: A multicenter, double-blind, randomized, placebo-controlled trial. Am. J. Respir. Crit. Care Med.

204: 209–221.

Zamanian, R.T., Hansmann, G., Snook, S., Lilienfeld, D., Rappaport, K.M., Reaven, G.M., et al. (2009). Insulin resistance in pulmonary arterial hypertension. Eur. Respir. J. *33*: 318–324.

Zandvoort, A., Postma, D.S., Jonker, M.R., Noordhoek, J.A., Vos, J.T.W.M., Geld, Y.M. van der, et al. (2006). Altered expression of the Smad signalling pathway: Implications for COPD pathogenesis. Eur. Respir. J. *28*: 533–541.

Zhang, G.X., Obata, K., Takeshita, D., Mitsuyama, S., Nakashima, T., Kikuta, A., et al. (2012). Evaluation of left ventricular mechanical work and energetics of normal hearts in SERCA2a transgenic rats. J. Physiol. Sci. *62*: 221–231.

Zhang, M., Chang, Z., Zhang, P., Jing, Z., Yan, L., Feng, J., et al. (2019). Protective effects of 18β-glycyrrhetinic acid on pulmonary arterial hypertension via regulation of Rho A/Rho kinsase pathway. Chem. Biol. Interact. *311*:.

Zhang, S., Yang, T., Xu, X., Wang, M., Zhong, L., Yang, Y., et al. (2015). Oxidative stress and nitric oxide signaling related biomarkers in patients with pulmonary hypertension: A case control study. BMC Pulm. Med. *15*:.

Zhao, L. (2010). Chronic hypoxia-induced pulmonary hypertension in rat: The best animal model for studying pulmonary vasoconstriction and vascular medial hypertrophy. Drug Discov. Today Dis. Model. *7*: 83–88.

Zhao, L., Long, L., Morrell, N.W., and Wilkins, M.R. (1999). NPR-A-deficient mice show increased susceptibility to hypoxia-induced pulmonary hypertension. Circulation *99*: 605–607.

Zhao, L., Mason, N.A., Strange, J.W., Walker, H., and Wilkins, M.R. (2003). Beneficial effects of phosphodiesterase 5 inhibition in pulmonary hypertension are influenced by natriuretic peptide activity. Circulation *107*: 234–237.

Zhao, Y., Lv, W., Piao, H., Chu, X., and Wang, H. (2014). Role of platelet-derived growth factor-BB (PDGF-BB) in human pulmonary artery smooth muscle cell proliferation. J. Recept. Signal Transduct. *34*: 254–260.

Zheng, S., Chen, Y., Ma, M., and Li, M. (2022). Mechanism of quercetin on the

improvement of ovulation disorder and regulation of ovarian CNP/NPR2 in PCOS model rats. J. Formos. Med. Assoc. *121*: 1081–1092.

Zhihao, L., Jingyu, N., Lan, L., Michael, S., Rui, G., Xiyun, B., et al. (2020). SERCA2a: a key protein in the Ca2+ cycle of the heart failure. Heart Fail. Rev. *25*: 523–535.

Zhou, C., Francis, C.M., Xu, N., and Stevens, T. (2018). The role of endothelial leak in pulmonary hypertension (2017 Grover Conference Series). Pulm. Circ. *8*:.

Zhu, H., Li, Y., Qu, S., Luo, H., Zhou, Y., Wang, Y., et al. (2012). MicroRNA expression abnormalities in limited cutaneous scleroderma and diffuse cutaneous scleroderma. J. Clin. Immunol. *32*: 514–522.

Zhu, Z., Godana, D., Li, A., Rodriguez, B., Gu, C., Tang, H., et al. (2019). Echocardiographic assessment of right ventricular function in experimental pulmonary hypertension. Pulm. Circ. *9*:.

Zimmer, H.G., Zierhut, W., Seesko, R.C., and Varekamp, A.E. (1988). Right heart catheterization in rats with pulmonary hypertension and right ventricular hypertrophy. Basic Res. Cardiol. *83*: 48–57.

Zisman, D.A., Schwarz, M., Anstrom, K.J., Collard, H.R., Flaherty, K.R., Hunninghake, G.W., et al. (2010). A controlled trial of sildenafil in advanced idiopathic pulmonary fibrosis. N. Engl. J. Med. *363*: 620–628.

Zolty, R. (2021). Novel experimental therapies for treatment of pulmonary arterial hypertension. J. Exp. Pharmacol. *13*: 817–857.

Zuckerbraun, B.S., Stoyanovsky, D.A., Sengupta, R., Shapiro, R.A., Ozanich, B.A., Rao, J., et al. (2007). Nitric oxide-induced inhibition of smooth muscle cell proliferation involves S-nitrosation and inactivation of RhoA. Am. J. Physiol. - Cell Physiol. *292*:.

Appendix

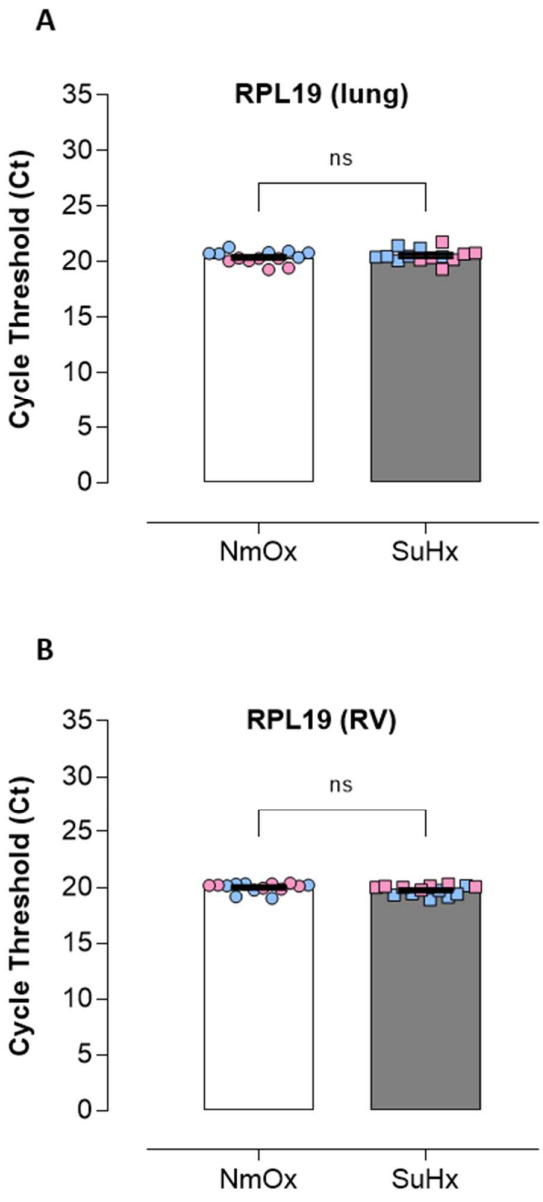

Supplementary Figure 1: Comparison of housekeeping gene mRNA expression in NmOx and SuHx mice

Ribosomal protein L19 (RPL19) mRNA expression in the lungs (*A*) and RV (*B*) of normoxic (NmOx) and Sugen + hypoxia (SuHx) wildtype mice. Data presented as mean ± *SEM*; blue and pink symbols represent individual values for male and female animals, respectively. Statistical analysis by Student's *t*-test; *ns*, not significant.

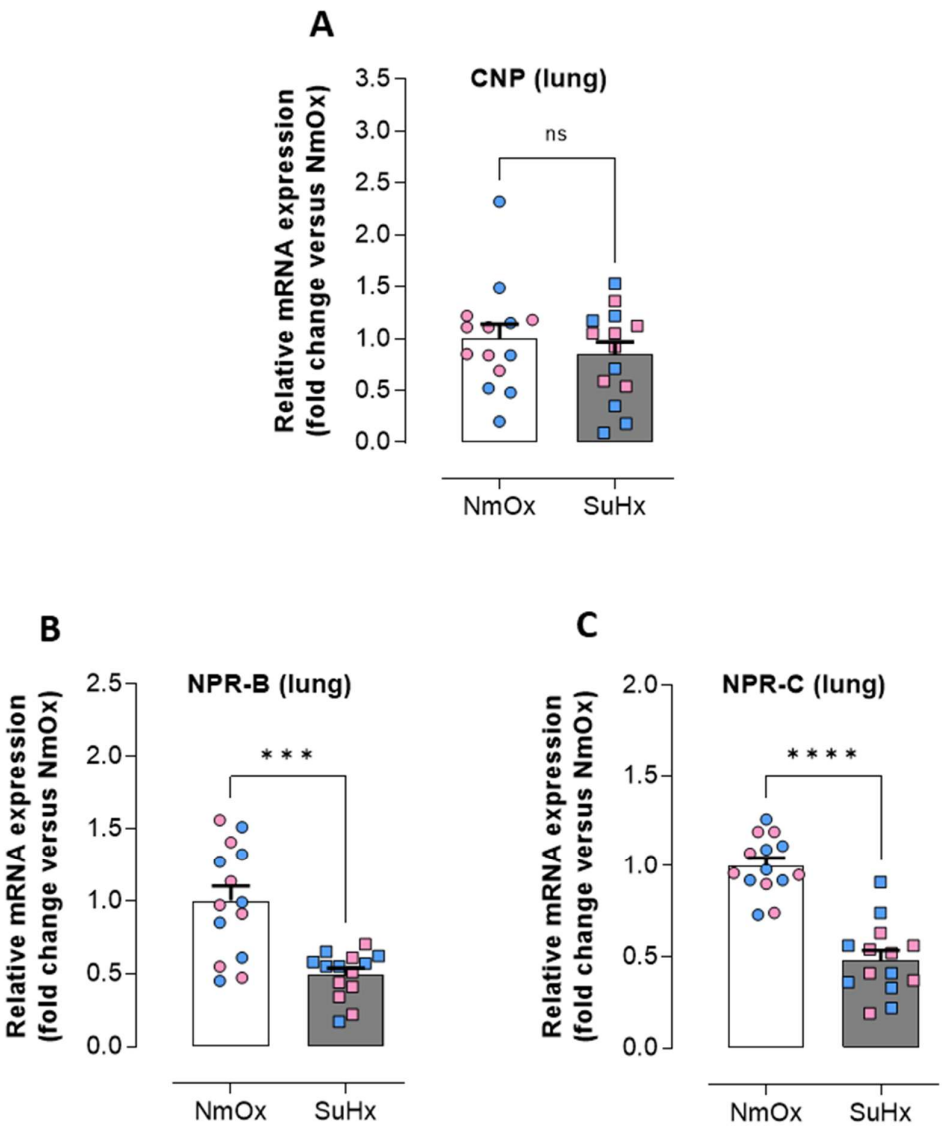

Supplementary Figure 2: Expression of CNP, NPR-B and NPR-C in the lungs of animals with experimental PH

Pulmonary mRNA expression of (*A*) CNP, (*B*) NPR-B, and (*C*) NPR-C in normoxic (NmOx) and Sugen + hypoxia (SuHx) wildtype mice. Data presented as mean ± *SEM*; blue and pink symbols represent individual values for male and female animals, respectively. Statistical analysis by Student's *t*-test. ***$P \leq 0.001$; ****$P \leq 0.0001$; *ns*, not significant.

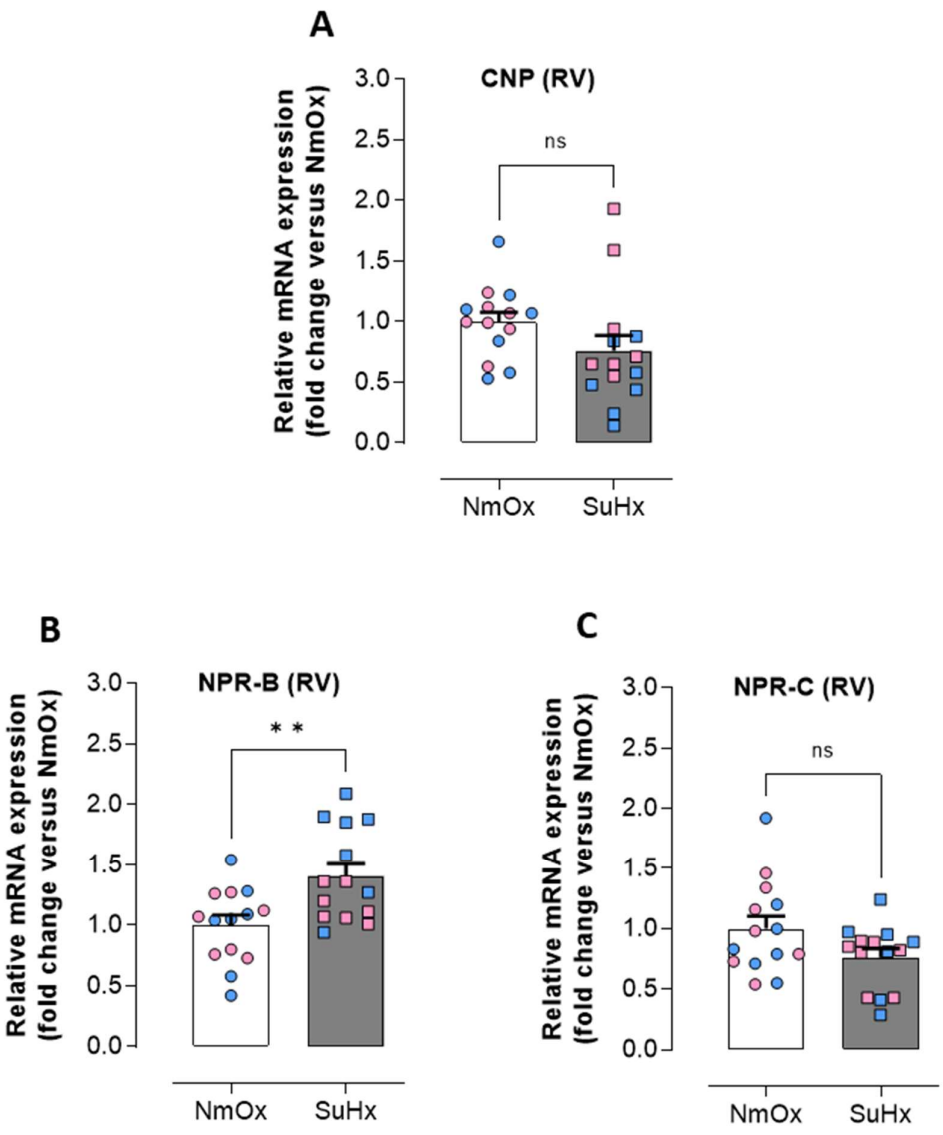

Supplementary Figure 3: Expression of CNP, NPR-B and NPR-C in the RV of animals with experimental PH

Right ventricular (RV) mRNA expression of (*A*) CNP, (*B*) NPR-B, and (*C*) NPR-C in normoxic (NmOx) and Sugen + hypoxia (SuHx) wildtype mice. Data presented as mean ± *SEM*; blue and pink symbols represent individual values for male and female animals, respectively. Statistical analysis by Student's *t*-test. $^{**}P \leq 0.01$; *ns*, not significant.

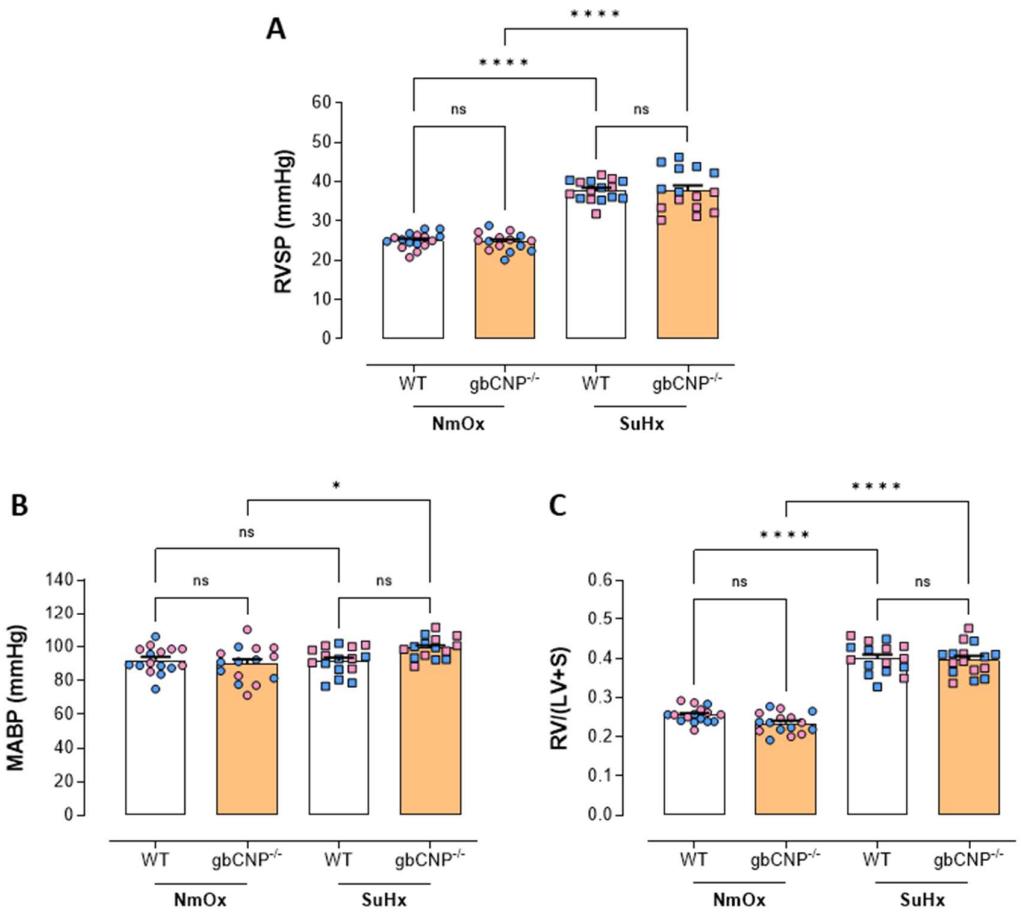

Supplementary Figure 4: The effect of global CNP deletion on the development of experimental PH

(A) Right ventricular systolic pressure (RVSP), (*B*) mean arterial blood pressure (MABP), and (*C*) right ventricle to left ventricle plus septum ratio; RV/(LV+S) in normoxic (NmOx) and Sugen + hypoxia (SuHx) wildtype (WT) and global CNP knockout (gbCNP$^{-/-}$) mice. Data presented as mean ± *SEM*; blue and pink symbols represent individual values for male and female animals, respectively. Statistical analysis by one-way ANOVA with Šidák post hoc test. *$P \leq 0.05$, ****$P \leq 0.0001$; *ns*, not significant (adjusted for multiplicity).

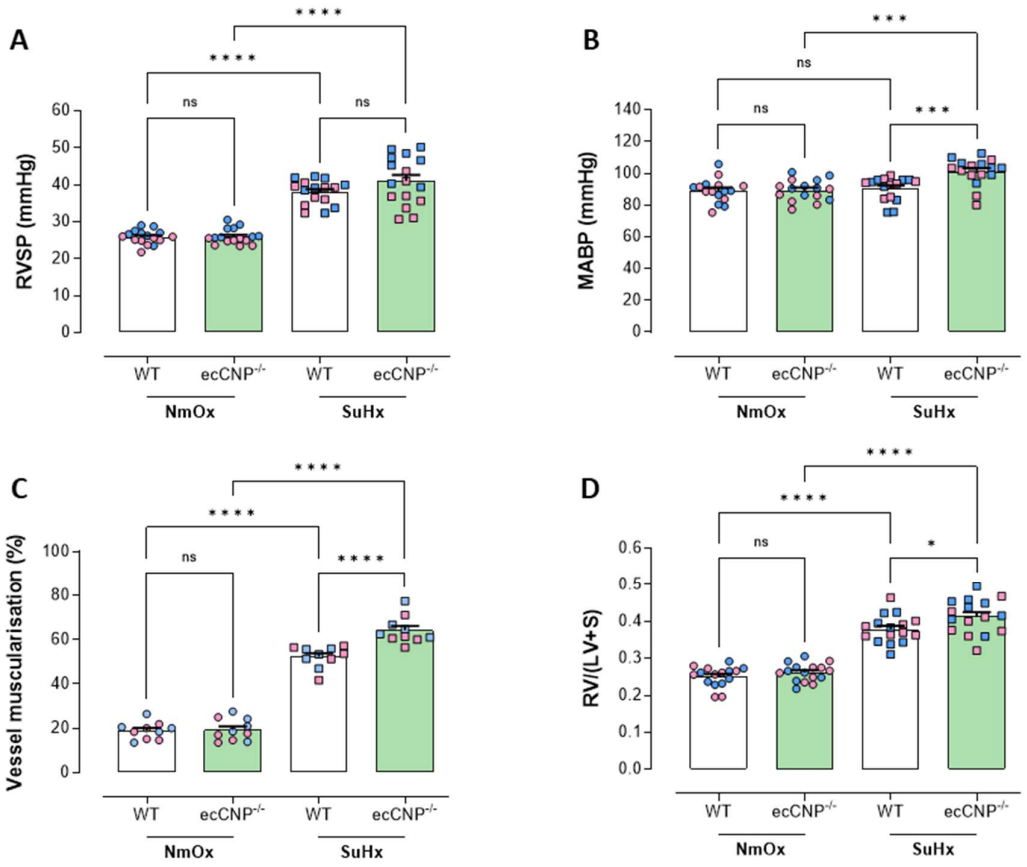

Supplementary Figure 5: The effect of endothelial CNP deletion on the development of experimental PH

(A) Right ventricular systolic pressure (RVSP), (*B*) mean arterial blood pressure (MABP), (*C*) pulmonary vessel muscularisation, and (*D*) right ventricle to left ventricle plus septum ratio; RV/(LV+S) in normoxic (NmOx) and Sugen + hypoxia (SuHx) wildtype (WT) and endothelial-specific CNP knockout (ecCNP$^{-/-}$) mice. Data presented as mean ± *SEM*; blue and pink symbols represent individual values for male and female animals, respectively. Statistical analysis by one-way ANOVA with Šidák post hoc test. **P* ≤ 0.05, ****P* ≤ 0.001, *****P* ≤ 0.0001; *ns*, not significant (adjusted for multiplicity).

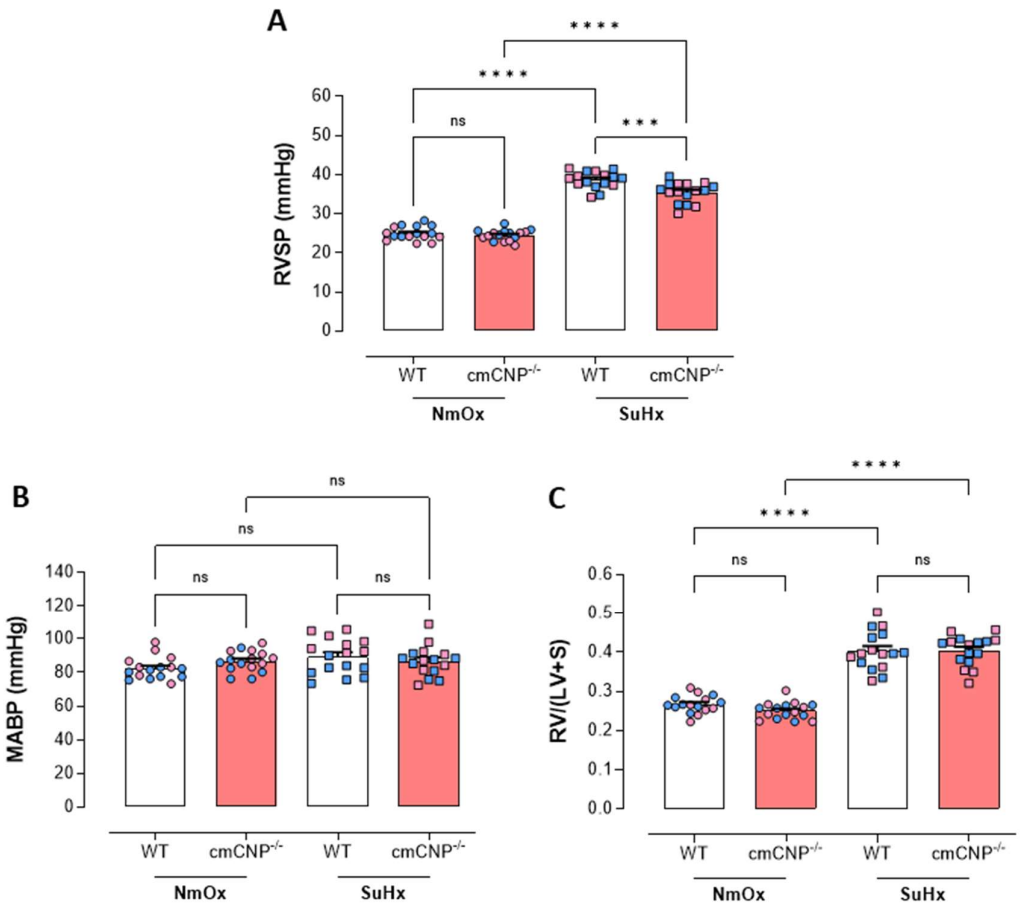

Supplementary Figure 6: The effect of cardiomyocyte CNP depletion on the development of experimental PH

(A) Right ventricular systolic pressure (RVSP), (*B*) mean arterial blood pressure (MABP), and (*C*) right ventricle to left ventricle plus septum ratio; RV/(LV+S) in normoxic (NmOx) and Sugen + hypoxia (SuHx) wildtype (WT) and cardiomyocyte-specific CNP knockout (cmCNP$^{-/-}$) mice. Data presented as mean ± *SEM*; blue and pink symbols represent individual values for male and female animals, respectively. Statistical analysis by one-way ANOVA with Šidák post hoc test. ***$P \leq 0.001$, ****$P \leq 0.0001$; *ns*, not significant (adjusted for multiplicity).

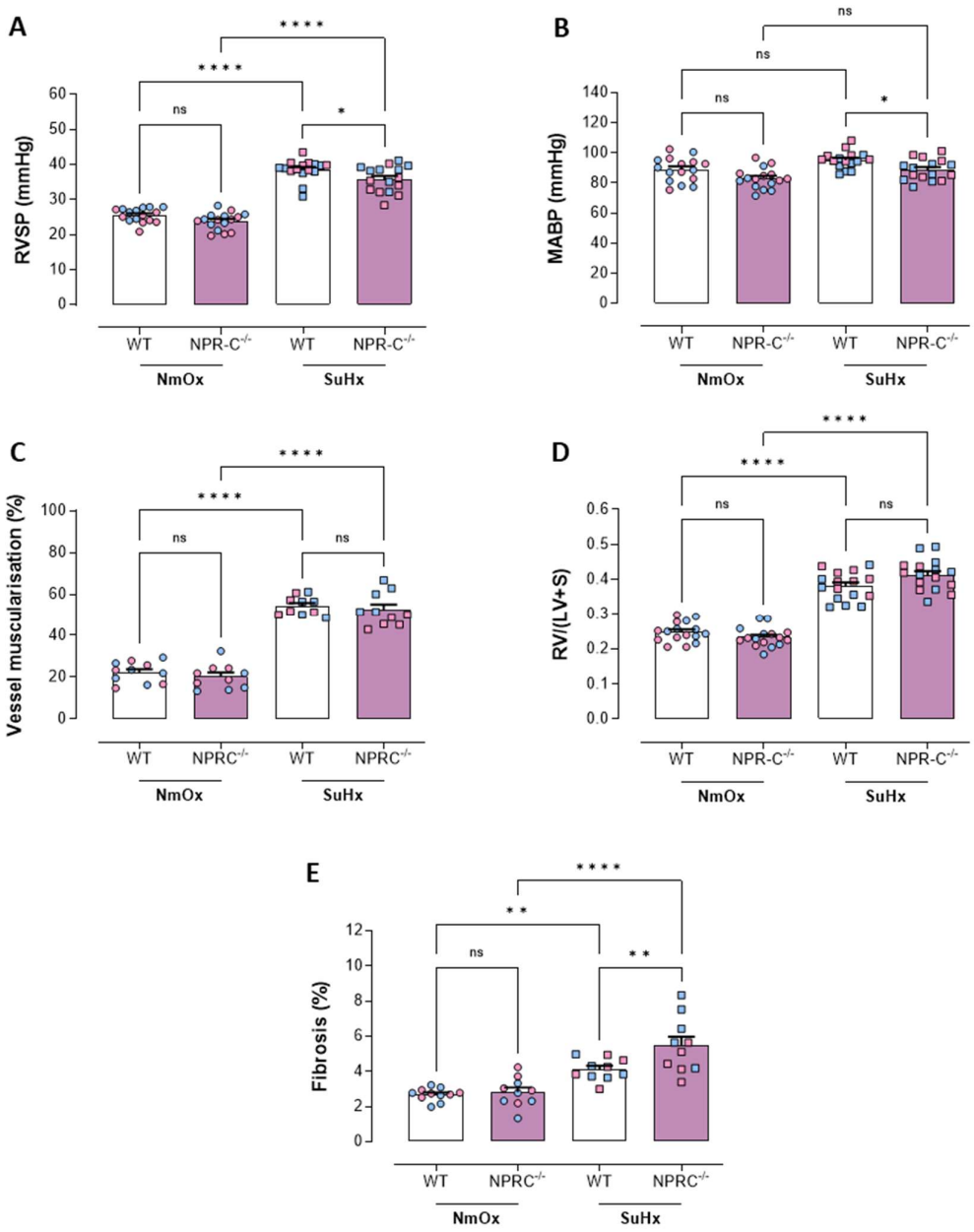

Supplementary Figure 7: The effect of global NPR-C deletion on the development of experimental PH

(A) Right ventricular systolic pressure (RVSP), (*B*) mean arterial blood pressure (MABP), (*C*) pulmonary vessel muscularisation, (*D*) right ventricle to left ventricle plus septum ratio; RV/(LV+S), and (*E*) RV fibrosis in normoxic (NmOx) and Sugen + hypoxia (SuHx) wildtype (WT) and global NPR-C knockout (NPR-C$^{-/-}$) mice. Data presented as mean ± *SEM*; blue and pink symbols represent individual values for male and female animals, respectively. Statistical analysis by one-way ANOVA with Šidák post hoc test. *$P \leq 0.05$, **$P \leq 0.01$, ****$P \leq 0.0001$; *ns*, not significant (adjusted for multiplicity).